

Bio-orthogonal Manipulation of Cellular Membranes for Biological Applications

Paul J. O'Brien

A Dissertation Submitted to the Faculty of Graduate Studies

In Partial Fulfillment of the Requirements

for the Degree of

Doctor of Philosophy

Graduate Program in Chemistry

York University

Toronto, Ontario

January, 2018

© Paul O'Brien, 2018

Abstract

Recent breakthroughs using novel chemistry and nanotechnology methodologies for cellular biology applications have spurred tremendous interest in the development of new technologies to manipulate cell-lines or cellular products for biotechnology applications, without complicated or permanent techniques used in academia and industry. Small molecule drugs, proteins, deoxyribonucleic acids (DNA) and ribonucleic acids (RNA) have been employed to manipulate and probe cellular behaviour with the intention of elucidating healthy and diseased molecular pathways for understanding human health.

This research focused on the application of liposomal delivery of bioorthogonal chemoselective chemistry to cellular membranes to control biological functions. These smart membranes were used to investigate cellular adhesion, cell spheroid aggregation kinetics and incorporation of ligands. In Chapters 2 and 3, NMR spectroscopy, oxime reaction kinetics and oxime cell surface engineered cell adhesion was correlated and probed under microfluidic conditions, while the robustness of adhesion and flexibility of cluster and tissue formation was established using live cell technique microfluidics. Using this as a base strategy, we developed a general method for the microfluidic manipulation and CSE of cells for dual labelling and flexible delivery of nucleic acids and small molecule ligands (Paul O'Brien et al. 2017, in preparation).

In Chapter 4, the bioorthogonal liposomal strategy originally utilized for cell adhesion and cell membrane ligand integration was modified and extended to transfect mammalian cell lines with nucleic acids, limiting the use of cationic charge as a mild and general method to tag and target cells in monocultures and co-cultures. The method was characterized using microscopy, protein production quantification and targeting in complex co-cultures for selective internalization.

Finally, in Chapter 5 a new chemical moiety termed “dialdehyde” was designed and synthesized for the easy and mild conjugation of primary amine containing molecules. This conjugation strategy was used to deliver small molecule ligands and macromolecules to bacterial and mammalian cell membranes using a generalized liposomal formation method. The dialdehyde was characterized and modified to contain two dialdehyde moieties with a Polyethylene Glycol (PEG) linker for crosslinking proteins, inorganic surface functionalization, organic bead assembly and cell aggregation for tissue formation.

Dedication

I want to thank my parents whom have motivated my progress by constantly asking about “when I am finishing and getting a job” and the unwavering support of my partner Janet. I dedicate my thesis to my lovely partner Janet, whom has encouraged and supported me throughout my PhD work at York. Her dedication to her own career advancement, hard work and love of life outside of her career inspired me to excel at my studies and focus on my skills outside of the lab.

Acknowledgements

This thesis is the culmination of many years of research, which would not have been possible without the support of many individuals. First, I wish to express my deepest thanks to my supervisor, Professor Muhammad N. Yousaf, for his guidance, patience, advice and occasional coffee discussions that shaped my graduate studies. I will never forget the teachable moments, both professional and personal. I would also extend thanks to my research committee advisors: Prof. Derek Wilson for support and guidance in branching into multi-disciplinary research efforts and support as MSc and PhD advisor; and Prof. Yi Sheng for her constructive criticism and analysis of my work to shape my understanding of biological experimentation. In addition, I also thank my internal and external examiners, Prof. Michael Connor and Prof. Craig Simmons, respectively, for approving to examine this thesis.

Next, I would wish to thank all of the past members of the Yousaf group. Each of you have impacted me greatly over the past years, making the day to day struggle of research bearable. I want to thank Sina Elahpanah and Dmitry Rogoznikov for their support and contributions to my work and wish them the best in the future.

Lastly, I want to thank my friends and family for their support.

Table of Contents

Abstract	ii
Dedication	iv
Acknowledgements	v
Table of Contents	vi
List of Figures	x
List of Abbreviations and Symbols	xiii
List of Publications	xv
Chapter 1: Cell Membrane Engineering for Cellular Manipulation Molecular Study and Cellular Adhesion Studies	1
1.1 Introduction	1
1.2 Traditional Techniques to Manipulate Cells	3
1.2.1 Genetic Engineering of Cellular Membranes	3
1.2.2 Cellular Membrane Manipulation using Polymers	7
1.2.3 Metabolic Labelling of Cellular Membranes	11
1.3 Bio-orthogonal Liposomes as Self-Assembled Nanoparticles for Delivery of Bio-orthogonal Ligands to Cells	14
1.3.1 Liposomes as Vehicles for Drugs or Molecular Delivery	14
1.3.2 Cellular Mechanisms of Liposome Uptake and Lipid Incorporation	17
1.3.3 Bio-orthogonal Lipid Incorporation into Cellular Membranes via Liposome Fusion	21
1.4 References	26
Chapter 2: Cell Surface Engineering in Flow Using Bio-orthogonal Liposomes	30
2.1 Introduction	31
2.2 Materials and Methods	38
2.2.1 Materials	38
2.2.2 Cell Culture	38
2.2.3 Surface Engineering Liposome Formulation	38
2.2.4 Assembly of Microfluidic Devices	39
2.2.5 Surface Engineering and Adhesion Studies in Flow	39
2.2.6 General Transfection and Assembly of Tissues in Flow using HDNF/RFP Cells and pHMGFP	41
2.2.7 Selective Transfection and Assembly of Tissues in Microfluidic Flow	42

2.2.8 Microfluidic CSE of Liposome Coupled Biotin and Streptavidin (FITC) to Cellular Membranes	43
2.2.9 Synthesis of (24) (E)-2-(dodecan-2-ylideneaminoxy) acetic acid.....	44
2.3 Results and Discussion.....	45
2.4 Conclusion.....	56
2.5 References	57
Chapter 3: Cell-Cell Tissue Assembly and Particle Kinetics in Microfluidic Flow	59
3.1 Introduction	60
3.2 Materials and Methods	67
3.2.1 Materials	67
3.2.2 Cell Culture	67
3.2.3 Microfluidic Device Fabrication and Design.....	67
3.2.4 Liposome Formation and Formulation	68
3.2.5 Cell Surface Modification using Liposome Fusion.....	69
3.2.6 Microtissue Generation in Microfluidic Device	69
3.2.7 Microtissue Generation vs. Flow Kinetics	70
3.2.8 Confocal Microscopy of RFP/GFP 3D Co-culture Microtissues	70
3.2.9 Confocal Microscopy of Three-cell line (red/green/blue) Microtissues	71
3.2.10 Three-Dimensional Co-culture 3D Multi-Layers of HMSCs and NIH3T3 Fibroblasts	72
3.2.11 Collagen Based RFP and GFP Tissue Formation (Fig. 3.7 O,P).....	72
3.2.12 Three-Dimensional Oriented Co-culture Multi-layers (RFP-GFP-RFP, thin) (Fig. 7E, F) 73	
3.2.13 Three-Dimensional Oriented Co-culture Multi-zones (RFP-GFP-RFP, thick) (Fig. 3.7 G, H)	73
3.2.14 Oxime Bond Formation (Synthesis of 2-(propan-2-ylideneaminoxy)acetic acid).....	74
3.2.15 Oxime Hydrolysis Analysis	74
3.2.16 Oxime Formation Kinetics Conditions	75
3.2.17 Spheroid Movies in Flow Experimental	75
3.2.18 Stem Cell Differentiation in Co-culture.....	75
3.3 Results and Discussion.....	76
3.4 Conclusion.....	87
Chapter 4: Application of Bio-orthogonal CSE for Directed Nucleic Acid Transfection	91
4.2 Materials and Methods	99

4.2.1 Preparation of Cell Cultures.....	99
4.2.2 Cellular Engineering Ketone Liposome Formulation and Cell Priming.....	99
4.2.3 General SnapFect Transfection of C3H/10T1/2 cells with phMGFP	100
4.2.4 Targeted Co-culture Method (HNDF/RFP and C3H/10T1/2) and phMGFP Transfection of HNDF cells.....	101
4.2.5 Firefly Luciferase Stability Assay.....	102
4.2.6 Western Blot Assay	103
4.2.7 Comparison Luciferase Assays Using Viafect and Lipofectamine 3000.....	104
4.2.8 Viability and Efficiency Comparison Assays Using phGFP of Viafect and Lipofectamine	104
4.2.9 Microfluidic Transfection in Flow	105
4.3 Results and Discussion.....	107
4.4 Conclusion.....	118
4.5 References	120
Chapter 5: Dialdehyde Reagents for Bioconjugation Applications	122
5.1 Introduction	123
5.2 Materials and Methods	128
5.2.1 Synthesis of Lipid Dialdehyde (9) and Conjugate (10).....	128
5.2.2 Synthesis of Acetonide Precursor (24).....	130
5.2.3 Synthesis of Dialdehyde Amide (29) and Conjugate (30).....	133
5.2.4 Synthesis of Phenyl Dialdehyde (33) and Conjugate (51)	135
5.2.5 Synthesis of Biotin Dialdehyde (37) and Conjugate (38).....	137
5.2.7 Synthesis of Lysine O-methyl Dialdehyde Conjugate (36).....	142
5.2.8 Synthesis of Dialdehyde Glass Surfaces	142
5.2.9 Immobilization of Fluorescent Beads onto Dialdehyde Glass Surfaces.....	143
5.2.10 Cell Surface Engineering via Liposome Fusion using Dialdehyde Liposomes (15).....	143
Dialdehyde Liposome (Pathway A)	143
5.2.11 Synthesis of Cell Surface Engineering Liposome Probes.....	145
5.2.12 Cell Surface Engineering via Liposome Fusion using Dialdehyde Liposomes (15).....	145
Dialdehyde Liposome (Pathway B)	145
5.2.13 Mammalian Cell Surface Engineering via Dialdehyde Conjugate Liposome (15)	147
5.2.14 Bacteria Cell Surface Engineering via Dialdehyde Conjugate Liposome (15)	149
5.2.15 Cell Surface Engineering via Liposome Fusion using Amine Liposomes (42)	149
Amine Liposome (Pathway A).....	149

5.2.16 Cell Surface Engineering via Liposome Fusion using Amine Liposomes (42)	151
Amine Liposome (Pathway B).....	151
5.2.17 Mammalian Cell Surface Engineering via Amine Conjugate Liposome (42).....	152
5.2.18 Bacteria Cell Surface Engineering via Amine Conjugate Liposome (42).....	154
5.2.19 Cross-linking of Protein LAR D1D2 and CS2 Domain	155
5.2.20 Cross-linking of Protein EA22.....	156
5.2.21 Cross-linking of Protein PP16	156
5.2.22 Dialdehyde Cross-linking and Acid Release of Commercial Latex-Amine Beads in Aqueous Solution	157
5.2.23 Cross-linker Dialdehyde Generation of Tissue Constructs.....	159
5.2.24 Synthesis of Dialdehyde Cross-linker (49).....	160
5.3 Results and Discussion.....	162
5.4 Conclusion.....	186
5.5 References	188
Chapter 6: Conclusions and Future Directions	190
6.1 Conclusions	191
6.2 Future Directions	192
6.3 References	194
7.0 Appendix.....	195

List of Figures

	Page
Figure 1.1 RBCs cell surface engineered with embedded Kell proteins and C-terminal coupled with sortase-mediated probes.....	4
Figure 1.2 Cells were site-specific labeled by genetic labeling and probed using ketone and biotin containing molecules.....	5
Figure 1.3 Schematic depicting a conducting polymer matrix imbedded with neuronal cells used to make sensitive measurements of neuronal cell conductivity in response to stimuli.....	8
Figure 1.4 UV activated polymer surface coatings of PMEDSAH promoted the adhesion and growth of hESCs with reduced reliance upon soluble growth factors.....	9
Figure 1.5 Microscopic images of polymer encapsulated pancreatic cells derived from HMSCs for implantation.....	10
Figure 1.6 Schematic for reacting metabolically incorporated Aha with soluble phosphine tagged reagents to form stable conjugates.....	12
Figure 1.7 Fluorescently labeled Jurkat cells with metabolically incorporated N-azidoacetylmannosamine were separately treated with DIFO terminated ssDNA for surface conjugation of complimentary binding of ssDNA populations.....	13
Figure 1.8 Depiction of three active mechanisms of endocytosis in cells.....	17
Figure 1.9 General depiction two membranes undergoing membrane fusion.....	18
Figure 1.10 Current model of SNARE-mediated fusion.....	19
Figure 1.11 Depiction of bio-orthogonal chemistry pairs used for chemical biology applications.....	21
Figure 1.12 Microfluidic gradient of O-hydroxylamine patterning on gold substrates for ketone terminated addition of RGD-ketones for cellular migration studies.....	23
Figure 2.1 Utility of bio-orthogonal CSE strategies for general microfluidic manipulation of cellular suspensions.	34
Figure 2.2 Depiction of the formulation and delivery of bio-orthogonal lipid engineered liposomes to achieve engineered cells and tissues in microfluidic flow.....	36
Figure 2.3 Microfluidic scheme depicting our integrated tissue formation assay.....	48
Figure 2.4 Complex spheroid and tissue formation using a simple microfluidic device to form three cell-line tissues and spheroids using three different CSE cell lines in flow.....	50
Figure 2.5 Multiplexed delivery of CSE engineering and nucleic acids through CSE-lipoplexes to HDNF RFP cells in flow.....	51
Figure 2.6 Single step selective nucleic acid transfection and microfluidic CSE assembly of tissues to produce complex transfected co-cultures containing two cell lines.....	53

Figure 2.7	Efficient microfluidic membrane incorporation of oxime coupled biotin and subsequent labeling with Streptavidin-FITC conjugate for flow cytometry.....	55
Figure 3.1	Schematic describing the cell surface tailoring strategy to generate complex co-culture tissue assemblies.....	65
Figure 3.2	Nuclear Magnetic Resonance (NMR) study of the kinetics and stability of the bio-orthogonal oxime conjugation reaction at physiological conditions.....	76
Figure 3.3	Schematic describing the use of microfluidic technology and tailored cell lines to generate multi-layer co-culture tissues.....	77
Figure 3.4	Images of cells at various stages of assembly in the microfluidic channel device.....	78
Figure 3.5	Schematic cartoon and fluorescent images of co-culture spheroid assembly via click chemistry ligation.....	80
Figure 3.6	3D plot presenting the relationship between flow rate, channel distance, cell density, and resulting cell cluster size (spheroid) assembled within a microfluidic channel.....	81
Figure 3.7	A range of confocal and bright-field images of various combinations of GFP NIH 3T3 fibroblasts, RFP neonatal fibroblasts, blue live stain C3H10T1/2 pluripotent embryonic fibroblast stem cells.....	83
Figure 3.8	Construction of a 3D tissue co-culture system via intercell click ligation and application to stem cell differentiation.....	85
Figure 4.1	A general scheme depicting the assembly, association and cell membrane adhesion of cationic charged based chemical lipoplexes with mammalian cell lines.....	94
Figure 4.2	Schematic of combined liposome fusion, bio-orthogonal chemistry and CSE strategy for selective nucleic acid transfection of cells (SnapFect).....	96
Figure 4.3	Schematic of procedure to transfect cells via bio-orthogonal chemistry and cell surface engineering (SnapFect).....	108
Figure 4.4	Evaluation and comparison of bio-orthogonal mediated transfection (SnapFect).....	112
Figure 4.5	Precision transfection via bio-orthogonal mediated ligation in co-cultures.....	116
Figure 5.1	Selection of primary amine conjugation reactions used in research and commercially available kits for reacting amines with small molecules or biomolecules	126
Figure 5.2	Scheme of the dialdehyde click reaction of primary amines under aqueous conditions to form a ligated conjugate molecule.....	128
Figure 5.3	Lipidated Dialdehyde reagent synthetic route.....	163
Figure 5.4	Reaction of lipidated dialdehyde (9) with propyl amine to produce the lipid conjugate (10).....	165

Figure 5.5	^1H NMR spectra comparison of the modified glutaraldehyde molecule (9) and the conjugated molecule (10).....	165
Figure 5.6	Reaction rate of primary amine (propylamine) and dialdehyde (9) to generate the dihydro pyridine conjugate (10).....	166
Figure 5.7	Scheme depicting the flexible liposome functionalization strategy using incorporated dialdehyde lipids.....	167
Figure 5.8	Flow cytometry scheme of cells rapidly treated with amine containing bio-molecular probes conjugated to lipid dialdehyde liposomes using CSE via liposome fusion.....	169
Figure 5.9	3D plots of various ligands delivered to the cell membrane by dialdehyde amine click chemistry using liposome fusion describing the relationship concerning the amount of ligand characterized using flow cytometry.....	171
Figure 5.10	A general synthetic methodology to generate dialdehyde reagents.....	173
Figure 5.11	List of synthesized dialdehyde molecules and dialdehyde conjugates utilized in this study.....	174
Figure 5.12	Scheme depicting the flexible liposome functionalization strategy using incorporated dialdehyde lipids.....	176
Figure 5.13	Depiction of dialdehyde terminated ligand delivery to cells using rapid CSE via liposome fusion using click chemistry and characterized using flow cytometry and fluorescence microscopy.....	178
Figure 5.14	Diagram and images depicting the production of a dialdehyde modified glass substrate for primary amine terminated immobilization	180
Figure 5.15	Scheme depicting the synthesis of crosslinking dialdehyde molecule (49).....	181
Figure 5.16	Depiction and data of protein stapling of LAR D1D21 (A) and Caskin 2 SAM2 (B) (47) using the dialdehyde cross-linker (49).....	182
Figure 5.17	Depiction of proteins PP16 and EA22, RNA binding and DNA translation proteins respectively, treated with dialdehyde cross-linker (49) conditions to form dimers and stapled protein complexes.....	183
Figure 5.18	Scheme depicting the assembly and release of primary amine presenting fluorescent beads using dialdehyde cross-linker (49).....	185
Figure 5.19	Cell assembly of large scale cell aggregates into 3D co-culture tissues using dialdehyde cross-linker (49).....	187

List of Abbreviations and Symbols

3D – three-dimensional

ACN – Acetonitrile

CMAC - CellTracker™ Blue CMAC (7-amino-4-chloromethylcoumarin)

CSE - Cell Surface Engineering

DCM – Dichloromethane

DMEM - Dulbecco's Modified Eagle Medium

DMPG - 1, 2-ditetradecanoyl-*sn*-glycero-3-phospho-(1'-*rac*-glycerol)

DNP – 2, 4-Dinitrophenol

DOTAP - 1,2-dioleoyl-3-trimethylammonium-propane

EDTA - Ethylenediaminetetraacetic acid

ESCs - Embryonic Stem Cells

FACS – Fluorescence-Activated Cell Sorting

FBS – Fetal Bovine Serum

FITC – Fluorescein isothiocyanate

FRET – Fluorescence Resonance Energy Transfer

GFP - Green Fluorescent Protein

HDNF - Human Dermal Neonatal Fibroblasts

HEK – Human Embryonic Kidney cell

HeLa – Henrietta Lacks cancerous cervical cell

Hex:EthOAc – Hexane:Ethyl acetate solution

MESF - Molecules of Equivalent Soluble Fluorochrome

NMR – Nuclear Magnetic Resolution

NSF - *N*-ethylmaleimide Sensitive Fusion protein

PBS - Phosphate-buffered saline

PEEK - Polyether Ether Ketone

PEDOT - poly(3,4-ethylenedioxythiophene)

PEG – Polyethylene Glycol

phMGFP - Monster Green® Fluorescent Protein phMGFP Vector

PMEDSAH - poly[2-(methacryloyloxy)ethyl dimethyl-(3-sulfopropyl)ammonium hydroxide]

POPC - 1-palmitoyl-2-oleoyl-*sn*-glycero-3-phosphocholine

PSS - Poly(styrene sulphonate)

PS - Penicillin Streptomycin

RBC – Red Blood Cell

RES - Reticuloendothelial System

RFP - Red Fluorescent Protein

RGD - Arginylglycylaspartic acid tripeptide

SDS-PAGE - sodium dodecyl sulfate polyacrylamide gel electrophoresis

SNARE – Soluble NSF Attachment Protein Receptor

STREPT - Streptavidin

STREPT-FITC – Streptavidin conjugated with Fluorescein TEG – Tetraethylene Glycol

THF – Tetrahydrofuran

TLC – Thin-Layer Chromatography

List of Publications

- 1) **O'Brien, P. J.**; Elahipanah, S.; Rogozhnikov, D.; Yousaf, M. N. *ACS Cent. Sci.* **2017**, 3 (5), 489–500. Bio-Orthogonal Mediated Nucleic Acid Transfection of Cells via Cell Surface Engineering.
- 2) Rogozhnikov, D.; **O'Brien, P. J.**; Elahipanah, S.; Yousaf, M. N. *Sci. Rep.* **2016**, 6, 39806. Scaffold Free Bio-orthogonal Assembly of 3-Dimensional Cardiac Tissue via Cell Surface Engineering.
- 3) Elahipanah, S.; **O'Brien, P. J.**; Rogozhnikov, D.; Yousaf, M. N. *Bioconjug. Chem.* **2017**, 28 (5), 1422–1433. General Dialdehyde Click Chemistry for Amine Bioconjugation.
- 4) Elahipanah, S., Radmanesh, P., Luo, W., **O'Brien, P. J.**, Rogozhnikov, D., & Yousaf, M.N. Rewiring Gram-Negative Bacteria Cell Surfaces with Bio-Orthogonal Chemistry via Liposome Fusion. *ACS Bioconjug Chem.* 27 (4), 1082–1089 (2016)
- 5) Rogozhnikov, D., Luo, W., Elahipanah, S., **O'Brien, P. J.** & Yousaf, M.N. Generation of a Scaffold-Free Three-Dimensional Liver Tissue via a Rapid Cell-to-Cell Click Assembly Process. *ACS Bioconjug. Chem.* 27 (9), 1991–1998 (2016).
- 6) **O'Brien, P. J.**; Luo, W.; Rogozhnikov, D.; Chen, J.; Yousaf, M. N. *Bioconjug. Chem.* **2015**, 26 (9), 1939–1949. Spheroid and Tissue Assembly via Click Chemistry in Microfluidic Flow.
- 7) **O'Brien, P. J.**, Elahipanah, S. & Yousaf, M.N. Microfluidic Cell Surface Engineering for Rapid Modulation of Cellular Membranes. (Submitted to *Angewandte Chemie Int. Ed.*).
- 8) Rogozhnikov, D., Luo, W., Elahipanah, S., **O'Brien, P. J.** & Yousaf, M.N. Assembly of Cells into 3D Tissues via Bio-orthogonal Chemistry and Preferential Differentiation of

Stem Cells in Co-cultures with Controlled Cell Orientations. (Submitted to Nature Communications).

Chapter 1

Cell Membrane Engineering for Cellular Manipulation Molecular Study and Cellular Adhesion Studies

1.1 Introduction

The creation of new platform biotechnologies to drive innovation necessitate the development of techniques to directly manipulate cells using transient methods to advance novel therapeutics, theranostics and basic research techniques. The benefit of transient techniques stems from preventing the introduction of permanent unpredictable alterations to germ-line gene expression, which can be a mixture of genetic, epigenetic and phenotypic changes. Therefore, cell manipulation methodologies must be general, have controllable characteristics, high cell viability and reduced cell death, have bio-orthogonal compatibility with natural cellular processes, but most importantly possess transient properties while harmlessly degrading or diluting with predictability.

Cell membranes are a dynamic and robust barrier containing both active and passive properties for the exchange of information and nutrients within the environment. Signal transduction of environmental cues through the membrane results in altered gene expression producing appropriate output responses. Cells typically respond to external stimuli stemming from extracellular surfaces, soluble molecules, exosomes and adjacent cells using membrane bound receptors, channels or transmembrane proteins to transduce signals through a combination of mechanical, chemical or protein cascades beginning at the membrane, through the cytosol to reach the nucleus and alter gene expression resulting in phenotypic changes and behavioral responses such as movement, growth, apoptosis and mitosis.^{1 2 3} Therefore, the cell membrane is a vital signaling gateway for behavioral responses. Thus techniques which can manipulate the

membrane directly are essential in order to control cellular behavior without introducing permanent changes to the cell.

Interest in directly manipulating cells spurred the development of numerous techniques to engineer the cellular membrane using genetic engineering,⁴ polymer matrices,^{5 6} metabolic labelling⁷ and cell surface engineering with bio-orthogonal ligands.⁸ These techniques aim to impart functionality to the cell by introducing exogenous proteins, chemical functionality or biophysical properties through adsorption or incorporation into the membrane. Manipulation of the membrane is a major hurdle to the study of human health, since it is the gateway to the cell interior which inhibits research to the study of complex cell membranes cellular interactions, tumor growth, juxtacrine, paracrine and autocrine signaling and cell migration within tissues. Therefore new techniques that manipulate the membrane are beneficial for understanding human biology and developing next generation therapeutics.

The plasma membrane is composed of a variety of amphiphilic lipid molecules which include a hydrophilic polar head and a hydrophobic lipid tail, with highly dynamic biophysical properties arising from polar and Van der Waals interactions to form a bilayer, which can be actively modulated by the cell. There are two main classes of proteins which are associated with membrane modulation by the cell, integral proteins and peripheral proteins. Integral proteins permanently associate with the membrane and can extend through the entirety of the membrane. These transmembrane proteins, act as transporters, channels or receptors controlling membrane morphology, allowing communication or gating functions between the external environment and the cytoplasm. Peripheral proteins however, temporarily associate with either the membrane or other surface proteins through electrostatic or hydrophobic interactions. The integral and peripheral membrane proteins play an intimate role in cellular adhesion, autocrine and paracrine

signalling, apoptosis, migration and cellular division. The integral proteins also mediate important active processes such as endocytosis and vesicle fusion, both of which are important signalling events and routes of cellular cytoplasmic entry exploited by chemical transfection reagents and liposome based drug delivery systems. Therefore, the introduction of groups or proteins on the cell surface which can mimic these adhesion molecules have great potential in manipulating the membrane and ultimately cellular behaviour.

1.2 Traditional Techniques to Manipulate Cells

1.2.1 Genetic Engineering of Cellular Membranes

The use of genetic engineering to insert, delete or change the functional expression of proteins has been widely used to discover and elucidate biological pathways of healthy organisms,⁹ disease states, as well as develop drugs, cell therapies,¹⁰ biologics, mono-clonal antibodies (mABs) and proteins for structural study. Genetic engineering has recently been used to redesign cell surfaces by altering surface marker expression in cell lines by changing surface protein expression or introducing exogenous ligands upon red blood cell (RBC) progenitor membranes.⁴ The modified expression of RBC surface markers, was achieved by developing blood cell progenitors that matured into RBCs expressing proteins containing C-terminus linked LPTETG peptide chains which can be easily modified using Sortase enzymatic action. The murine RBCs were engineered to express exogenous human glycophorin A-LPTETG and targeted using Sortase-A enzymes from *Staphylococcus aureus*, which recognise the short peptide sequences of LPTETG to couple molecular probes containing a glycine cap (Figure 1.1).⁴ Importantly, these peptide chains were selectively targeted and enzymatically coupled with exogenous molecules without damaging the cell. This methodology was also used to selectively

introduce biotin and single domain antibodies onto the cell surface to demonstrate that these altered cells were viable and did not significantly affect circulation survival time in mice. Engineered RBCs are potentially advantageous as therapeutic carriers for drugs or molecules to inhibit autoimmune responses, the process of terminal differentiation from modified erythroid progenitors removes the nucleus and genetic content of the cell, leaving no trace of the genetic modification. Although the technique requires the use of RBCs, without removal of the genetic content within the cell, its therapeutic value becomes difficult to justify to healthcare regulatory agencies and does not lend to other general applications that do not require RBCs.

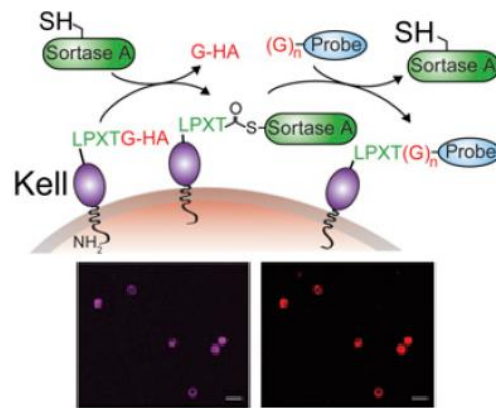


Figure 1.1: RBCs cell surface engineered with embedded Kell proteins and C-terminal coupled with sortase-mediated probes. The labelling of probes with GGG epitopes (biotin/HA) allows conjugation using Sortase-A to the LPXTG-HA epitope allowing ease of coupling in the presence of live cells. (Taken from Shi et al, 2014).⁴

Another application of genetic engineering of cellular membranes involved the introduction of surface recombinant proteins tagged with peptide recognition sequences which can be subsequently targeted by small molecules bearing bio-orthogonal chemical groups as site specific reaction handles.¹¹

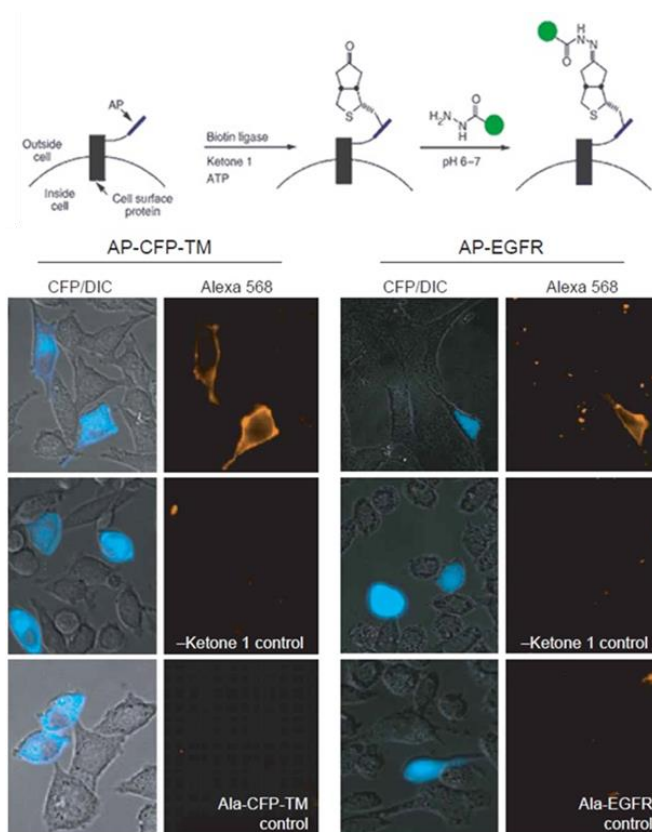


Figure 1.2: Cells were site-specific labeled by genetic labelling and probed using ketone and biotin containing molecules. HeLa or HEK cells were transfected with either acceptor protein (AP-CFP-TM) or (AP-EGFR) to express on the cell surface, then treated with a biotin containing carboxylic acid and biotin ligase. Then the biotin was targeted with a bi-functional hydrazine molecule to allow conjugation to Streptavidin-Alexa 658 or hydrazine containing fluorescent probe. (Taken from Chen et al. 2005).¹¹

Human embryonic kidney (HEK) cells were transfected with a cyan fluorescent protein fused with an acceptor peptide, which was attached to the transmembrane domain of the platelet-derived growth factor receptor. The acceptor peptide was then targeted with an exogenous biotin ligase (BirA) enzyme from *Escherichia coli*, which accepts biotin containing ligands (Figure 1.2). Once expressed on the surface of HEK or HeLa cells, they can be treated with a biotin labelled small molecule with an attached probe or ketone functional group, followed by treatment *in vitro* with hydrazine or hydroxylamine containing biophysical probes for functional analysis. This method allowed the rapid incorporation of recombinant proteins into the cellular

membrane for study, while maintaining a flexible platform for the targeted use of different synthetic biophysical probes.

There has also been interest in using genetic engineering of cell surfaces for antiviral therapies, to either remove or block bacterial or viral points of entry into the cell. A recent breakthrough in human immunodeficiency virus (HIV) treatments have shown that genetic manipulation of T-cells, a class of white blood cells that protect the body, can be made resistant to infection by the HIV virus.¹² By altering viral or bacterial antigen recognition sites on mammalian cells, the infection rates can be altered or halted, by blocking viral docking with the cell membrane. Recently, in a small clinical population of CD4 T cells, an important immune system component directly targeted by HIV using the chemokine (C-C) motif (CCR5) surface receptor, was rendered permanently dysfunctional through gene editing that produced CD4 T cells resistant to the virus. Selected HIV infected patients were treated with autologous CD4 T-cells by deleting the human CCR5 gene.¹³ Since this surface receptor contains an HIV binding site, deletion of the gene removes or hinders the virus's capability to penetrate the T-cell membrane.

Although permanent gene editing technologies for cell surface engineering have shown potential for niche research and clinical applications, there are major bottlenecks to the use of the technology and scope of its application. Genomic manipulation for plasma membrane localization of exogenous proteins involves both the complicated production of the protein of interest, as well as altering pathways for protein localization that lead from the endoplasmic reticulum (ER) or Golgi apparatus to the membrane by hindering phosphorylation,¹⁴ S-palmitoylation, N-terminal myristylation and C-terminal prenylation protein amendments or modifications.^{15 16} Many membrane associated proteins play multiple roles in the membrane

contributing to fluidity, lipid raft formation, membrane stability, endocytosis and exocytosis to name a few. Changes in these proteins or associated pathways can result in the disruption of the cellular membrane itself through over-expression, fluidity and poor lipid content regulation, impacting fluid dynamics resulting in poor proliferation, oxidative stress and increased in apoptotic signalling. These changes can result in false positive results for gene pathway elucidation, incorrect conclusions about gene regulation and false avenues of inquiry for academic and industrial research leading to wasted time, expense and effort.

1.2.2 Cellular Membrane Manipulation using Polymers

Synthetic and natural polymer research has generated a variety of methodologies to directly modify cell behaviour through layering or adhesion of polymers to the cellular membrane, imparting tunable functionality to the cell. Polymers are a broad class of high molecular weight molecules composed of repeating subunits called monomers, which are covalently linked together to form linear or branching chains.¹⁷ Polymers occupy a special class of chemistry and biology due to their emergent macroscopic characteristics which arise from their unique chemical and mechanical traits. These macroscopic properties can be modulated based upon a number of explored factors, such as subunit chemical structure and placement, the amount of branching, chain length, molecular weight and mechanical processing to produce a wide array of polymer structures with vastly different properties. Developments using polymers such as cellular or membrane coatings can be used for autoimmune resistance *in vitro*,¹⁸ tissue engineering,^{19 20} cancer models,²¹ hypoxia studies,²² as well as cellular migration and delivery.²³ This research allowed the scientific community to develop a variety of synthetic polymers and characterized many naturally occurring biological polymers, enabling the creation of a variety of plastics and reagents with a broad range of properties.

Control of cellular behaviour using ionic polymers has developed over the past 10 years to include cellular coatings, delivery and electronic control of cellular signalling.^{24 25 26} Recent work has produced novel methodologies using ionic polymers and neuronal cells to create an organic electronic ion pump for the study of cellular signalling of calcium ions.²⁷ The group synthesized poly(3,4-ethylenedioxythiophene) (PEDOT) doped with poly(styrene sulphonate) (PSS) as a proof of concept to control ion homeostasis in single neuronal cells through confinement in micron-sized devices (Figure 1.3).

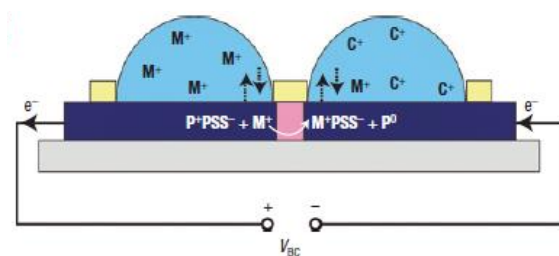


Figure 1.3: Schematic depicting a conducting polymer matrix imbedded with neuronal cells used to make sensitive measurements of cell conductivity in response to stimuli. (Taken from Isaksson et al. 2007).²⁷

These non-toxic polymers acted as an electronic connection to the neuron cells to control the electronic environment of the cells, stimulating the release or inhibition of calcium ions through translation of the electronic signal into an ion flux. The group determined that in Human Cortical Neuronal (HCN-2) cells, activation of the pump induced an increase in the intracellular calcium and potassium, mimicking manual loading of potassium sulfate into the medium. Molecular control of ionic flux through polymer engineering of the cell surface produced meaningful data essential for the development of new systems biology approaches to research and clinical understanding of disease.

Two dimensional adherent surfaces composed of inorganic, synthetic or natural polymeric materials can promote growth, cellular migration and prolonged health of cellular

colonies.^{28 29} Polymer surfaces have been used to promote the growth of difficult or sensitive cells lines such as embryonic stem cells (ESCs) without inducing differentiation or variability, while limiting the use of soluble media factors. Adhesive polymer based cellular growth surfaces have recently been developed using polymer surface coating technique using poly[2-(methacryloyloxy)ethyl dimethyl-(3-sulfopropyl)ammonium hydroxide] (PMEDSAH) to sustain hEMCs, removing the requirement of animal derived matrix (Matrigel) for long term growth *in vivo* (Figure 1.4).³⁰

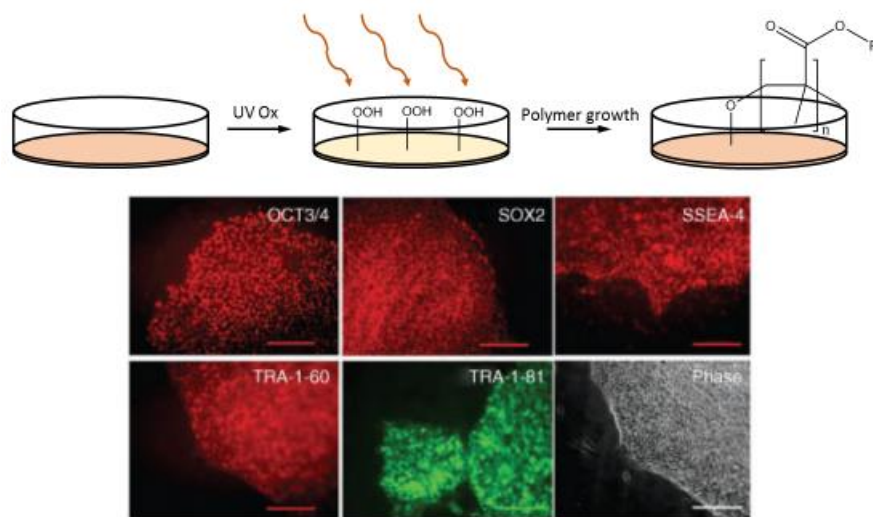


Figure 1.4: UV activated polymer surface coatings of PMEDSAH promoted the adhesion and growth of hESCs with reduced reliance upon soluble growth factors. (Taken from Villa-Diaz et al, 2010).³⁰

This demonstrated that chemically defined surface engineering can displace inconsistent animal derived sources to produce better growth methodologies.

Type I diabetes affects over 300 million people worldwide, in which the pancreas does not produce sufficient amounts of the hormone insulin, a hormone regulating the cellular uptake of glucose for energy production. To treat this disease, there have been a number of approaches used, such as gene therapy, injected beta cell autografts, xenografts and pancreatic transplants in

an attempt to restore insulin function.³¹ However, detrimental autoimmune responses can arise in the host body. To combat autoimmune responses, researchers have used polymers to mask the grafted cells from the host immune system using permeable membranes but few have moved toward cell surface engineering as a solution. To protect implanted cells such as stem cell derived pancreatic cells for transplantation, they are encapsulated with the porous biomaterial triazole-thiomorpholine dioxide (TMTD) modified alginate (Figure 1.5).

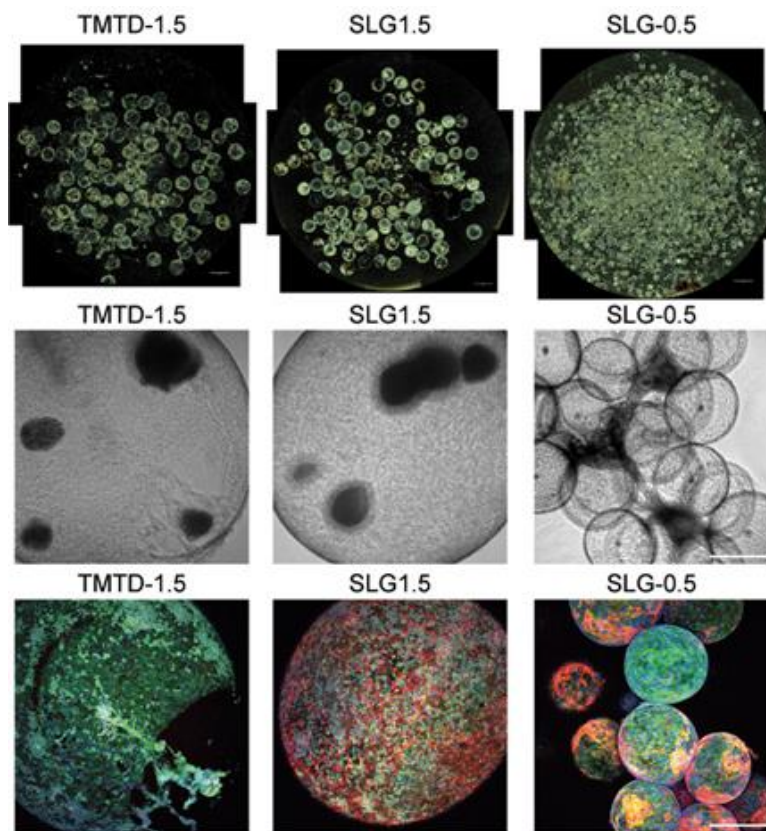


Figure 1.5: Microscopic images of polymer encapsulated pancreatic cells derived from Human Mesenchymal Stem Cells (HMSCs) for implantation. Cells were encapsulated with porous polymer materials to limit or eliminate autoimmune rejection by the host body. (Taken from Vegas et al, 2016).³²

With spheroids consisting of SC- β cells in TMTD alginate spheres, long-term control of the glycemic forming porous encapsulated response can be obtained without the use of an immunosuppressive drug regime.

Although polymers for cell based applications have been useful in niche applications, they have a number of drawbacks which limit their use in therapeutics and research applications. Polymers can be difficult to synthesize and purify in the lab, where batch to batch variability can be high, but most importantly controlled degradation of the polymers in a cellular context can be very difficult to control or predict. Polymers in living systems are constantly being degraded through active or natural processes and replaced as needed, such as in wound healing. For the most part, synthetic polymers react poorly to degradation producing toxic by-products, changing local pH, or introducing pockets of hypoxia to name a few. Naturally obtained polymers however, are expensive and contain significant batch to batch variability in composition, producing wildly varying results. Therefore, systems which are cheap, readily quantified and without by-products would be an ideal system to perform cellular membrane engineering, where molecular solutions can be transiently incorporated into the cells existing structures.

1.2.3 Metabolic Labelling of Cellular Membranes

A recently developed method for cell surface engineering termed metabolic labelling introduces molecular handles onto the cell membrane through the metabolic incorporation of unnatural sugars into the primary structure of surface glycans, proteins and peptides. Once added, the chemical groups residing on or in the functionalized cells can be used to incorporate carbohydrates,^{33 7 34} containing bio-orthogonal click-functional groups to be selectively targeted for imaging proteins,³⁵ assembling small spheroids,^{34 8} labelling DNA,³⁶ DNA ligation,³⁷ as well

as DNA and protein cross-linking.^{38 39} Metabolic labelling typically requires the chemical modification of naturally occurring biological monomers such as sugars, sialic acids, amino acids or nucleotides, as shown in Figure 1.6 to include bio-orthogonal groups such as alkynes, where following incorporation can be targeted with other molecules such as azide tagged fluorescent probes to monitor active cellular processes.⁴⁰ To incorporate chemistry into live protein within cellular structures, reactive analogues of natural cellular metabolites were exposed to cells as media additives of azidohomoalanine (Aha), a bio-orthogonal analogue of methionine (Met), in Met depleted cellular media.⁴¹ Once incorporated, the Aha azido bio-orthogonal group is targeted using the Staudinger ligation reaction with a phosphine labeled fluorescence molecule (Figure 1.6) for structural elucidation and protein localization studies *in vivo* and *in vitro*.⁴² These bio-orthogonal groups can be targeted using soluble fluorescent molecules, magnetic beads, radioactive tracers or labelled biomolecules containing the complementary bio-orthogonal reaction group to quickly and reliably incorporate it into the functionalized proteins.

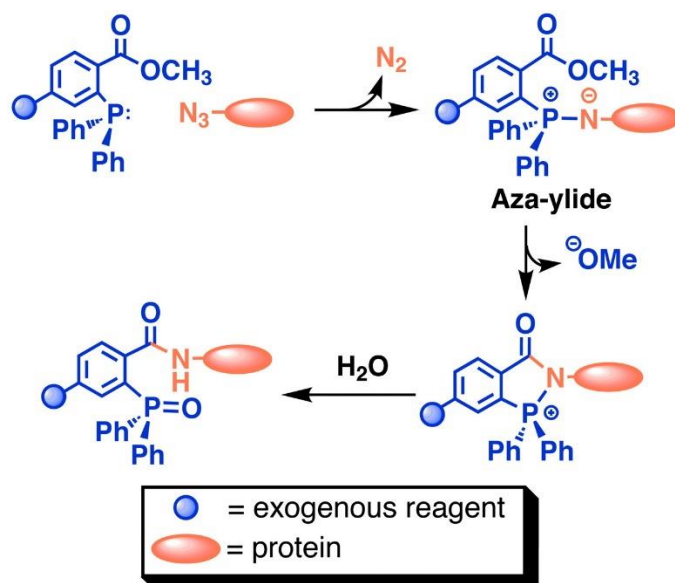


Figure 1.6: Schematic for reacting metabolically incorporated Aha with soluble phosphine tagged reagents to form stable conjugates. (Taken from Kiick et al, 2002).⁴¹

An important application of live cell metabolic labelling involved the assembly of microtissues with the introduction of N-azidoacetylmannosamine to cellular media. These azide bearing sialic acid residues were applied to two separate fluorescent immune cell populations of Jurkat cells and then reacted with complimentary single stranded DNA (ssDNA) partners respectively (Figure 1.7A).⁸ These ssDNA strands contained a difluorinated cyclooctyne (DIFO)-conjugating group to react with azide containing surface sugars to complete a bio-orthogonal copper-free ligation reaction. Two separate cell populations with complimentary ssDNA strands were then combined, resulting in strong polyvalent hydrogen bonding through complimentary base pairing to produce cell spheroids of 4-5 cells (Figure 1.7DEG).

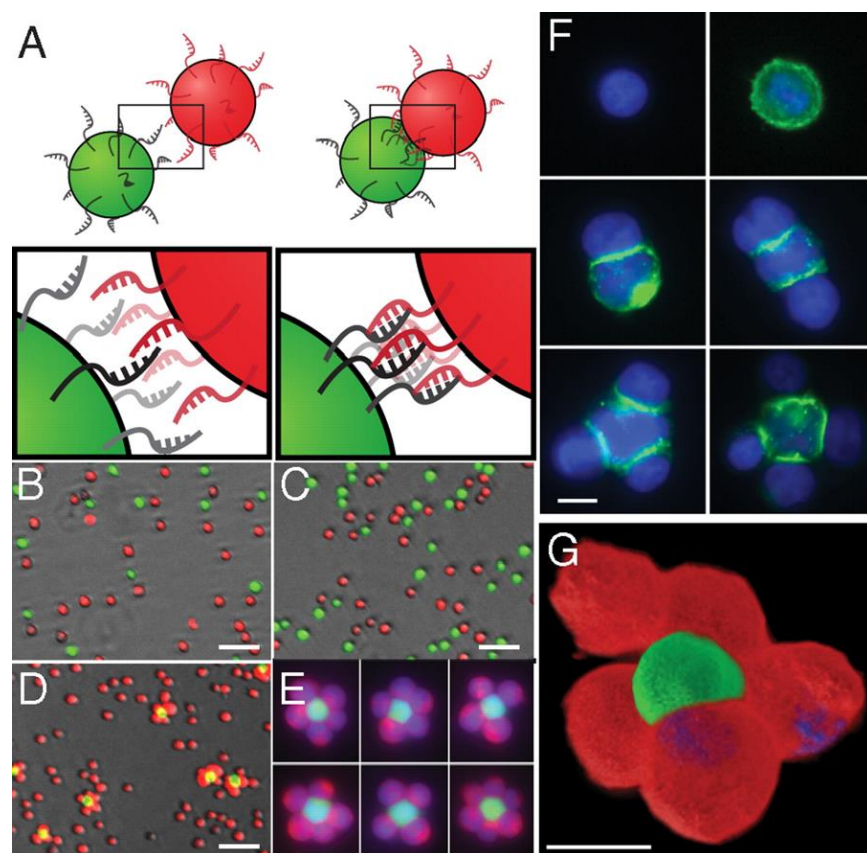


Figure 1.7: Fluorescently labeled Jurkat cells with metabolically incorporated N-azidoacetylmannosamine were separately treated with DIFO terminated ssDNA for surface conjugation of complimentary binding of ssDNA populations. These oligonucleotides direct the formation of 3-dimensional multicellular spheroids entrapped within Matrigel®. (Taken from Gartner et al, 2009).⁸

A recent extension of this methodology of spheroid production method by developing ssDNA programmed assembly of cells to generate larger tissues using epithelial and Human Umbilical Vein Cells (HUVEC) cell lines as micro-tissues imbedded within a Matrigel extracellular matrix (ECM).⁴³

1.3 Bio-orthogonal Liposomes as Self-Assembled Nanoparticles for Delivery of Bio-orthogonal Ligands to Cells

1.3.1 Liposomes as Vehicles for Drugs or Molecular Delivery

Liposomes were first described by Alec Bangham and colleagues, whom outlined a swollen phospholipid system, forming the basis of a model membrane.^{44 45} Liposomes refer to a

simple closed spherical bilayer structure composed of associated amphiphilic lipids, that contain a hydrophilic polar headgroup and nonpolar hydrophobic tail, when in an aqueous medium resemble the fundamental structure of biological membranes. Lipid polar head groups orient towards the interior and exterior aqueous phase while the acyl groups associate to form an internal hydrophobic environment, which has enabled these structures to be used extensively in commercial applications. The presence of an internal aqueous compartment and hydrophobic bilayer phase of liposomes provides these particles with tremendous capabilities as both hydrophilic and hydrophobic carriers for drug delivery,⁴⁶ and use in the cosmetic and food industry.^{47 48 49 50} These molecules self-assemble in aqueous media through hydration of the headgroup and strong association of the acyl tails through Van Der Waals forces and electrostatics to produce the bilayer structure (lamella). Lipid bilayers systems such as liposomes, micelles and lipid-rafts have been used as model systems for the fundamental study of lipid mixing,⁵¹ membrane fusion⁵² and biological exosome trafficking.⁵³ Although synthetic liposomes are simplified models of cellular membranes, they also occur naturally as exosomes, cell-derived particles found in biological fluids implicated in inter-cellular signaling, mRNA trafficking, waste excretion and coagulation.⁵⁴

Over the past 50 years, major technical advances have been made in synthetic liposomes to serve as potent applications for research and therapeutics. The development of better techniques for promote drug loading, homogeneous size, ligand targeting, triggered release and multiple drug delivery have enabled clinical trials for various cancer, fungal and antibiotic drugs previously thought impossible with traditional administration.⁵⁵ With liposomal particles, optimal methods of formation and molecular loading to achieve specific practical biological applications must be determined. There are several biological factors which guide liposome

selection including the clearance of liposomes by antibody recognition (vesicle opsonisation) of foreign particles and phagocytic scavenging by the reticuloendothelial system (RES),^{56 57} absorption and disruption of phospholipid membranes by serum proteins in plasma or cell culture media,⁵⁸ size (increased size results in decreased half-life caused by higher clearance rates by the liver and spleen),⁵⁹ and passive targeting of organs such as lungs using large multilamellar vesicles (MLVs) and solid tumors.⁶⁰ The utility of liposomes as drug delivery agents for pharmaceuticals has been well established, where physical liposomal characteristics enable the generation of new drug formulations and the re-purposing of previously discarded agents for use as cancer drugs. Drug delivery using liposome encapsulation of active pharmaceutical agents has resulted in the development of 15 liposomal based drugs including Abelcet®, Deposcy® and Lipo-Dox®, to treat a wide variety of indications including fungal infections, malignant lymphomatous meningitis, Kaposi's sarcoma, breast cancer and influenza. This is possible as a result of the dynamic nature of the lipid particle, which can be tailored using a variety of different lipid components to increase drug circulation times, hinder metabolic degradation and target tissues of interest.

Liposomes can be made to vary in size from 20 nm-100 nm as small unilamellar vesicles (SUVs), 100 nm-400 nm large unilamellar vesicles (LUVs) and giant unilamellar vesicles (>1 µm) through the use of different lipids and additives as well as different formation techniques. Liposomes can be synthesized with multiple discrete internal lamella using advanced fabrication techniques such as extrusion or microfluidics to produce MLVs containing concentric discrete vesicles or multivesicular vesicles (MVVs), which consist of multiple individual vesicles with a similar appearance to cellular organelles.⁶¹ To prepare lipid dispersion for liposome self-assembly, there are two general methods: mechanical and solvent dispersion. Mechanical

dispersion is the most common and robust method to obtain liposomes and includes sonication, extrusion and freeze-thaw techniques, while solvent dispersion includes solvent vaporization, ethanol injection and reverse phase evaporation.

Sonication is the most common mechanical technique due to its speed and the production of a general uniform size distribution of the liposome particles. It involves the use of cavitation in aqueous media to break up or induce budding of liposome structures from lipid aggregates in aqueous suspension resulting in SUVs from hydrated lipid suspensions. Sonication produces SUVs with a typical average size of 70 nm depending on the length of exposure, and can be performed using either tip or bath sonicators. Although sonication allows for fast and efficient production of liposomes, the main disadvantages of this method include low encapsulation efficiency, protein degradation, metallic contamination and the production of a mixture of SUVs and MLVs within the liposome suspension.

1.3.2 Cellular Mechanisms of Liposome Uptake and Lipid Incorporation

Endocytosis plays a significant role as an active mechanism for critical cellular metabolic processes such as nutrient uptake, antigen presentation, pathogen entry, receptor regulation, synaptic transmission and autocrine signalling. There are three major mechanisms which involve active cellular trafficking of material through the plasma membrane, including phagocytosis, pinocytosis and receptor-mediated endocytosis (Figure 1.8). The immune system of multicellular organisms typically use phagocytosis to remove cellular debris generated through apoptosis or engulfing foreign particles such as bacteria into internal compartments called phagosomes.⁶² These phagosomes fuse with lysosomes, containing acidic pH or hydrolytic enzymes, to destroy the phagosome contents for later absorption. Pinocytosis closely resembles phagocytosis, but involves the internalization of small molecules for hydrolysis in lysosomes,

commonly seen as an “eating or drinking” mechanism for the cell to obtain nutrients. A well-studied form of receptor-mediated endocytosis termed Clathrin-mediated endocytosis has been shown to be a ubiquitous internalization mechanism for cells, that involves Clathrin, a large cytosolic protein located on the proximal surface of the cellular membrane, which interacts with distal receptors such as the low-density lipoprotein (LDL) receptor and transferrin to remove LDL from the blood and ferric ions respectively, through internalization.^{63 64}

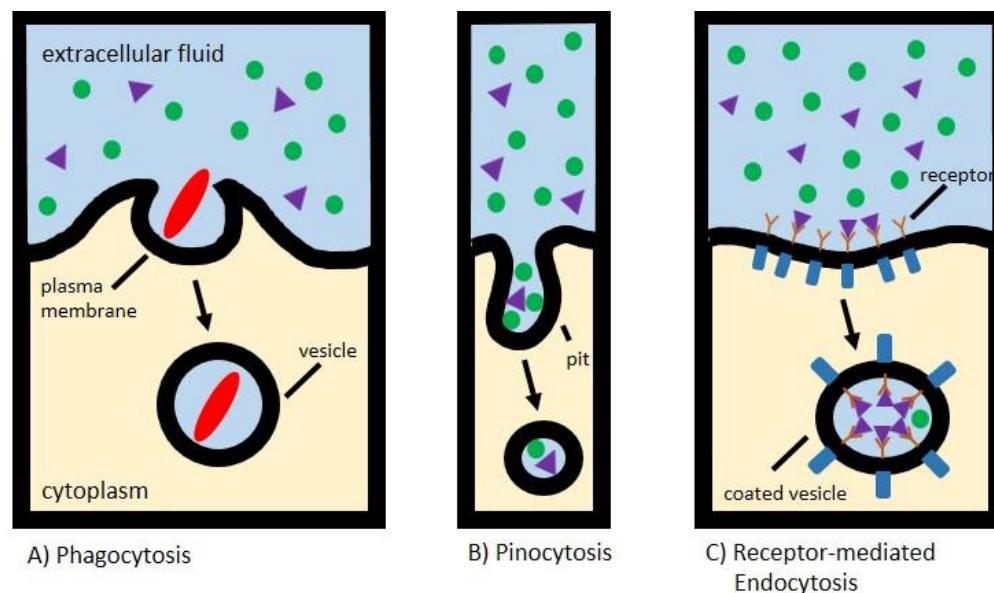


Figure 1.8: Depiction of three general active mechanisms of endocytosis in cells. (A) Phagocytosis allows for cells to deform their plasma membrane and engulf a solid particle, commonly used by immune cells to ingest pathogens, through recognition of pathogen associated molecular patterns (PAMPs). (B) Pinocytosis involves the formation of pits in the plasma membrane for non-selective uptake of nutrients and liquids. (C) Receptor-mediated endocytosis utilizes specific transmembrane receptors to bind ligands which trigger actin reorganization for invagination of the plasma membrane and internalization.

Clathrin proteins aggregate in patches on the inner membrane causing the formation of membrane buds, which pinch off creating cytosolic Clathrin coated vesicles, which can be trafficked within the cell. The plasma membrane of many cells types also contain Caveolae, small flask shaped pits consisting of the Vip21 cholesterol binding protein, which commonly

occur in smooth muscle, fibroblasts and adipocytes.⁶⁵ Liposome fusion also plays an important role in cellular entry for internal functions, such as lipid shuttling within the ER and signal transduction in neuronal cells.

Model lipid bilayer systems such as liposomes have been crucial for elucidating and mimicking the biophysical structure and fundamental behavior of biological membranes and membrane fusion. Membrane fusion occurs where two discrete bilayers merge lipid bilayers resulting in the mixing of both the lipid and internal aqueous environments. Lipid bilayers undergo three general stages to achieve fusion: (1) Membrane Contact (stalk formation), (2) Merging (hemifusion), and (3) Pore Formation (Figure 1.9).

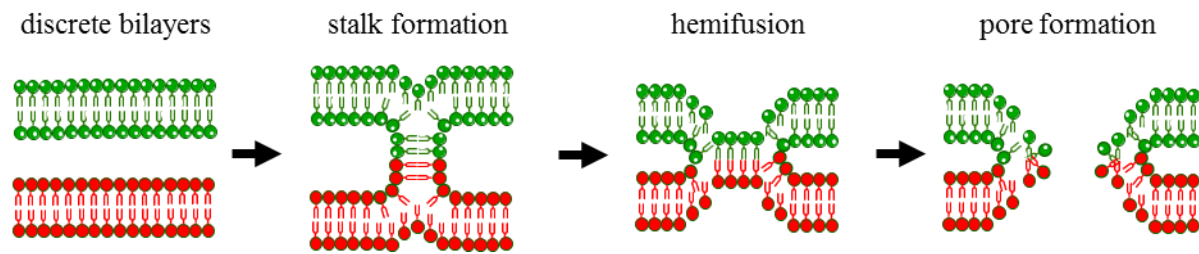


Figure 1.9: General depiction of two membranes undergoing membrane fusion. Initiated through close proximity, stalk structures form to bridge the proximal lipid layers. The membrane structures then become unstable resulting in hemifusion, where the distal layers interact, followed by pore formation and complete lipid mixing of the membrane lipids.

Initiation of membrane fusion occurs when two proximal membrane layers come into close contact, overcoming both head group electrostatic repulsion and the dehydration of the interstitial water boundary layer, for approach within a few angstroms. Once in contact the layers must undergo destabilization, either through active protein complexation, covalent adhesion or electrostatic charge driven mixing. These destabilized transition or intermediate membrane states are not fully understood but literature best describes the formation of stalk like structures (Figure 1.9), which rearrange into the hemifused structure as the distal boundary layers approach,

resulting in a pseudo-merging of the lipid layers. This hemifused structural intermediate then proceeds to form the pore structure, resulting in the merging and mixing of the two membrane layers. These fluid bilayer fusion mechanisms are also reflected in biological systems which use protein structures to deform or aid the thermodynamic process of membrane fusion to enable faster biological processing.

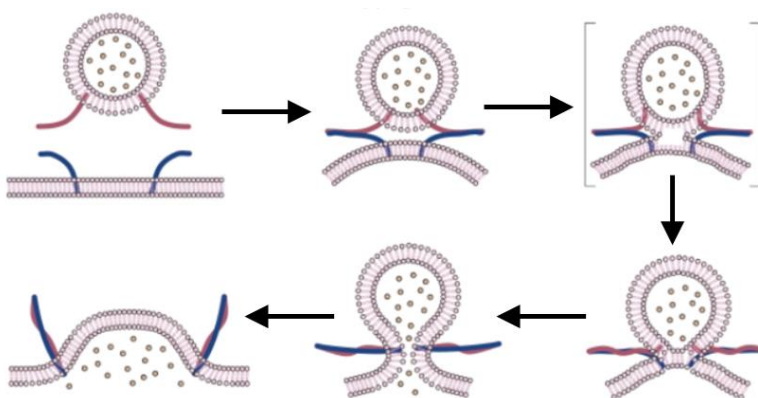


Figure 1.10: Current model of Soluble NSF Attachment Protein Receptor (SNARE)-mediated fusion. The distal membrane leaflets come into close proximity but the SNAREs are not yet interacting. SNARE complexes interact and begin zipping from the amino-terminal end, drawing the membranes closer together. The zippering continues, increasing the membrane curvature and lateral tension of the individual membranes, exposing the hydrophobic interior of the bilayer. Hemifusion spontaneously occurs as the membranes are close enough in proximity. The lateral tension causes membrane breakdown to form a fusion pore, where the pore expands causing a reduction in membrane curvature surface tension. (Taken from Hu et al, 2007).⁶⁶

The biological use of membrane fusion allows for the rapid movement of intracellular factors, which have been well studied in neuronal synaptic signalling of the presynaptic membrane.⁶⁷ Figure 1.10 demonstrates how vesicular surface markers interact with target membrane receptors for selective fusion of liposome-like delivery vesicles using N-ethylmaleimide sensitive fusion (NSF) receptors, to mediate vesicle fusion of neurotransmitter carriers to target neuronal membranes. Synthetic liposomal carriers for cellular delivery exploit natural mechanisms either using specific receptor recognition events for molecular localization,

or non-specific interactions such as electrostatics or nanometer sized liposomes (high membrane curvature) to deliver cargo for passage through the plasma membrane.^{68 69}

Cationic liposome based nucleic acid delivery has been commonly used to introduce both endogenous and exogenous genes into cells for discovery of protein and cellular behavior pathways. Initially biophysical and biological methods such as electroporation and viral transfection respectively, were used to deliver macromolecules into cells.^{70 71} Recently, chemical methods have been developed to deliver oligonucleotides or other electrostatically charged molecules into the cell with charged liposome particles. The introduction of chemical based transfection reagents such as Lipofectamine® and Viafect® for cationic lipid-based delivery of anionic nucleic acids, allowing for cheaper and easier methods for elucidation of new biological processes and pathways using knock-in, knock out and gene silencing strategies to the benefit of life sciences and the clinical understanding of disease mechanisms. These methods generally utilize cationic liposome or lipid formulations to encapsulate anionic nucleic acids resulting in beneficial properties such as protection from degradation and delivery of encapsulated material into the cytosol.

1.3.3 Bio-orthogonal Lipid Incorporation into Cellular Membranes via Liposome Fusion

Developing novel liposome based cell surface engineering strategies over previous methodologies requires a general set of criteria for improvement and adoption into cellular based research: (1) The method must deliver and label the outer plasma leaflets of any cell-type, without permanently altering the genomic content of the cell, (2) embedded engineering must selectively react under physiological or cell culture conditions, (3) applied ligands must be easy to synthesize, while displaying fast kinetics and stability in the plasma membrane with a

conjugation partner, (4) the system must be robust and programmable to enable cell labelling and cell surface reactions to take place with high cell economy and stoichiometry, (5) the method must be modular and compatible with existing techniques such as microfluidics, inorganic and organic surfaces as a complimentary technology.

The Yousaf group has focused on developing methodology using bio-orthogonal chemistries upon inorganic and organic surfaces to probe, influence and model cellular behavior *in vitro* (Figure 1.11). Bio-orthogonal chemistry functional groups have recently been

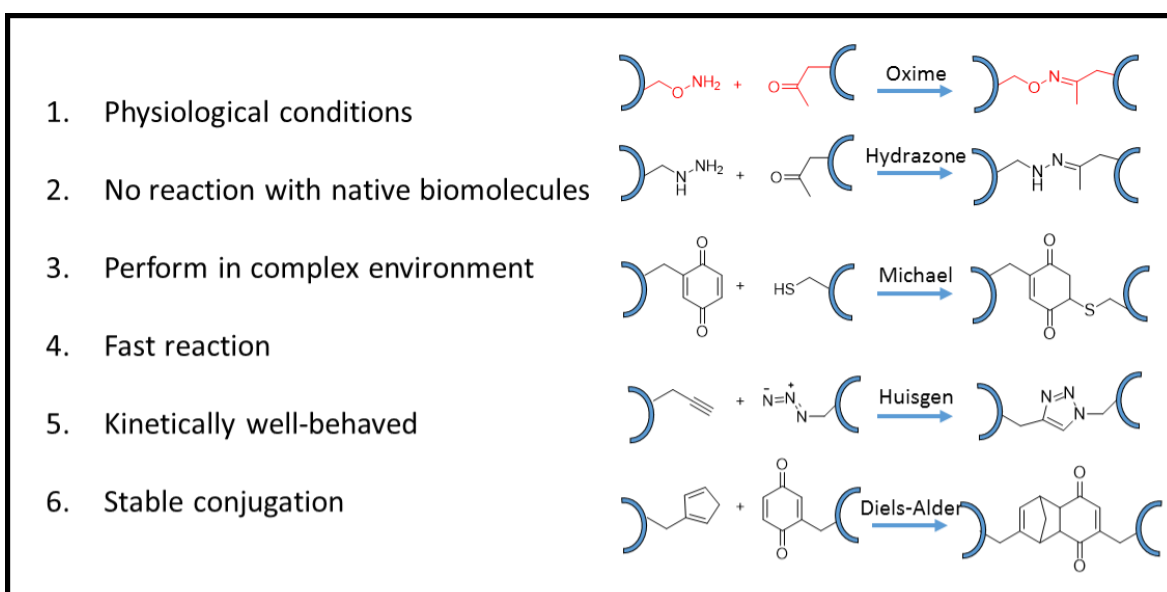


Figure 1.11: Depiction of bio-orthogonal chemistry pairs used for chemical biology applications. These pairs can be incorporated into biomolecules and cellular structures without interfering with native biochemistry and can undergo reactions in complex cellular environments.

popularized for use in chemical biology applications, such as genetic engineering techniques,^{72 73}

⁷⁴ polymers,^{75 76 77} metabolic products,^{78 79} conjugating proteins,⁸⁰ antibodies,⁸¹ and small

molecules on bioactive surfaces to name a few. Most notably, the recent development of Cu²⁺

free reaction of strained cyclooctynes with azides (Huisgen Reaction) revived interest in using

chemistry to probe and affect biology.⁸² The use of strained cyclic alkynes enabled the removal

of cytotoxic copper from these reactions to produce a true ‘click’ two body reaction with utility in cellular media and in the presence of live cells.

Oxime chemistry is a bio-orthogonal reaction where N-hydroxylamine functional groups quickly and selectively react with ketone moieties under aqueous physiological conditions.⁸³ Oxime reaction partners are beneficial to chemical biology applications, as opposed to other bio-orthogonal methodologies, due to ease of synthesis and fewer synthetic steps. Initial work of oxime chemistry focused on using modified inorganic surfaces and liposomal cell surface engineering to create dynamic surfaces and inorganic surface functionalization for biological studies, rather than using genetic, polymer or metabolic based techniques.

The Yousaf group pioneered the development of model gold surfaces patterned with molecular gradients of hydroxylamine terminated self-assembled monolayers (SAMs) (Figure 1.12). These hydroxylamine gradients were then modified with Arginylglycylaspartic acid (RGD)-ketone molecules to create gradients of RGD peptides to study cell adhesion, polarity and migration.⁸⁴ Diffusion and bio-orthogonal chemistry can be used to introduce a new functionality to inorganic surfaces for biological studies without interfering with biological processes, while modifying a surface simply and effectively. The method can be used widely for research in stem cell differentiation,⁸⁵ high-throughput adhesive studies,⁸⁶ switchable electroactive surfaces for protein structure,⁸⁷ as well as cellular division on these bio-orthogonal gradient surfaces.⁸⁸

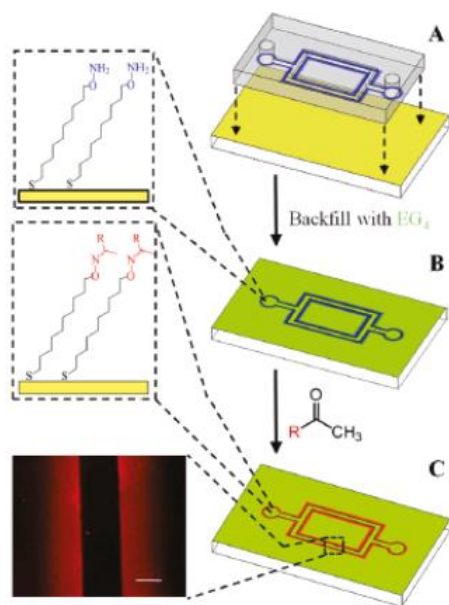


Figure 1.12: Microfluidic gradient of O-hydroxylamine patterning on gold substrates for ketone terminated addition of RGD-ketones for cellular migration studies. (Taken from Yousaf et al.)⁸⁴

To enhance and provide greater control of the membrane, rather than modify adhesive substrates, the cell membrane can be directly modified to obtain a higher degree of cellular manipulation. Since previous work studied hydroxylamine SAMs on gold surfaces, indium tin oxide (ITO) surfaces and liposomes deposited onto glass surfaces which modelled the cellular surfaces and membranes for cell adhesion assays. Applying lipid bio-orthogonal chemistry directly into the cellular membrane became the next step in the evolution of this innovative surface modifying technology. Initial experiments applying bio-orthogonal lipids into the cellular membrane focused on the delivery of lipids for Fluorescence Resonance Energy Transfer (FRET) and fluorescent molecule targeting for imaging.⁸⁹ The liposomal strategy has been successful in delivering liposome oxime conjugated fluorophores, as well as ketone lipids to cell membranes and conjugated in live cell culture with hydroxylamine fluorophores.

The overarching objective of this thesis work is to develop a robust and enabling methodology based upon our CSE technology to perform microfluidic cellular manipulation, cell membrane labelling and cargo delivery applications. Over the course of this thesis I developed a CSE technology that enables new biological experiments through the ability to reliably and rapidly manipulate the plasma membrane, which led to separate downstream applications. To develop our CSE strategy as an enabling platform for biological research, we demonstrated the liposome technique as a microfluidic reagent to label cells rapidly and robustly, which is important for flow cytometry, mass spectrometry, cell sorting and sensing applications. To enable new experiments, we developed methods to label and build tissue structures with multiple different cell types with spatial orientation that have applications in tissue engineering, transplantation, drug assays and therapeutics. We demonstrated CSE strategy for cargo delivery using transfection as a model system which has applications in gene therapy, small molecule, cell surface protein delivery and mixed multi-modal delivery techniques. Finally, we developed a novel amine conjugation reaction with applications in protein labelling, antibody drug conjugates (ADCs) and future CSE abilities through conjugation with liposomes. The elucidation and development of our CSE technique over these fields of application will validate the unique and enabling properties across multiple research areas and applications.

1.4 References

- (1) Li, S. *Int. J. Biol. Sci.* **2005**, *1* (4), 152.
- (2) Cappuccio, A.; Zollinger, R.; Schenk, M.; Walczak, A.; Servant, N.; Barillot, E.; Hupé, P.; Modlin, R. L.; Soumelis, V. **2015**, *6*, 6847.
- (3) Fulda, S.; Gorman, A. M.; Hori, O.; Samali, A. *Int. J. Cell Biol.* **2010**, *2010*.
- (4) Shi, J.; Kundrat, L.; Pishesha, N.; Bilate, A.; Theile, C.; Maruyama, T.; Dougan, S. K.; Ploegh, H. L.; Lodish, H. F. *Proc. Natl. Acad. Sci. U. S. A.* **2014**, *111* (28), 10131–10136.
- (5) Liechty, W. B.; Kryscio, D. R.; Slaughter, B. V.; Peppas, N. A. *Annu. Rev. Chem. Biomol. Eng.* **2010**, *1* (1), 149–173.
- (6) Park, K. M.; Gerecht, S. **2014**, *5*, 4075.
- (7) Laughlin, S. T.; Bertozzi, C. R. *Nat. Protoc.* **2007**, *2* (11), 2930–2944.
- (8) Gartner, Z. J.; Bertozzi, C. R. *Proc. Natl. Acad. Sci. U. S. A.* **2009**, *106* (12), 4606–4610.
- (9) Fernandez-Suarez, M.; Baruah, H.; Martinez-Hernandez, L.; Xie, K. T.; Baskin, J. M.; Bertozzi, C. R.; Ting, A. Y. *Nat Biotech* **2007**, *25* (12), 1483–1487.
- (10) Smith, D. J.; Liu, S.; Ji, S.; Li, B.; McLaughlin, J.; Cheng, D.; Witte, O. N.; Yang, L. *Proc. Natl. Acad. Sci.* **2015**, *112* (5), 1523–1528.
- (11) Chen, I.; Howarth, M.; Lin, W.; Ting, A. Y. *Nat. Methods* **2005**, *2* (2), 99–104.
- (12) Leslie, G. J.; Wang, J.; Richardson, M. W.; Haggarty, B. S.; Hua, K. L.; Duong, J.; Secreto, A. J.; Jordon, A. P. O.; Romano, J.; Kumar, K. E.; DeClercq, J. J.; Gregory, P. D.; June, C. H.; Root, M. J.; Riley, J. L.; Holmes, M. C.; Hoxie, J. A. *PLOS Pathog.* **2016**, *12* (11), e1005983.
- (13) Tebas, P.; Stein, D.; Tang, W. W.; Frank, I.; Wang, S. Q.; Lee, G.; Spratt, S. K.; Suroskey, R. T.; Giedlin, M. A.; Nichol, G.; Holmes, M. C.; Gregory, P. D.; Ando, D. G.; Kalos, M.; Collman, R. G.; Binder-Scholl, G.; Plesa, G.; Hwang, W.-T.; Levine, B. L.; June, C. H. *N. Engl. J. Med.* **2014**, *370* (10), 901–910.
- (14) Silhavy, T. J.; Benson, S. A.; Emr, S. D. *Microbiol. Rev.* **1983**, *47* (3), 313–344.
- (15) Li, L.; Haynes, M. P.; Bender, J. R. *Proc. Natl. Acad. Sci.* **2003**, *100* (8), 4807–4812.
- (16) Linder, M. E.; Deschenes, R. J. *Nat Rev Mol Cell Biol* **2007**, *8* (1), 74–84.
- (17) Crosby, A. J.; Lee, J. *Polym. Rev.* **2007**, *47* (2), 217–229.
- (18) Tzianabos, A. O. **2000**, *13* (4), 523–533.
- (19) Dhandayuthapani, B.; Yoshida, Y.; Maekawa, T.; Kumar, D. S. **2011**, *20* (ii).
- (20) Place, E. S.; George, J. H.; Williams, C. K.; Stevens, M. M. *Chem. Soc. Rev.* **2009**, *38* (4), 1139–1151.
- (21) Petersen, R. C. **2013**, *2013*.
- (22) Fonseca, A. C.; Serra, A. C.; Coelho, J. F. J. *EPMA J.* **2015**, *6*, 22.
- (23) De Vos, P.; Lazarjani, H. A.; Poncelet, D.; Faas, M. M. *Adv. Drug Deliv. Rev.* **2014**, *67–68*, 15–

- (24) Bushuyev, O. S.; Brown, P.; Maiti, A.; Gee, R. H.; Peterson, G. R.; Weeks, B. L.; Hope-Weeks, L. *J. J. Am. Chem. Soc.* **2012**, *134* (3), 1422–1425.
- (25) Zhang, Y.; Chen, X.; Lan, J.; You, J.; Chen, L. *Chem. Biol. Drug Des.* **2009**, *74* (3), 282–288.
- (26) Balint, R.; Cassidy, N. J.; Cartmell, S. H. *Acta Biomater.* **2014**, *10* (6), 2341–2353.
- (27) Isaksson, J.; Kjäll, P.; Nilsson, D.; Robinson, N. D.; Berggren, M.; Richter-Dahlfors, A. *Nat. Mater.* **2007**, *6* (9), 673–679.
- (28) Kato, D.; Takeuchi, M.; Sakurai, T.; Furukawa, S.; Mizokami, H.; Sakata, M.; Hirayama, C.; Kunitake, M. *Biomaterials* **2003**, *24* (23), 4253–4264.
- (29) Niu, J.; Lunn, D. J.; Pusuluri, A.; Yoo, J. I.; O'Malley, M. A.; Mitragotri, S.; Soh, H. T.; Hawker, C. J. *Nat Chem* **2017**, *9* (6), 537–545.
- (30) Villa-Diaz, L. G.; Nandivada, H.; Ding, J.; Nogueira-de-Souza, N. C.; Krebsbach, P. H.; O'Shea, K. S.; Lahann, J.; Smith, G. D. *Nat Biotech* **2010**, *28* (6), 581–583.
- (31) Bruni, A.; Gala-Lopez, B.; Pepper, A. R.; Abualhassan, N. S.; Shapiro, A. M. J. *Diabetes, Metab. Syndr. Obes. Targets Ther.* **2014**, *7*, 211–223.
- (32) Vegas, A. J.; Veiseh, O.; Gürtler, M.; Millman, J. R.; Pagliuca, F. W.; Bader, A. R.; Doloff, J. C.; Li, J.; Chen, M.; Olejnik, K.; Tam, H. H.; Jhunjhunwala, S.; Langan, E.; Aresta-Dasilva, S.; Gandham, S.; McGarrigle, J. J.; Bochenek, M. A.; Hollister-Lock, J.; Oberholzer, J.; Greiner, D. L.; Weir, G. C.; Melton, D. A.; Langer, R.; Anderson, D. G. *Nat. Med.* **2016**, *22* (3), 306–311.
- (33) Ngo, J. T.; Adams, S. R.; Deerinck, T. J.; Boassa, D.; Rodriguez-Rivera, F.; Palida, S. F.; Bertozzi, C. R.; Ellisman, M. H.; Tsien, R. Y. *Nat Chem Biol* **2016**, *12* (6), 459–465.
- (34) Chang, P. V.; Chen, X.; Smyrniotis, C.; Xenakis, A.; Hu, T.; Bertozzi, C. R.; Wu, P. *Angew. Chemie* **2009**, *121* (22), 4090–4093.
- (35) Saxon, E.; Bertozzi, C. R. *Science* (80-.). **2000**, *287* (5460), 2007 LP-2010.
- (36) Merkel, M.; Arndt, S.; Ploschik, D.; Cserép, G. B.; Wenge, U.; Kele, P.; Wagenknecht, H.-A. *J. Org. Chem.* **2016**, *81* (17), 7527–7538.
- (37) Roloff, A.; Seitz, O. *Chem. Sci.* **2013**, *4* (1), 432–436.
- (38) Dadová, J.; Vrábel, M.; Adámik, M.; Brázdová, M.; Pohl, R.; Fojta, M.; Hocek, M. *Chem. - A Eur. J.* **2015**, *21* (45), 16091–16102.
- (39) Hu, F.; Lamprecht, M. R.; Wei, L.; Morrison, B.; Min, W. **2016**, *6*, 39660.
- (40) Laughlin, S. T.; Baskin, J. M.; Amacher, S. L.; Bertozzi, C. R. *Science* (80-.). **2008**, *320* (5876), 664–667.
- (41) Kiick, K. L.; Saxon, E.; Tirrell, D. A.; Bertozzi, C. R. *Proc. Natl. Acad. Sci. U. S. A.* **2002**, *99* (1), 19–24.
- (42) Beatty, K. E.; Szychowski, J.; Fisk, J. D.; Tirrell, D. A. *Chembiochem* **2011**, *12* (14), 2137–2139.
- (43) Todhunter, M. E.; Jee, N. Y.; Hughes, A. J.; Coyle, M. C.; Cerchiari, A.; Farlow, J.; Garbe, J. C.; LaBarge, M. A.; Desai, T. A.; Gartner, Z. J. *Nat Meth* **2015**, *12* (10), 975–981.

- (44) Bangham, A. D.; Standish, M. M.; Watkins, J. C. *J. Mol. Biol.* **1965**, *13* (1), 238–IN27.
- (45) Bangham, A. D.; Standish, M. M.; Watkins, J. C.; Weissmann, G. Bolis, L., Capraro, V., Porter, K. R., Robertson, J. D., Eds.; Springer Vienna: Vienna, 1967; pp 183–187.
- (46) Pattni, B. S.; Chupin, V. V.; Torchilin, V. P. *Chem. Rev.* **2015**, *115* (19), 10938–10966.
- (47) Perrie, Y.; Kastner, E.; Khadke, S.; Roces, C. B.; Stone, P. Fox, C. B., Ed.; Springer New York: New York, NY, 2017; pp 127–144.
- (48) Raj, S.; Jose, S.; Sumod, U. S.; Sabitha, M. *J. Pharm. Bioallied Sci.* **2012**, *4* (3), 186–193.
- (49) Mohammadi, R.; Mahmoudzade, M.; Atefi, M.; Khosravi-Darani, K.; Mozafari, M. R. *Int. J. Dairy Technol.* **2015**, *68* (1), 11–23.
- (50) Taylor, T. M.; Weiss, J.; Davidson, P. M.; Bruce, B. D. *Crit. Rev. Food Sci. Nutr.* **2005**, *45* (7–8), 587–605.
- (51) Duzgunes, N.; Allen, T. M.; Fedor, J.; Papahadjopoulos, D. *Biochemistry* **1987**, *26* (25), 8435–8442.
- (52) Liu, J.; Jiang, X.; Ashley, C.; Brinker, C. J. *J. Am. Chem. Soc.* **2009**, *131* (22), 7567–7569.
- (53) Tian, T.; Zhu, Y.-L.; Hu, F.-H.; Wang, Y.-Y.; Huang, N.-P.; Xiao, Z.-D. *J. Cell. Physiol.* **2013**, *228* (7), 1487–1495.
- (54) Thery, C.; Zitvogel, L.; Amigorena, S. *Nat Rev Immunol* **2002**, *2* (8), 569–579.
- (55) Allen, T. M.; Cullis, P. R. *Adv. Drug Deliv. Rev.* **2013**, *65* (1), 36–48.
- (56) Gregoriadis, G.; Gregoriadis, G.; Piper, J. R.; Papahadjopoulos, D.; Ghyczy, M.; Etschenberg, J.; Holstein, A. F. *Trends Biotechnol.* **1985**, *3* (9), 235–241.
- (57) Moghimi, S. M.; Hunter, A. C. *Pharm. Res.* **2001**, *18* (1), 1–8.
- (58) Jones, M. N.; Nicholas, A. R. *Biochim. Biophys. Acta - Biomembr.* **1991**, *1065* (2), 145–152.
- (59) Ishida, T.; Harashima, H.; Kiwada, H. *Biosci. Rep.* **2002**, *22* (2), 197–224.
- (60) Gabizon, A.; Papahadjopoulos, D. *Proc. Natl. Acad. Sci. U. S. A.* **1988**, *85* (18), 6949–6953.
- (61) Torchilin, V. P. *Adv. Drug Deliv. Rev.* **2012**, *64*, 302–315.
- (62) Bilyy, R. O.; Shkandina, T.; Tomin, A.; Muñoz, L. E.; Franz, S.; Antonyuk, V.; Kit, Y. Y.; Zirngibl, M.; Fürnrohr, B. G.; Janko, C.; Lauber, K.; Schiller, M.; Schett, G.; Stoika, R. S.; Herrmann, M. *J. Biol. Chem.* **2012**, *287* (1), 496–503.
- (63) Marsh, M.; McMahon, H. T. *Science* (80-.). **1999**, *285* (5425), 215 LP-220.
- (64) Anderson, R. G. W.; Brown, M. S.; Goldstein, J. L. *Cell* **2017**, *10* (3), 351–364.
- (65) Parton, R. G.; Simons, K. *Nat Rev Mol Cell Biol* **2007**, *8* (3), 185–194.
- (66) Hu, C.; Hardee, D.; Minnear, F. *Exp. Cell Res.* **2007**, *313* (15), 3198–3209.
- (67) Chen, Y. A.; Scheller, R. H. *Nat Rev Mol Cell Biol* **2001**, *2* (2), 98–106.
- (68) Robinson, M. S. *Trends Cell Biol.* **2017**, *7* (3), 99–102.
- (69) Helwa, Y.; Dave, N.; Liu, J. *Soft Matter* **2013**, *9* (26), 6151–6158.

- (70) Neumann, E.; Schaefer-Ridder, M.; Wang, Y.; Hofschneider, P. H. *EMBO J.* **1982**, *1* (7), 841–845.
- (71) Gardlík, R.; Pálffy, R.; Hodosy, J.; Lukács, J.; Turna, J.; Celec, P. *Med. Sci. Monit.* **2005**, *11* (4), RA110-A121.
- (72) Lang, K.; Davis, L.; Torres-Kolbus, J.; Chou, C.; Deiters, A.; Chin, J. W. *Nat Chem* **2012**, *4* (4), 298–304.
- (73) Elliott, T. S.; Bianco, A.; Chin, J. W. *Curr. Opin. Chem. Biol.* **2014**, *21*, 154–160.
- (74) Nguyen, D. P.; Elliott, T.; Holt, M.; Muir, T. W.; Chin, J. W. *J. Am. Chem. Soc.* **2011**, *133* (30), 11418–11421.
- (75) Wu, C.; Jin, Y.; Schneider, T.; Burnham, D. R.; Smith, P. B.; Chiu, D. T. *Angew. Chemie Int. Ed.* **2010**, *49* (49), 9436–9440.
- (76) Devaraj, N. K.; Thurber, G. M.; Keliher, E. J.; Marinelli, B.; Weissleder, R. *Proc. Natl. Acad. Sci.* **2012**, *109* (13), 4762–4767.
- (77) Gattás-Asfura, K. M.; Stabler, C. L. *ACS Appl. Mater. Interfaces* **2013**, *5* (20), 9964–9974.
- (78) Homann, A.; Qamar, R.; Serim, S.; Dersch, P.; Seibel, J. *Beilstein J. Org. Chem.* **2010**, *6*, 24.
- (79) Chang, P. V.; Chen, X.; Smyrniotis, C.; Xenakis, A.; Hu, T.; Bertozzi, C. R.; Wu, P. *Angew. Chemie Int. Ed.* **2009**, *48* (22), 4030–4033.
- (80) Kim, C. H.; Axup, J. Y.; Schultz, P. G. *Curr. Opin. Chem. Biol.* **2013**, *17* (3), 412–419.
- (81) Colombo, M.; Sommaruga, S.; Mazzucchelli, S.; Polito, L.; Verderio, P.; Galeffi, P.; Corsi, F.; Tortora, P.; Prosperi, D. *Angew. Chemie Int. Ed.* **2012**, *51* (2), 496–499.
- (82) Agard, N. J.; Prescher, J. A.; Bertozzi, C. R. *J. Am. Chem. Soc.* **2004**, *126* (46), 15046–15047.
- (83) Agten, S. M.; Dawson, P. E.; Hackeng, T. M. *J. Pept. Sci.* **2016**, *22* (5), 271–279.
- (84) Lamb, B. M.; Park, S.; Yousaf, M. N. *Langmuir* **2010**, *26* (15), 12817–12823.
- (85) Luo, W.; Yousaf, M. N. *J. Colloid Interface Sci.* **2011**, *360* (2), 325–330.
- (86) Pulsipher, A.; Yousaf, M. N. *Chem. Commun.* **2011**, *47* (1), 523–525.
- (87) Lamb, B. M.; Yousaf, M. N. *J. Am. Chem. Soc.* **2011**, *133* (23), 8870–8873.
- (88) Lamb, B. M.; Luo, W.; Nagdas, S.; Yousaf, M. N. *ACS Appl. Mater. Interfaces* **2014**, *6* (14), 11523–11528.
- (89) Dutta, D.; Pulsipher, A.; Luo, W.; Mak, H.; Yousaf, M. N. *Bioconjug. Chem.* **2011**, *22* (12), 2423–2433.

Chapter 2

Cell Surface Engineering in Flow Using Bio-orthogonal Liposomes

Contributions

M.N.Y designed the study. P.J.O., D.R., and S.E. performed the experiments. M.N.Y., P.J.O., and S.E. analyzed the data. P.J.O. and M.N.Y. wrote the manuscript.

2.1 Introduction

Lack of efficient, cost-effective and general techniques to manipulate cells and the plasma membrane is a major challenge to the complex study of human health, where 3D cellular interactions in tissues, cell membranes, tumour growth, paracrine and autocrine signalling and cell migration within tissues are critical but difficult to explore. As a result, tremendous progress has been directed towards manipulating cellular membranes using molecular biology,¹ synthetic metabolic incorporation via biosynthesis,^{2 3 4} natural or synthetic polymer coatings,^{5 6} and polymeric constructs.^{7 8} The Yousaf group has developed a complimentary general CSE methodology to introduce bio-orthogonal ‘click’ lipids to eukaryotic,⁹ and bacterial¹⁰ phospholipid bilayers via liposome fusion for membrane probes, cell migration studies¹¹ and tissue engineering applications through cell-cell ligation and rapid complex spheroid assembly through microfluidic control.¹²

The combination of bio-orthogonal chemistry and liposome fusion for CSE provides numerous benefits over other methodologies for the manipulation of cellular membranes and cellular behavior: (1) bio-orthogonal CSE provides a general methodology to transiently alter the plasma membrane of different cell types, without manipulating genomic content, (2) bio-orthogonal ligands, particularly ketone and hydroxylamine functional groups, can be relatively easy to synthesize as amphiphilic lipids or molecular probes, (3) bio-orthogonal chemical groups can react selectively in the presence of live cell culture conditions, without interfering with native biochemistry, (4) bio-orthogonal reactions undergo fast and stable conjugation under cell culture conditions, (5) liposome fusion and mixing of liposomes with cellular membranes is fast and well-understood through previously published literature, and lastly (6) the method can be

modular and compatible with other existing techniques such as microfluidics as a complimentary or enabling technology.

To rewire and explore the capabilities of this integrated bio-orthogonal liposome approach to cellular manipulation using cell surface engineering, we focused on using microfluidics to study the efficiency, utility and speed of our method to undergo membrane fusion, cell functionalization and subsequent applications. Figure 2.1 describes the CSE microfluidic methodology for the rapid delivery of complimentary bio-orthogonal ligands and moieties directly to the cell surface using membrane fusion to form engineered cell lines. By integrating microfluidics with our CSE delivery technique we can probe the utility of membrane functionalization as well as quantify the amount of CSE necessary for various applications. Incorporating internal aqueous cargo in addition to membrane incorporated bio-orthogonal functionality, we demonstrate this dual delivery methodology as an example of the multiplexing ability via liposome technology. Using a tandem payload delivery, multiplexed experiments enable the incorporation of nucleic acids, bio-orthogonal CSE and membrane probes for tissue assembly, transfection of complex tissues and molecular probe delivery.

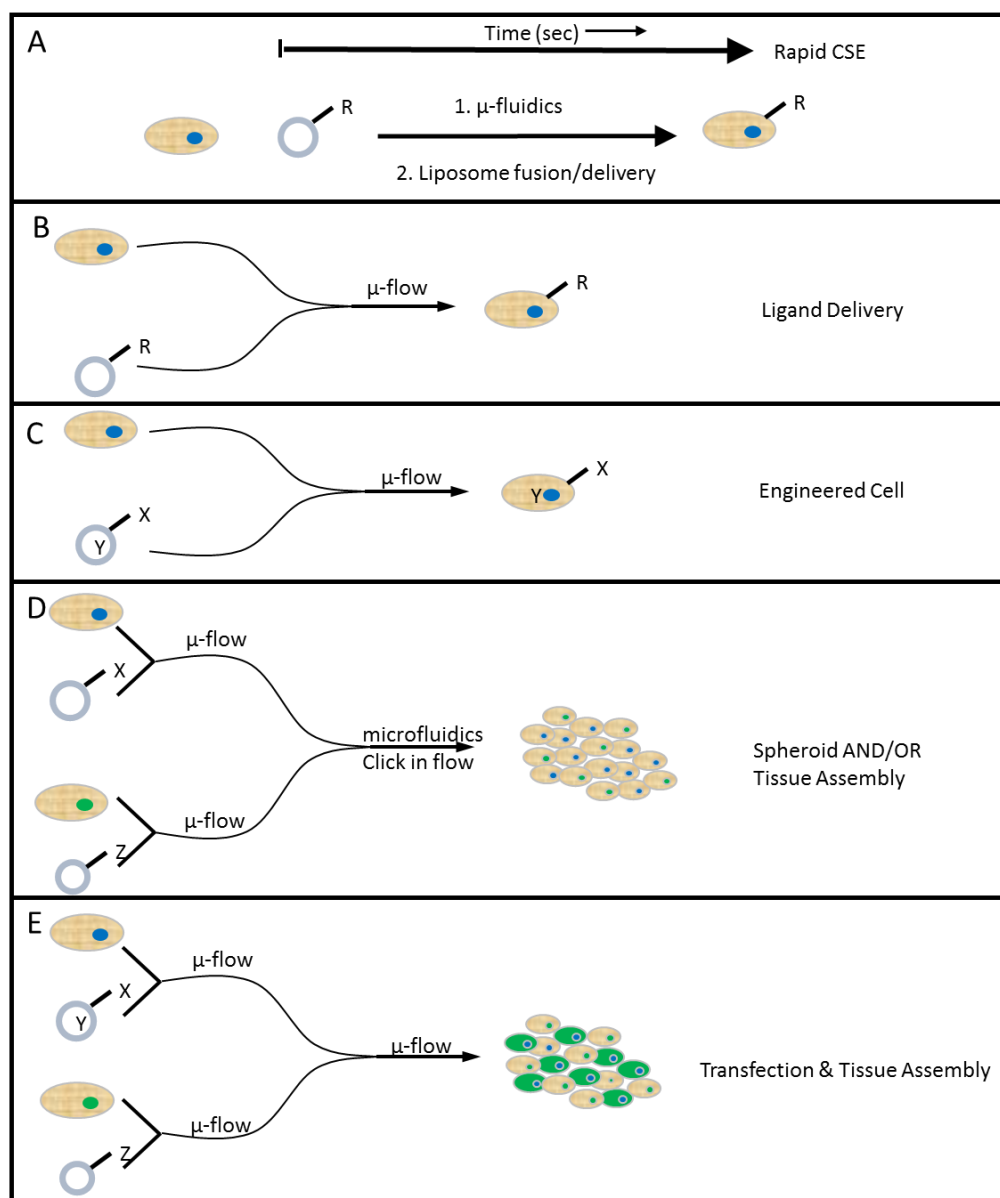


Figure 2.1: Schematic depicting the utility of bio-orthogonal CSE strategies for general microfluidic manipulation of cellular suspensions. (A) The combination of liposomes and cellular suspensions in microfluidics can be produced simply and rapidly to engineer cell membranes (R). (B) Combining lipid delivery of any small molecule (R) with liposome delivery strategies enables membrane fusion and mixing of the liposome leaflets into the plasma membrane for probe incorporation. (C) Bio-orthogonal chemistry embedded in the liposome membrane (X) does not interfere with hydrophilic cargo encapsulation (Y), allowing increased scope by enabling multiplexed reagents for cellular manipulation. (D) Highly multiplexed microfluidic devices in combination with bio-orthogonal CSE (X) and (Z) can be used to form complex spheroid assemblies and tissues. (E) Bio-orthogonal CSE can also be used for dual purpose biological applications such as simultaneous transfection (Y) and tissue assembly applications (X) and (Z) using microfluidics.

The combination of microfluidics, liposomes and bio-orthogonal chemistry can be a powerful enabler of new methodologies, while also incorporating a simple microfluidic delivery system of synthetic bio-orthogonal pairs to cellular membranes via liposome fusion to impart rapid and useful functionalities. Figure 2.2 depicts the composition of CSE liposomes and the base microfluidic system for treating cells for the formation of multiple cell-type tissues, dual assembly-nucleic acid transfected tissues and molecular probe delivery all within a single device. Liposomes engineered with bio-orthogonal lipids can be easily combined with other technologies such as nucleic acid transfection and small ligand delivery acting as probes for tissue formation and complex transfection of tissue constructs. The use of liposomes to deliver bio-orthogonal ligands was demonstrated to be mild, fast and efficient producing tissues and spheroids rapidly without purification in microfluidic flow. Using this methodology, we demonstrate the production of complex three cell-type spheroids and tissues, hybrid transfected tissue constructs in microfluidics and the delivery of oxime coupled biotin to mammalian cell lines.

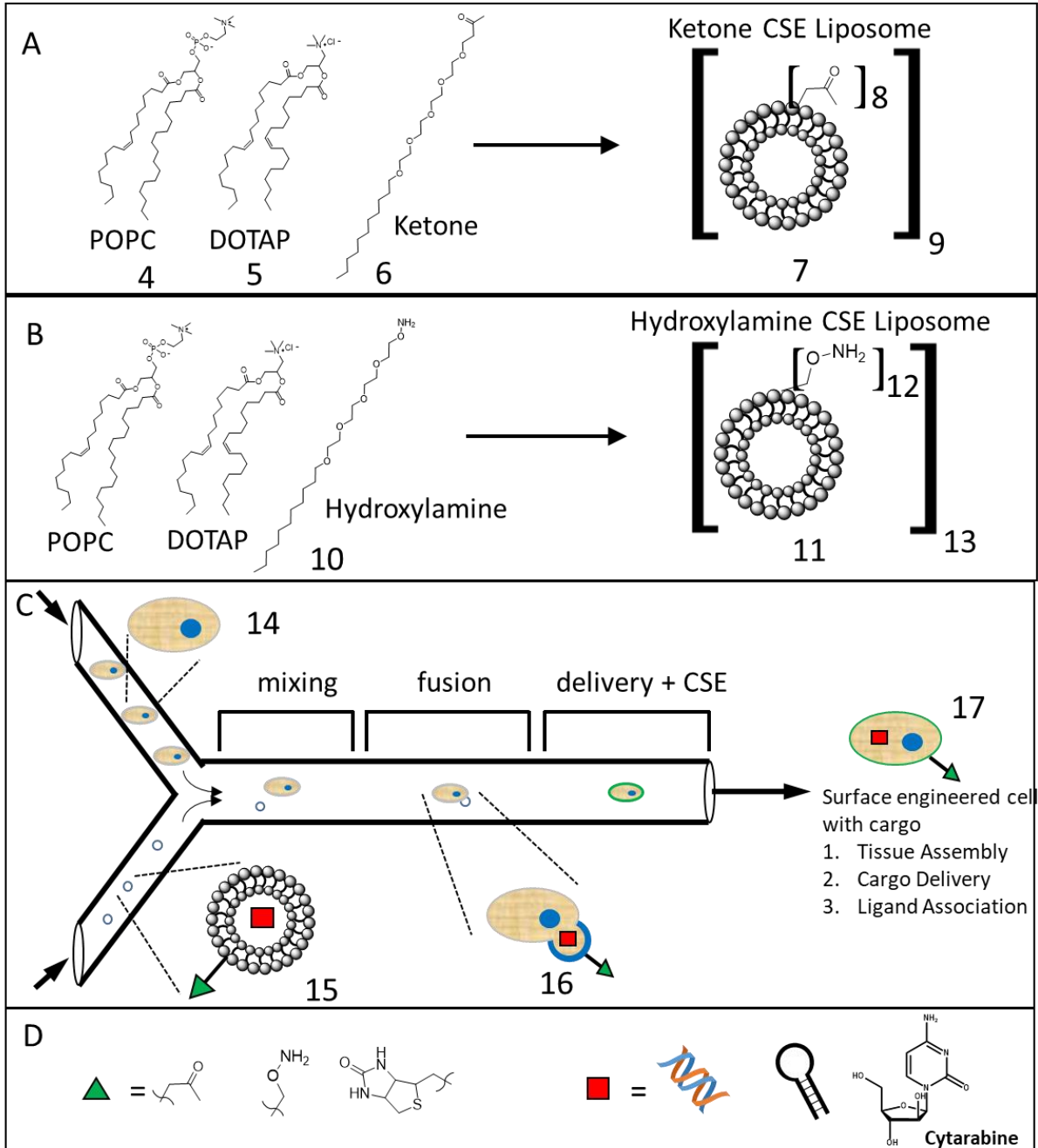


Figure 2.2: Depiction of the formulation and delivery of bio-orthogonal lipid engineered liposomes to achieve engineered cells and tissues in microfluidic flow. (A) Bio-orthogonal liposomes used for CSE delivery and spheroid or tissue formation are composed of POPC (4), DOTAP (5) and synthetic ketone lipids (6) to form a ketone CSE liposome (7) in varying ratios of lipids (8) and total liposome concentration (9) to determine cellular adhesion efficiency. (B) Complimentary hydroxylamine CSE liposomes are composed of POPC (4), DOTAP (5) and synthetic hydroxylamine lipid (10) to form hydroxylamine liposomes (11) in varying ratios of lipids (12) and total liposome concentration (13) for cellular fusion to suspension cells in microfluidic devices. (C) General microfluidic scheme depicting setup of a Y-channel microfluidic device used to engineer suspended native cells (14) through simultaneous injection with CSE liposomes (15), in combination with other aqueous soluble molecular agents (RED). Under flow conditions, the liposome and cell suspension mix rapidly and undergo rapid membrane fusion (16) to achieve CSE cells (17), which can be probed using complimentary hydroxylamine CSE HNDP RFP cells or fluorescent imaging with hydroxylamine-Biotin/Streptavidin(FITC) binding. (D) Small molecule membrane embedded ligands (GREEN) and cargo (RED) used to potentially enhance liposomal delivery systems.

Cell populations were engineered using bio-orthogonal liposomal formulations containing readily available lipids 1-palmitoyl-2-oleoyl-*sn*-glycero-3-phosphocholine (POPC) (4) and 1,2-dioleoyl-3-trimethylammonium-propane (DOTAP) (5) and then combined with synthetic bio-orthogonal ketone (6) and hydroxylamine (10) lipids to form separate populations of ketone (7) and hydroxylamine (11) forming the liposomes shown in Figure 2.2A, B. Figure 2.2C describes the microfluidic treatment of cells with bio-orthogonal liposomes (15), which can be easily varied to determine optimal CSE application to cell populations (14) for both tissue formation and ligand delivery. Ratios of ketone and hydroxylamine (8) and (12) lipids were varied, along with overall liposome concentration (9) and (13) to determine the minimum CSE necessary for polyvalent adhesion to occur. These liposome populations can be used together or individually as CSE carriers (16) with one or more payloads in microfluidic flow to engineer native cells (14) to achieve CSE cell lines (17). Microfluidics impart precision control of injected reagents, mixing, liposome fusion and elution of CSE cells (17) that can be further modified by adding additional channels and inlets. The small channel cross-sectional volume and large surface contact within microfluidic channels promote rapid mixing along the axis of flow, where

cells and liposomes associate through electrostatics resulting in increased uniform delivery of liposomes to the cellular surface. Microfluidic devices have led to innovations in genetic sequencing,¹³ cell sorting applications,¹⁴ enzyme kinetics,¹⁵ cell biology¹⁶ and biomedical research¹⁷ through the use of micron-sized reaction chambers which impart unique physical properties to the flow stream. Cell populations consisting of ketone and hydroxylamine CSE cells become rapidly labelled and in flow associate within 70 seconds, while controls missing either one or both bio-orthogonal chemical groups did not assemble. However, bio-orthogonal CSE cells which are cultured after application proliferate over time resulting in dilution of our labelling chemistry and retain viability.

Liposomal drug delivery methodologies are well established and understood as delivery vesicles for a variety of therapeutics such as the cancer agents Myocet® and DaunoXome®, imaging technology,¹⁸ nucleic acid transfection^{19 20} and drug delivery.²¹ Liposome strategies have also been essential for the fundamental study of cell membrane dynamics and membrane biology through their utility as model membranes.^{22 23 24} Extending the capabilities of liposome technologies through bio-orthogonal CSE allows for additional functionality by adding complimentary complexity without inhibiting the ease of use or overall utility. Bio-orthogonal functional groups are a collection of chemoselective ‘click’ reactions which couple two molecules under physiological conditions rapidly and without side reactions,^{25 26} which has enabled greater understanding of molecular biology in areas such as proteomics²⁷ and genetic regulation.^{28 29} Microfluidic technology was applied to control our CSE liposome fusion to create CSE cells and incorporate methods for subsequent applications.³⁰

2.2 Materials and Methods

2.2.1 Materials

Fluorescent dyes were obtained from Fisher Scientific (Mississauga, Ont), fluorescence mounting media was obtained from Invitrogen (Carlsbad, CA), monster green fluorescing protein (MGFP) vector was obtained from Promega (Fitchburg, WI), cell samples C3H/10T1/2, NIH3T3/RFP and Neonatal Dermal Fibroblasts/GFP were obtained from ATCC (Manassas, VA). All other materials were obtained from Sigma Aldrich (St. Louis, MO). O-dodecyloxyamine-tetra(ethylene)glycol was synthesized as previously described.³¹ 1-Palmitoyl-2-oleoyl-sn-glycero-3-phosphocholine (POPC) and 1, 2-dioleoyl-3-trimethylammonium-propane (DOTAP) were purchased from Avanti Polar Lipids (Alabaster, AL).

2.2.2 Cell Culture

C3H/10T1/2 mouse embryonic fibroblast cells were cultured and incubated for 3 days at 37°C and 5 % CO₂ in 10 cm culture plates with media changed every other day using DMEM with 1 % v/v PS and 10 % FBS as additives. NIH3T3/GFP expressing cells were obtained fresh from ATCC and cultured from liquid nitrogen storage and maintained using DMEM with 1 % v/v PS and 10 % FBS as additives. Human Neonatal Dermal Fibroblasts (HDNF)/RFP cells were obtained and cultured from liquid nitrogen storage and maintained using DMEM with 1 % v/v PS, 10 % FBS, 0.5 % w/w blasticidine hydrochloride, 5 mL L-glutamine and 5 mL non-essential Amino Acid Solution as additives. Cell cultures used for experiments were between 2 and 12 passages.

2.2.3 Surface Engineering Liposome Formulation

To form separate liposome solutions bearing ketone and hydroxylamine functionalities, sterile 5 mL vials were used and 60 µL, 30 µL, 10 µL and 1.0 µL of 2-dodecanone (10 mg/mL in CHCl₃)

or undecyloxyamine (10 mg/mL in CHCl_3) was added, followed by 454 μL POPC (10 mg/mL in CHCl_3) followed by 10 μL of DOTAP (Avanti Polar Lipids) (10 mg/mL in CHCl_3), which were then allowed to dry for 24 hours. Once the CHCl_3 was evaporated, 3 mL of fresh PBS was added, followed by tip sonication. Sonication of the lipid suspensions was carried out over 10 minutes using a 23°C water bath under 30 W. Subsequent suspensions were stored at 4°C. No liposome suspension was used past one week. For bilayer formation experiments, 2-dodecanone or undecyloxyamine bearing liposomes were diluted using PBS after sonication to 5 %, 2.5 %, 1 % and 0.5 % of the initial liposome concentration for subsequent microfluidic cell surface engineering experiments using tissue formation as our assay.

2.2.4 Assembly of Microfluidic Devices

The dual Y-reactor device used four luer-lock connectors (UpChurch Scientific) with four sections of PEEK tubing (McMaster Carr). Each PEEK tube had an inner diameter of 254 μm and a length of 8.0 cm. The four 8.0 cm lengths of tubing were connected to syringes and low flow volume T-mixer (UpChurch Scientific) passes into the subsequent reactor tube with a diameter of 254 μm , length of 68.5 mm and a total swept volume of 3.47 mm^3 . The flow was driven by two Hamilton Dual low flow rate dual syringe pumps.

2.2.5 Surface Engineering and Adhesion Studies in Flow

HDNF/RFP cells were grown in a 10 cm tissue culture dish using high glucose DMEM media containing 10 % FBS and 1 % Penicillin/Streptomycin (P/S) over 3 days, incubated at 37°C and 5 % CO_2 . Cells used for experiments were approximately 90 % confluent. HDNF/RFP cell suspensions were prepared by washing the culture plates with 3 mL PBS, followed by aspiration, treated with 3 mL trypsin 0.25 % EDTA for 3 minutes and then quenched with 6 mL of serum media. The suspension was then transferred to a 15 mL tube and centrifuged at 800 RPM for 5

minutes. The media was decanted and the pellet re-suspended in fresh growth serum containing media to 4 million cells/mL scored using a hemocytometer. Then 250 μ L of this suspension was loaded into a sterile 1 mL Hamilton gas-tight syringe, which was then attached using a luer lock connector to the assembled microfluidic device. To surface engineer the cellular suspension, 250 μ L of separately prepared undecyloxyamine (hydroxylamine) bearing liposomes was injected into a separate 1 mL Hamilton gas-tight syringe and connected to the microfluidic device alongside the HNDF/RFP cell suspension injector, using a luer lock connector. NIH3T3/GFP expressing cells were grown in 10 cm culture plates to approximately 90% confluency alongside HDNF/RFP cells.

The cell suspension was prepared for use by being washed with 3 mL of PBS, aspiration and subsequent treatment with 3 mL trypsin 0.25 % EDTA for 3 minutes and quenched with 6 mL of growth media. The suspension was transferred to a 15 mL tube and centrifuged at 800 RPM for 5 minutes, followed by decanting and re-suspending the pellet in fresh growth media to obtain a suspension concentration of 4 million cells/mL using a hemocytometer. Then 250 μ L of the 4 million cells/mL RFP suspension was loaded into a sterile 1 mL Hamilton gas-tight syringe which was then attached using a luer lock connector to the assembled microfluidic device. A separately prepared 250 μ L suspension of 2-dodecanone (ketone) bearing liposomes were loaded into a separate 1 mL Hamilton gas-tight syringe and connected alongside the NIH3T3/GFP cell suspension syringe to the microfluidic device using a luer lock connector. The microfluidic device and syringes were sterilized by flowing 75 % ethanol through the assembled device, followed by sterile PBS for 5 minutes at 41.0 μ L/min to remove any remaining ethanol and gas bubbles. Once the cell suspension and liposome syringes were connected to the microfluidic device, the syringes were attached to the Hamilton syringe pumps with a vertical configuration

and the flow was started from a high flow rate (41.0 $\mu\text{L}/\text{min}$) to low flow rate (0.69 $\mu\text{L}/\text{min}$) with mixing times ranging from 300 seconds to 5.0 seconds respectively, with the removal and discarding of the eluted head volume after 5 minutes so that flow equilibrium was established before cell deposition begins. Once flow equilibrium was established, the eluted flow volume was directly eluted onto prepared 1 cm^2 glass slides placed in 35 mm culture plates containing 2 mL of NIH3T3/GFP growth media, enough to immerse the glass slide. Once 20 μL of equilibrated flow volume was eluted onto the glass slide it was placed carefully in a cell culture incubator at 37°C and 5 % CO_2 for 16 hours. For analysis, the samples were fixed for 20 minutes using 4 % formalin solution, drained and washed with PBS and then mounted on glass slides to perform confocal microscopy using a Zeiss LSM 700 to determine tissue assembly, growth and formation of multilayers.

2.2.6 General Transfection and Assembly of Tissues in Flow using HDNF/RFP Cells and phMGFP

HDNF/RFP cells were cultured using standard protocols using 10% FBS and 1% P/S High Glucose DMEM in 10 cm culture plates over 2 days to 75 % confluency. To prepare the cellular suspension for microfluidic injection, HDNF/RFP cells were trypsinized using 3 mL of 0.25 % trypsin for 3 minutes, followed by quenching with 6 mL of growth media. The suspension was then transferred to a 15 mL tube and centrifuged at 800 RPM for 5 minutes. The supernatant was decanted and the pellet was re-suspended in growth media to 4 million cells/mL using a hemocytometer and 250 μL of the suspension was loaded into two sterile 1 mL Hamilton gas-tight syringes. To a sterile 1.5 mL Eppendorf tube, 60 μL of prepared ketone liposome suspension containing 410 μL POPC (10 mg/mL), 80 μL DOTAP (10 mg/mL) and 120 μL 2-dodecanone (10 mg/mL) was added followed by the addition of 10 μL of (1.4 $\mu\text{g}/\mu\text{L}$) phMGFP.

This mixture was then incubated at 23°C for 30 minutes and then diluted with 200 µL of serum free DMEM media and loaded into a 1 mL Hamilton syringe. To a second sterile 1.5 mL Eppendorf tube, 60 µL of a prepared hydroxylamine liposome suspension containing 410 µL POPC (10 mg/mL), 80 µL DOTAP (10 mg/mL) and 120 µL undecyloxyamine (10 mg/mL) was added, followed by the addition of 10 µL of pHMGFP (1.4 µg/µL). This mixture was incubated at 23°C for 30 minutes and diluted with 200 µL of serum free DMEM media and loaded into a 1 mL Hamilton gas-tight syringe. Both of these syringes were then connected to our microfluidic device and flowed at 3.4 µL/min and eluted over 1 cm² glass slides immersed in 2 mL of serum free media for 20 minutes, followed by incubation for 1 hour at 37°C and 5 % CO₂. The media was aspirated and replaced with FBS containing growth media and incubated for 48 hours. The slides were fixed by washing 3 times with 3 mL PBS, followed by the addition of 5 % formalin solution for 15 minutes. The formalin solution was aspirated and the cells washed once with PBS, followed by mounting on glass cover slips for fluorescent microscopy using an Zeiss LSM 700 Ziess microscope.

2.2.7 Selective Transfection and Assembly of Tissues in Microfluidic Flow

C3H/10T1/2 cells were cultured using standard protocols using 10 % FBS and 1 % P/S High Glucose DMEM in 10 cm culture plates over 2 days to 75 % confluency. HDNF/RFP cells were also cultured using standard protocols using 10% FBS and 1% P/S High Glucose DMEM in 10 cm culture plates over 2 days to 75 % confluency. Once cells reached 75 % confluency, 5 % (v/v) ketone liposomes were added to the media, and incubated with cells at 37°C and 5 % CO₂ for 1 hour to create ketone-tailored cells. To prepare the C3H/10T1/2 and ketone-tailored HDNF/RFP cellular suspensions for microfluidic injection, the cell cultures were trypsinized using 3 mL of 0.25 % trypsin for 3 minutes, followed by quenching with 6 mL of growth media.

The suspensions were then transferred to 15 mL tubes and centrifuged at 800 RPM for 5 minutes. The supernatant was decanted and the pellet was re-suspended in growth media to 4 million cells/mL using a hemocytometer and 250 μ L of the suspension was loaded into two sterile 1 mL Hamilton gas-tight syringes. To a sterile 1.5 mL Eppendorf tube, 60 μ L of a prepared ketone liposome suspension containing 410 μ L POPC (10 mg/mL), 80 μ L DOTAP (10 mg/mL) and 120 μ L undecyloxyamine (10 mg/mL) was added, followed by the addition of 10 μ L of (1.4 μ g/ μ L) pHMGFP. This mixture was then incubated at 23°C for 30 minutes and then diluted with 200 μ L of serum free DMEM media and loaded into a 1mL Hamilton syringe. The C3H/10T1/2 and pHMGFP oxyamine liposome syringes were then connected to our microfluidic device, followed by the addition of the ketone-tailored HDNF/RFP suspension to the downstream luer lock connection and connected to a Hamilton 11 Plus syringe pump with a flow rate of 3.4 μ L/min and eluted over 1 cm² glass slides immersed in 2 mL of serum free media for 20 minutes, followed by incubation for 1 hour at 37°C and 5 % CO₂. The media was then aspirated and replaced with FBS containing growth media and incubated for 48 hours. The slides were fixed by washing 3 times with 3 mL PBS followed by the addition of 5 % formalin solution for 15 minutes. The formalin solution was aspirated and the cells washed once with PBS followed by mounting on glass cover slips for time-course fluorescent microscopy using an Zeiss LSM 700 3D confocal microscope.

2.2.8 Microfluidic CSE of Liposome Coupled Biotin and Streptavidin (FITC) to Cellular Membranes

To synthesize Biotin containing liposomes, to a sterile 5 mL glass vial 460 μ L of POPC (10 mg/mL), 10 μ L DOTAP (10 mg/mL) and 120 μ L, 240 μ L and 360 μ L of oxime-tethered biotinylated lipid **24** (10 mg/mL) were added and the solvent was allowed to evaporate over 10

hours. To the dried lipids, 3 mL of PBS was added and then tip sonicated for 10 minutes at 30 W using a 23°C water bath. The liposomes were then stored at 4°C for no longer than 7 days. For CSE experiments, C3H/10T1/2 cells were cultured using standard protocols to 75% confluency, followed by washing with 3 mL PBS and subsequent treatment with 3 mL trypsin 0.25% EDTA for 3 minutes and then quenched with 6 mL of serum containing media. The cell suspension was then centrifuged in a 15 mL tube at 800 RPM for 5 minutes, followed by decanting and re-suspension of the pellet in fresh media to 4 million cells/mL using a hemocytometer. Then 250 μ L of the untailed cell suspension was loaded into a 1 mL Hamilton gas-tight syringe and attached to the device using a luer lock connection. To a separate 1 mL syringe 250 μ L of the prepared Biotin **24** containing liposomes were loaded and connected in tandem with the native C3H/10T1/2 syringe to our simple Y-channel device. The syringes were then attached to a Hamilton 11 Plus syringe pump and simultaneously injected at 6.8 μ L/min for a residence time of 30 seconds before being eluted into serum containing media for dilution. After 20 minutes the flow was stopped and the diluted solution was centrifuged at 800 RPM for 5 minutes followed by decanting and re-suspension of the pellet in 500 mL PBS and 60 μ L of 1 mg/mL Streptavidin-FITC conjugate was added and incubated for 1 hour followed by dilution with 9 mL PBS, centrifuged, decanted and re-suspended in 500 μ L PBS for flow cytometry.

2.2.9 Synthesis of (24) (E)-2-(dodecan-2-ylideneaminoxy) acetic acid

To a 10 mL dry argon filled vial containing a magnetic stir bar 120 μ L of 2-dodecanone (100.0 mg, 184.32 g/mol, 0.542 mmol) (Sigma Aldrich) was added and dissolved in 2.5 mL of freshly distilled tetrahydrofuran (THF). To a separate vial 65.1 mg of *o*-(Carboxymethyl)hydroxylamine hemihydrochloride (109.30 g/mol, 0.596 mmol) (Sigma Aldrich) was added and dissolved in 2.5 mL of freshly distilled THF. The solution of hydroxylamine was then cannulated into the

solution of 2-dodecanone and stirred overnight at 23°C. The next day the solvent was evaporated and the remaining solid was weighed (152.0 mg) and dissolved in ethyl acetate and passed through a small pad of celite. The solvent was evaporated to yield the isolated product **24** (126.0 mg, 90 %). ^1H NMR (CDCl_3 , 300 MHz) δ 4.63-4.59 (m, 2H), 2.41-2.36 (m, 1H), 2.22-2.15 (t, 2H), 1.90 (s, 3H), 1.45 (s, 2H), 1.27 (s, 14H), 0.917-0.875 (t, 3H) ppm. ^{13}C NMR (CDCl_3 , 300 MHz) δ 174.1, 161.5, 69.6, 35.6, 31.8, 29.5, 29.4, 29.3, 29.2, 29.1, 26.2, 22.6, 14.3, 14.1 ppm.

2.3 Results and Discussion

The combined generation and application of CSE cells in microfluidic flow has potential applications in many areas of the life sciences. But to be an effective technology platform CSE delivery and manipulation must be robust and rapid. The efficient delivery of CSE liposomes has real world applications including imaging, cell purification, transfection and three-dimensional (3D) printing of tissues. Microfluidic devices have useful physical properties as analytical tools to integrate unit operations efficiently into single small devices, while accurately and rapidly (within seconds) mixing reagents within micron-sized channels. Microfluidic devices have been incorporated into many existing commercial technologies such as flow cytometry, mass spectrometry and 3D printing because of the unique physical and analytical properties these devices impart, such as particle sorting, short mixing regimes and liquid partitioning.

Figure 2.3 describes our integrated microfluidic approach to apply CSE for cell-cell assembly, with potential applications for printing 3D tissues. Bio-orthogonal CSE delivery and assembly was probed through varying microfluidic flow rate, bio-orthogonal lipid ratios and overall liposome concentration to determine total efficiency of the CSE application and tissue

assembly. A three Y-joint microfluidic device was constructed and used to probe our integrated approach for applying ketone CSE (7) to NIH3T3/GFP (14) and hydroxylamine CSE (11) to tailor HNDF/RFP (17), followed by mixing for cell-cell assembly to produce two cell type spheroids (21) without purification (Figure 2.3). By varying residence time, composition and concentration of CSE liposomes, it was determined that cell labelling occurred at low total liposome concentrations (0.62 mM) for tissue engineering within 30 seconds and at low (1 %) ratios of both bio-orthogonal lipids (Supplementary Info.). The successful assembly of tissues using both low concentration and low percent ratios of bio-orthogonal lipids demonstrates the robust and efficient delivery and utility of CSE using microfluidics, where the number of polyvalent surface molecules (approx. ~1000) was sufficient to induce assembly.

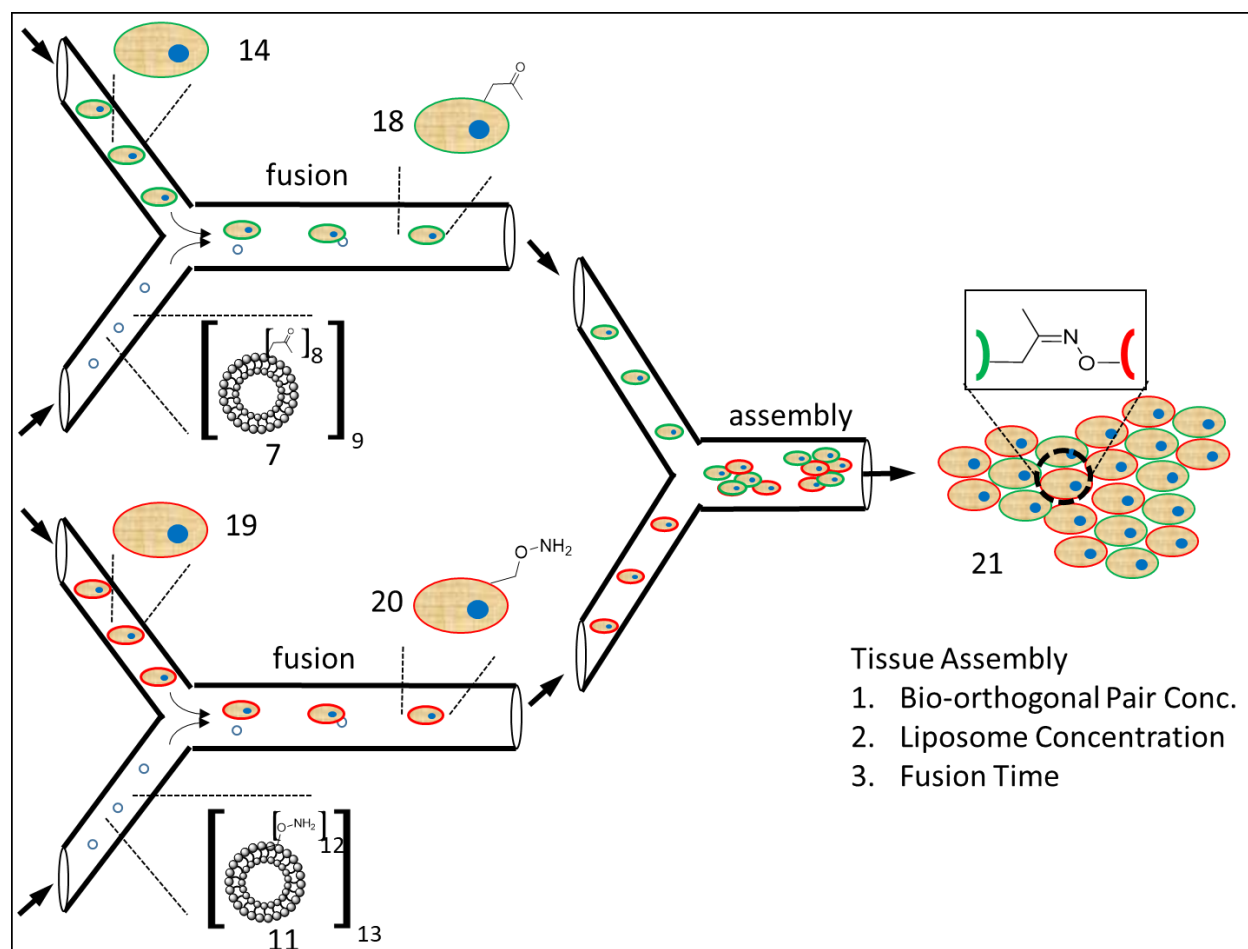


Figure 2.3: Microfluidic scheme depicting our integrated tissue formation assay using microfluidic flow networks to perform CSE on cells in suspension, by simultaneously engineering NIH3T3-GFP (14) and HNDF-RFP (19) cell lines with ketone (7) and hydroxylamine (11) liposomes to produce tissues (21) in a continuous methodology. To determine CSE efficacy, the ratio of both liposomes (9) and (13) and bio-orthogonal components ketone (6) and hydroxylamine (10) were varied respectively. (Top) GFP expressing cells (14) were combined in flow with ketone presenting liposomes (7) to produce ketone presenting GFP cells (18). (Bottom) RFP expressing cells (19) were combined in flow with hydroxylamine presenting liposomes (11) to produce hydroxylamine presenting RFP cells (20). (Middle) CSE cells are directly mixed in a third microfluidic channel without further manipulation, which combine and assemble through polyvalent “velcro-like” oxime reactions to produce spheroids and tissues in culture (21). Probing assembling efficacy was accomplished by varying the ratio of the bio-orthogonal pair, the liposome concentration and the ratio of individual lipids were varied to determine the minimum conditions necessary to produce tissue assemblies (21), which were probed using fluorescence microscopy.

Spheroid and tissue assembly of complex multicellular model structures for systems biology and other research applications using polymer scaffolds or metabolic labelling have several drawbacks which limit their general utility and adoption. More advanced systems are needed to enable three or more cell type assemblies to introduce better approximations of native tissue function using simple and robust methodologies. Figure 2.4 demonstrates our integrated microfluidic approach to rapidly label and generate bio-orthogonal CSE assemblies of three cell type spheroids and tissues using microfluidics. With the advancement of 3D printing engineering technology, the need for viable tissue constructs containing multiple cell lines with very high cell density is a major hurdle for many rapid therapeutic and tissue applications. To demonstrate rapid development of complex tissues and spheroids in flow, we developed a three-inlet microfluidic PMMA device shown in Figure 2.4A, with a standard Y-joint followed by a downstream inlet to allow for the injection of additional cell lines. We combined hydroxylamine tailored HDNF/RFP cells (28) and ketone tailored NIH3T3/GFP (29) in suspension, where they were mixed and combined with another suspension of live stained ketone tailored C3H/10T1/2 (30) cells for assembly (31). The eluted spheroids were deposited for live cell fluorescence microscopy resulting in a range of spheroids sizes shown in Figure 2.4B-C. The three cell aggregation process was observed to be rapid, (within 30 seconds) fully forming three cell type spheroids. Tissues were generated through the deposition of higher quantities of spheroids shown in Figure 2.4D, with thicknesses ranging from 30 μm -300 μm which adhere upon contact and induces natural cell contact adhesion over 16 hours.

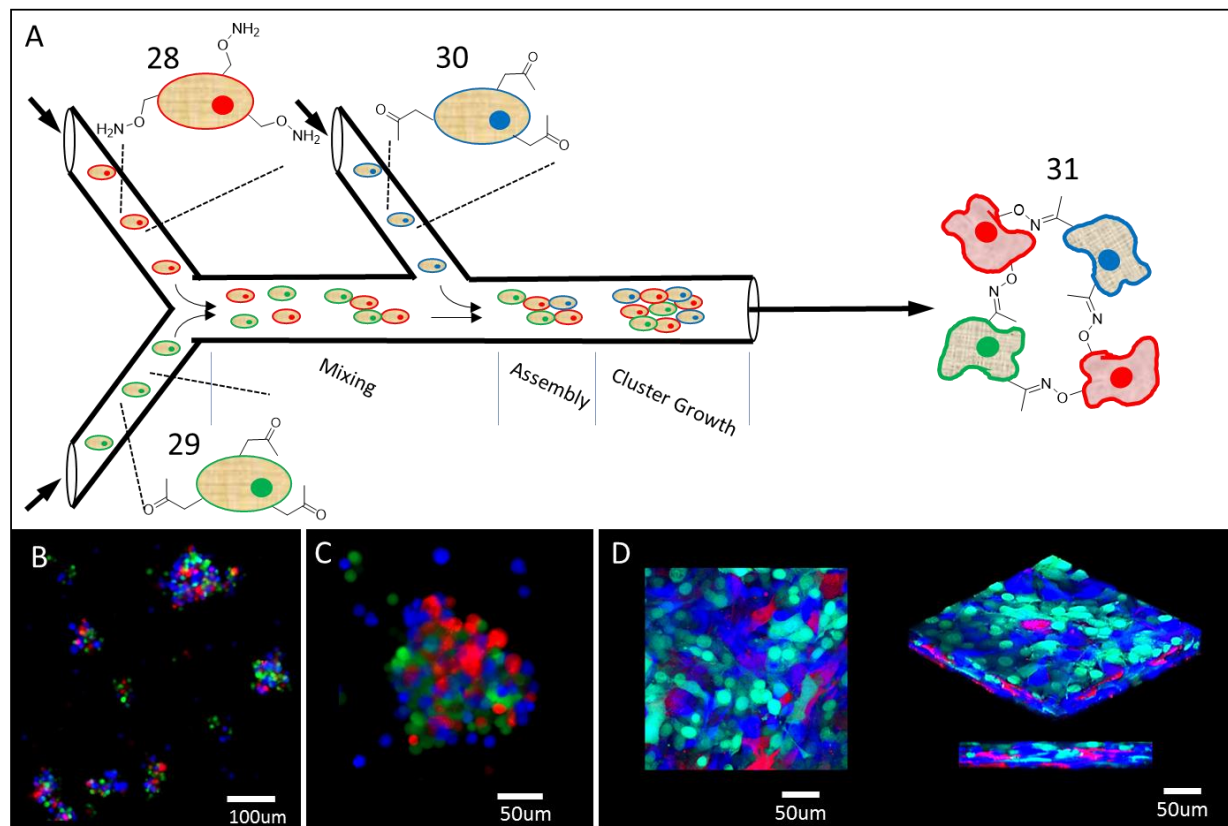


Figure 2.4: Complex spheroid and tissue formation using a simple microfluidic device to form three cell-line tissues and spheroids using three different CSE cell lines in flow. (A) Using a three inlet microfluidic device, a combination of ketone engineered HDNF/RFP cells (28) and hydroxylamine engineered NIH3T3/GFP (29) were injected, followed by the addition of CMSO (blue) stained ketone engineered C3H/10T1/2 cells (30) resulted in cell-cell assembly of multiple cell line spheroids through oxime adhesion (31) within 70 seconds, with an average size range of 50 µm - 70 µm. (B) Direct elution and dilution of the spheroid suspension resulted in three color spheroids (20X) under fluorescence microscopy without the use of trapping agents or fixation to produce stable live spheroids. (C) Three color spheroids (40X) demonstrates that HDNF/RFP cells are primary adhesive cells driving aggregation with a consistency of roughly 2:1:1 (HDNF/RFP: NIH3T3/GFP: CMSO C3H/10T1/2). (D) Images of concentrated deposition of incubated three cell type tissues (40X) over 24 hours using Zeiss LSM 700 confocal microscope.

Cell based combinatory methodologies have been crucial components in the advancement of medical technologies, such as printing 3D tissues, closed medical diagnostic devices and cellular transfection. Microfluidic devices have largely been developed for analytical purposes to disassemble cells for DNA sequences, separation, purification of small particles and recently tissue engineering and cellular assays. Figure 2.5 demonstrates the flexibility of our modular

microfluidic combinatorial approach. CSE liposome pairs containing bio-orthogonal hydroxylamine and ketone groups were combined with nucleic acids to perform dual purpose assembly and transfection using microfluidics. To form multiplexed liposomes, ketone (7) and hydroxylamine (11) liposomes were combined with pHMGFP to produce tailored CSE lipoplexes (33). Stably transfected RFP expressing HDNF cells (32) were treated with ketone-tailored pHMGFP lipoplexes (33) to produce GFP-RFP (orange) monolayers (Figure 2.5). Figure 2.5E shows the production of transfected spheroids using our microfluidic device, where populations of HDNF/RFP (32) cells were treated with ketone and hydroxylamine tailored lipoplexes respectively to produce GFP transfected HDNF/RFP (orange) spheroids. This demonstrates that CSE availability can be used for delivery of complex cargo, such as nucleic acids while the bio-orthogonal ligands remain active in the plasma membrane for cellular assembly of contact inhibited cell lines.

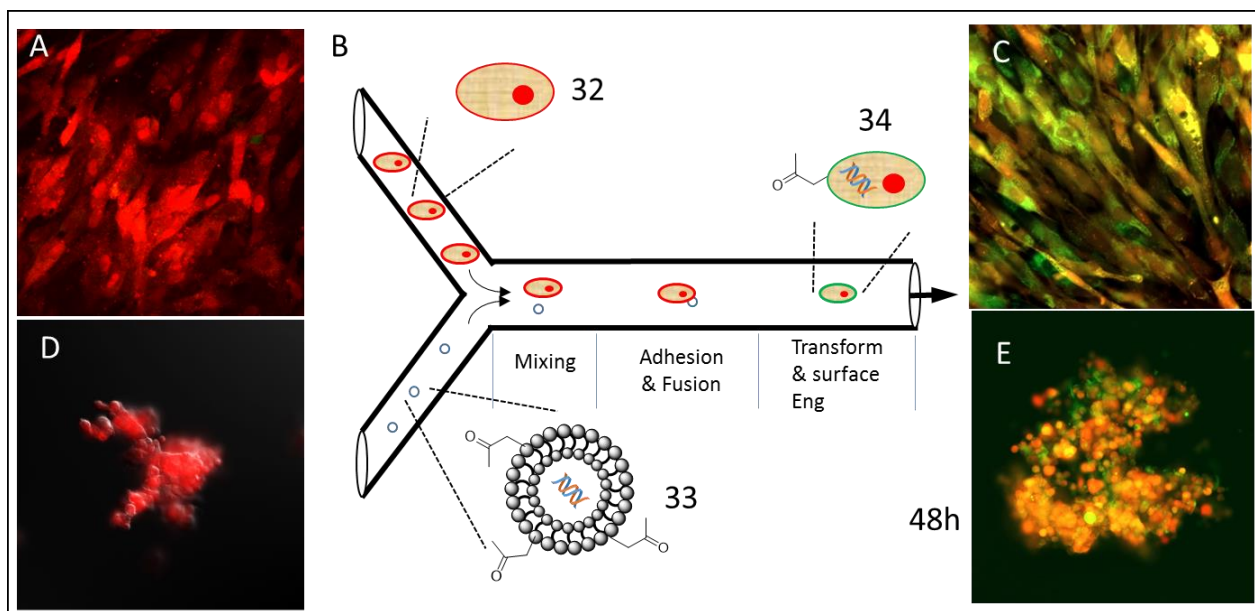


Figure 2.5: Multiplexed delivery of CSE engineering and nucleic acids through CSE-lipoplexes to HDNF/RFP cells in flow. (A) Control monolayer of non-CSE HDNF/RFP cultured cells (20X) adhered to 1 cm² glass plates. (B) Scheme depicting microfluidic injection of HDNF/RFP cells (32) in suspension along with ketone engineered pGFP-lipoplex suspension (33), which undergo mixing, adhesion and transfection (34) in flow. (C) Deposited monolayer of flow delivered ketone CSE pGFP transfected HDNF/RFP cells (20X) which transform from red to orange upon GFP expression after 24 hours. (D) Fluorescent microscopy image (20X) of microfluidic generated oxime assembled RFP HDNF cell spheroid using of CSE ketone and hydroxylamine liposomes. (E) Ketone and hydroxylamine CSE pGFP transfected HDNF/RFP cells (20X) assembled using separate ketone CSE and hydroxylamine pGFP-lipoplexes over 24 hours.

The flexibility of CSE liposomal technology in combination with microfluidic devices can also rapidly synthesize novel mixed transfected tissue constructs using flow processes that do not require further manipulation. In Figure 2.6, we designed a single step process to tailor and selectively transfect cell lines for advanced tissue engineering applications. Using tailored ketone nucleic acid lipoplexes (33) and co-injected native cells (14) to deliver both CSE and nucleic acids (35) producing dual engineered cell lines (36), while a downstream inlet was used to introduce hydroxylamine tailored cells (28) to form mixed transfected spheroids without

purification. Initial spheroids did not express phMGFP (Figure 2.6B) but after 6-12 hours of incubation, spheroids become positive for GFP expression (Figure 2.6C). Using increasing cell density, we rapidly accessed tissues where (dark) cells (14) do not express GFP (Figure 2.6E), while after 24 hours GFP expression was localized in C3H/10T1/2 cells. This unique strategy produced tissues rapidly, while leveraging the properties of microfluidics to selectively express GFP, while HDNF/RFP (28) showed no GFP transfection. This strategy has many applications for systems biology, where knock-in and knock out methodologies can be used to determine cell-cell interactions in a variety of organ-like contexts such as the kidney, blood brain barrier, cardiac and neuronal growth. This is a beneficial strategy over current methods where native cell-cell interactions can be studied over time in the context of decreases or increases a gene of interest protein pathway.

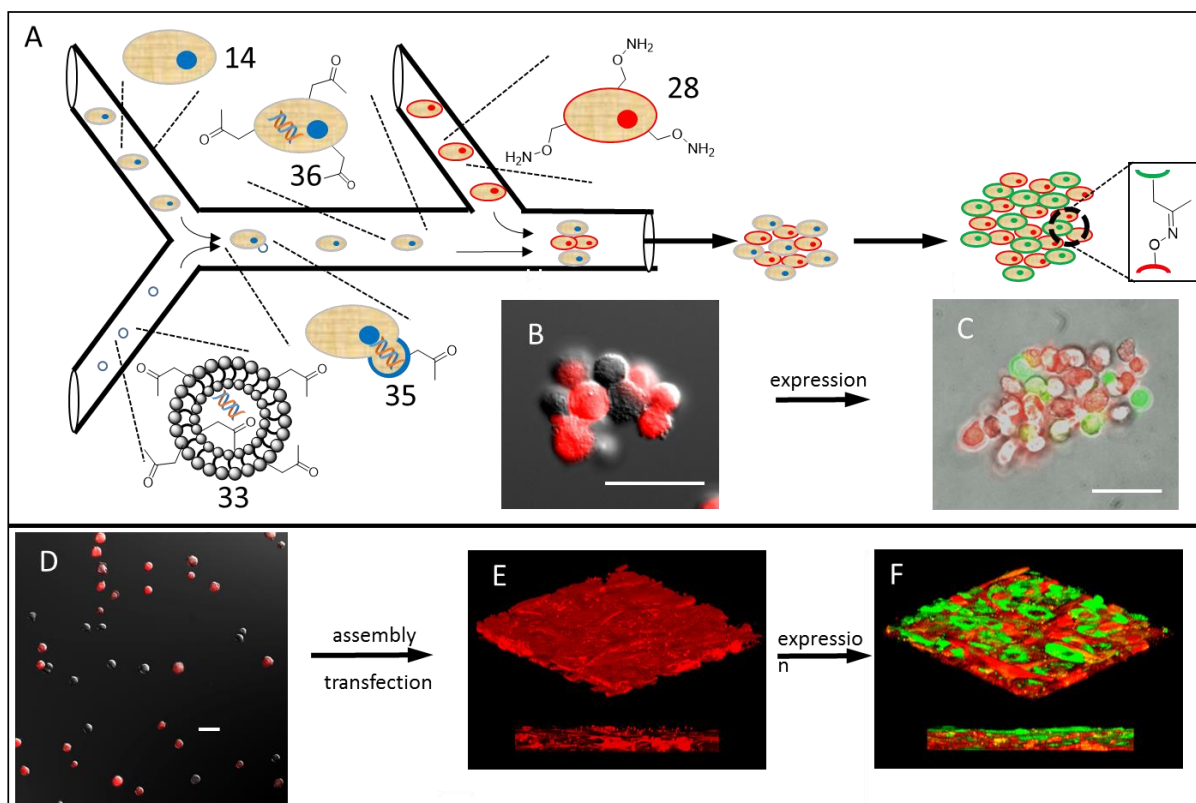


Figure 2.6: Single step selective nucleic acid transfection and microfluidic CSE assembly of tissues to produce complex transfected co-cultures containing two cell lines. (A) Schematic of microfluidic device for injection of suspended C3H/10T1/2 cells (14) with ketone engineered phMGFP-lipoplex solution (33), where both suspensions undergo mixing in the microchannel for 30 seconds. During mixing the lipoplex and cells undergo mixing and adhesion (35) resulting in fusion (36) to produce CSE ketone displaying cells containing added phMGFP plasmids. An additional downstream inlet adds pre-engineered hydroxylamine HNDP/RFP cells (28) into the flow channel resulting in cell-cell assembly with CSE ketone phMGFP transfected cells through oxime ligation. (B) Mixed ketone engineered HNDP/RFP cells and hydroxylamine phMGFP transfected C3H/10T1/2 cells after microfluidic elution (40X). (C) Mixed ketone engineered RFP HNDP cells and hydroxylamine phMGFP C3H/10T1/2 cells after 12 hours of incubation (40X). (D) Control mixed HNDP/RFP cells and C3H/10T1/2 cells. (E) Top and side 40X confocal images of tissues composed of phMGFP transfected keto-C3H/10T1/2 cells and oxy-HNDP/RFP cells incubated for 2 hours, resulting in a thickness of approximately 30 μm . (F) Top and side images of mixed tissue composed of transfected keto-C3H/10T1/2 cells and oxy-HNDP/RFP cells incubated for 24 hours, where GFP is expressed (40X).

To quantify the rapid and efficient incorporation of bio-orthogonal liposome CSE using microfluidics devices we utilized oxime coupled Biotin and Streptavidin-FITC (Strept-FITC) as CSE reporters to determine membrane incorporation of delivered lipids using varying

concentrations (Figure 2.7). Cells in suspension (14) were combined with biotin containing liposome (37) which were generated using ketone tailored liposomes (38) treated with hydroxylamine-biotin (39). Rates of bio-orthogonal liposome incorporation were measured using flow cytometry after treatment with Strept-FITC (41). Incorporation experiments show increased cell membrane incorporation of biotin using our liposomal format compared to treatment with free biotin conjugate (39) (Figure 2.7B-E). We quantified the transfer of our biotin liposome (37) to the cellular membrane using Molecules of Equivalent Soluble Fluorescence (MESF) based on Strept-FITC, to quantify delivery of lipids with 30 seconds of microfluidic treatment. Using 30 seconds as our benchmark treatment time, we altered the ratio of biotin lipid (38), resulting in a near linear increase in MESF response. Interestingly, we observed fast turnover of biotin on the cellular membrane using live cell flow cytometry through rapid depletion of Streptavidin-FITC signal over time (to background levels) after 30 minutes.

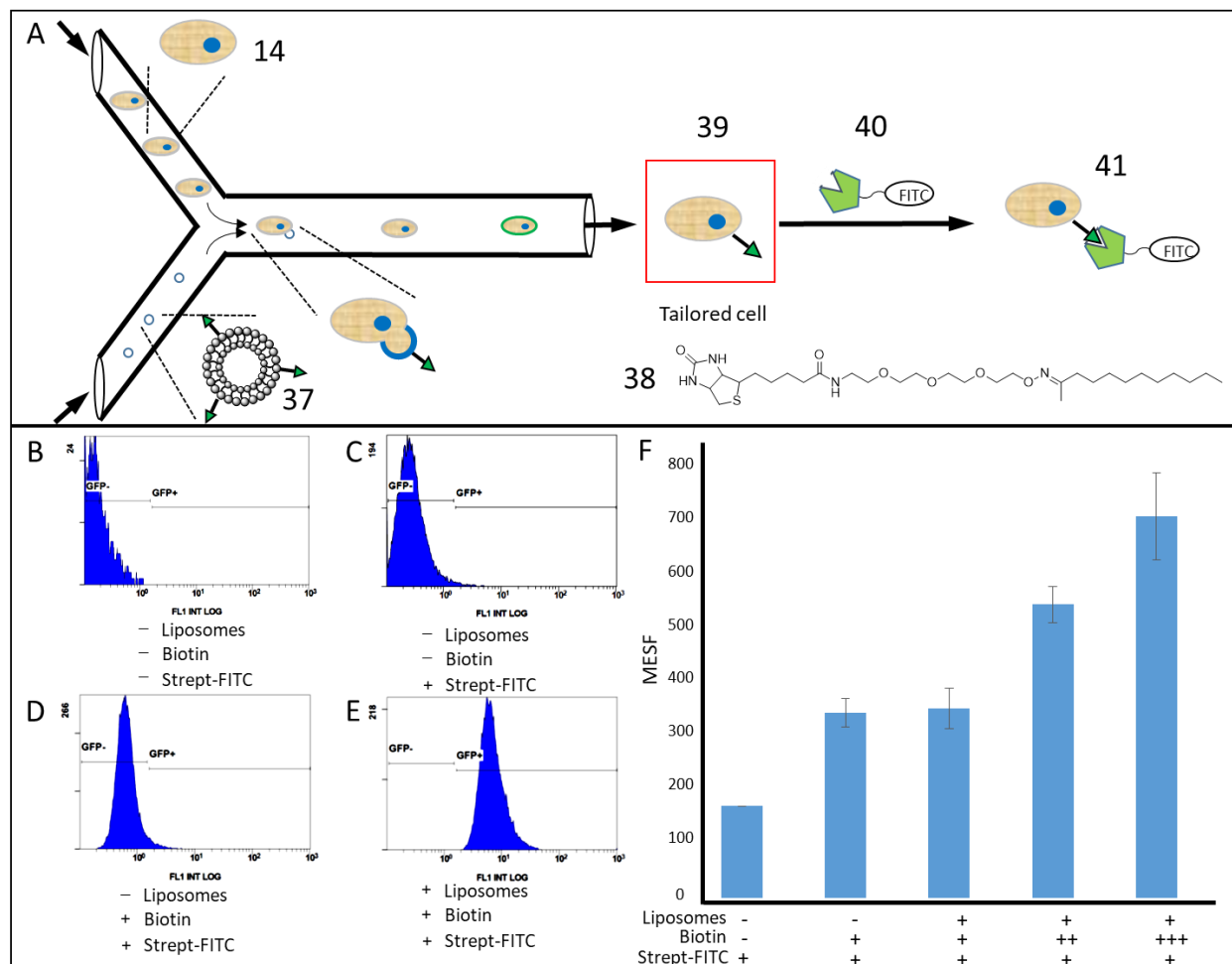


Figure 2.7: Efficient microfluidic membrane incorporation of oxime coupled biotin and subsequent labelling with Strept-FITC conjugate for flow cytometry. (A) C3H/10T1/2 cell suspensions (14) were injected into a Y-joint microfluidic device with liposomes (37) containing oxime biotin conjugate (38) to produce biotin surface engineered cells (39) within 30 seconds. The biotin engineered cells were separately labelled with Strept-FITC marker (40) for flow cytometry (41). (B) Flow data of native C3H/10T1/2 cells using the microfluidic device for 30 seconds. (C) Flow data of native cells flowed through our microfluidic device for 30 seconds, then incubated with Strept-FITC. (D) C3H/10T1/2 cells treated with non-liposomal oxime biotin molecule through microfluidic mixing for 30 seconds and incubated with Strept-FITC. (E) C3H 10T1\2 cells treated with liposomal biotin through microfluidic mixing for 30 seconds, produces a strong fluorescent signal with subsequent Strept-FITC incubation. (F) Graph depicting number of fluorescent Strept-FITC molecules on C3H/10T1/2 cell surfaces using flow cytometry (MESF). As the amount of biotin conjugate is increased (1X, 2X and 3X) the amount biotin available on the cell surface increases linearly.

2.4 Conclusion

In summary, CSE liposomes and microfluidics can be used as a modular strategy to control CSE of cells and their use in co-culture tissue formation, gene and drug delivery as well as exogenous membrane ligand incorporation. The combination of CSE using liposome fusion delivery has also been demonstrated to be quick and efficient using microfluidics and flow cytometry. The oxime liposome fusion strategy rapidly imparts useful molecular agents to engineer cells *in situ* for real world applications and research for next generation therapeutic studies. Flexibility of the CSE strategy for incorporation into existing delivery methodologies has been shown to be useful for the critical adaptability in a range of applications. By varying flow rate and the length of microfluidic reactor channel, as well as the liposome composition, the optimal reaction time and liposome content can be rapidly determined and used for downstream applications quickly and efficiently, since cell types can have a range of division times and metabolic activity which may effect the amount of CSE available on the cell surface over time. Without altering the molecular biology or metabolic biosynthetic pathways of cells, this methodology serves as a platform for the development of new cellular capabilities using microfluidics to create medical devices capable of rapidly engineering cells for therapeutics and theranostics. Using our platform, we developed methods for modular microfluidic devices for use in flow cytometry, 3D printing and rapid automated drug testing. This methodology can potentially be used to tailor inorganic, polymeric or nanoparticles surfaces for the development of sensors, analytical devices and biological applications.

2.5 References

- (1) Shi, J.; Kundrat, L.; Pishesha, N.; Bilate, A.; Theile, C.; Maruyama, T.; Dougan, S. K.; Ploegh, H. L.; Lodish, H. F. *Proc. Natl. Acad. Sci. U. S. A.* **2014**, *111* (28), 10131–10136.
- (2) Lu, L.; Gao, J.; Guo, Z. *Angew. Chemie* **2015**, *127* (33), 9815–9818.
- (3) Laughlin, S. T.; Bertozzi, C. R. *Nat. Protoc.* **2007**, *2* (11), 2930–2944.
- (4) Nguyen, D. P.; Elliott, T.; Holt, M.; Muir, T. W.; Chin, J. W. *J. Am. Chem. Soc.* **2011**, *133* (30), 11418–11421.
- (5) Rabuka, D.; Forstner, M. B.; Groves, J. T.; Bertozzi, C. R. *J. Am. Chem. Soc.* **2008**, *130* (18), 5947–5953.
- (6) Schmitt, S. K.; Trebatoski, D. J.; Krutty, J. D.; Xie, A. W.; Rollins, B.; Murphy, W. L.; Gopalan, P. *Biomacromolecules* **2016**, *17* (3), 1040–1047.
- (7) Park, K. M.; Gerecht, S. **2014**, *5*, 4075.
- (8) West, J. L.; Hubbell, J. A. *Macromolecules* **1999**, *32* (1), 241–244.
- (9) Pulsipher, A.; Dutta, D.; Luo, W.; Yousaf, M. N. *Angew. Chemie Int. Ed.* **2014**, *53* (36), 9487–9492.
- (10) Elahipanah, S.; Radmanesh, P.; Luo, W.; O'Brien, P. J.; Rogozhnikov, D.; Yousaf, M. N. *Bioconjug. Chem.* **2016**, *27* (4), 1082–1089.
- (11) Lee, E.; Luo, W.; Chan, E. W. L.; Yousaf, M. N. *PLoS One* **2015**, *10* (6), e0118126.
- (12) O'Brien, P. J.; Luo, W.; Rogozhnikov, D.; Chen, J.; Yousaf, M. N. *Bioconjug. Chem.* **2015**, *26* (9), 1939–1949.
- (13) Abate, A. R.; Hung, T.; Sperling, R. A.; Mary, P.; Rotem, A.; Agresti, J. J.; Weiner, M. A.; Weitz, D. A. *Lab Chip* **2013**, *13* (24), 4864–4869.
- (14) Wyatt Shields IV, C.; Reyes, C. D.; Lopez, G. P. *Lab Chip* **2015**, *15* (5), 1230–1249.
- (15) Sjostrom, S. L.; Joensson, H. N.; Svahn, H. A. *Lab Chip* **2013**, *13* (9), 1754–1761.
- (16) Kim, D.; Wu, X.; Young, A. T.; Haynes, C. L. *Acc. Chem. Res.* **2014**, *47* (4), 1165–1173.
- (17) Sackmann, E. K.; Fulton, A. L.; Beebe, D. J. *Nature* **2014**, *507* (7491), 181–189.
- (18) Stephan, M. T.; Irvine, D. J. *Nano Today* **2011**, *6* (3), 309–325.
- (19) Wasungu, L.; Hoekstra, D. J. *Control. Release* **2006**, *116* (2), 255–264.
- (20) Elouahabi, A.; Ruysschaert, J.-M. *Mol. Ther.* **2005**, *11* (3), 336–347.
- (21) Liu, J.; Jiang, X.; Ashley, C.; Brinker, C. J. *J. Am. Chem. Soc.* **2009**, *131* (22), 7567–7569.
- (22) Pattni, B. S.; Chupin, V. V.; Torchilin, V. P. *Chem. Rev.* **2015**, *115* (19), 10938–10966.
- (23) Matos, C.; Moutinho, C.; Lobão, P. J. *Membr. Biol.* **2012**, *245* (2), 69–75.
- (24) Chan, Y.-H. M.; Boxer, S. G. *Curr. Opin. Chem. Biol.* **2007**, *11* (6), 581–587.
- (25) Bertozzi, C. R. *Acc. Chem. Res.* **2011**, *44* (9), 651–653.

- (26) McKay, C. S.; Finn, M. G. *Chem. Biol.* **2014**, *21* (9), 1075–1101.
- (27) Weigt, D.; Hopf, C.; Médard, G. *Clin. Epigenetics* **2016**, *8* (1), 76.
- (28) Dieterich, D. C.; Lee, J. J.; Link, A. J.; Graumann, J.; Tirrell, D. A.; Schuman, E. M. *Nat. Protoc.* **2007**, *2* (3), 532–540.
- (29) Elliott, T. S.; Bianco, A.; Chin, J. W. *Curr. Opin. Chem. Biol.* **2014**, *21*, 154–160.
- (30) Whitesides, G. M. *Nature* **2006**, *442* (7101), 368–373.
- (31) Dutta, D.; Pulsipher, A.; Luo, W.; Mak, H.; Yousaf, M. N. *Bioconjug. Chem.* **2011**, *22* (12), 2423–2433.

Chapter 3

Cell-Cell Tissue Assembly and Particle Kinetics in Microfluidic Flow

This work has been published in *Bioconjugate Chemistry*, Volume 9, pages 1939-1949 in 2015 under the title “Spheroid and Tissue Assembly via Click Chemistry in Microfluidic Flow”. It is reprinted with permission (© ACS Publishing Group 2015). O’Brien, P. J.; Luo, W.; Rogozhnikov, D.; Chen, J.; Yousaf, M. N. are co-authors of this work.

Contributions

M.N.Y designed the study. P.J.O., D.R., W.L. and S.E. performed the experiments. M.N.Y., P.J.O., D.R. and S.E. analyzed the data. P.J.O. and M.N.Y. wrote the manuscript.

3.1 Introduction

In vitro generated spheroids and tissues are crucial for next generation therapeutics, serving as human model systems to investigate paracrine and autocrine signalling, tumour growth, invasion models and commercial applications such as tissue chips for drug screening, organ grafting and organ replacement therapies.^{1 2 3 4 5 6 7} Due to the need for these types of organ-like constructs, tremendous progress towards spheroid and tissue formation has been made through manipulating cell adhesion properties via molecular biology, non-natural metabolite incorporation, polymer and de-cellularized tissue scaffolds.^{8 9 10 11} Current tissue engineering technologies lack control over the formation of cell-cell interactions and subsequent 3D architecture of tissue assemblies.

The Yousaf group recently developed the use of liposomes bearing bio-orthogonal oxime chemistry as a method to engineer contact inhibited cell lines using liposome fusion to deliver molecules to the plasma membrane. This is an important methodology that circumvents difficulties encountered with polymer scaffolds and metabolic and genetic engineering to adhere cells as a method to directly adhere cells together to create better tissue mimics of *in vivo* tissues. Mammalian cells largely exist within natural 3D environments, consisting of other cell types and secreted ECM where cell types and spatial orientation directly influence function and viability of tissues and organs. Tissue engineering has seen an explosion in the use of natural and synthetic biomaterials to reconstruct these tissues *in vitro* using materials such as collagen, hydrogels, Matrigel®, peptide coupled polymers, polymers containing signalling agents and biodegradable polymers. Although these materials have shown some promise as *in vitro* models for basic research, these technologies have not seen wide spread adoption or development into products for regenerative medicine. Current challenges include the formation of continuous cell-cell

contacts across the millimeter scale, multiple cell type adhesion and controlling 3D spatial orientation.

In higher-order organisms, cell-cell and cell-ECM interactions coupled with control over spatial and temporal architecture are vital for function and survival. Tissue engineering seeks to recapitulate these functions in damaged or diseased human organs and tissues for both life-saving and quality of life applications. Current advanced methods in tissue engineering use a number of different techniques to assemble cells into tissue-like structures in attempts to recreate natural 3D environments such as natural ECMs, de-cellularization of natural organs, followed by re-cellularization using autologous cells to re-establish function, growth of organs from single stem cells, protein interactions to adhere cells and a newly developed liposome fusion cell treatments to produce self-adherent cell lines. Therefore, tissue engineering techniques require approaches that are simple, with transient stable cell-cell conjugation techniques that do not alter biomolecular pathways, as a general application. Using liposome leaflets as vectors for small molecule bio-orthogonal lipids has been shown as a viable method for the surface modification of cells for tissue assembly and cell-imaging that addresses many of the above issues. To understand the assembly of surface modified cells and control subsequent tissue orientation, we used microfluidics as a biophysical analytical tool to study the *in situ* assembly process directly to determine not only assembly kinetics but also cluster architecture using a combination of bright-field, fluorescent and confocal microscopy.

Microfluidics has been utilized extensively as a method to efficiently mix reagents, sort micro and nanoparticles, conduct high-throughput chemical reactions, increase analytical sensitivity and has been applied to a multitude of bioanalytical and healthcare applications. Microfluidics use micro sized channels to move and mix fluids for analytical and biological

assays using small amounts of reagents. These devices have the benefit of low reagent usage, multiplexed stepwise processing, small size, efficient mixing and highly controlled reagent addition. These properties allow efficient chemical and nanoparticle formation for optical and analytical analysis using transparent materials, such as glass, poly (methyl methacrylate) (PMMA) and Polydimethylsiloxane (PDMS). By merging microfluidics and liposomal cell surface engineering, high throughput manufacturing of tissue generation and research using off shelf technologies can be achieved. Microfluidic flow reactors typically have a tube-like design with at least one cross-sectional dimension of less than 500 μm in a closed system. By incorporating microfluidic technology and liposomal cell surface rewiring control can be exerted over assembly kinetics and spheroid compositions, which cannot be performed using traditional mixing techniques. This is an advantageous system, where density, flow rate control and small reactor size can enhance efficiency, optimize assembly and reagent addition through the tight control of reagents, cellular aggregation and spheroid patterning in shorter time frames.

Herein, we describe a new platform strategy to rewire cell surfaces with bio-orthogonal groups via liposome fusion delivery and use microfluidic technology to control the rapid assembly of co-culture micro-tissues via an interfacial ‘click’ chemical reaction in flow. The interfacial bio-orthogonal groups delivered to the cell surfaces act as chemoselective molecular ‘velcro’ to induce a stable click (cell-cell) adhesion process.

As a methodology to deliver cargo to cells, liposome formulation and fusion is well-established for drug therapeutics and imaging technology.^{12 13} Many fundamental studies of lipid membrane fluidity and membrane biology have been advanced by using liposomes as model membranes.^{14 15} To design cells with the capability to associate with any other cell type we chose to modify cell surfaces with bio-orthogonal lipids as handles for ligation. Bio-orthogonal

chemistry is a powerful suite of chemical conjugation reactions that can ligate molecules in a physiological environment rapidly and without side reactions.¹⁶ The reactions have led to pioneering developments with many applications in cell biology and proteomics.^{17 18} To control the cell assembly process, we used microfluidic technology as a bioanalytical method to control spheroid morphology and subsequent tissue orientation. Microfluidic technology has revolutionized biomedical research and its programmable features have led to diverse innovations in genomics, cell sorting, material science and chemical research.^{19 20 21 22} However, until now microfluidic technology has not been used for assembling cells in flow to generate microtissues due to weak or non-existent cell-cell adhesion processes.

To rewire cell surfaces with chemical groups that function as bio-orthogonal molecular velcro, we first focused on the delivery strategy by generating two different liposome populations with complementary ligation groups. Figure 3.1 describes the cell surface tailoring strategy to generate complex co-culture tissue assemblies. We used the reaction between ketone groups and hydroxylamine groups, which form a stable and bio-orthogonal oxime as the ligation strategy. We have previously shown the utility of this strategy for making co-culture spheroids and thick tissue multi-layers.^{23 24 25 26} Each liposome pair was generated with background lipids of POPC and DOTAP with the incorporation of either ketone lipid (3) or hydroxylamine lipid (4) (Ratio POPC:DOTAP:Bio-orthogonal Lipid 49:49:2). Once formed, the ketone liposome (5) was then added to cells in culture (7) containing serum for 1 hour for rapid fusion and delivery of the ketone lipid to the cell surface (9). Similarly, hydroxylamine liposome (6) was added to a second cell type to generate hydroxylamine presenting cells (10). Upon the mixing of ketone (9) and hydroxylamine (10) presenting cells, rapid co-culture cell assemblies formed due to the fast and polyvalent oxime click chemistry ligation between cells. As a control, no cell assemblies

were generated when either the ketone or hydroxylamine groups were not present on the cell surface. Fluorescence-activated cell sorting (FACS) analysis was also used to determine the amount of bio-orthogonal lipid present on cell surfaces. Previous studies have shown cell viability is not affected by the liposome fusion method or the incorporation of bio-orthogonal lipids into membranes.²⁷

Current tissue engineering methodologies include polymeric scaffolds, decellularized scaffolds, organoid formation and layer by layer approaches. Polymeric scaffolds use synthetic polymers such as Poly Lactic-co-Glycolic Acid (PLGA), Poly Lactic acid (PLLA), Poly ethylene glycol (PEG) or natural materials such as collagen, Matrigel, elastin and agarose to embed or encapsulate cells into solid structures to create tissue-like constructs.²⁸ Although these methods of collecting individual contact inhibited cell lines into a solid macroscale structure can provide mechanical support, engineered growth factors and a adhesive substrate, they also have a number of drawbacks such as a lack of fine microscale structure, no initial or low subsequent cell-cell contact (signaling), low cell loading and most polymers tend to product toxic metabolic by-products. Decellularized scaffolds while providing the fine microstructure and large scale mechanical support of the original tissue, also provides signaling factors to newly perfused cells. Although these scaffolds seem to present a leap forward in tissue engineering, they suffer from similar disadvantages as polymer scaffolds such as low cell seeding density and little or no cell-cell contacts generated due to the limitations of the prepared cells, while also the scaffold can contain detrimental factors arising from the death of original organ tissue. Organoid structures developed from stem cell culture are excellent for the study of developmental biology are not suitable for large scale applications due to growth (time) restraints, manufacturing difficulties and unreliable induction of organ growth.

We propose that our CSE methodology for the rewiring of the cellular membrane will result in more advanced and stable tissue constructs for use as microtissues for biological research as well as macrotissues for the study of organ behaviour and tissue transplantation techniques. Our CSE technique for cell-cell assembly has incredible potential as both as a standalone methodology and a modular technique to improve existing tissue assembly technologies such as polymer scaffolding and cadaverous organ de-cellularization. Two important benefits of our CSE technology allow cell-cell contacts to form during contact but also enabling the integration of multiple cell types into a single tissue with microstructure such as epithelial single cell layer membranes in combination with other cells or mixed layers. This is beneficial for the development of physiologically relevant tumor models (containing cancerous and non-cancerous cell-types), as well as *in vivo* tissue mimics for system biology study. Since the CSE molecules delivered to the cell membrane are chemoselective for only complimentary labeled cells, layers can be easily incorporated into our designed tissues resulting in single layer or thick tissue structures commonly observed in *in vivo* tissues. These physical structures are incredibly important to the properties and function of *in vivo* tissues in many contexts such as the Blood Brain Barrier (BBB) or skin, acting as physical barriers to the environment or promoting specific cell-cell interactions.

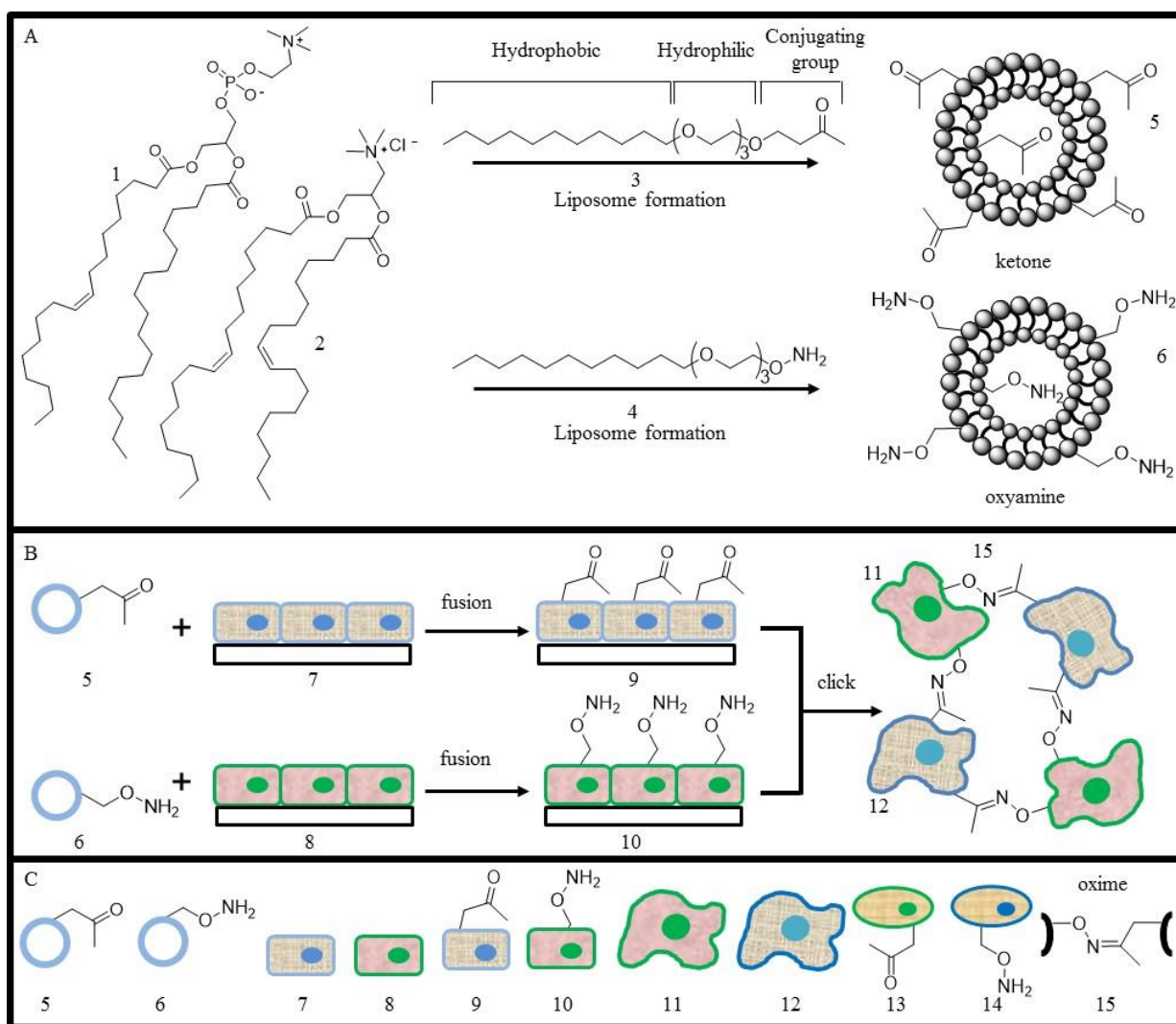


Figure 3.1: Schematic describing the cell surface tailoring strategy to generate complex co-culture tissue assemblies. The combination of bio-orthogonal lipids, liposome formation and liposome fusion result in the generation of engineered cell surfaces that can subsequently be assembled through an interfacial click reaction. (A) Bio-orthogonal liposomes are formed by mixing POPC (1), DOTAP (2) and either a ketone (3) or hydroxylamine (4) terminated presenting lipid-like molecule. (B) Cell surfaces were engineered to present ketones or hydroxylamines via liposome fusion and delivery. The tailored cells were then mixed and formed rapid assemblies via the bio-orthogonal oxime click ligation. (C) (5) ketone bearing CSE liposome, (6) hydroxylamine bearing CSE liposome, (7) or (8) separate native cells lines, (9) ketone CSE cell line, (10) hydroxylamine CSE cell line, (11) and (12) adhered or spread out cell line, (13) detached ketone CSE cell line, (14) detached hydroxylamine CSE cell line, (15) oxime bond formed upon reaction in cell culture conditions between hydroxylamine and ketone moieties.

3.2 Materials and Methods

3.2.1 Materials

O-dodecylhydroxylamine was synthesized as previously described.²³ 1-palmitoyl-2-oleoyl-sn-glycero-3-phosphocholine (POPC) and 1,2-dioleoyl-3-trimethylammonium-propane (DOTAP) were purchased from Avanti Polar Lipids (Alabaster, AL). All other chemicals were obtained from Sigma-Aldrich or Fisher Scientific. C3H/10T1/2 mouse embryonic fibroblast cells, RFP Expressing Human Neonatal Dermal Fibroblasts (HDNF), GFP expressing NIH3T3 cells were obtained from ATCC. Human mesenchymal stem cell (hMSC), hMSC basic, growth, and differentiation media were obtained from Lonza.

3.2.2 Cell Culture

C3H/10T1/2 were cultured in petri dishes at 37°C and 5% CO₂ with DMEM media containing 10 % fetal bovine serum (FBS) and 1 % penicillin/streptomycin (P/S). HDNF/RFP were maintained in DMEM containing 5 % FBS and 1 % P/S. The cell cultures used for experiments were between 3 and 8 passages. NIH3T3/GFP cells were cultured in Dulbecco's Modified Eagle Medium (DMEM) (Gibco), with 10% FBS, 0.1 mM MEM Non-Essential Amino Acids, 2 mM L-glutamine, 1 % P/S, and 10 µg/mL Blasticidin. 3T3 Swiss albino mouse fibroblasts were cultured in containing 10 % fetal bovine serum (FBS) and 1 % P/S at 37°C at 5 % CO₂. hMSCs were cultured in growth media at 37°C in 5 % CO₂. Adipogenic differentiation was induced by induction and maintenance media as described in the Lonza protocol.

3.2.3 Microfluidic Device Fabrication and Design

The microchannel was designed as a simple Y-shape, where cell suspensions are brought together in the Y-mixer channel. In order to make a simple, cheap and robust device, PMMA blocks were used as the substrate. The experimental devices with micron-sized channels were

created using laser ablation etching on PMMA blocks (1/8 in thickness, 1.25 in length and 1.42 in width). The channels were laser etched on the PMMA surface using Versalaser 2.30 with a CO₂ laser at 14.25 W power to produce parabolic channels with a measured base width of 170 μ m, a peak height of 200 μ m, and a channel length of 1.5 cm. The two fluid inlet connections were fabricated using 406 μ m (0.016 in) OD stainless steel capillary tubes with an 203 μ m (0.008 in) ID and a length of 2.0 cm, which were embedded into the PMMA blocks using thermal heating to be in line with the channel flow axes. The fluid outlet capillary was cut to 2.0 cm and embedded by thermal heating and applied pressure similar to the fluid inlets and then allowed to cool. The top block of PMMA is used to cap the channel through thermal bonding (with the etched bottom block) in a convection oven for 2 hours at 275°C and allowed to cool completely to 23°C for 2 hours under pressure. Once cooled, the fluid connections were completed by slipping poly ethyl ethylene ketone (PEEK) tubing (ID 203 μ m/ 0.008 in) over the metal capillary and sealed using epoxy resin (3M). Finally, high pressure HPLC 1 mL Luer lock glass syringes (Hamilton) were connected to the PEEK tubing using finger tight female Luer connectors (UpChurch Scientific).

3.2.4 Liposome Formation and Formulation

To prepare liposomes bearing ketone or hydroxylamine functionalities, 60 μ L of 2-dodecanone (10 mM in CHCl₃) or *O*-dodecylhydroxylamine (10 mM in CHCl₃) was mixed with 430 μ L POPC (10 mg/mL in CHCl₃) and 10 μ L of DOTAP (10 mg/mL in CHCl₃), and then thoroughly dried using N₂. After the CHCl₃ was evaporated, the lipid mixture was suspended in 3 mL of PBS, followed by tip sonication for 15 min until the suspension became clear.

3.2.5 Cell Surface Modification using Liposome Fusion

Once cells reached 90% confluency, 5% (v/v) liposomes (ketone or hydroxylamine bearing) were added to the cell culture media, and incubated with cells at 37°C and 5% CO₂ for 1 hour to create ketone- or hydroxylamine-tailored cells.

3.2.6 Microtissue Generation in Microfluidic Device

GFP and RFP cells were grown to approximately 90% confluency and then treated with hydroxylamine and ketone bearing liposomes, respectively using the standard protocol. Once the cells were surface engineered, they were washed 3 times with PBS and then detached by 0.25% trypsin/EDTA at 37°C and 5 % CO₂. Once the cells were detached and neutralized by DMEM media (10 % FBS), cell suspensions were transferred to separate 15 mL tubes and spun down at 800 RPM for 5 minutes. The supernatant was discarded, the remaining pellet was re-suspended in DMEM media to reach a final concentration of 4×10^6 /mL. Once the ketone and hydroxylamine-tailored cell suspensions were ready, 250 µL of each cell suspension was immediately loaded into separate sterilized 1mL gastight Luer lock Hamilton gas chromatography syringes. The connection tubing and microfluidic device were sterilized by passing 1 mL 70% ethanol solution, followed by 1 mL of PBS buffer. Once sterilized, the loaded syringes were finger tightened onto male Luer connections and placed onto a Harvard 11 PLUS syringe pump. The flow rate was set to 8 µL/min for 5 minutes to purge air bubbles from the system, then lowered to 0.4 µL/min for 5 minutes, where the fluid is discarded and the subsequent eluent was collected onto 1 cm² glass slides. The 1 cm² glass slides were prepared in advance and sterilized by sonication in 70 % ethanol solution for 30 min. The microfluidic experiments typically lasted around 45 minutes. Once experiments were complete, the collecting slides were transferred to tissue culture plates and incubated at 37°C and 5% CO₂ for 25 minutes.

The cells on the slides were then fixed using 3.8% formaldehyde solution for 15 minutes, followed by gentle washing with PBS. The cell samples were observed and imaged using a Nikon Eclipse TE2000-U Fluorescence Microscope.

3.2.7 Microtissue Generation vs. Flow Kinetics

Ketone and hydroxylamine engineered C3H/10T1/2 cells were collected to reach a specific cell density for cell cluster formation. Once the cell suspension with different cell densities were ready, 250 μL of each suspension was immediately loaded into separate sterile 1 mL gas-tight Luer lock Hamilton gas chromatography syringes. The connection tubing and microfluidic device were sterilized by passing 1 mL 70% ethanol solution, followed by 1 mL of PBS buffer. The loaded syringes are attached to the fluid system using Luer connectors and placed onto a Harvard 11 PLUS syringe pump. The flow rate was set to 8 $\mu\text{L}/\text{min}$ for 5 minutes to purge air bubbles from the system, then the flow rate was lower to the experimental flow rate (0.2 $\mu\text{L}/\text{min}$ -0.6 $\mu\text{L}/\text{min}$) for 5 minutes to discard fluid head before collecting cell clusters. Live cell images were obtained *in situ* at 10X using an Olympus CKX41 microscope to record cluster size and growth. Images of cell clusters were recorded at 0 mm, 7.5 mm, and 15.0 mm of the microfluidic channel (to collect data of cluster size), while flow rate and cell density were changed to study the relationship between microtissue generation and microfluidic flow conditions as shown in the 3D plot (Figure 3.4).

3.2.8 Confocal Microscopy of RFP/GFP 3D Co-culture Microtissues

To obtain confocal images of co-culture microtissues, GFP and RFP cells were grown to approximately 95% confluency and treated with hydroxylamine and ketone bearing liposomes respectively, using our standard protocol. Engineered cells (250 μL , $2 \times 10^6/\text{mL}$) were immediately loaded into separate sterilized 1 mL gas-tight Luer lock Hamilton gas

chromatography syringes, which were finger tightened onto male Luer connections and placed onto a Harvard 11 PLUS syringe pump. The flow rate was set to 8 $\mu\text{L}/\text{min}$ for 5 minutes to purge air bubbles from the system, and then lowered to 0.4 $\mu\text{L}/\text{min}$ for 5 minutes. After that, cell collection began. Flow experiments were performed for 3 hours, before the collecting slides were transferred to tissue culture plates and incubated at 37°C and 5% CO_2 . After culturing the cell clusters for 12 hours, cell samples were fixed with 3.8% formaldehyde, washed with PBS and mounted onto thin glass slides with LIGHT DIAGNOSTICS Mounting Fluid (Millipore) for 3D confocal microscopy using a Zeiss LSM 700.

3.2.9 Confocal Microscopy of Three-cell line (red/green/blue) Microtissues

To generate microtissues composed of three-cell lines to be observed then by confocal microscopy, hydroxylamine engineered C3H/10T1/2 cells were treated with 0.3 % v/v of CellTracker™ Blue CMAC (Life Technologies) for 45 minutes, and then mixed with ketone engineered GFP cells and RFP cells. Blue-stained C3H/10T1/2 cells presenting hydroxylamine ($4 \times 10^6/\text{mL}$) were loaded into a 1 mL Hamilton glass syringe, while ketone engineered GFP cells ($2 \times 10^6/\text{mL}$) and ketone engineered RFP cells ($2 \times 10^6/\text{mL}$) were loaded into another 1 mL Hamilton glass syringe. The two syringes were connected to the microfluidic device and the flow rate was set at 0.4 $\mu\text{L}/\text{min}$. Cell clusters were dispensed onto 1 cm^2 glass slides for 45 minutes and then incubated in tissue culture plates for 12 hours at 37°C with 5 % CO_2 . Cell samples were fixed with 3.8% formaldehyde, washed with PBS and mounted onto thin glass slides with LIGHT DIAGNOSTICS Mounting Fluid (Millipore) for 3D confocal microscopy using a Zeiss LSM 700.

3.2.10 Three-Dimensional Co-culture 3D Multi-Layers of HMSCs and NIH3T3 Fibroblasts

HMSCs and NIH3T3 fibroblasts were surface engineered with ketone and hydroxylamine liposomes respectively. NIH3T3 fibroblasts presenting hydroxylamines were then trypsinized and added (10^5 cells/mL) to the hMSCs. These cells were co-cultured in adipogenic induction hMSC Adipogenic BulletKit media (Lonza), hMSC Fibroblast BulletKit media (Lonza) and hMSC Osteogenic BulletKit media (Lonza) resulting in the 3D multi-layered, tissue-like structures of adipocytes, NIH3T3 fibroblasts and osteoblasts using the standard Lonza protocol. The 3D co-cultures were fixed after one day and two weeks using formaldehyde (4 % in PBS, 30 minutes). Substrates were then immersed in a solution containing water and 60 % isopropyl alcohol (3-5 minutes), followed by staining with Oil Red O (5 minutes) and Harris Hemotoxylin (1 minute). Substrates were visualized by phase contrast microscopy using a Zeiss inverted microscope.

3.2.11 Collagen Based RFP and GFP Tissue Formation (Fig. 3.7 O,P)

To make macro-size ($2 \times 2 \text{ cm}^2$) robust tissue, collagen was introduced. Hydroxylamine tailored GFP cells (2 mL, $4 \times 10^6/\text{mL}$) and ketone tailored RFP cells (2 mL, $4 \times 10^6/\text{mL}$) were loaded into the microfluidic device to generate RFP/GFP microtissue. The flow rate was set to $8 \mu\text{L}/\text{min}$ for 5 minutes to purge air bubbles from the system, and then lowered to $0.4 \mu\text{L}/\text{min}$ for 5 minutes. After that, cell collection began. Cell clusters were collected onto a $2 \times 2 \text{ cm}^2$ slide loaded with liquid collagen solution. Following collection, the collagen/cell hybrid was transferred to a tissue culture plate and incubated at 37°C and 5 % CO_2 for 30 minutes to allow the collagen solution to solidify. Cell culture media was then added and the collagen/cell hybrid tissue was incubated for 12 hours before being carefully peeled off the glass slide. The collagen supported macrotissue was then fixed with 3.8% formaldehyde, washed with PBS and mounted onto thin glass

slides with LIGHT DIAGNOSTICS Mounting Fluid (Millipore) for 3D confocal microscopy using a Zeiss LSM 700.

3.2.12 Three-Dimensional Oriented Co-culture Multi-layers (RFP-GFP-RFP, thin) (Fig. 7E, F)

Microscope glass cover slips were cut into small pieces in advance and placed into a 96-well microplate. RFP cells were grown on slips in the microplate and grown to 95 % confluency. Through standard liposome treatment, the RFP cells were surface engineered to present ketone groups. GFP cells presenting hydroxylamine (200 μ L, 5×10^5 /mL) were then loaded by the standard microfluidics procedure onto the ketone tailored RFP cells and cultured for 12 hours. After removing most of the media, ketone tailored RFP cells (200 μ L, 5×10^5 /mL) were loaded into the wells by microfluidics and cultured for 6 hours. The slips inside the microplate were then gently removed and fixed in 3.8 % formaldehyde, washed with PBS and mounted onto thin glass slides with LIGHT DIAGNOSTICS Mounting Fluid (Millipore) for 3D confocal microscopy using a Zeiss LSM 700.

3.2.13 Three-Dimensional Oriented Co-culture Multi-zones (RFP-GFP-RFP, thick) (Fig. 3.7 G, H)

Microscope glass cover slips were cut into small pieces in advance and put into a 96-well microplate. Ketone tailored RFP cells (150 μ L, 1×10^6 /mL) and hydroxylamine tailored RFP cells (150 μ L, 1×10^6 /mL) were loaded by standard microfluidics procedure onto the cover slips in the microplate, and cultured for 12 hours. After removing most media, ketone tailored GFP cells (150 μ L, 1×10^6 /mL) and hydroxylamine tailored GFP cells (150 μ L, 1×10^6 /mL) were loaded by microfluidics onto the RFP cells, and then cultured for 12 hours. After removing most media, ketone tailored RFP cells (150 μ L, 1×10^6 /mL) and hydroxylamine tailored RFP cells (150

μL , $1 \times 10^6/\text{mL}$) were loaded by microfluidics again, and cultured for 6 hours. The slides inside the microplate were then gently picked up and fixed in 3.8 % formaldehyde, washed with PBS, and mounted onto thin glass slides with LIGHT DIAGNOSTICS Mounting Fluid (Millipore) for 3D confocal microscopy using a Zeiss LSM 700.

3.2.14 Oxime Bond Formation (Synthesis of 2-(propan-2-ylideneaminoxyl)acetic acid)

To a 10 mL flask containing a magnetic stir bar, 100 mg (1.1 mmol) of *o*-(Carboxymethyl)hydroxylamine hemihydrochloride was added and purged with Argon gas. Freshly distilled acetone (3 mL) was then added using a syringe and stirred at 23°C for 4 hours. Excess acetone was removed using a rotary evaporator to (0.140 g, 99 %) convert to the oxime product 2-(propan-2-ylideneaminoxyl) acetic acid as a white solid. ^1H -NMR (D_2O , 300 MHz): δ 4.45 (s, 2H), 1.85 (s, 3H), 1.79 (s, 3H); ^{13}C -NMR (D_2O , 400 MHz): δ 175.45, 160.82, 69.81, 20.61, 15.31.

3.2.15 Oxime Hydrolysis Analysis

Oxime hydrolysis experiments were conducted by adding (1.5 mg, 11 μmol) 2-(propan-2-ylideneaminoxyl) acetic acid into five separate scintillation vials, followed by preparation of 0.1 M buffered D_2O solutions using pyridine (pH 11.0), sodium bicarbonate (pH 8.0), PBS (pH 7.4), sodium carbonate (pH 5.0) and sodium formate (pH 3.0), respectively. Once the 5 separate samples of 2-(propan-2-ylideneaminoxyl) acetic acid were dissolved in 0.5 mL each of the pH buffered D_2O solutions, their respective NMR spectra were taken ($n=8$). Data was gathered initially at 3 hour intervals, followed by once a day, then once a week to determine the rate of hydrolysis of the starting material.

3.2.16 Oxime Formation Kinetics Conditions

Pseudo-first order rate experiments were conducted using ^1H -NMR (300 MHz) spectroscopy. These experiments were performed in typical NMR tubes by dissolving methhydroxylamine hydrochloride (1.5 mg, 83.52 g/mol, 18 μmol) and freshly distilled acetone (150 μL , distilled over drying agents) in 0.25 mL PBS buffered D_2O (pH 7.4) at 37.0°C, respectively. The two solutions were quickly mixed together in the NMR tube and placed into the spectrometer. The first time point was taken immediately, with subsequent data points recorded every 40 seconds. This experiment was repeated using 2-(propan-2-ylideneaminoxyl) acetic acid (11 mg, 109.30 g/mol, 11 μmol) dissolved in 0.25 mL PBS buffered D_2O (pH 7.4) in a NMR tube at 37.0°C. Freshly distilled acetone was added into 0.25 mL PBS buffered D_2O (pH 7.4) and warmed to 37.0°C. The two solutions were then mixed in a NMR tube and placed into the spectrometer. The first time point was taken immediately, with subsequent data points recorded every 40 seconds.

3.2.17 Spheroid Movies in Flow Experimental

The microfluidic device was mounted on a Nikon Eclipse TE2000-U Fluorescence Microscope. Ketone engineered GFP cells ($2 \times 10^6/\text{mL}$) and hydroxylamine engineered GFP cells ($2 \times 10^6/\text{mL}$) were prepared in PBS and loaded into the Hamilton glass syringes separately. The two syringes were connected to the microfluidic device and flow rate was set at 0.4 $\mu\text{L}/\text{min}$. Live recording of the two cell populations flowing through the microfluidic channels were taken automatically by the microscope over 10-20 second intervals.

3.2.18 Stem Cell Differentiation in Co-culture

hMSCs were induced to differentiate for 2 weeks. Total RNA was then extracted using a RNA isolation kit (Qiagen). 1 μg of total RNA was converted to cDNA using AMV reverse transcriptase and random hexamer primers (Promega). The resulting cDNA was used in PCR

with the following primer, LPL (sense 5'-GAG ATT TCT CTG TAT GGC ACC-3', antisense 5'-CTG CAA ATG AGA CAC TTT CTC-3'), PPAR γ 2 (sense 5'-GCT GTT ATG GGT GAA ACT CTG-3', antisense 5'-ATA AGG TGG AGA TGC AGG CTC-3'), Collagen I (sense 5'-TGC TGG CCA ACC ATG CCT CT-3', antisense 5'-TTG CAC AAT GCT CTG ATC-3'), Collagen II (sense 5'-ATG ACA ACC TGG CTC CCA AC-3', antisense 5'-GCC CTA TGT CCA CAC CGA-3'), RUNX2 (sense 5'-GAT GAC ACT GCC ACC TCT GAC TT-3', antisense 5'-CCC CCC GGC ACC ATG GGA AAC TG-3'), ALPL (sense 5'-CCA TTC CCA CGT CTT CAC ATT-3', antisense 5'-GAG GGC CAG CGC GAG CAG CAG GG-3'), at annealing temperatures of 52°C, 55°C, 53°C, 57°C, 61°C, 66°C, respectively. Amplification reactions were carried out for 1 min through 30 cycles and the reaction products were subjected to 1 % agarose gel electrophoresis. The reaction products are 276 bp (LPL), 351 bp (PPAR γ 2), 489 bp (Collagen I), 359 bp (Collagen II), 362 bp (RUNX2), and 418 bp (ALPL), respectively.

3.3 Results and Discussion

To rapidly generate co-culture assemblies based on bio-orthogonal ligation chemistry in microfluidic flow, we determined that the inter-cell surface reaction to be fast and stable. Several bio-orthogonal strategies were available, including Diels-Alder and Huisgen 3+2 copper catalyzed cyclo-additions but we chose oxime ligation involving the reaction between hydroxylamine and ketone groups due to their ease of incorporation into simple lipid-like molecules. Figure 3.2 describes the kinetics of formation and stability of the oxime reaction at physiological conditions (pH 7.4, 37°C). In solution, a model reaction forms the oxime with a half-life of approximately 9 seconds and is stable for many weeks with minimal hydrolysis. However, we surmised that on the surface of a cell oxime formation would be several orders of magnitude faster, due to the polyvalent nature and fluid mosaic ability of the membrane allowing

for the ketone and hydroxylamine lipids within the membrane to rapidly diffuse and thus dramatically change their local concentration density.

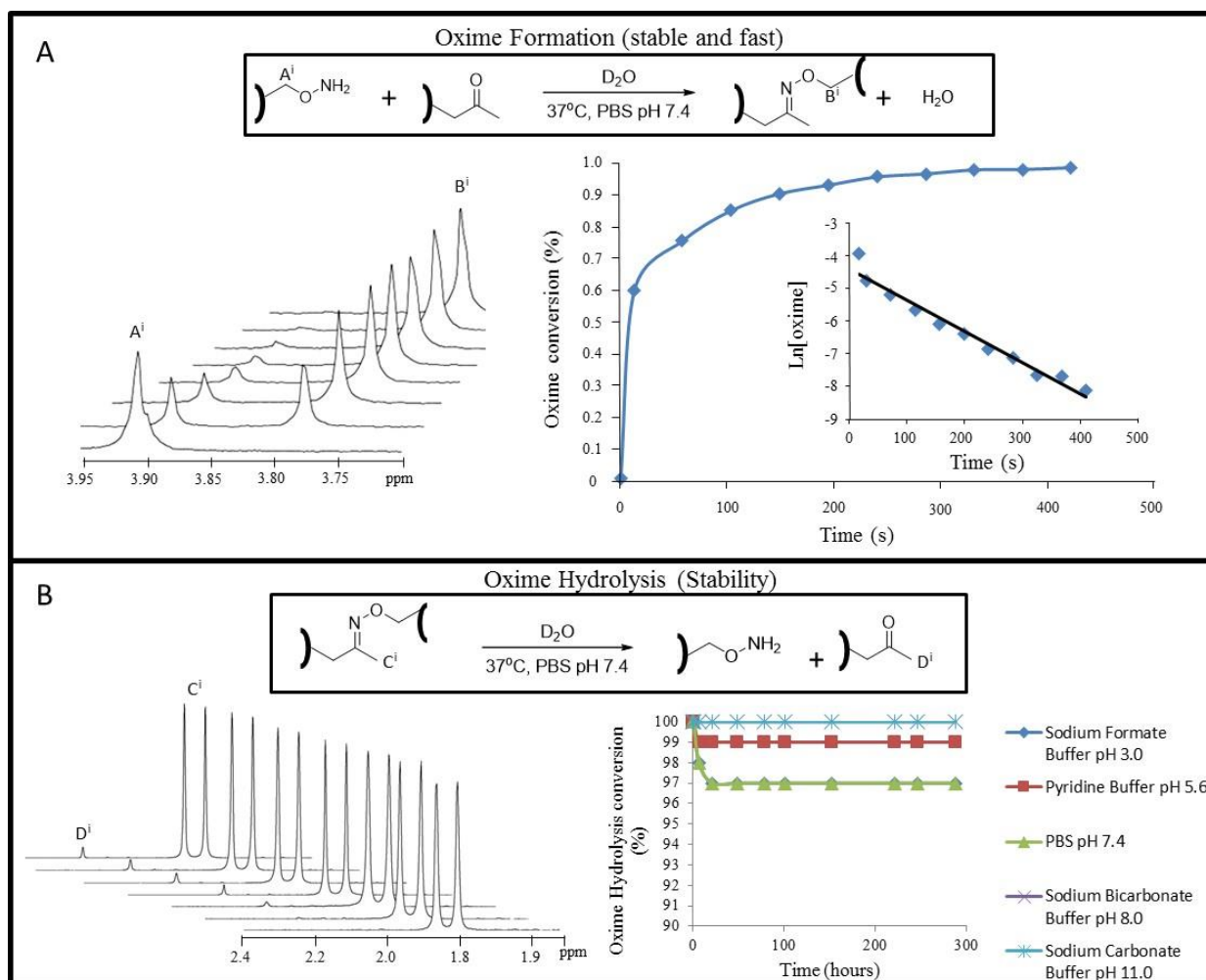


Figure 3.2: Nuclear Magnetic Resonance (NMR) study of the kinetics and stability of the bio-orthogonal oxime conjugation reaction at physiological conditions under pseudo first order condition. (A) The reaction of a ketone and hydroxylamine at physiological conditions results in the rapid formation of the covalent and stable oxime bond. The alpha proton of the hydroxylamine (A^i) was compared to the oxime alpha proton (B^i) to obtain a ratio of starting material to product to calculate conversion and rate constant. ^1H -NMR was used to determine the oxime formation kinetics ($k=0.98 \times 10^{-2} \text{ Ms}^{-1}$, $t_{1/2} = 9 \text{ sec}$). (B) The stability of the oxime bond was studied under hydrolytic conditions with ^1H NMR using a variety of biological buffers (pH 3.0, 5.6, 7.4, 8.0 and 11.0). The oxime product was formed with high purity and studied using the alpha oxime proton (C^i) and compared to the alpha keto proton of the ketone hydrolysis product (D^i). The oxime bond was stable with no hydrolysis observed after 3 weeks in pH 3.0 and 5.6. At physiological conditions (pH 7.4), there was a 3 % hydrolysis over 3 weeks.

Figure 3.3 describes the overall strategy for the generation of co-culture assemblies in microfluidic flow using potential automated systems. First, multiple different cell lines were cultured in microwell plates as single monolayers. To these cell cultures, liposomes with either ketone or hydroxylamine groups were added, which rapidly fuse and tailor the cell surfaces. These cells were then detached and transferred to the standard Y-joint PMMA microfluidic device. Each inlet of the microfluidic channel injects a separate cell line tailored with either the ketone or hydroxylamine groups. As the cells flow through, they arrive at the mixing channel where they come in contact and collide with the complimentary CSE cells, instantly forming adhesions due to the inter-cell polyvalent bio-orthogonal oxime reaction. As the spheroid assemblies flow through the channel they associate with more cells to generate larger spheroids. As the microtissues flow through the channel they were deposited onto microwells to form 3D multi-layer tissues. This microfluidic and CSE strategy allows for the rapid assembly of complex co-culture tissues for studies of spheroid autocrine and paracrine signalling, tumours and the formation of 3D multi-layer tissues for a range of applications. Controls clearly show that no cell assemblies form when cell surfaces do not present the oxime pair. Furthermore, only a monolayer or single cells in solution are generated when either the ketone or hydroxylamine is absent on the cell surfaces.

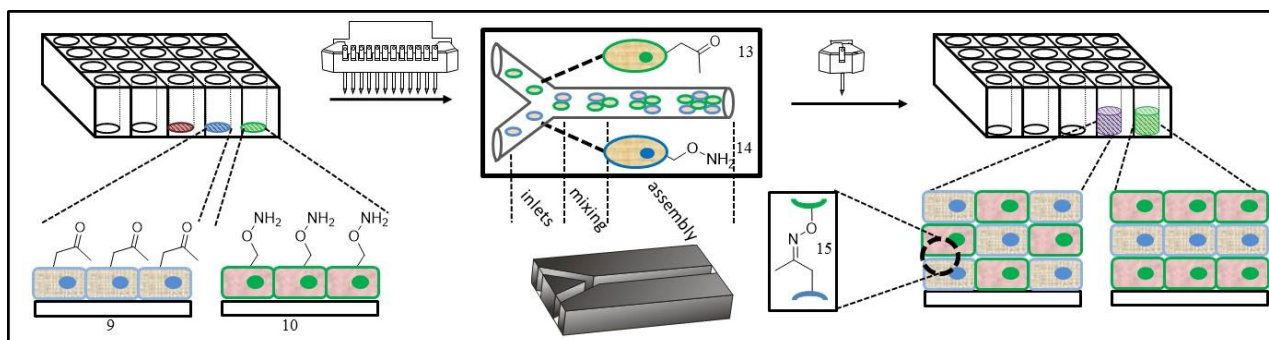


Figure 3.3: Schematic describing the use of microfluidic technology and tailored cell lines to generate multi-layer co-culture tissues. (Left) Different cell lines were grown in microwell arrays to generate 2D contact inhibited single layers. Liposomes containing either ketone or hydroxylamine are added to the microwells. The liposomes quickly fuse to the cells and deliver the functional groups to rapidly produce engineered cell surfaces presenting ketone (9) or hydroxylamines (10). (Middle) The engineered cells are then transferred via pin arrays to a simple microfluidic device. As the cells are flowed through the channels they come into contact and assemble into co-culture spheroids through oxime click chemistry. The size of the spheroids are determined by flow rate, cell concentration and length of the assembly chamber. (Right) The spheroids are then transferred to a microwell plate where they adhere and form co-culture multi-layered 3D tissues. As controls, cells without the bio-orthogonal functional groups produce no spheroids upon mixing in the microfluidic channels and results in no 3D assemblies produced, where only standard 2D single cell layer sheets are formed.

Figure 3.4 presents various images of spheroid sizes generated along the length of the microchannel. Figure 3.4A describes the relationship between the spheroid size generated versus flow rate and position within the channel. As the flow rate decreases and the position along the channel increases, the size of the spheroid clusters become larger. It is remarkable that the oxime ligation chemistry between cells can adhere cells together while subjected to shear forces under flow conditions. The generated spheroids and multi-layers are stable, do not fall apart or require additional support, such as entrapment within Matrigel® or other polymer based scaffolds.

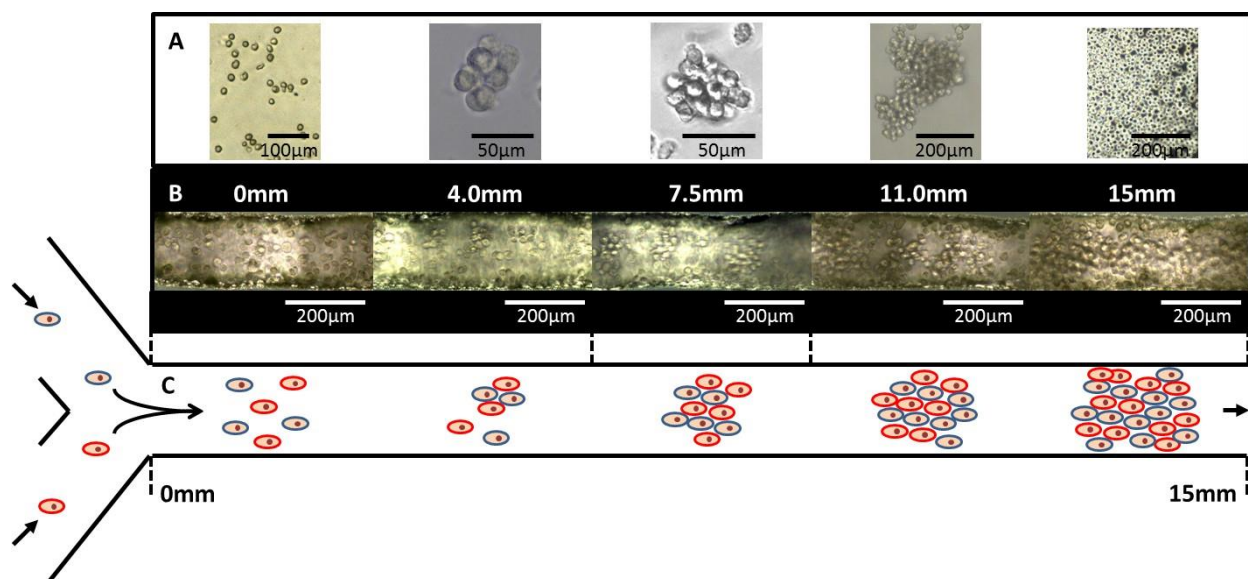


Figure 3.4: Images of cells at various stages of assembly in the microfluidic channel device. (A) Illustration of the PMMA microfluidic device showing the flow of cells in the Y-joint followed by mixing and assembly at different lengths of the channel. (B) Images of cells flowing through the microfluidic device at different flow points. Larger spheroid cell assemblies are produced at longer lengths of the channel. (C) Images of representative cell cluster (20X) sizes at different flow points along the channel.

To generate a range of co-culture spheroids by microfluidic assisted assembly, we used several fluorescent cell lines tailored with the bio-orthogonal lipids. Figure 3.5 shows a description of the polyvalent nature of the inter-cell co-culture oxime spheroid assembly. GFP and RFP cells were used to demonstrate the assembly of co-culture cells in flow. By adjusting the initial cell density flowed through the channels, several different co-culture cell ratio spheroids could be generated. By adjusting the ratio (stoichiometry) of the two cell types many different co-culture assembly combinations could be generated. For example, in Figure 3.5C an 8:1 ratio of RFP to GFP cells flowed through the channels resulted in spheroids containing a single RFP surrounded by GFP cells. Figure 3.5E shows three cell types forming spheroids by combining equal numbers of RFP-ketone, GFP-ketone and blue live-dye –hydroxylamine cells. Figure 3.5F-G shows GFP and RFP cell spheroid formation based on two sets of cells with

complementary ketone and hydroxylamine cell surface chemistry. Figure 3.5H shows fluorescent and bright field combined images of a 1:1 RFP to GFP cell spheroids.

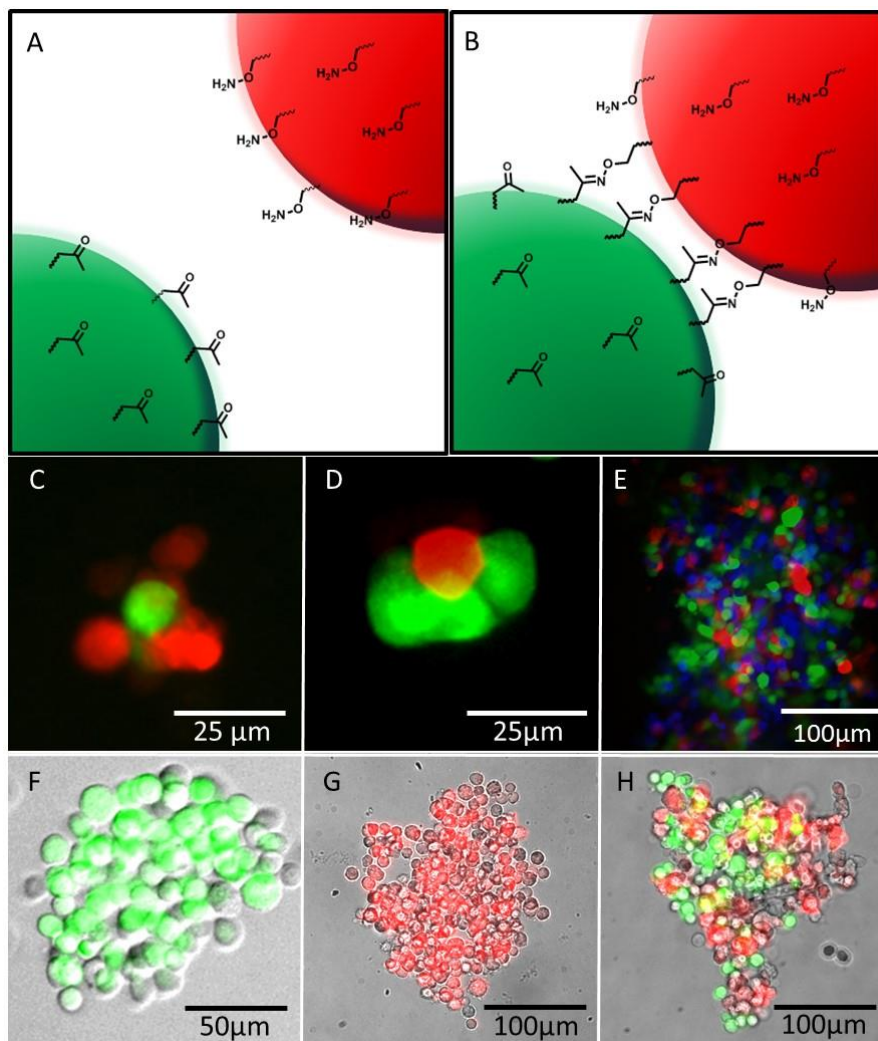


Figure 3.5: Schematic illustration and fluorescent images of co-culture spheroid assembly via click chemistry ligation. (A, B) Illustration of co-culture assembly based on oxime ligation between two different cell types. (C, D) Images depict how changing the ratio of input cells in microfluidic flow result in different ratios of co-culture spheroids. A 8:1 ratio (RFP:GFP) of cell input results in a single NIH 3T3/GFP cell surrounded by HDNF/RFP cells (C). Reversing the ratio to 1:8 (GFP:RFP) results in a single HDNF/RFP cell surrounded by NIH 3T3/GFP cells (D). (E) Image of a large 3 cell type spheroid generated by mixing of a 1:1:1 ratio of GFP:RFP:Blue C3H10T1/2 cells CMAC (7-Amino-4-Chloromethylcoumarin) in flow. The GFP and RFP cells presented ketones and the Blue cells presented hydroxylamine groups. (F) A large spheroid of GFP cells obtained by combining two different populations of GFP cells that present ketone and hydroxylamine groups. (G) A large spheroid of RFP cells obtained by combining two different populations of RFP cells that present ketone and hydroxylamine groups. (H) A large spheroid of

RFP and GFP cells obtained by flowing a 1:1 ratio of cells in the microfluidic device. By adjusting the flow rate, cell density and ratio of cell density inputs a range of stoichiometric co-culture spheroid assemblies and size of spheroids could be generated.

Figure 3.6 depicts a 3D plot of spheroid cluster size of complimentary CSE cells in our microfluidic device by adjusting the flow rate, reaction time and injected cell density. The assembly of spheroids in microchannels can be accurately controlled through the careful selection microfluidic conditions for different cell assembly applications, although in this work resulting spheroids were imaged but not used for subsequent experiments. Figure 3.6 demonstrates an inverse relationship of cluster size to flow rate, where doubling of flow rate from 0.2 to 0.4 $\mu\text{L}/\text{min}$ results in a 54% reduction in average cluster size from 22.6 to 10.3 cells per spheroid cluster. This was not a surprising result, as increasing shear stress as a result of laminar flow ($\text{Re} \sim 1$) from increased flow rate would prevent cell-cell assembly from initiating. Channel distance or residence time in channel for assembly to occur had a roughly linear positive relationship to cluster size, where doubling the channel length resulted in a doubling of cluster size. Increasing the injected cell density results in increasing cluster size but is not linear due to laminar flow which prevents turbulent mixing of cells in the microchannel (relatively large 10 μm spheres) and relies on diffusion mixing calculated to be ($T_{\text{diff}} = 13110 \text{ min}$) across the width of the microchannel. Therefore high densities are necessary for spheroid assembly to occur while lower densities (500K cells/mL) do not result in spheroid assembly (Supplementary Info.).

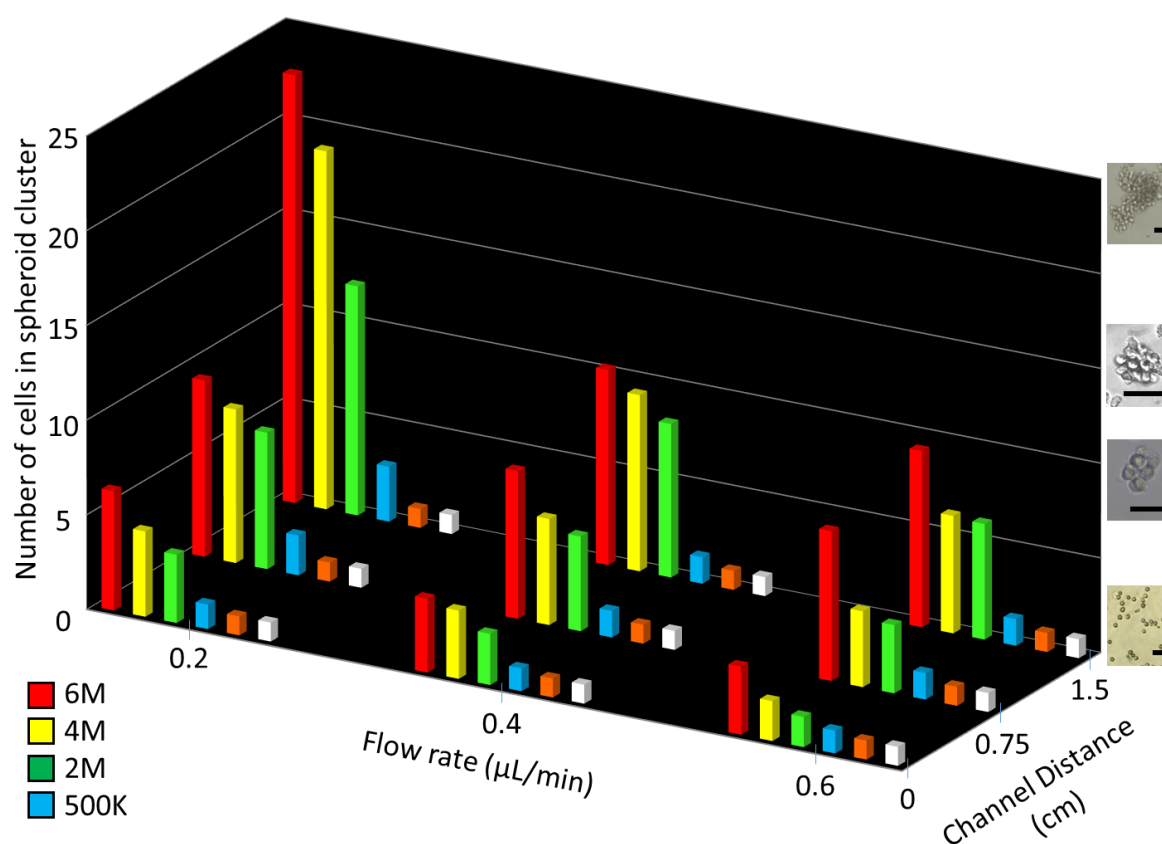


Figure 3.6: 3D plot representing the relationship between flow rate, channel distance, cell density, and resulting cell cluster size (spheroid) assembled within a microfluidic channel. As the cell density increases and flow rate decreases, spheroids assemble at a faster rate. The absence of one (orange) or both (white) surface chemistries results in no spheroid formation. Statistical analysis showed cluster size was within 5 % for each condition. Images of cellular clusters consist of representative samples of eluted cell clusters. Scale bars (left side) = 50 μm .

To demonstrate the flexibility of this methodology, several co-culture assemblies were generated via microfluidic flow and evaluated. Figure 3.7A-B shows a control monolayer of GFP expressing cells that are contact inhibited in culture. Without the bio-orthogonal click chemistry on the cell surface, most cells adhere and proliferate until they become contact inhibited and form a single monolayer in the x-y plane in culture. These cells do not grow on top of each other (in the Z plane, vertical direction) in normal standard cell culture *in vitro* conditions. However, upon delivering bio-orthogonal lipids via liposome fusion the cells will form co-culture multi-

layers in the Z plane to form multi-layers or 3D tissues. Figure 3.7C-D shows confocal images of RFP and GFP cells assembled sequentially in microfluidic flow and then deposited onto cell culture dishes to generate oriented co-culture layers. Complex zones of varying thickness of multiple cell lines (GFP and RFP) can be generated by simple alteration of the number of cells and sequence of cell deposition (Figure 3.7E-H). By depositing many cells onto each other using bio-orthogonal chemistry thick layers can be formed and cells proliferate. As described previously, the ketone and hydroxylamine lipids dilute over time on the cells via a transient transfection model while naturally excreted ECM is produced by the cells taking over as the tissue adhesive.²⁹

Therefore, the oxime chemistry is slowly diluted and the ECM holds the tissue layers together. Figure 3.7K-L, shows a thick multi-layer of hMSC and fibroblast cells that can be induced to differentiate distinct lineages based on the orientation of the cells within the multi-layer (stem cell studies). Figure 3.7M-N shows the formation of 3 cell types in a mixed multi-layer via bio-orthogonal chemistry. RFP and GFP ketone containing cells were mixed with blue (CMAC) stained hydroxylamine cells and assembled spheroids in microfluidics, then deposited onto tissue culture plates to generate 3D mixed multi-layers consisting of 3 cell lines. Figure 3.7O-P shows the combination of the cell assembly click strategy combined with collagen scaffolds. Upon cell seeding, the collagen scaffold is filled with cells almost instantly since bio-orthogonal cells can simultaneously adhere to each other and to the collagen scaffold. This strategy allows for a very high cell seeding density, which causes rapid filling of polymer scaffolds or de-cellularized materials.

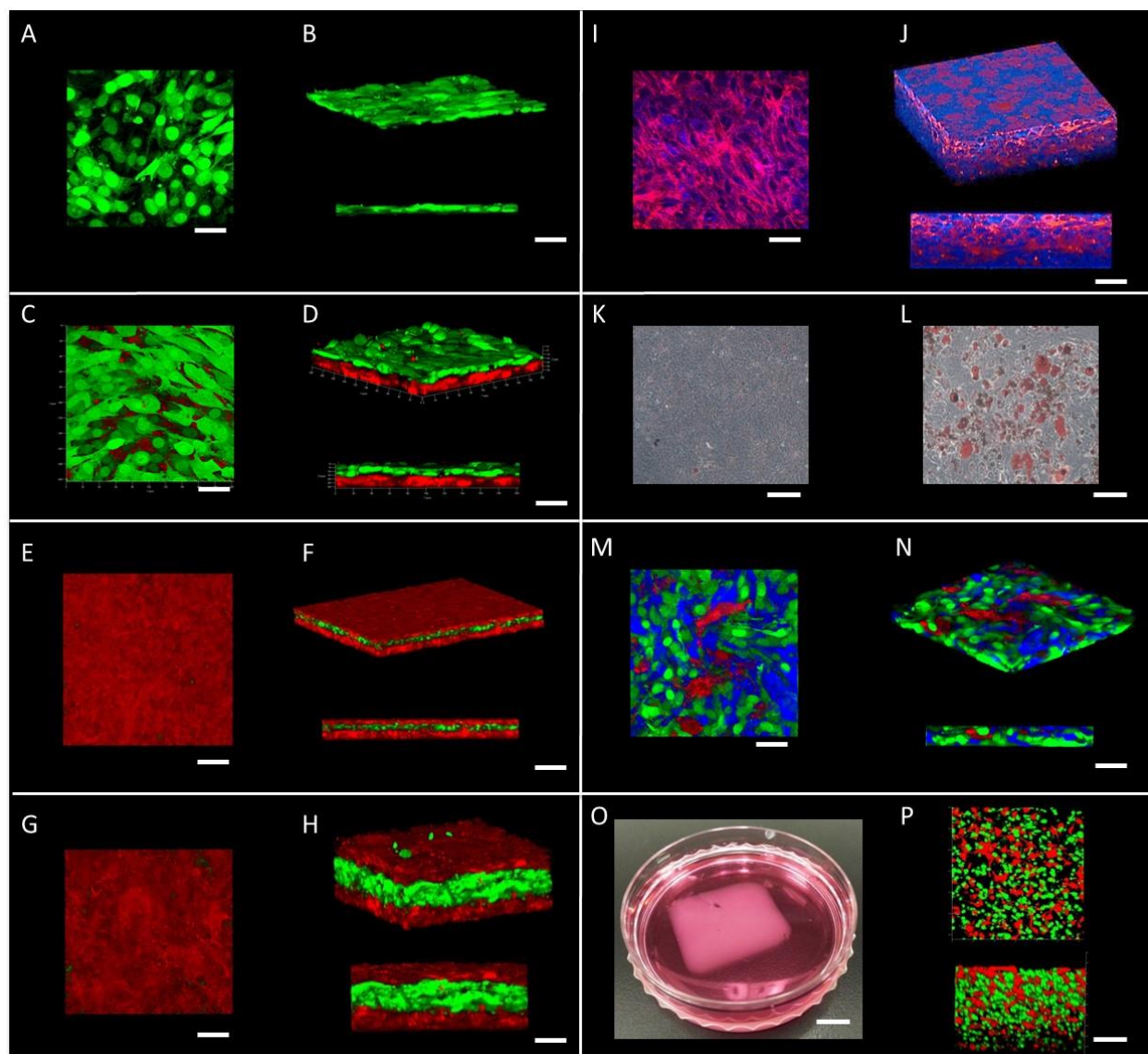


Figure 3.7: A range of confocal and bright-field images of various combinations of NIH 3T3/GFP, HDNF/RFP, Blue live stain C3H/10T1/2 pluripotent embryonic fibroblast stem cells, hMSC cells and NIH3T3 cells. (A) Top view of a standard contact inhibited single monolayer of NIH 3T3/GFP cells in culture. (B) Angle and side view of monolayer showing a thickness of approximately 6 μm . (C) Top view image of RFP-GFP bilayer multi-layer generated by first assembly in microfluidic flow of GFP spheroids followed by deposition onto glass slides to generate GFP multi-layer. To this GFP multi-layer, RFP spheroids were added as they were generated in microfluidic flow. The sequential spheroid and multi-layer generation resulted in a bilayer of multi-layers of GFP and RFP cells (30 μm thick). (E, F, G, H) Image of serial RFP and GFP spheroid assembly in flow followed by sequential deposition resulted in control of co-culture orientation multi-layers and thickness (E, F, 30 μm thick) (G, H, 120 μm thick). (I, J) Image of Tetramethylrhodamine (TRITC) and 4',6-diamidino-2-phenylindole (DAPI) stained thick multi-layers of NIH3T3 fibroblasts (140 μm thick). (K, L) Brightfield image of multi-layers of hMSC cells mixed with NIH3T3 fibroblasts. (L) After culturing for 10 days the hMSC cells differentiated

to adipocytes in the co-culture. (M, N) Image of 1:1:1 RFP:GFP:Blue C3H/10T1/2 cells mixed multi-layers generated by assembly in flow followed by deposition onto glass slides. The RFP and GFP cells presented ketones and the Blue cells presented hydroxylamines. (O) Photograph of a 2 cm x 2 cm x 0.5 cm thick collagen tissue containing RFP-ketone and GFP-hydroxylamine cells. Spheroids of RFP:GFP cells were generated in flow and then mixed with collagen. (P) Top and side views of co-culture cells in collagen. High cell density within collagen was achieved by the adhesion of large spheroids. The cells adhere to the collagen and to each other, therefore generating high cell density thick tissues instantly.

To demonstrate the utility of our CSE methodology, a series of experiments were performed using the microfluidic scaffold-free co-culture formation of hMSCs and fibroblasts to determine differentiation under CSE assembly (Figure 3.8). Ketone and hydroxylamine presenting hMSC and Swiss 3T3 fibroblasts were mixed and induced with differentiation factors to form adipocytes, fibroblasts and osteoblasts using typical induction conditions. The cells were assembled into multi-layer cultures and assayed after 1 day and 2 weeks to establish a lineage. Figure 3.8A-F demonstrates the stability and expression of gene markers over long periods for lineage differentiation. This demonstrates the utility of the CSE assembly methodology to study

the influence of second cell types in stem cell niche-like conditions that may alter rate and final differentiation lineage.

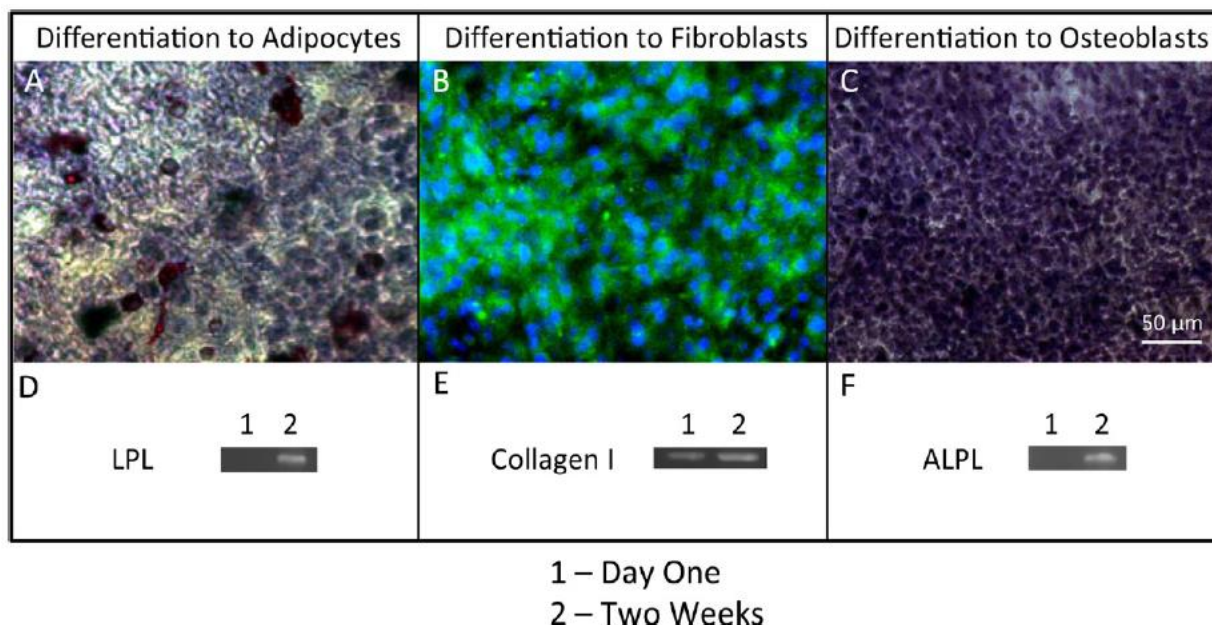


Figure 3.8: Construction of a 3D tissue co-culture system via intercell click ligation and application to stem cell differentiation. (A–C) Co-culture system of hMSCs/fibroblasts were assembled and then made to differentiate to adipocytes (A), fibroblasts (B) and osteocytes (C) via corresponding induction conditions. Adipocytes, fibroblasts and osteoblasts were stained red, green and blue, respectively. Images were taken by phase contrast microscopy (20X). Corresponding gene markers (LPL for adipocytes, Collagen I for fibroblasts, ALPL for osteoblasts) were studied over 2 weeks. (1: day one; 2: 2 weeks) and are represented by the gels shown in D, E and F, respectively.

3.4 Conclusion

In summary, we have developed a straightforward strategy to rapidly generate co-culture cell assemblies and tissues in flow using bio-orthogonal groups to rewire cells. Liposome fusion delivery of the bio-orthogonal lipid like groups to the cell surface is efficient, fast and inexpensive. The cell surface oxime ligation strategy is kinetically well behaved, stable and allows for rapid complex co-culture and multi-layer tissue construction. It is also simple to incorporate existing cargo strategies within the liposomes for simultaneous delivery of payloads and lipid molecules to surfaces for multiplex applications, ranging from imaging to theranostics

(combined diagnostics and therapy agents). Due to the flexibility of the methodology, many other click chemistry reactions may be used and multiple different click chemistries can be incorporated on cell surfaces simultaneously. These methods can be used to tailor surfaces with a range of molecules, probes, biomolecules and nanoparticles. Since there is no metabolic biosynthetic manipulation of the cells, a large scope of novel cell surface capabilities may be possible through bio-orthogonal conjugation. Furthermore, autocrine, paracrine, tissue or spheroid studies and regenerative medicine applications are now available due to the ease of delivery and manipulation of primary cell surfaces. By using more complex microfluidic technology it may be possible to incorporate multiple cell lines with *in situ* liposome fusion in flow, followed by cell sorting to engineer cells in various ways. Since the rewired cell acts as the scaffold, there is no need to use polymers for tissue construction due to the efficient cell economy assembly process. However, the methodology can also be complementary to polymer scaffolds, allowing for the rapid filling of molds as cells can adhere to each other and to the polymer. The ability to generate spheroids, thick multi-layers and oriented architectures may have applications in generating various skin and tissue chips for drug screening or tissue grafting and replacement. CSE has the potential to greatly impact clinical and basic science research, enabling faster and more in-depth studies using easily generated 3D tissue models and cellular manipulation.

3.5 References

- (1) Sutherland, R. M. *Science* (80-.). **1988**, 240 (4849), 177–184.
- (2) Torisawa, Y.; Takagi, A.; Nashimoto, Y.; Yasukawa, T.; Shiku, H.; Matsue, T. *Biomaterials* **2007**, 28 (3), 559–566.
- (3) Tejavibulya, N.; Youssef, J.; Bao, B.; Ferruccio, T.-M.; Morgan, J. R. *Biofabrication* **2011**, 3 (3), 34110.
- (4) Gartner, Z. J.; Bertozzi, C. R. *Proc. Natl. Acad. Sci. U. S. A.* **2009**, 106 (12), 4606–4610.
- (5) Gong, P.; Zheng, W.; Huang, Z.; Zhang, W.; Xiao, D.; Jiang, X. *Adv. Funct. Mater.* **2013**, 23 (1), 42–46.
- (6) Matsunaga, Y. T.; Morimoto, Y.; Takeuchi, S. *Adv. Mater.* **2011**, 23 (12), H90–H94.
- (7) Peng, Y.; Kim, D. H.; Jones, T. M.; Ruiz, D. I.; Lerner, R. A. *Angew. Chemie Int. Ed.* **2013**, 52 (1), 336–340.
- (8) Lutolf, M. P.; Hubbell, J. A. *Nat Biotech* **2005**, 23 (1), 47–55.
- (9) Selden, N. S.; Todhunter, M. E.; Jee, N. Y.; Liu, J. S.; Broaders, K. E.; Gartner, Z. J. *J. Am. Chem. Soc.* **2012**, 134 (2), 765–768.
- (10) Huang, L.-L.; Lu, G.-H.; Hao, J.; Wang, H.; Yin, D.-L.; Xie, H.-Y. *Anal. Chem.* **2013**, 85 (10), 5263–5270.
- (11) Ott, H. C.; Matthiesen, T. S.; Goh, S.-K.; Black, L. D.; Kren, S. M.; Netoff, T. I.; Taylor, D. A. *Nat Med* **2008**, 14 (2), 213–221.
- (12) Torchilin, V. P. *Nat Rev Drug Discov* **2005**, 4 (2), 145–160.
- (13) Csiszár, A.; Hersch, N.; Dieluweit, S.; Biehl, R.; Merkel, R.; Hoffmann, B. *Bioconjug. Chem.* **2010**, 21 (3), 537–543.
- (14) Chen, Y.-F.; Sun, T.-L.; Sun, Y.; Huang, H. W. *Biochemistry* **2014**, 53 (33), 5384–5392.
- (15) Chan, Y.-H. M.; Boxer, S. G. *Curr. Opin. Chem. Biol.* **2007**, 11 (6), 581–587.
- (16) Bertozzi, C. R. *Acc. Chem. Res.* **2011**, 44 (9), 651–653.
- (17) McKay, C. S.; Finn, M. G. *Chem. Biol.* **2014**, 21 (9), 1075–1101.
- (18) Dieterich, D. C.; Lee, J. J.; Link, A. J.; Graumann, J.; Tirrell, D. A.; Schuman, E. M. *Nat. Protoc.* **2007**, 2 (3), 532–540.
- (19) Berg, L. S. and J. G. B. and M. J. and E. T. C. and A. van den. *Nanotechnology* **2011**, 22 (49), 494013.
- (20) Gunther, A.; Jensen, K. F. *Lab Chip* **2006**, 6 (12), 1487–1503.
- (21) Autebert, J.; Coudert, B.; Bidard, F.-C.; Pierga, J.-Y.; Descroix, S.; Malaquin, L.; Viovy, J.-L. *Methods* **2012**, 57 (3), 297–307.
- (22) Watts, P.; Haswell, S. J. *Curr. Opin. Chem. Biol.* **2003**, 7 (3), 380–387.
- (23) Dutta, D.; Pulsipher, A.; Luo, W.; Yousaf, M. N. *J. Am. Chem. Soc.* **2011**, 133 (22), 8704–8713.

- (24) Dutta, D.; Pulsipher, A.; Luo, W.; Mak, H.; Yousaf, M. N. *Bioconjug. Chem.* **2011**, 22 (12), 2423–2433.
- (25) Pulsipher, A.; Dutta, D.; Luo, W.; Yousaf, M. N. *Angew. Chemie Int. Ed.* **2014**, 53 (36), 9487–9492.
- (26) Luo, W.; Pulsipher, A.; Dutta, D.; Lamb, B. M.; Yousaf, M. N. *Sci. Rep.* **2015**, 4 (1), 6313.
- (27) Bilyy, R. O.; Shkandina, T.; Tomin, A.; Muñoz, L. E.; Franz, S.; Antonyuk, V.; Kit, Y. Y.; Zirngibl, M.; Fürnrohr, B. G.; Janko, C.; Lauber, K.; Schiller, M.; Schett, G.; Stoika, R. S.; Herrmann, M. *J. Biol. Chem.* **2012**, 287 (1), 496–503.
- (28) Dhandayuthapani, B.; Yoshida, Y.; Maekawa, T.; Kumar, D. S. **2011**, 20 (ii).
- (29) Rogozhnikov, D.; O'Brien, P. J.; Elahipanah, S.; Yousaf, M. N. *Sci. Rep.* **2016**, 6, 39806.

Chapter 4

Application of Bio-orthogonal CSE for Directed Nucleic Acid Transfection

This work has been published in ACS Central Science, Volume 3, pages 489-500 in 2017 under the title “Bio-Orthogonal Mediated Nucleic Acid Transfection of Cells via Cell Surface Engineering’. It is reprinted with permission (© ACS Publishing Group 2017). O’Brien, P. J.; Elahipanah, S.; Rogozhnikov, D.; Yousaf, M. N. are co-authors of this work.

Contributions

M.N.Y designed the study. P.J.O., D.R., and S.E. performed the experiments. M.N.Y. and P.J.O. analyzed the data.

P.J.O. and M.N.Y. wrote the manuscript.

4.1 Introduction

The ability to efficiently deliver nucleic acids into cells (transfection) plays a pivotal role in the advancement of our understanding of human health.¹ Transfection has revolutionized fundamental studies in cell biology, biotechnology, agriculture, microbiology, genetics, cancer, medicine and biomedical research.^{2 3 4 5 6 7} Cutting edge research relies on the efficient delivery of nucleic acids into a range of cell types for various applications that span gene editing, fundamental cell biology studies, therapeutic and vaccine development, human and plant biotechnology and scaling protein production.^{8 9 10 11} Although transfection is of central importance and arguably one of the most vital tools in biological research, most cell types are not easily transfected with foreign nucleic acids due to variations in nucleic acid stability, delivery and host cell defense mechanisms. Furthermore, transfecting cells with nucleic acids *in vitro* and *in vivo* is not always straightforward due to rapid nucleic acid degradation in serum containing media or *in vivo* conditions. Since, transfection is an initial step in many biological studies, poor cell transfection results in tremendous waste of time and effort spent in multiple rounds of transfection to improve cell count and money spent in extra labor and reagents. Due to its critical importance, reagents that promote transfection have become essential in research in the life sciences and commercial market is estimated to be over \$1.5 billion/year.¹²

The delivery of nucleic acids to mammalian cell lines has been revolutionized over the last 20 years through the development of cationic polymer (Viafect, Promega) or cationic lipid based (Lipofectamine, Life Technologies) technologies for biological assays. Gene delivery technologies insert coding (cDNA) into the cell nucleus, typically in the form of circular DNA or plasmids which interact with endogenous transcription factors to produce changes in messenger RNA (mRNA) protein expression. Mammalian cell line transfection of plasmid DNA (pDNA),

short interfering RNA (siRNA) and other genetic hybrid molecules is a substantial field of study encompassing protein production, genetic discovery and manipulation, signal pathway elucidation and cellular imaging.

Genetic engineering transfection generally involves the delivery of oligonucleotides for identification or clone isolation of partial genetic content of whole single cells to change cellular behaviour, produce desired biological outcomes or elucidate biological signalling pathways. Permanent changes to the genome can be achieved through gene editing techniques such as molecular scissors, nucleases and most recently Clustered Regularly Interspaced Short Palindromic Repeats (CRISPR)-Cas9 to introduce heritable changes to reveal gene functionality, new therapeutic targets, improve human gene therapy and the commercial production of therapeutic agents from standard host cells such as yeast or mammalian cell lines. Current methods to introduce permanent changes to the cell involve the use of mega-nucleases such as Zinc-Finger (ZF), Transcription activator-like effector nucleases (TALEN) and CRISPR-Cas9, were first discovered as viral defence mechanisms within bacterial cells. They employ site-specific DNA cleavage producing DNA double stranded breaks while reducing off target gene changes.

Although mega-nuclease complexes and their mechanism of action have been refined through tremendous effort in the biological community, with even further improvements and optimization on the horizon, these gene editing techniques do however suffer from a common caveat, they all require a vector for delivery to the cytoplasm of the cell. To make any changes to the interior of the cell, a mechanism for breaching the robust and protective cell membrane is required. The plasma membrane is a significant barrier to polar aqueous soluble molecules, and can be highly resistant to DNA and RNA not only through passively blocking physical entry but

also employing active mechanisms to repel or inactivate foreign genetic information. To circumvent these defense mechanisms, researchers have developed instrumental (physical), biological (viral) and reagent (chemical) based methods to transfect cell lines by using vectors to insert foreign genetic content.

Physical based transfection methods employ high strength electromagnetic fields, femto-lasers, microneedles or gold nanoparticles to introduce physical pores or holes in the membrane that allow diffusion of oligonucleotides from the surrounding medium into the cytosol.¹³ These methodologies have aided academic research by enabling transfection of difficult to transfect cell lines such as MSCs and primary cell lines. However, these methods are expensive, highly cytotoxic and can only be used cultured cell lines.

After the initial discovery of viral mechanisms for entry into mammalian cells, the development of viral vectors for gene editing was quickly established by Paul Berg using recombinant DNA to insert bacteriophage genes into the *E. coli* genome using SV 40 viruses.¹⁴ Viral gene editing has progressed to include lentivirus, adeno-associated and adenovirus vectors as replication deficient delivery vehicles for streamlined and efficient transfection. Viral techniques utilized whole engineered viral particles to package and deliver DNA payloads for genomic integration, where viral protein coat receptors target mammalian membrane receptors to hijack endocytic pathways, allowing viral DNA entry into the cytosol. Once inside the nuclear envelope the DNA is incorporated into the host genome, while viral replication is disabled to inhibit viral propagation and subsequent cell death. However, viral insertion has several limitations preventing widespread use in academia, industry and clinical applications including limited transgenic length, targeting difficulties and mutagenesis.^{15 16}

Chemical based transfection reagents include chemical or molecular substances that when combined with plasmids or oligonucleotide sequences produce aggregate complexes termed ‘lipoplexes,’ which promote the delivery of DNA into cells. Chemical transfection methods include calcium phosphate, cationic polymers, cationic lipids and cationic amino acids to produce self-assembled lipoplexes with RNA or DNA. The key challenge for efficient and usage scope of cell transfection is found at the molecular level: How can negatively charged nucleic acids be delivered to negatively charged cells at physiological conditions in serum, with the fewest number of steps, while ensuring high viability, efficiency and no post sorting of transfected and non-transfected cells? To address this complex question a range of delivery, instruments and viral methods have been developed for transfection but each suffer from various drawbacks related to cost, viability and efficiency.^{17 18}

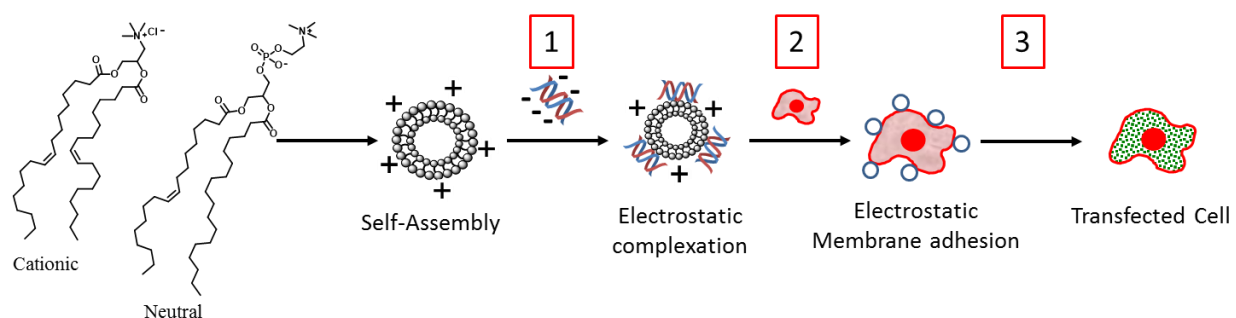


Figure 4.1: A general scheme depicting the assembly, association and cell membrane adhesion of cationic charge based chemical lipoplexes with mammalian cell lines.

The overwhelming strategy for nucleic acid delivery has been based on chemical reagents binding to nucleic acids, followed by adhesion and cellular uptake. Figure 4.1 outlines three main steps in chemical based nucleic acid delivery to cells: 1) The electrostatic reagent forms a complex with nucleic acids (Packaging). 2) The complex undergoes adhesion to cell surfaces, followed by endocytosis (Delivery). 3) The complex achieves lysosomal escape, where the

nucleic acid begins expression within the nucleus (Release). To be useful to the broad research community, these processes must be designed with a minimal number of steps, while retaining high viability and efficiency. Current strategies and products focus on combining nucleic acids via electrostatic complexation of anionic nucleic acids with the excess positive charge of polyamine polymers or small molecules.¹⁷ The resultant cationic lipid and anionic nucleic acid complex or ‘lipoplex,’ is then added to cell media where serum proteins can rapidly absorb or degrade a significant fraction of the complex, while the remaining active complex associates electrostatically with anionic cell surfaces. The nucleic acid complex undergoes endocytosis and a small but functional fraction escapes the lysosome to be expressed or transfect the cell.

To significantly advance transfection technology and cell biology research, new methods that look for alternatives to supplement electrostatic lipoplexes may broaden the scope of cellular transfection. Our novel method comprises a combined CSE and bio-orthogonal strategy to package and deliver nucleic acids using rapid artificial surface labelling and targeting, while reducing the requirement for cytotoxic cationic charge to drive cellular adhesion. This method generates a nucleic acid complex with bio-orthogonal groups and CSE to label cell membranes with complementary bio-orthogonal chemistry for adhesion and delivery. This method is based on selective oxime ‘click’ chemistry which limits non-specific electrostatic interactions between the nucleic acid complex and the cell. The methodology we term SnapFect® is: 1) Mild. 2) Efficient. 3) High cell viability. 4) Has no post cell sorting steps. 5) Precision targeting of specific cells in co-culture. 6) Compatible with complex media. 7) Transient CSE. 8) Does not alter cell behaviour using the mild liposomal and bio-orthogonal protocol. 9) Simple two step protocol.

Liposome fusion has been used as a strategy for the delivery of chemical and biological cargo into mammalian cells for a variety of bio-sensing and drug studies as well as therapeutic applications.^{19 20} In this study, we used the liposome strategy to deliver lipid-like functional molecules efficiently to the cell surface, where liposome fusion capitalizes on the hydrophobic interactions of micelles and lipid bilayers to insert the liposomal bilayer contents with the outer plasma membrane structure. In addition, the composition of the liposome background lipids play a significant role in inducing particle adhesion and fusion.

In order to tailor both the cell surface and the nucleic acid complex with complementary molecules that can undergo a chemo-selective click reaction *in vitro* and *in vivo* without side reactions, we used bio-orthogonal chemistry. Bio-orthogonal chemistry refers to a special suite of organic chemistry reactions that can be performed at physiological conditions in complex mixtures including serum containing media.^{21 22} Tremendous research has been performed to investigate and expand the scope of these special chemical reactions. Several types of click bio-orthogonal reactions have been used, such as hydrazone, thiol-ene, Diels-Alder, Staudinger, Huisgen 3+2 strained alkyne and azides, as well as oxime chemistry for many biological applications ranging from *in vivo* targeting, drug delivery, antibody drug conjugates, to protein engineering, proteomics, imaging and bio-sensing.^{23 24} Figure 4.2 outlines our novel CSE approach for cell nucleic acid transfection which integrates liposome fusion, bio-orthogonal chemistry and CSE (SnapFect).

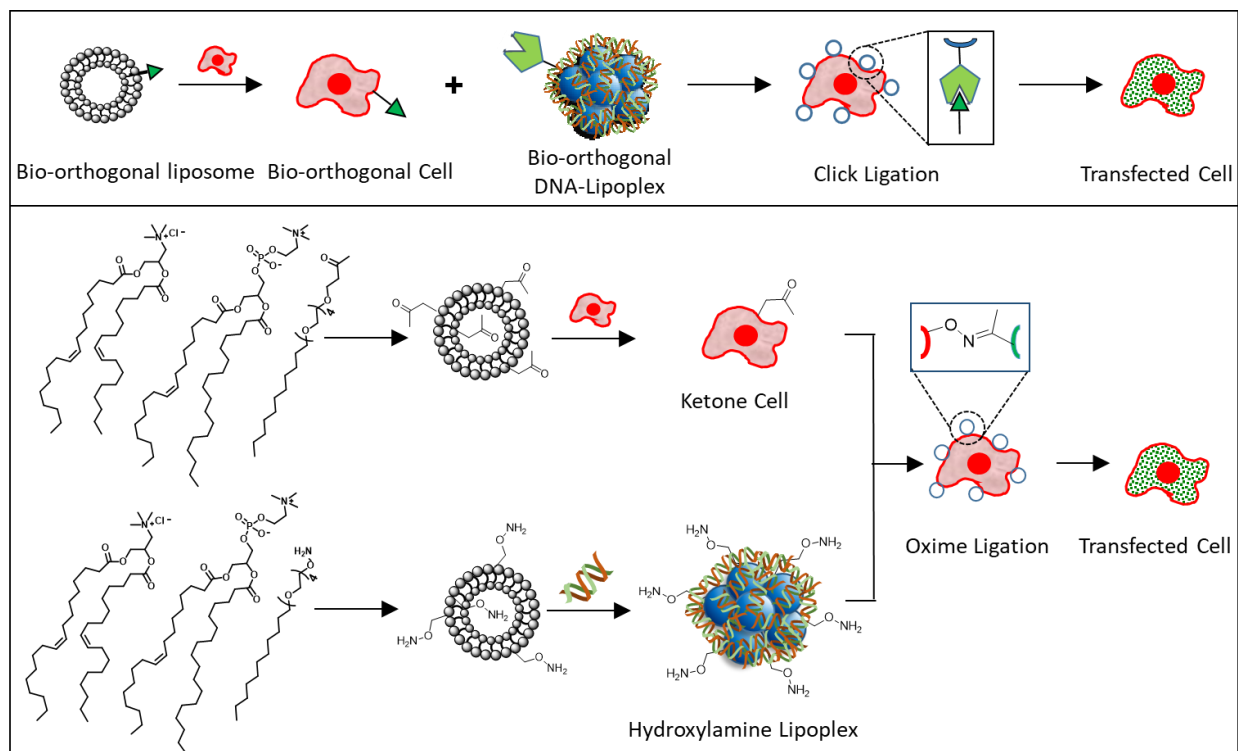


Figure 4.2: Schematic of combined liposome fusion, bio-orthogonal chemistry and CSE strategy for selective nucleic acid transfection of cells (SnapFect). (Top) A liposome containing a bio-orthogonal like lipid molecule is delivered to the cell surface via rapid liposome fusion. A complementary bio-orthogonal nucleic acid/liposome complex is formed and added to the tailored cell. The nucleic acid/liposome complex undergoes a fast click reaction at the cell surface. The nucleic acid/lipoplex is then endocytosed where the nucleic acid/lipoplex dissociates and is translated. (Bottom) A molecular view of the mild and selective bio-orthogonal mediated transfection of cells. A bio-orthogonal liposome containing a ketone group is synthesized and added to cell culture. The ketone group is presented on the cell surface through rapid liposome fusion. A complementary hydroxylamine liposome is complexed with nucleic acids. The hydroxylamine/nucleic acid lipoplex is then added to the ketone presenting cells where rapid oxime formation occurs at the cell surface. The nucleic acid is then endocytosed and released within the cell. No transfection occurs if either component of the bio-orthogonal pair is missing.

We have previously shown that fast and efficient delivery of lipid like bio-orthogonal molecules to cell surfaces via liposome fusion provides cells with a new range of capabilities for photochemical, redox and biosensing applications.^{25 26 27} Using CSE we influence the association of the lipoplex to the cell membrane during the second step of the transfection process to produce a more general approach to lipoplex-cell adhesion with polyvalent oxime reactions rather than electrostatic interactions to induce transfection. This approach will present new capabilities into

transfection reagents through the use of selective oxime chemistry to drive the cellular adhesion process.

4.2 Materials and Methods

4.2.1 Preparation of Cell Cultures

For our model system we used C3H/10T1/2 mouse embryonic fibroblast cells which were cultured and incubated for 3 days at 37°C and 5 % CO₂ in 10 cm culture plates (Fisher Scientific) with media replaced every other day using DMEM (Sigma Aldrich) with 1% v/v PS (Sigma Aldrich) and 10% FBS (Sigma Aldrich) as additives. Cells used for experiments were between 2 and 6 passages. RFP expressing human neonatal dermal fibroblasts were cultured from liquid nitrogen storage and maintained using DMEM (Sigma Aldrich) with 1 % v/v PS (Sigma Aldrich) and 10 % FBS (Sigma Aldrich) as additives and passaged every 3 days. Cells used for experiments were between 2 and 6 passages. All cell lines were obtained from ATCC.

4.2.2 Cellular Engineering Ketone Liposome Formulation and Cell Priming

To form liposome solutions bearing ketone functionalities, into a 5 mL vial 120 µL of 2-dodecanone (Sigma Aldrich) (10 mg/mL in CHCl₃) was added, followed by 454 µL POPC (Avanti Polar Lipids) (10 mg/mL in CHCl₃) and 10 µL of DOTAP (Avanti Polar Lipids) (10 mg/mL in CHCl₃), which were then allowed to evaporate over 24 hours. Once the CHCl₃ evaporated, 3 mL fresh PBS (Sigma Aldrich) was added, followed by tip sonication. Sonication of the lipid suspensions was performed for 10 minutes in a 23°C water bath and stored at 4°C at 30W. To apply ketone CSE to cultured cells, they need to be between 75-80 % confluency, the cell culture media was then aspirated, followed by the addition of fresh serum containing media (2 mL) and 5 % v/v ketone liposome suspension (100 µL) and incubated with the cells under

standard growth conditions for 5 minutes followed by three 3 mL washes of PBS and the addition of fresh growth media to the cells prior to transfection.

4.2.3 General SnapFect Transfection of C3H/10T1/2 cells with phMGFP

C3H/10T1/2 cells were cultured using standard protocols with 10 % FBS and 1 % Penicillin Streptomycin High Glucose DMEM in 10 cm culture plates over 2 days to 75% confluency before use. The C3H/10T1/2 cells were then for 3 minutes trypsinized using 3 mL of 0.25 % trypsin followed by quenching with 6 mL of growth media and centrifugation at 800 RPM for 5 minutes. The pellet was then isolated and re-suspended in growth media 1×10^4 cells/mL and seeded onto 1 cm^2 prepared glass slides (180 μL). The following day the cells were treated using the general ketone cell surface engineering protocol, followed by the immediate addition of the prepared hydroxylamine lipoplex. To form the hydroxylamine lipoplex into a sterile 1.5 mL Eppendorf tube, 15 μL of the hydroxylamine liposome suspension containing 210 μL POPC (10 mg/mL), 60 μL DOTAP (10 mg/mL) and 120 μL dodecyl (tetraethylene glycol) hydroxylamine (10 mg/mL) in 3 mL PBS, using tip sonication over 10 minutes in a 23°C water bath and stored at 4°C at 30 W, the fluorescent protein of interest was added, typically 2.0 μg of phMGFP (1.4 $\mu\text{g}/\mu\text{L}$). This mixture was then incubated at 23°C for 30 minutes, diluted with 200 μL of serum free DMEM media and then carefully pipetted onto the slide and incubated at 37°C at 5 % CO_2 for 5 minutes. After the 5 minute incubation period, the samples were given HNDF serum containing growth media and incubated for another 24-48 hours. The slides were then fixed by washing three times with 3 mL PBS followed by the addition of 5 % formalin solution for 15 minutes. The formalin solution was then drained and washed once with PBS followed by mounting to glass cover slips for fluorescent microscopy using an inverted Zeiss AX10 Fluorescence Microscope.

4.2.4 Targeted Co-culture Method (HNDF/RFP and C3H/10T1/2) and phMGFP

Transfection of HNDF cells

HNDF cells were grown in 10 cm culture plates using the standard growth protocol with 10 % FBS and 1 % P/S High Glucose DMEM media to 80 % confluency and then trypsinized using 3 mL 0.25 % trypsin for 3 minutes followed by quenching with 6 mL of growth media and centrifugation at 800 RPM for 5 minutes. The pellet was then isolated and re-suspended in growth media for 5×10^3 cells/mL and seeded onto 1 cm² prepared glass slides (180 μ L). The cells were then incubated for 4 hours at 37°C at 5 % CO₂, followed by the addition of 2 mL fresh growth media. The following day (approximately 16 hours) the cell media was replaced with fresh media and 5 % v/v ketone liposome suspension (100 μ L) was added to the growth media and incubated for 5 minutes, followed by three 3 mL washes of PBS. C3H/10T1/2 cells were grown in 10 cm culture plates using the standard protocol and once they reached 75 % confluency were trypsinized using 3 mL trypsin for 3 minutes followed by the addition of 6 mL growth media and centrifuged at 800 RPM for 5 minutes. The pellet was isolated and resuspended in growth media to 1×10^4 cells/mL. The tissue plates containing slides with adherent HNDF/RFP cells were then drained of media and then 180 μ L of C3H/10T1/2 cell suspension was added and incubated for 4 hours at 37°C and 5% CO₂ followed by the addition of 2 mL of fresh growth media and incubated for 16 hours. The lipoplex suspension was freshly prepared each time. To a sterile 1.5 mL Eppendorf tube, 60 μ L of the hydroxylamine liposome suspension containing 410 μ L POPC (10 mg/mL), 60 μ L DOTAP (10 mg/mL) and 120 μ L dodecyl (tetraethylene glycol) hydroxylamine (10 mg/mL) was added followed by the addition of 2.0 μ g of phMGFP (1.4 μ g/ μ L). This mixture was then incubated at 23°C for 30 minutes and then diluted with 700 μ L of serum free DMEM media. Then 1 cm² glass slides were washed

twice with 3 mL PBS, with the PBS drained, 200 μ L of the lipoplex solution was carefully pipetted onto the slide and incubated at 37°C at 5 % CO₂ for 5 minutes. After the 5 minute incubation period, the samples were given HNF serum containing growth media and incubated for another 24-48 hours. The slides were then fixed by washing 3 times with 3 mL PBS followed by the addition of 5% formalin solution for 15 minutes. The formalin solution was then drained and washed once with PBS followed by mounting to glass cover slips for fluorescent microscopy using an inverted Zeiss AX10 Fluorescence Microscope.

4.2.5 Firefly Luciferase Stability Assay

C3H/10T1/2 cells were cultured and incubated for 3 days at 37°C and 5 % CO₂ in 10 cm culture plates with media replaced every second day using DMEM with 1 % v/v PS and 10 % FBS as additives. Cell cultures used for experiments were between 2 and 6 passages. Cells were then transferred using 3 mL trypsin into 6 well plates using 7.5×10^3 cells/well. The cells were grown overnight and transfected using the general transfection protocol and incubated for 24 hours. The cells were surfaced engineered with a liposome solution bearing ketones functionalities, where in a clean 5 mL vial 120 μ L of 2-dodecanone (10 mg/mL in CHCl₃) was added, followed by 454 μ L POPC (10 mg/mL in CHCl₃) followed by 10 μ L of DOTAP (10 mg/mL in CHCl₃), which were then allowed to evaporate over 24 hours. Once the CHCl₃ is evaporated 3 mL of fresh PBS is added, followed by tip sonication. Sonication of the lipid suspensions was performed for 10 minutes in a 23°C water bath and stored at 4°C at 30 W.

Using optimal conditions for transfecting pGFP outlined above, we substituted pGFP for Firefly Luciferase (pRL) (Promega) to transfect C3H/10T1/2 cells. pRL lipoplex liposomes were synthesized using a sterile 1.5 mL Eppendorf tube 60 μ L of the hydroxylamine liposome suspension containing 210 μ L POPC (10 mg/mL), 60 μ L DOTAP (10 mg/mL) and 120 μ L

dodecyl (tetraethylene glycol) hydroxylamine (10 mg/mL) was added followed by the addition of 2.0 µg of pRL (1.4 µg/µL). This mixture was then incubated at 23°C for 30 minutes and then diluted with 200 µL of serum free DMEM media and carefully pipetted onto the slide and incubated at 37°C and 5 % CO₂ for 5 minutes. Following the 5 minute incubation period, the samples were washed with 3 mL PBS and given HNDF serum containing growth media and incubated for another 24 hours. Control experiments omitted ketone lipids to the pre-treatment of the cells before transfection, while retaining the original ratio of background lipids, as well as through the absence of hydroxylamine bearing lipids from the formulation of the lipoplex. Transfected cell culture plates were then transferred to a 0°C ice bath and washed twice with 2 mL of PBS treated with 160 µL of lysis buffer and mechanically scrapped from the dishes and then transferred into 1.5 mL Eppendorf tubes. The lysate was then heated to 100°C using a heating block (Labnet Accublock) for 5 minutes and frozen at -80°C overnight. The following day, pRL expression was quantified using an automated Berthold Lumat 3 (LB 9508) with luminol.

4.2.6 Western Blot Assay

Expression using pRFP was conducted in parallel to pRL luciferase expression analysis. C3H/10T1/2 cells were collected using NP-40 lysis buffer (0.5 % [vol/vol] Nonidet P-40, 50 mM Tris-HCl [pH 8.0], 150 mM NaCl, 10 mM sodium pyrophosphate, 1 mM EDTA [pH 8.0], and 0.1 M NaF) containing 10 µg/ml (each) leupeptin and aprotinin, 5 µg/ml pepstatin A, 0.2 mM phenylmethylsulfonyl fluoride, and 0.5 mM sodium orthovanadate. Protein extracts were denatured in SDS loading buffer at 95°C for 5 minutes and then run on a 10 % SDS-PAGE gel, transferred to a polyvinylidene difluoride membrane (Millipore), and blocked in 5 % skim milk for 1 hour prior to antibody incubation, using rabbit RFP Antibody (Life Technologies).

4.2.7 Comparison Luciferase Assays Using Viafect and Lipofectamine 3000

Viafect (Promega) and Lipofectamine 3000 (Life Technologies) reagents were optimized for use with C3H/10T1/2 with phGFP and optical microscopy to determine the highest transfection efficiency using the recommended manufacturer and our general SnapFect protocol. Using the standard growth protocol for C3H/10T1/2 cells, the cells were seeded into 6 well plates at 3.5×10^4 cells/well overnight. The following day 2.0 μg of pRL (0.14 $\mu\text{g}/\mu\text{L}$) was mixed with 6.0 μL of Viafect reagent and incubated at 23°C for 10 minutes, then diluted to 200 μL of total volume using non serum containing media. Then the 200 μL of Viafect solution were added to the cells containing 2 mL of serum containing media and incubated for 24 hours at 37°C at 5% CO_2 . For Lipofectamine, the following day 9.8 μg of pRL (1.4 $\mu\text{g}/\mu\text{L}$) was mixed with 4.0 μL of P3000 reagent for 5 minutes and diluted to 125 μL in serum-free media. Then 4.4 μL of Lipofectamine 3000 reagent was diluted with 125 μL of serum free media, then the two solutions were mixed and incubated at 23°C for 10 minutes. Then the 250 μL of complex solution was added to the cells containing 2.0 mL of serum containing media and incubated for 24 hours at 37°C at 5 % CO_2 . Then the cells were investigated using our above Luciferase protocol. The control and experimental trials were completed in technical triplicate.

4.2.8 Viability and Efficiency Comparison Assays Using phGFP of Viafect and Lipofectamine

Viability was determined using the above scaled up Luciferase protocol. Viafect (Promega) and Lipofectamine 3000 (Life Technologies) reagents were used to transfect C3H/10T1/2 cells with phGFP and optical microscopy was used to determine viability and efficiency through cell counting using the recommended manufacturer protocols. Using the general growth protocol for C3H/10T1/2 cells, the cells were seeded onto 6 well plates at 3.5×10^4 cells/well overnight. The

following day 2.0 µg of phGFP (1.4 µg/µL) was mixed with 6.0 µL of Viafect reagent and incubated at 23°C for 10 minutes, then diluted to 200 µL of total volume using non-serum containing media. Then the 200 µL of Viafect solution were added to the cells containing 2 mL of serum containing media and incubated for 24 hours at 37°C and 5 % CO₂. For Lipofectamine, the following day 9.8 µg of phGFP (1.4 µg/µL) was mixed with 4.0 µL of P3000 reagent for 5 minutes and diluted to 125 µL in serum-free media. Then 4.4 µL of Lipofectamine 3000 reagent was diluted with 125 µL of serum-free media, then the two solution were mixed and incubated at room temperature for 10 min. Then 250 µL of complex solution was added to the cells containing 2.0 mL of serum containing media and incubated for 24 hours at 37°C at 5% CO₂. The experiments were all performed in parallel. Viability was determined through vital dye staining using 0.4% Trypan blue (Sigma Aldrich) using the manufacturer protocol, in addition to a (Bright-Line) visual hemocytometer for cell counting. Cell efficiency was determined using the above-mentioned transfection protocols for Viafect, Lipofectamine and Snapfect, where following a 24 hour incubation period with the relevant reagent the cells were fixed and observed using fluorescence microscopy. The visually fluorescent cells were scored as transfected while dark cells were counted as non-transfected using ImageJ (National Institute for Health) and compared with cell counts of control populations. Nine images from each well were averaged to determine efficiency of the reagent.

4.2.9 Microfluidic Transfection in Flow

Microfluidic Device Fabrication and Design: The micro-channel was designed with a simple Y-shape, where cell suspensions are brought together in the Y-joint mixing zone. In order to make a simple, cheap and robust device, poly methyl methacrylate (PMMA) blocks were used as the device substrate. The experimental device was created using laser ablation to etch PMMA blocks

(1/8 in thickness, 1.25 in length, and 1.42 in width). The PMMA channels were laser etched using Versalaser 2.30 with a CO₂ laser at 14.25 W power to produce parabolic channels with a measured base width of 170 μm , a peak height of 200 μm and a channel length of 1.5 cm. The fluid inlet connections were fabricated using 406 μm (0.016 in) OD stainless steel capillary tubes with an 203 μm (0.008 in) inner diameter (ID) and a length of 2.0 cm, which were embedded into the PMMA blocks using thermal heating (to be in line with the channel flow axes), while the fluid outlet capillary was cut to 2.0 cm and embedded by thermal heating and pressure similarly to the fluid inlets and allowed to cool. The top block of PMMA is used to cap the channel through thermal bonding with the etched bottom block in a convection oven for 2 hours at 275°C and allowed to cool completely to 23°C over 2 hours under pressure. Once cooled, the fluid connections were completed by slipping polyether ether ketone (PEEK) tubing (ID 203 μm /0.008 in) over the metal capillary and sealed using epoxy resin (3M). Finally, high pressure HPLC 1 mL Luer lock glass syringes (Hamilton) were connected to the PEEK tubing using Luer tubing connections (UpChurch Scientific).

C3H/10T1/2 and HNDF/RFP cells were grown to approximately 80 % confluency in 10 cm plastic growth plates and then treated with 5 % v/v ketone bearing liposomes in serum containing media, respectively, for 1 minute followed by aspiration of the media. Cells were washed 3 times with PBS and then detached using 0.25 % trypsin/EDTA at 37°C and 5 % CO₂. Once the cells were detached and neutralized by DMEM media (10 % FBS), the cell suspension was transferred to 15 mL tubes and spun down at 800 RPM for 5 minutes. The supernatant was discarded and the remaining pellet was re-suspended in DMEM media to reach a final concentration of 2×10^5 cells/mL. The SnapFect reagent was generated using our hydroxylamine liposomes using the above general method for SnapFect liposomes. Once the ketone tailored cell suspensions were

prepared, 250 μ L of the ketone tailored C3H/10T1/2 suspension was loaded into a sterilized 1 mL gastight Luer lock Hamilton gas chromatography syringe, while 15 μ L of the SnapFect reagent was diluted in 250 μ L of non-serum containing media and loaded into a sterilized 1 mL gastight Luer lock Hamilton gas chromatography syringe. The connection tubing and microfluidic device were sterilized by passing 1 mL 70 % ethanol solution, followed by 1 mL of PBS buffer. Once sterilized, the loaded syringes were attached to Luer connections to complete the fluid connection to the device and placed onto a Harvard 11 PLUS syringe pump. The flow rate was set to 8 μ L/min for 5 minutes to purge air bubbles from the system and then reduced to 0.4 μ L/min for 5 minutes, with a residence time within the device of approximately 1 min, where the initial fluid was discarded and subsequent eluent was collected onto 1 cm² glass slides with serum containing media. The 1 cm² glass slides were prepared in advance and sterilized by sonication in 70 % ethanol solution for 30 minutes. After microfluidic flow was completed, the collecting slides were transferred to tissue culture plates and incubated at 37°C and 5 % CO₂ for 25 minutes. Then 3 mL of serum containing media was added and the slides were incubated under standard growth conditions for another 24 hours. The transfected cells were then fixed by 3.8 % formaldehyde solution for 15 minutes, followed with gentle washing using PBS. The cell samples were mounted and observed with a Zeiss AX10 Fluorescence Microscope.

4.3 Results and Discussion

In this study, the bio-orthogonal liposome fuses rapidly to a range of cell types to present the functional group on the cell surface. Our liposome CSE strategy for tailoring cell surfaces shown in Figure 4.3A is fast and efficient and does not require complex, slow or laborious molecular biology or invasive metabolic biosynthesis techniques. The liposome fusion CSE strategy is mild and does not alter cell viability or cell behaviour (Figure 4.3B, C). A

complementary bio-orthogonal liposome was then used to complex with nucleic acids and generate a hybrid bio-orthogonal tailored lipoplex. Upon addition of the bio-orthogonal lipoplex to the engineered cell, a rapid click ligation occurs at the cell surface. The nucleic acid/lipoplex is then internalized, released and expressed for efficient transfection of the cell.

We have previously shown the use of liposome fusion to deliver and install ketone and hydroxylamine groups on cell surfaces for applications in co-culture spheroid and tissue engineering. The current application in transfection changes the engineered partners from a complimentary engineered cell to a lipid based engineered nanoparticle. However, lipoplex and cell association is based on a bio-orthogonal click oxime ligation method and not through electrostatics or physical adsorption processes, followed by the typical process of endocytosis and release.

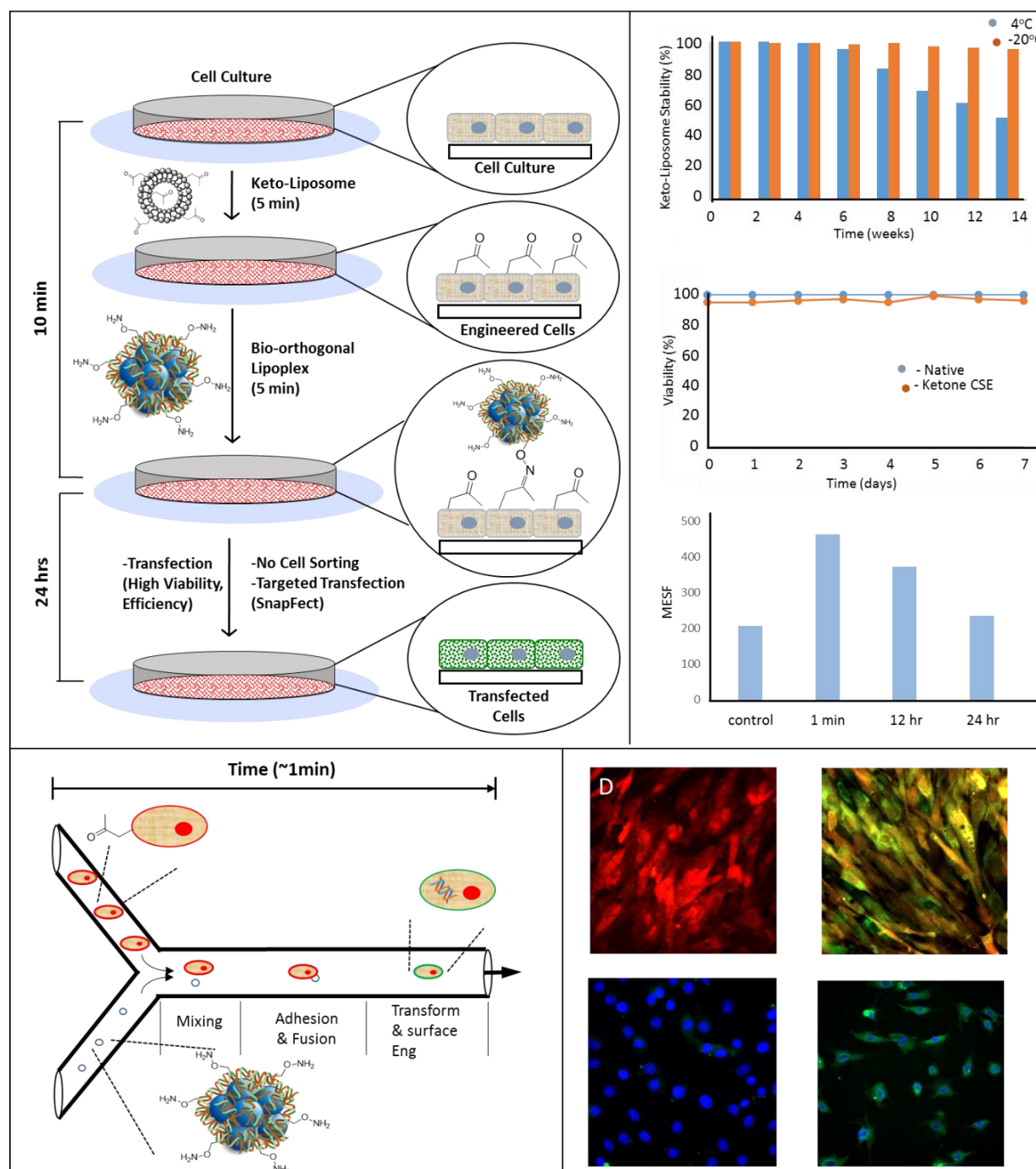


Figure 4.3: Schematic of the procedure to transfect cells via bio-orthogonal chemistry and cell surface engineering (SnapFect). (A) A keto-liposome is added to cells in culture. The liposome rapidly fuses with cells and presents the ketone groups on the surface within seconds. To the keto-engineered cells, a DNA/hydroxylamine lipoplex is added. The bio-orthogonal DNA/lipoplex quickly clicks onto the cell surface via oxime ligation. The oxime reaction is fast, mild and can be performed at physiological conditions in vitro and in vivo. The DNA is then endocytosed/released and transfects the cell. The procedure is straightforward and uses minimal

time. Steps can be performed on adhered or suspended cells and in serum containing cell culture. (B) Stability of the liposome-ketone reagent for CSE at various temperatures and durations. (C) Viability of the cells after liposome-ketone fusion treatment. The liposome fusion method is mild and there is no difference in viability or behaviour between treated and normal untreated (native) cells. (D) The liposome-ketone fusion to present ketones on the cell surface is transient. After 1 minute of liposome-ketone fusion treatment, the cells have approximately 2000 ketones (determined by flow cytometry), which are rapidly reduced on the cell surface after 24 hours due to dilution via growth and division of the cells. (E) The bio-orthogonal mediated nucleic acid transfection strategy is fast and can be performed in a microfluidic format. The mixing of the keto-tailored cells with the nucleic acid lipoplex for transfection occurs in less than 1 minute. The cells are then visualized after 24 hours and show high viability and transfection efficiency. (F) RFP expressing fibroblasts that are transfected with GFP in the microfluidic format. The cells turn yellow and green after GFP transfection via the fast microfluidic method (G). (H) Stained NIH3T3 fibroblasts are flowed through the microfluidic channel and mixed with GFP nucleic acid lipoplex (1 minute). (I) The fibroblasts are visualized after 24 hours are efficiently transfected and show green fluorescence with high viability and efficiency.

Although key parameters for successful cell transfection involve viability, efficiency and scope of cell types to be transfected, an equally important consideration for the practical utility of transfecting cells are the number of steps, cost of reagents and the duration of the transfection. Ideally, the transfection reagents are stable and can be stored without significant degradation or loss of transfection ability for long periods, the number of steps are minimal and performed in serum containing cell culture media. Figure 4.3A shows the general SnapFect transfection procedure based on bio-orthogonal mediated reagents. We found efficient installation of the ketone group on the cell surface within seconds to minutes of liposome exposure. The bio-orthogonal hydroxylamine lipoplex is formed through straightforward addition of the hydroxylamine lipoplex to pDNA. To the ketone engineered cells, the bio-orthogonal hydroxylamine lipoplex is added for 5 minutes. Interfacial oxime ligation occurs at the cell surface and the cells are then evaluated after 24 hours for transfection viability and efficiency. The overall SnapFect transfection procedure is two steps and takes less than 10 minutes to complete. Figure 4.3B depicts the stability of the liposome ketone reagent compared to viability for engineering the cell, where storage in the liposome format for months at low temperatures

does not result in loss of transfection ability. Figure 4.3C describes the viability of cells undergoing the liposome fusion procedure to install ketones on the cell surface, demonstrating that the liposome fusion procedure is mild and fast, while CSE cells are indistinguishable from native cells in behaviour and viability. Figure 4.3D displays that ketone groups on the cell surface after liposome fusion are transient and decrease over time due to cell growth and proliferation. Flow cytometry and viability studies show that the number of bio-orthogonal groups on the cell surface are fewer in number and degrade after only a few rounds of cell division.

After 24 hours, the amount of ketone groups on cell surfaces are reduced and treated cells are indistinguishable from non-treated (control) native cells. This transient nature of ketone group dilution from the cell surface is a key feature of our strategy and is important for various pre and post-transfection applications. Figure 4.3E shows that the bio-orthogonal mediated transfection method is compatible with various technologies and can also be performed in microfluidic flow. We observed that less than 1 minute is required for cells to be efficiently decorated with ketone groups and less than 1 minute for lipoplex adhesion in microfluidic flow (0.8 $\mu\text{L}/\text{min}$) to occur. Cells were evaluated after 24 hours and showed high transfection efficiency and viability (>90%). RFP keto-tailored cells were flowed through a microfluidic channel, where a bio-orthogonal hydroxylamine lipoplex (containing pGFP) rapidly adhered with the cell. After 24 hours, all the RFP cells were expressing GFP and turned either yellow or green. The microfluidic integration with transfection demonstrates the flexibility of the SnapFect strategy and the ability to combine this method with advanced multiplex technologies.

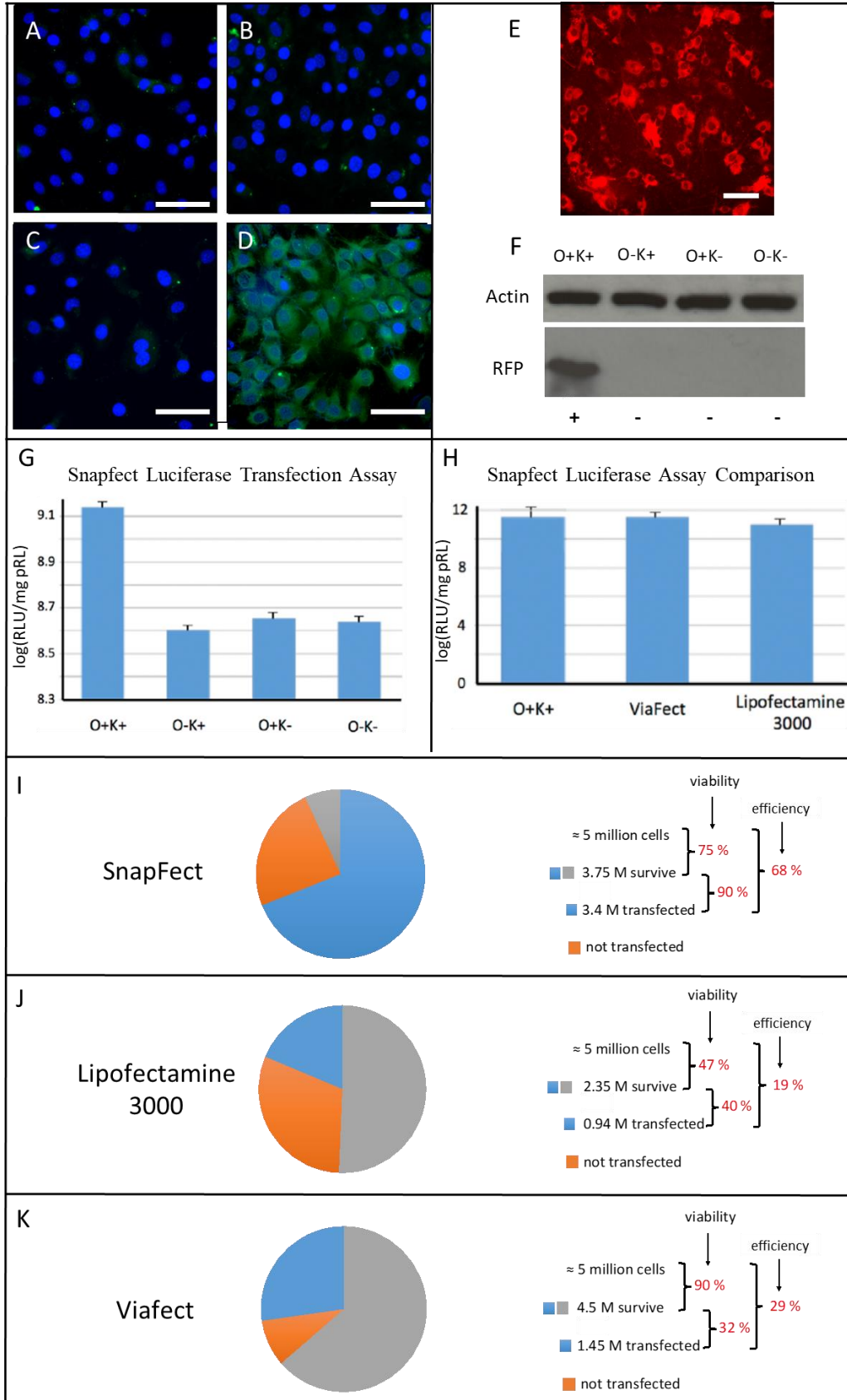


Figure 4.4: Evaluation and comparison of bio-orthogonal mediated transfection (SnapFect).

(A) Fluorescent image of native C3H/10T1/2 cells with DAPI Nuclei stain. (B) Fluorescent image of native C3H/10T1/2 cells treated with hydroxylamine containing DNA-lipoplex. No transfection occurred since the cells did not present ketone groups on their cell surface. (C) Fluorescent image of native C3H/10T1/2 cells and (D) image of the cells presenting ketone groups exposed to GFP hydroxylamine lipoplex after 24 hours. GFP expression resulted due to specific bio-orthogonal mediated transfection. (E) Image of RFP transfected fibroblast cells via click chemistry mediated transfection. (F) A protein gel demonstrating that the expression of RFP is mediated by the correct pairing of the bio-orthogonal chemistry functional groups on the cell surface and on the DNA-lipoplex. (O+ and K+) represent hydroxylamine containing lipoplexes (O+) and ketone presenting cells (K+) were used for RFP transfection. (O- and K-) represent conditions where either hydroxylamine or ketone were absent from the cell surface or DNA-lipoplex. Only the correct combination resulted in bio-orthogonal mediated transfection. (G, H) Luciferase transfection assay for fibroblasts using the bio-orthogonal mediated transfection strategy. (H) Comparison of luciferase assay transfection for the bio-orthogonal mediated strategy (SnapFect) and leading commercial transfection reagents. (I-K) Comparison of viability, efficiency and amount of cells transfected between SnapFect and other commercial transfection reagents. Initially 5 million cells were used and the amount of surviving cells that were transfected resulted in the percent efficiency of transfection. SnapFect has the highest ratio of viable cells to viable and transfected cells. Therefore it does not require further separation of cells and requires less cells for transfection. For example Snapfect requires only 5 million cells to generate 3.4 million transfected cells without post-sorting, whereas Lipofectamine and Viafect require 18 million and 11.5 million cells respectively, to obtain 3.4 million transfected cells with the additional step of separating viable transfected versus viable non-transfected cells.

To demonstrate the bio-orthogonal mediated transfection (SnapFect) of cells, we performed and evaluated several standard transfection assays. Figure 4.4A shows a fluorescent image of native C3H/10T1/2 cells stained with 4', 6-diamidino-2-phenylindole (DAPI), which stains nuclei of cells in culture. Figure 4.4B shows these same cells after treatment with a bio-orthogonal GFP-hydroxylamine lipoplex. No transfection occurred when C3H/10T1/2 cells did not present ketones on their surface. Figure 4.4C, D shows that when C3H/10T1/2 cells present ketone groups they are efficiently transfected with GFP delivered via a bio-orthogonal nucleic acid/hydroxylamine lipoplex. Figure 4.4E depicts the result of the transfection of pRFP to ketone presenting fibroblasts. Western blot analysis Figure 4.4F demonstrates that only when the right combination of bio-orthogonal pairs is presented on the cell surface and on the nucleic acid lipoplex respectively, does transfection occur. Fibroblasts presenting ketone groups via liposome

fusion and delivery (K+) on their surfaces are efficiently transfected with pRFP hydroxylamine/lipoplexes (O+). Any other combination does not result in transfection, clearly demonstrating that transfection is mediated by the bio-orthogonal click reaction and not by an electrostatic or other non-specific interaction process.

Figure 4.4G depicts our transfection assay based on luciferase expression in fibroblast cells. Both complimentary chemistries on the cell surface and lipoplex are necessary, while the lack of either or both chemistries leads to no transfection and no luciferase expression. Figure 4.4H shows a comparison of luciferase expression in cells of SnapFect compared to two cationic based commercial reagents. Figure 4.4I-K shows a comparison of viability and efficiency of transfection between SnapFect and other commercial reagents. For these sets of experiments, a population of 5 million cells were used and compared for transfection viability and efficiency after transfection using commercial reagents. Viability was calculated based on the number of cells that survived compared to the initial population (5 million) after treatment with a transfection reagent. The efficiency of transfection was then calculated in two ways. The '1st efficiency' is the ratio of the number of viable transfected cells to the number of viable surviving cells after treatment. The second (overall efficiency) is determined by the number of viable transfected cells to the initial number of total cells (5 million). For SnapFect, the viability is 75 % (3.75 million cell survived over 5 million initial cells) and the efficiency is 90 % (3.4 million transfected cells over 3.75 million cells) and overall efficiency is 68 % (3.4 million transfected cells over 5 million initial cells). One key consideration is that the number of cells that survive compared to the number of cells transfected (1st efficiency) is very high for SnapFect compared with other reagent products. With such high 1st efficiency, no additional sorting step is required for post processing, since almost all the cells that survive have also been transfected. However,

for the other reagents the 1st efficiency is 40 % and 32 %, respectively. This requires a post-sorting step to separate the surviving non-transfected cells and the surviving transfected cells, increased time, cost and effort required to produce a transfected population of cells. As a comparison, SnapFect requires only 5 million cells to generate 3.4 million transfected cells without post-sorting, whereas Lipofectamine and Viafect require 18 million and 11.5 million cells respectively, to obtain the same 3.4 million population of transfected cells, with the added step of separating via FACS to obtain viable transfected cells. Due to the mild nature of bio-orthogonal mediated transfection delivered by SnapFect, fewer cells, reagents, media, time and labour are necessary and the additional post-sorting step of other methods is eliminated.

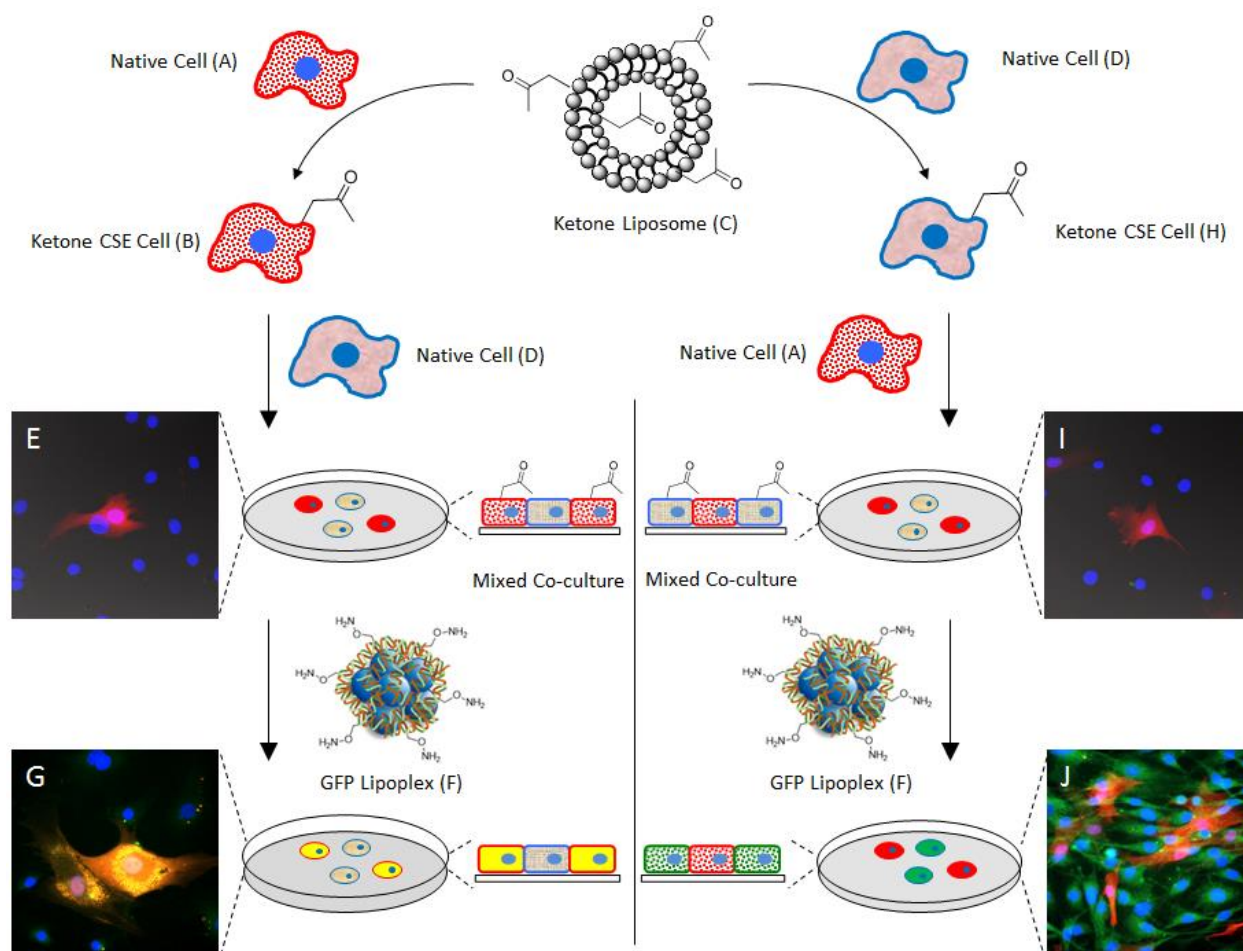


Figure 4.5: Precision transfection via bio-orthogonal mediated ligation in co-cultures. (Left) RFP expressing HDNF cells (A) are cell surface engineered to present ketone groups (B) via rapid liposome fusion (C). Non-fluorescent C3H/10T1/2 cells (D) and ketone presenting HDNF cells (B) are mixed to generate a co-culture (E). To this co-culture, a bio-orthogonal hydroxylamine presenting GFP-lipoplex (F) is added. Only the ketone presenting cells (B) are targeted for selective transfection via the hydroxylamine presenting lipoplex (E) via oxime ligation. (G) Fluorescent image showing only HDNF presenting ketones are transfected with GFP (yellow). (Right) Non-fluorescent C3H/10T1/2 cells (D) are cell surface engineered to present ketone groups (H) via rapid liposome fusion (C). Red fluorescent HDNF cells (A) and ketone presenting C3H/10T1/2 cells (H) are mixed to generate a co-culture (I). To this co-culture a bio-orthogonal hydroxylamine presenting GFP-lipoplex (F) is added. Only the ketone presenting cells (H) are targeted for selective transfection via the hydroxylamine presenting lipoplex (F) via oxime ligation. (J) Fluorescent image showing only C3H/10T1/2 cells presenting ketones are transfected with GFP (green). These co-culture results show transfection is only mediated through targeted bio-orthogonal chemistry and not non-specific electrostatic interactions.

The ability to selectively target a specific cell or cell type for gene and drug delivery in a co-culture *in vitro* and *in vivo* is of fundamental interest and a common major hurdle in many therapeutic applications for cancer and other chronic diseases. Figure 4.5 demonstrates a novel precision transfection capability of SnapFect to selectively transfect a single cell type in co-cultures. To selectively deliver pDNA two cell populations were chosen, [HDNF/RFPs (A) and C3H/10T1/2 (D)] where each cell surface was engineered with ketone liposomes and then mixed with a second untreated native cell type. In one scenario this produced a co-culture containing keto-RFP HDNF (B) cells and native C3H/10T1/2 cells (D), with another co-culture containing native RFP-HDNF (A) cells and keto-C3H/10T1/2 cells (H). Both co-cultures were then treated with an identical bio-orthogonal pGFP hydroxylamine-lipoplex (F). Fluorescence microscopy of DAPI stained keto-RFP HDNF cells and native C3H/10T1/2 cells (Figure 4.5E) show that upon treatment with oxy-lipoplexes of pGFP, only RFP-HDNF cells are transfected and turn yellow due to a combination of red and green fluorescence within the cell shown in Figure 4.5G. Fluorescence imaging of DAPI stained native RFP-HDNF cells and keto-C3H/10T1/2 cells (Figure 4.5I) shows co-culture formation. Upon treatment with bio-orthogonal hydroxylamine-lipoplex pGFP (F) keto-C3H/10T1/2 (H) cells express GFP protein selectively and turn green, while the non-labelled RFP-HDNF cells remain unaffected (Figure 4.5J). These results demonstrate that the SnapFect method is able to precision target and transfect a specific cell type in a co-culture. Since the transfection is only mediated by bio-orthogonal chemistry and not electrostatic or other non-specific interactions, this selectivity enables new possibilities for targeted delivery in complex cellular environments and transfect cells *in vitro* and *in vivo* for new applications using our artificial receptors.

4.4 Conclusion

In summary, our SnapFect strategy integrates liposome fusion, CSE and bio-orthogonal chemistry for a rapid and efficient nucleic acid cell transfection method with new capabilities compared to existing transfection technologies. The approach installs a bio-orthogonal molecule on the surface of a cell, while the complementary bio-orthogonal functional group is associated with a nucleic acid that subsequently performs an interfacial click reaction at the cell surface for efficient nucleic acid delivery. Unlike conventional reagent transfection methods that use various molecules composed of positively charged polyamines to complex with nucleic acids which then are associated with negatively charged cells via electrostatic association, the SnapFect method relies on a precise chemo-selective click chemistry. The method was designed to have broad scope and utility, which is mild, efficient, with minimal steps, no additional sorting (of viable transfected and viable non-transfected cells), and can be performed on a range of cell types and in various cell culture conditions. Furthermore, selective cell transfection and gene silencing can be performed in co-cultures due to the specific requirement that only cells presenting bio-orthogonal groups are targeted for transfection.

We also show the SnapFect transfection method can occur in microfluidic flow, which opens numerous applications using the power of microfluidic technology. The liposome fusion method is fast and can be used to simultaneously engineer the cell surface with bio-orthogonal groups and to deliver various other small molecules and cargoes into the cell. We have demonstrated a bio-orthogonal CSE approach to generate cells with photoactive, redox and fluorescent capabilities. Also, we have used this method to generate co-culture spheroids and scaffold free 3D tissues for stem cell differentiation studies, liver and cardiac tissue on-a-chip applications.^{28 29} The key feature in this strategy is the rapid placement of an artificial receptor

(bio-orthogonal group) on the cell surface without the use of invasive molecular biology or the use of modified metabolites. This strategy is a platform technology that can be used to label and deliver a range of molecules to cells *in vitro* and *in vivo*. Future studies to tailor cell surfaces with various bio-orthogonal groups, nanoparticles or fluorescent probes may be pursued for various theranostic and systems biology type applications and studies.^{30 31} The SnapFect method provides a new way of thinking about delivery and targeting cells for various applications in fundamental biological studies from gene editing to immunotherapy.^{32 33} The method is compatible with other nucleic acid based biotechnologies such as CRISPR-Cas9 and RNA. We have previously shown that the CSE approach also functions in a wide range of cell types including stem cells and primary cells, while also showing applicability in bacteria. The ability to install a range of molecules on the cell surface will have broad utility in cell biology, tissue engineering and act as a molecular handle for a range of bio-analytical sorting and tracking technologies.³⁴

4.5 References

- (1) Naldini, L. *Nature* **2015**, 526 (7573), 351–360.
- (2) Pichon, C.; Billiet, L.; Midoux, P. *Curr. Opin. Biotechnol.* **2010**, 21 (5), 640–645.
- (3) Wurm, F. M. *Nat Biotech* **2004**, 22 (11), 1393–1398.
- (4) Sharei, A.; Zoldan, J.; Adamo, A.; Sim, W. Y.; Cho, N.; Jackson, E.; Mao, S.; Schneider, S.; Han, M.-J.; Lytton-Jean, A.; Basto, P. A.; Jhunhunwala, S.; Lee, J.; Heller, D. A.; Kang, J. W.; Hartoularos, G. C.; Kim, K.-S.; Anderson, D. G.; Langer, R.; Jensen, K. F. *Proc. Natl. Acad. Sci.* **2013**, 110 (6), 2082–2087.
- (5) Naldini, L.; Blomer, U.; Gallay, P.; Ory, D.; Mulligan, R.; Gage, F. H.; Verma, I. M.; Trono, D. *Science* (80-.). **1996**, 272 (5259), 263–267.
- (6) Hewapathirane, D. S.; Haas, K. *J. Vis. Exp.* **2008**, No. 17, 705.
- (7) Kohli, V.; Robles, V.; Cancela, M. L.; Acker, J. P.; Waskiewicz, A. J.; Elezzabi, A. Y. *Biotechnol. Bioeng.* **2007**, 98 (6), 1230–1241.
- (8) Tagalakis, A. D.; Kenny, G. D.; Bienemann, A. S.; McCarthy, D.; Munye, M. M.; Taylor, H.; Wyatt, M. J.; Lythgoe, M. F.; White, E. A.; Hart, S. L. *J. Control. Release* **2014**, 174, 177–187.
- (9) Kenny, G. D.; Bienemann, A. S.; Tagalakis, A. D.; Pugh, J. A.; Welser, K.; Campbell, F.; Tabor, A. B.; Hailes, H. C.; Gill, S. S.; Lythgoe, M. F.; McLeod, C. W.; White, E. A.; Hart, S. L. *Biomaterials* **2013**, 34 (36), 9190–9200.
- (10) Schnoor, M.; Buers, I.; Sietmann, A.; Brodde, M. F.; Hofnagel, O.; Robenek, H.; Lorkowski, S. *J. Immunol. Methods* **2009**, 344 (2), 109–115.
- (11) Zhong, S.; Malecek, K.; Perez-Garcia, A.; Krogsgaard, M. *J. Vis. Exp.* **2010**, No. 44, 2307.
- (12) Parvizi-Bahktar, P.; Mendez-Campos, J.; Raju, L.; Khalique, N. A.; Jubeli, E.; Larsen, H.; Nicholson, D.; Pungente, M. D.; Fyles, T. M. *Org. Biomol. Chem.* **2016**, 14 (11), 3080–3090.
- (13) Nayerossadat, N.; Maedeh, T.; Ali, P. A. *Adv. Biomed. Res.* **2012**, 1, 27.
- (14) Jackson, D. A.; Symons, R. H.; Berg, P. *Proc. Natl. Acad. Sci. U. S. A.* **1972**, 69 (10), 2904–2909.
- (15) Gardlík, R.; Pálffy, R.; Hodosy, J.; Lukács, J.; Turna, J.; Celec, P. *Med. Sci. Monit.* **2005**, 11 (4), RA110-A121.
- (16) Collins, M.; Thrasher, A. *Proc. R. Soc. B Biol. Sci.* **2015**, 282 (1821).
- (17) Kim, T. K.; Eberwine, J. H. *Anal. Bioanal. Chem.* **2010**, 397 (8), 3173–3178.
- (18) Zuris, J. A.; Thompson, D. B.; Shu, Y.; Guilinger, J. P.; Bessen, J. L.; Hu, J. H.; Maeder, M. L.; Joung, J. K.; Chen, Z.-Y.; Liu, D. R. *Nat Biotech* **2015**, 33 (1), 73–80.
- (19) Nicolson, G. L. *Biochim. Biophys. Acta - Biomembr.* **2014**, 1838 (6), 1451–1466.
- (20) Torchilin, V. P. *Nat Rev Drug Discov* **2005**, 4 (2), 145–160.
- (21) Kramer, J. R.; Onoa, B.; Bustamante, C.; Bertozzi, C. R. *Proc. Natl. Acad. Sci.* **2015**, 112 (41), 12574–12579.

- (22) Sletten, E. M.; Bertozzi, C. R. *Angew. Chemie Int. Ed.* **2009**, *48* (38), 6974–6998.
- (23) Patterson, D. M.; Nazarova, L. A.; Prescher, J. A. *ACS Chem Biol* **2014**, *9*.
- (24) McKay, C. S.; Finn, M. G. *Chem. Biol.* **2014**, *21* (9), 1075–1101.
- (25) Dutta, D.; Pulsipher, A.; Luo, W.; Mak, H.; Yousaf, M. N. *Bioconjug. Chem.* **2011**, *22* (12), 2423–2433.
- (26) Dutta, D.; Pulsipher, A.; Luo, W.; Yousaf, M. N. *J. Am. Chem. Soc.* **2011**, *133* (22), 8704–8713.
- (27) Elahipanah, S.; Radmanesh, P.; Luo, W.; O'Brien, P. J.; Rogozhnikov, D.; Yousaf, M. N. *Bioconjug. Chem.* **2016**, *27* (4), 1082–1089.
- (28) Rogozhnikov, D.; O'Brien, P. J.; Elahipanah, S.; Yousaf, M. N. *Sci. Rep.* **2016**, *6*, 39806.
- (29) Rogozhnikov, D.; Luo, W.; Elahipanah, S.; O'Brien, P. J.; Yousaf, M. N. *Bioconjug. Chem.* **2016**, *27* (9), 1991–1998.
- (30) Lim, E.-K.; Kim, T.; Paik, S.; Haam, S.; Huh, Y.-M.; Lee, K. *Chem. Rev.* **2015**, *115* (1), 327–394.
- (31) Chuang, H.-Y.; Hofree, M.; Ideker, T. *Annu. Rev. Cell Dev. Biol.* **2010**, *26* (1), 721–744.
- (32) Khalil, D. N.; Smith, E. L.; Brentjens, R. J.; Wolchok, J. D. *Nat Rev Clin Oncol* **2016**, *13* (5), 273–290.
- (33) Sander, J. D.; Joung, J. K. *Nat Biotech* **2014**, *32* (4), 347–355.
- (34) Chen, R.; Greene, E. L.; Collinsworth, G.; Grewal, J. S.; Houghton, O.; Zeng, H.; Garnovskaya, M.; Paul, R. V.; Raymond, J. R. *Am. J. Physiol. - Ren. Physiol.* **1999**, *276* (5), F777 LP-F785.

Chapter 5

Dialdehyde Reagents for Bioconjugation Applications

This work has been published in Bioconjugate Chemistry, Volume 5, pages 1422-1433 in 2017 under the title “General Dialdehyde Click Chemistry for Amine Bioconjugation”. It is reprinted with permission (© ACS Publishing Group 2017). Elahipanah, S.; O’Brien, P. J.; Rogozhnikov, D.; Yousaf, M. N. are co-authors of this work.

Contributions

M.N.Y designed the study. S.E., P.J.O., and D.R. performed the experiments. M.N.Y., S.E. and P.J.O. analyzed the data. S.E., P.J.O. and M.N.Y. wrote the manuscript.

5.1 Introduction

The delivery of bioactive reagents to cells is an important aspect of most biological research programs and life science commercial efforts. Chapters 1-4 included the implementation of bio-orthogonal lipids or reagents to impart functionality to the cell through liposome fusion CSE, which did not react with native biochemistry. Although bio-orthogonal reactions are efficient, rapid and non-cytotoxic, they have several drawbacks as a general methodology for commercially available small molecules and macromolecules. Bio-orthogonal moieties are difficult to synthetically incorporate into biological reagents and biophysical probes, reducing the utility of bio-orthogonal strategies where molecules become prohibitively expensive or difficult to synthesize. Liposome delivery and bioconjugation strategies have applications for the delivery of macromolecules, particularly proteins, peptides and antibodies for drug targeting, peptide signalling and functionalization of cell surfaces for research or therapeutic applications, which necessitate the use of easily performed and high yield coupling reactions. Simple methodologies are necessary to couple these large molecules to delivery agents or liposomes that use naturally occurring chemical functional groups to limit difficult engineering on proteins.

Primary amines are an important base and nucleophile used in organic synthesis and ligation of biological molecules for labelling, purification and stabilization.^{1 2 3} Biological systems utilize primary amine functional groups in every amino acid subgroup and subsequently are found in most proteins as lysine amino acids which are critical for hydrogen bonding, zwitterion formation, aqueous buffers and nucleophiles in enzymatic reactions.^{4 5 6} Primary amines are also found in antibody drug-conjugates as well as other biologic based drugs making primary amines an incredibly abundant and important functional group to chemo-selectively target for ligation and labelling applications.

There are several existing bioconjugation strategies for reacting primary amines which involve either directly reacting the amine with an electrophilic partner such as halides, or activating moieties such as carboxylic acids to form amide bonds. Figure 5.1 shows several primary amine reaction strategies including NHS-esters, isocyanates, isothiocyanates and reductive amination of imines that are widely available as commercial reagents or kits.^{7 8 9 10 11} A classic amine reaction technique relies upon carboxylic acid activation using N-hydroxy succinimide-dicyclocarbodiimide (NHS-DCC) to form stable amide bonds, which has provided a powerful strategy for conjugation but suffers several limitations. First, the production of toxic by-products can be produced in significant quantities, depending upon the strategy. Second, the reagents are generally expensive. Third, activated acids are sensitive to air and moisture due to rapid hydrolysis. Fourth, poor atom economy, requiring multiple reagents and producing significant by-products which are not incorporated into the desired molecule. These issues have limited the field, where expensive proteins or macromolecules are wasted through purification steps and incomplete reactions.

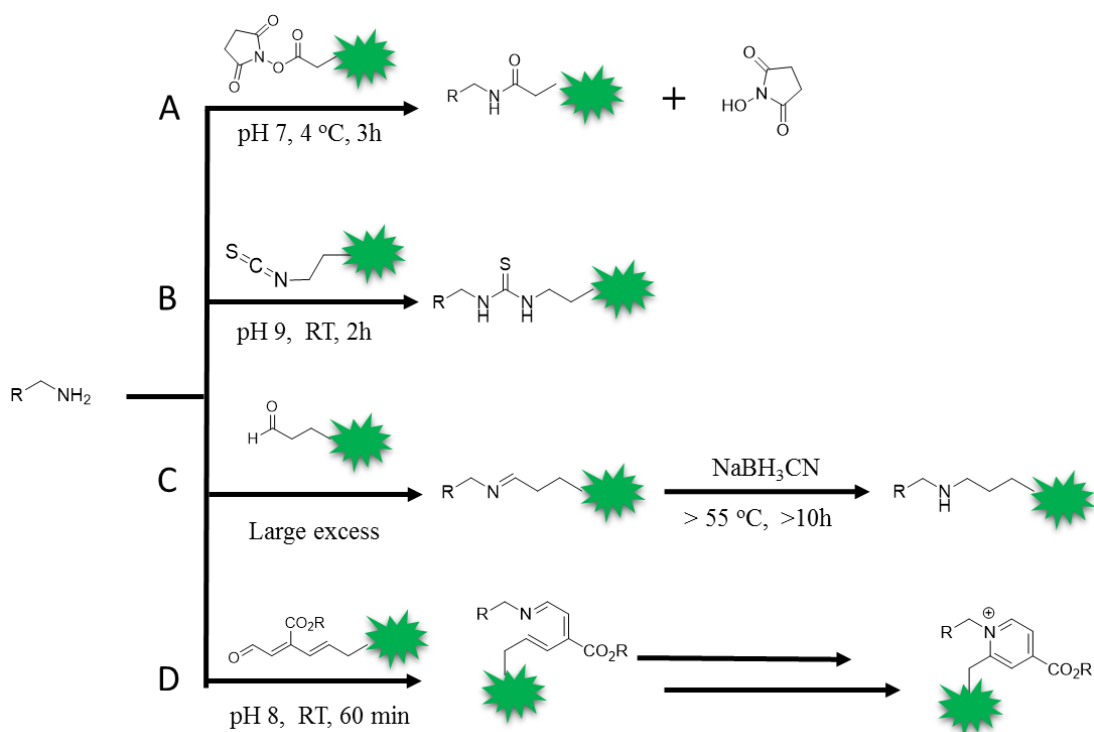


Figure 5.1: Selection of primary amine conjugation reactions used in research and commercially available kits for reacting amines with small molecules or biomolecules. (A) NHS-esters, (B) Isocyanates, (C) reductive amination of imines and (D) Amine cyclization.

To design bioconjugation reactions for applications with broad scope a few basic criteria must be met: 1) the reaction between the native biomolecule functional group and the conjugation partner must display fast kinetics under aqueous conditions; 2) the reaction must be chemo-selective for the desired functional group; 3) there should be minimal or no by-products; 4) the conjugation reagent must be relatively easy and efficient to synthesize using convergent synthesis techniques; 5) the reaction should use an existing chemical moiety commonly found on biomolecules or reagents such as amines, to reduce the number of functionalization steps.

Therefore, reactions which accommodate these criteria can be successful methods to attach a variety of probes, small molecules or macromolecules to primary amine bearing molecules under mild, aqueous conditions, selectively with high yields.

As inspiration for a new type of bioconjugation reaction we used glutaraldehyde as our base methodology, which has been used as a fixation agent in cellculture. Glutaraldehyde acts as a cross-linking agent for proteins both inside and outside the cell, since the small molecule can pass through the cell membrane to easily reach the cytosol, fixing the dynamic structures of the cell using primary amines for examination using microscopy.¹² To achieve primary amine conjugation a retro synthetically designed glutaraldehyde functional group was synthesized to conjugate amine containing molecules such as PEG, alkyl groups, biotin and 2,4-nitrophenol (DNP) for surface labelling, protein cross-linking and tissue engineering applications. Figure 5.2 demonstrates the model dialdehyde molecule for the general conjugate of primary amine containing amino acid side chains eg. Lysine.¹³ The rationale using glutaraldehyde as our base conjugation scheme was first informed by modifying the 3-position of the glutaraldehyde backbone for placement of functional groups (R_1 and R_2) to form a stable molecule which hinders aldol-type self-condensations. Second, the 1,5-pentanedial group has the correct carbon length (5 carbons) to act as an intramolecular trap to quickly perform a six-membered ring closing reaction. The ring closing reaction occurs through initial intermolecular condensation to form an imine via the primary amine attack with a single C1 aldehyde, then rapidly condenses again through an intramolecular reaction with the C5 aldehyde to form the final six-membered dihydropyridine ring (Figure 5.2).

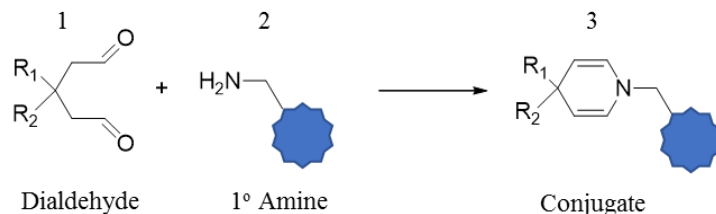


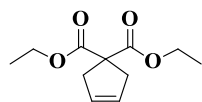
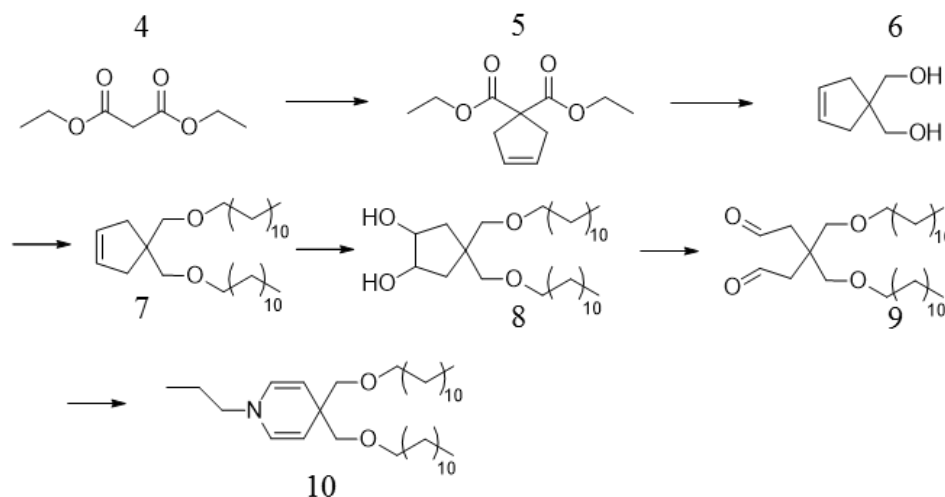
Figure 5.2: Scheme of the dialdehyde click reaction of primary amines under aqueous conditions to form a ligated conjugate molecule. The reaction occurs at 23°C to generate a dihydro pyridine moiety with a quaternary carbon which can consist of different groups (R_1 and R_2). The reaction has efficient atom economy, while requiring no purification and produces water as the byproduct with high yields.

Instability of aldehydes to oxidation in air has been a known issue as well as aldol-type condensations, resulting in polymerized products which could deactivate the 1, 5-pentanedial moiety. To mitigate these issues, we formed a quaternary carbon at the 3-carbon position, where steric hindrance would limit self-reaction but would also result in a protected and stable intramolecular hydrate (hemiacetal cyclic pyran). Not only does this quaternary carbon prevent self-condensation, it also provides an installation handle for a range of molecules to the dialdehyde, such as fluorescent molecules, biophysical probes or hydrophobic lipid tails.

To demonstrate the utility and benefits of our modified dialdehyde moiety to conjugate primary amines, we reacted the moiety with a variety of molecules spanning small molecules, peptides, amino acids, proteins, beads and live cells for our strategy. Characterization was performed using NMR, microscopy, flow cytometry and confocal microscopy to visualize and elucidate the both capabilities and limitations of using this novel backbone modified glutaraldehyde strategy.

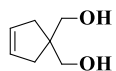
5.2 Materials and Methods

5.2.1 Synthesis of Lipid Dialdehyde (9) and Conjugate (10)



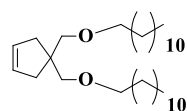
diethyl cyclopent-3-ene-1,1-dicarboxylate (5). To a solution of diethyl malonate

4 (2.00g, 12.48 mmol) in 50 mL *t*-butanol and metallic Na (*s*) (0.287 g, 12.48 mmol) was added *cis*-1,4-dichlorobut-2-ene was added. The mixture was stirred until a yellow solution was obtained, only then another portion of (0.287 g, 12.48 mmol) of metallic sodium was added and stirred for 12 hours. *t*-butanol was distilled off under vacuum and the mixture was diluted with dichloromethane (DCM). The organic solution was filtered and washed with H₂O (6 x 50 mL), saturated NH₄Cl (3 x 50 mL), and H₂O (2 x 50 mL), dried over MgSO₄, and purified with silica Hex:EtOAc (2:8) to afford a clear oil solid (11.23 mmol, 90%) ¹H-NMR (400 MHz; CDCl₃): δ 5.62 (s, 2H), 4.21 (d, *J* = 7.1 Hz, 2H), 3.03 (s, 4H), 1.27 (d, *J* = 7.2 Hz, 3H). ¹³C-NMR (700 MHz; CDCl₃): δ 172.2, 127.8, 61.5, 58.8, 40.8, 14.0.

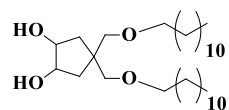


cyclopent-3-ene-1,1-diol (6). To a suspension of lithium aluminum hydride (1.706 g, 44.92 mmol) in dry 100 mL tetrahydrofuran (THF) at -78°C, diethyl cyclopent-3-ene-1,1-dicarboxylate (**5**) (2.38 g, 11.23 mmol) was added dropwise over 1 hour. The mixture was

stirred for 5 hours, and then quenched with 15 mL 1M NaOH. The mixture was stirred for an additional 2 hours, then concentrated and up taken in diethyl ether and dried over MgSO₄ to afford white solid (9.54 mmol, 85%). ¹H-NMR (700 MHz; CDCl₃): δ 5.65 (s, 2H), 3.73 (s, 4H), 2.24 (s, 4H).

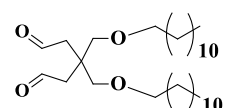


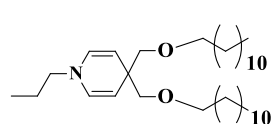
4,4-bis(dodecyloxymethyl)cyclopent-1-ene (7). To a suspension of excess NaH in dry 100 mL dry THF at -78°C was added cyclopent-3-ene-1,1-diyldimethanol (**6**) (1.222 g, 9.54 mmol) and stirred for 1 hour. Temperature was gradually increased to -40°C and bromododecane (7.104 g, 28.62 mmol) was added drop wise over 30 minutes. The mixture was mildly refluxed overnight. THF was distilled off under vacuum and the mixture was diluted with DCM. The organic solution was filtered and washed with H₂O (6 x 50 mL), saturated NH₄Cl (3 x 50 mL), and H₂O (2 x 50 mL), dried over MgSO₄, and purified with silica Hex:EtOAc (2:8) to afford a clear oil solid (7.60 mmol, 80%) ¹H-NMR (700 MHz; CDCl₃): δ 5.60 (s, 2H), 3.43 (t, *J* = 6.7 Hz, 4H), 3.33 (s, 4H), 2.21 (s, 4H), 1.57 (dd, *J* = 9.4, 5.2 Hz, 4H), 1.28 (s, 20H), 0.90 (t, *J* = 7.1 Hz, 6H).



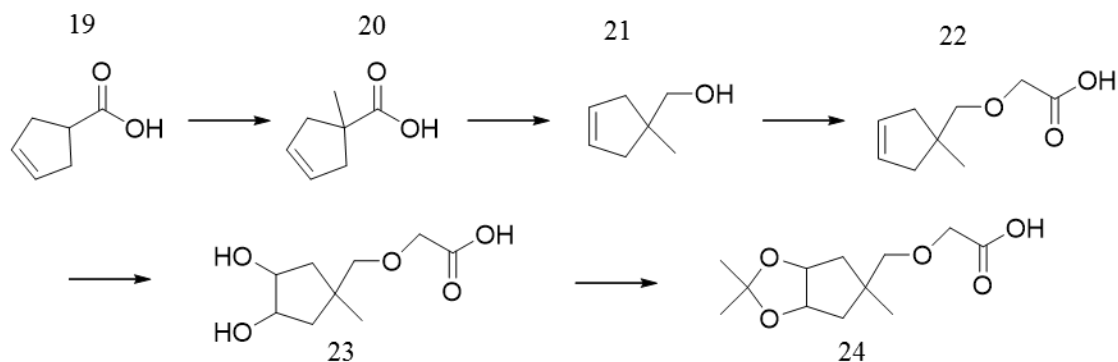
4,4-bis(dodecyloxymethyl)cyclopent-1-ene-1,2-diol (8). To a solution of 4,4-bis(dodecyloxymethyl)cyclopent-1-ene (**7**) (3.541 g, 7.60 mmol) in acetone: acetonitrile (1:1) was added catalytic amount of OsO₄ and excess *N*-methylmorpholine *N*-oxide 50% in H₂O. Reaction was monitored with thin layer chromatography (TLC) for complete disappearance of starting material. Solvent was distilled off under vacuum and the product was taken into diethyl ether and dried over MgSO₄, further purified with silica Hex:EtOAc (3:7) to afford a white solid (6.84 mmol, 90%) ¹H-NMR (700 MHz; CDCl₃): δ 3.93 (d, *J* = 7.2 Hz, 2H), 3.53 (t, *J* = 6.7 Hz, 2H), 3.38 (t, *J* = 6.6 Hz, 2H), 3.29 (s, 2H), 3.16 (s, 2H), 1.85 (dd, *J* = 14.1, 6.2 Hz, 2H), 1.69 (dd, *J* = 14.2, 5.0 Hz, 2H), 1.63 (t, *J* = 7.3 Hz, 2H), 1.55 (t, *J* = 7.0 Hz, 2H), 1.31 (d,

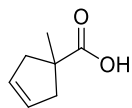
$J = 6.8$ Hz, 40H), 0.90 (t, $J = 7.1$ Hz, 6H). ^{13}C -NMR (700 MHz; CDCl_3): δ 77.19, 77.01, 76.94, 76.83, 76.1, 74.4, 71.86, 71.68, 45.0, 37.6, 31.9, 29.68, 29.64, 29.62, 29.55, 29.49, 29.46, 29.40, 29.36, 26.17, 26.12, 22.7, 14.1

 **3,3-bis(dodecyloxymethyl)pentanedial (9).** To a solution of (8) (3.4063 g, 6.84 mmol) in H_2O : methanol (1:9) was added NaIO_4 . Mixture was stirred for 1 hour until a flaky white, solid iodate salt, was obtained. Solvent was distilled off under vacuum and the product was taken into diethyl ether and dried over MgSO_4 and used for subsequent reactions.

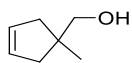
 **4,4-bis((dodecyloxy)methyl)-1-propyl-1,4-dihydropyridine (10).** To a solution of (9) (20 mg, 0.4032 mmol) in DCM was added excess propylamine and stirred for 15 min at 23°C . Solvent and excess propylamine were distilled off under vacuum and the final product was taken into diethyl ether and dried over MgSO_4 to afford pure clear oil. ^1H -NMR (700 MHz; CDCl_3): δ 5.91 (d, $J = 7.7$ Hz, 2H), 4.27 (d, $J = 7.8$ Hz, 2H), 3.43 (t, $J = 6.7$ Hz, 4H), 3.28 (s, 4H), 2.99 (t, $J = 7.0$ Hz, 2H), 1.55 (dq, $J = 23.0, 7.3$ Hz, 6H), 1.32 (t, $J = 6.9$ Hz, 36H), 0.90 (t, $J = 7.1$ Hz, 9H). ^{13}C -NMR (700 MHz; CDCl_3): δ 130.8, 99.9, 71.7, 55.0, 40.6, 31.9, 29.71, 29.69, 29.67, 29.61, 29.55, 29.54, 29.52, 29.50, 29.44, 29.38, 26.22, 26.18, 23.4, 22.7, 14.1, 11.1

5.2.2 Synthesis of Acetonide Precursor (24)

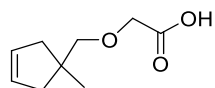




1-methylcyclopent-3-enecarboxylic acid (20). To a solution of cyclopent-3-enecarboxylic acid (**19**) (0.5000, 4.459 mmol) in 50 mL dry THF at -78°C under inert atmosphere (Ar) was added *t*-butyl lithium 1.7M (9 mL, 13.37 mmol, 3 eq) over 1 hour. The mixture was stirred at the same temperature for an additional 30 minutes until dianion is successfully generated, then excess iodomethane was added gently. A white precipitate forms to produce a suspension, which dissolves at 45°C overnight. The mixture is quenched by 1 mL of H₂O and stirred for 15 minutes, then solvent THF is stripped off under vacuum and the remaining crude is diluted with DCM. The organic solution was filtered and washed with H₂O (6 x 50 mL), saturated NH₄Cl (3 x 50 mL), and H₂O (2 x 50 mL), dried over MgSO₄, and purified with silica Hex:EtOAc (2:8) to afford a clear oil solid (3.121 mmol, 80%), repeating the experiment on the crude will yield 100% product. ¹H-NMR (700 MHz; CDCl₃): δ 5.64 (s, 2H), 2.98 (d, *J* = 14.7 Hz, 2H), 2.28 (d, *J* = 14.8 Hz, 2H), 1.36 (s, 3H). ¹³C-NMR (700 MHz; CDCl₃): δ 184.1, 128.2, 47.6, 44.6, 25.7.

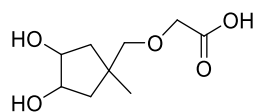


(1-methylcyclopent-3-enyl)methanol (21). To a suspension of lithium aluminum hydride (0.3358 g, 8.837 mmol, 3 eq) in dry 100 mL THF at -78°C, cyclopent-3-enecarboxylic acid (**20**) (0.3704 g, 2.945 mmol) was added drop wise over 1 hour. The mixture was stirred for 6 hours, and then quenched with 15 mL 1M NaOH. The mixture was stirred for an additional 2 hours, then concentrated and up taken in diethyl ether and dried over MgSO₄ to afford clear liquid (1.885 mmol, 63%). ¹H-NMR (700 MHz; CDCl₃): δ 5.64-5.63 (m, 2H), 3.47 (s, 3H), 2.35-2.32 (m, 2H), 2.12-2.07 (m, 2H), 1.13 (s, 3H). ¹³C-NMR (700 MHz; CDCl₃): δ 129.2, 71.4, 43.0, 24.9



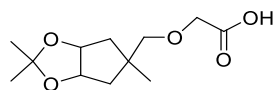
2-((1-methylcyclopent-3-enyl)methoxy)acetic acid (22)

To a suspension of excess NaH in 100 mL of dry THF at 0°C was added (1-methylcyclopent-3-enyl)methanol (**21**) (0.4494 g, 4.008 mmol) and stirred for 15 minutes. Then 2-chloroacetic acid (0.3767 g, 4.008 mmol) pre-dissolved in dry cool THF was added to the suspension via syringe. The mixture was mildly refluxed overnight. THF was distilled off under vacuum and the mixture was diluted with DCM. Content was treated with 1N NaOH to remove the organic impurities, then treated with 1N HCl and uptaken in DCM and dried over MgSO₄ to afford white solid (3.206 mmol, 80%) ¹H-NMR (700 MHz; CDCl₃): δ 5.63 (s, 2H), 4.15 (s, 2H), 3.43 (s, 2H), 2.38 (d, *J* = 14.3 Hz, 2H), 2.11 (d, *J* = 14.2 Hz, 2H), 1.16 (s, 3H). ¹³C-NMR (700 MHz; CDCl₃): δ 172.3, 129.0, 80.4, 68.4, 42.1, 25.4



2-((3,4-dihydroxy-1-methylcyclopentyl)methoxy)acetic acid (23)

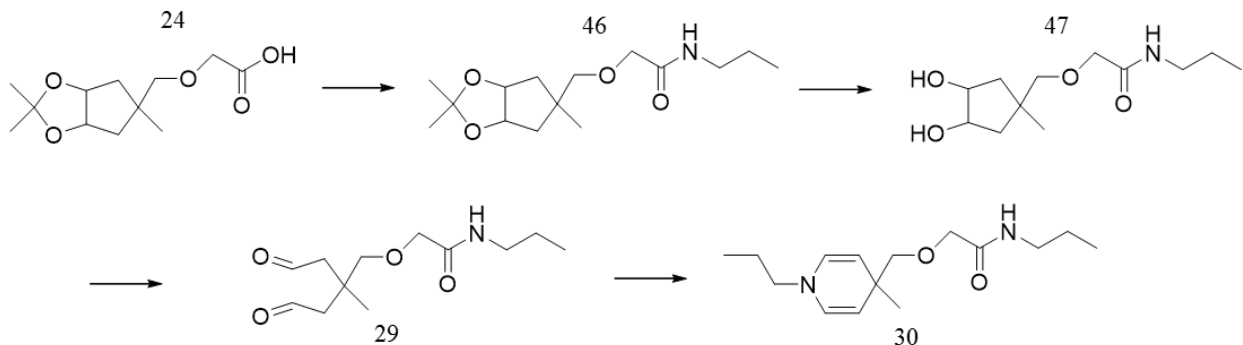
To a solution of crude product in previous step (**22**) (0.5456 g, 3.206 mmol) in acetone: acetonitrile (1:1) was added catalytic amount of OsO₄ and excess *N*-methylmorpholine *N*-oxide 50% in H₂O at pH 8. Reaction was monitored with TLC for complete disappearance of the starting material. Solvent was distilled off under vacuum and the product was taken into ethyl acetate and dried over MgSO₄, further purified with silica Hex:EtOAc (5:5) to afford a white solid as a mixture of isomers (2.308 mmol, combined 72%) ¹H-NMR (700 MHz; CDCl₃): δ 4.16 (t, *J* = 4.4 Hz, 2H), 4.14 (s, 2H), 3.27 (s, 2H), 1.99 (dd, *J* = 13.7, 6.2 Hz, 2H), 1.61 (dd, *J* = 13.7, 4.9 Hz, 2H), 1.22 (s, 3H). ¹³C-NMR (700 MHz; CDCl₃): δ 171.1, 81.0, 76.6, 74.4, 68.1, 41.8, 39.8, 27.4

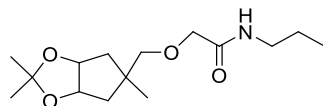


2-((2,2,5-trimethyltetrahydro-3aH-cyclopenta[d][1,3]dioxol-5-

yl)methoxy)acetic acid (24) To a solution of (**23**) mixture of isomers, (0.4713, 2.308 mmol) in dry THF and catalytic amount of *p*-TsOH was added a large excess of 2,2-dimethoxypropane. Reaction was monitored with TLC for complete disappearance of starting material. THF was distilled off under vacuum and the mixture was diluted with DCM. The organic solution was filtered and washed with H₂O (2 x 50 mL), dried over MgSO₄, and purified with silica Hex:EtOAc (7:3) to afford a mixture of diastereomers as white solid (2.193 mmol, combined 95%) ¹H-NMR (700 MHz; CDCl₃) Isomer I: δ 4.73-4.72 (m, 2H), 4.13 (s, 2H), 3.29 (s, 2H), 1.87 (dt, *J* = 14.5, 2.2 Hz, 2H), 1.74 (d, *J* = 14.2 Hz, 2H), 1.54 (s, 3H), 1.32 (s, 3H), 1.26 (s, 3H). ¹H-NMR (700 MHz; CDCl₃): δ 4.72 (dd, *J* = 3.4, 2.2 Hz, 3H), 4.16 (s, 2H), 4.13 (s, 2H), 3.61 (s, 2H), 3.28 (s, 2H), 2.01 (d, *J* = 14.8 Hz, 2H), 1.90 (ddd, *J* = 14.7, 4.9, 1.5 Hz, 2H), 1.72 (d, *J* = 14.1 Hz, 2H), 1.54 (s, 4H), 1.51 (s, 3H), 1.31 (d, *J* = 6.8 Hz, 6H), 1.25 (s, 3H), 1.10 (s, 3H). ¹³C-NMR (700 MHz; CDCl₃): δ 173.5, 172.6, 110.18, 110.06, 81.7, 81.4, 80.5, 78.6, 68.5, 68.2, 44.49, 44.46, 41.81, 41.71, 26.41, 26.23, 25.9, 24.5, 23.7, 23.4

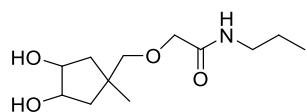
5.2.3 Synthesis of Dialdehyde Amide (**29**) and Conjugate (**30**)





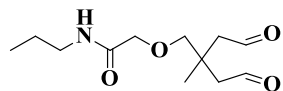
***N*-propyl-2-((2,2,5-trimethyltetrahydro-3aH-cyclopenta[d][1,3]dioxol-**

5-yl)methoxy)acetamide (46) To a solution of **(24)** mixed isomers (0.2000 g, 0.8196 mmol) in DCM/Acetonitrile (ACN) and excess of sodium bicarbonate was added along with 2-(1H-benzotriazol-1-yl)-1,1,3,3-tetramethyluronium hexafluorophosphate (HBTU) (0.3426 g, 0.9016 mmol, 1.1 eq). Reaction was monitored with TLC for complete disappearance of starting material. Once the activated carboxylic acid is generated, confirmed by disappearance of carboxylic acid intermediate, excess of propylamine was dispensed. Mixture was stirred for 30 minutes, then concentrated and flushed through a pad of silica Hex:EtOAc (4:1) to afford clear oil (0.7786 mmol, 95%) Mixture of Isomers: ¹H-NMR (400 MHz; CDCl₃): δ 4.72 (t, *J* = 2.1 Hz, 2H), 3.95 (s, 2H), 3.29 (q, *J* = 6.7 Hz, 2H), 3.22 (s, 2H), 1.77 (d, *J* = 3.0 Hz, 4H), 1.57 (dd, *J* = 13.3, 8.0 Hz, 9H), 1.32 (s, 3H), 1.28 (s, 3H), 0.96 (t, *J* = 7.4 Hz, 3H).



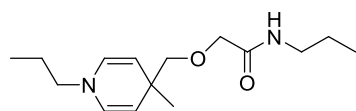
2-((3,4-dihydroxy-1-methylcyclopentyl)methoxy)-*N*-propylacetamide

(49) To a solution of **(46)** (0.1900 g, 0.7786 mmol) in methanol:H₂O (1:1), 3 drops of 1N HCl was added. Reaction was monitored with TLC for complete disappearance of starting material. Solvent was distilled off under vacuum and the product was taken into ethyl acetate and dried over MgSO₄, further purified with silica MeOH:EtOAc (0.5:9.5) to afford a white solid (0.7786 mmol, 100%) ¹H-NMR (700 MHz; CDCl₃): δ 4.12 (t, *J* = 4.3 Hz, 2H), 3.94 (s, 2H), 3.27 (q, *J* = 6.8 Hz, 2H), 3.18 (s, 2H), 1.92-1.90 (m, 2H), 1.61-1.53 (m, 2H), 1.20 (s, 3H), 0.94 (t, *J* = 7.4 Hz, 3H). ¹³C-NMR (700 MHz; CDCl₃): δ 169.5, 80.8, 74.4, 70.9, 41.9, 40.5, 39.9, 27.5, 22.9, 11.3



2-(2-methyl-4-oxo-2-(2-oxoethyl)butoxy)-*N*-propylacetamide (29) To a solution of **(47)** (190.7 mg, 0.7786 mmol) in H₂O:methanol (1:9) was

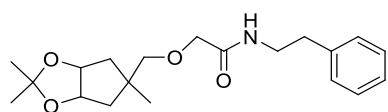
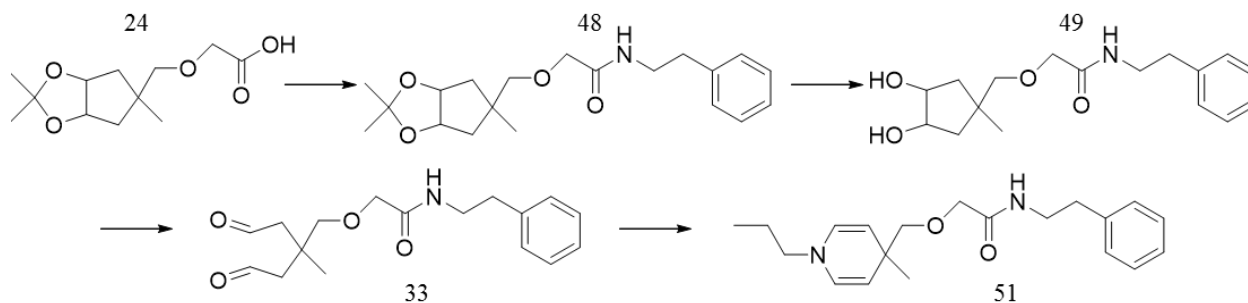
added NaIO₄ and stirred for 1 hour until a flakey white, solid iodate salt appeared. Solvent was distilled off under vacuum and the product was taken into diethyl ether and dried over MgSO₄ and used for subsequent reactions.



2-((4-methyl-1-propyl-1,4-dihydropyridin-4-yl)methoxy)-N-

propylacetamide (30) To a solution of **(29)** (20 mg, 0.4000 mmol) in DCM was added excess propylamine and stirred for 30 minutes at 23°C. Solvent and excess propylamine were distilled off under vacuum and the final product was taken into diethyl ether and dried over MgSO₄ to afford clear oil.

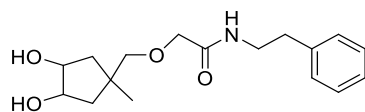
5.2.4 Synthesis of Phenyl Dialdehyde (33) and Conjugate (51)



N-phenethyl-2-((2,2,5-trimethyltetrahydro-3aH-

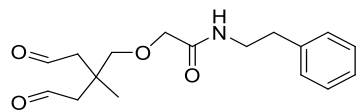
cyclopenta[d][1,3]dioxol-5-yl)methoxy)acetamide (48) To a solution of **(24)** mixed isomers (0.2000 g, 0.8196 mmol) in DCM/ACN and excess of sodium bicarbonate was added HBTU (0.3426 g, 0.9016 mmol, 1.1 eq). Reaction was monitored with TLC for complete disappearance of the starting material. Once the activated carboxylic acid was generated, confirmed by TLC, phenethylamine (0.0991 g, 0.8196 mmol) is added to the reaction vessel. Mixture was stirred for 30 minutes, then concentrated and flushed through a pad of silica Hex:EtOAc (4:1) to afford clear

oil (0.7377 mmol, 90 %) ^1H -NMR (700 MHz; CDCl_3): δ 7.33-7.31 (m, 1H), 7.25-7.23 (m, 1H), 7.21-7.20 (m, 1H), 4.62-4.61 (m, 2H), 3.89 (s, 2H), 3.59 (q, $J = 6.5$ Hz, 2H), 3.09 (s, 2H), 2.84 (t, $J = 6.8$ Hz, 2H), 1.62 (d, $J = 7.8$ Hz, 2H), 1.58 (s, 3H), 1.52 (s, 3H), 1.30 (s, 3H), 1.14 (s, 3H). ^{13}C -NMR (700 MHz; CDCl_3): δ 169.5, 138.6, 128.7, 126.7, 110.1, 81.5, 80.4, 70.8, 44.2, 41.7, 39.6, 35.5, 26.3, 24.4, 23.6.



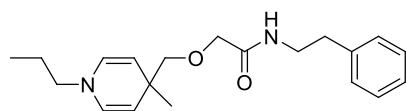
2-((3,4-dihydroxy-1-methylcyclopentyl)methoxy)-N-

phenethylacetamide (49): To a solution of **(48)** (0.2560 g, 7.377 mmol) in methanol: H_2O (1:1), 3 drops of 1N HCl was added. The reaction was monitored with TLC for complete disappearance of the starting material. Solvent was distilled off under vacuum and the product was taken into ethyl acetate and dried over MgSO_4 , further purified with silica MeOH:EtOAc (0.5:9.5) to afford a clear oil (7.377 mmol, 100 %) ^1H -NMR (700 MHz; CDCl_3): δ 7.33 (t, $J = 7.5$ Hz, 1H), 7.24 (d, $J = 7.3$ Hz, 1H), 7.21 (d, $J = 7.4$ Hz, 1H), 3.96 (d, $J = 3.5$ Hz, 2H), 3.90 (s, 2H), 3.61 (d, $J = 19.4$ Hz, 2H), 3.07 (s, 2H), 2.85 (d, $J = 13.4$ Hz, 2H), 1.76 (dd, $J = 13.8, 6.4$ Hz, 2H), 1.49 (dd, $J = 13.8, 5.2$ Hz, 2H), 1.08 (s, 3H). ^{13}C -NMR (700 MHz; CDCl_3): δ 169.5, 138.6, 128.89, 128.76, 126.6, 80.7, 74.3, 70.8, 41.7, 39.73, 39.55, 35.5, 27.4.



2-(2-methyl-4-oxo-2-(2-oxoethyl)butoxy)-N-phenethylacetamide

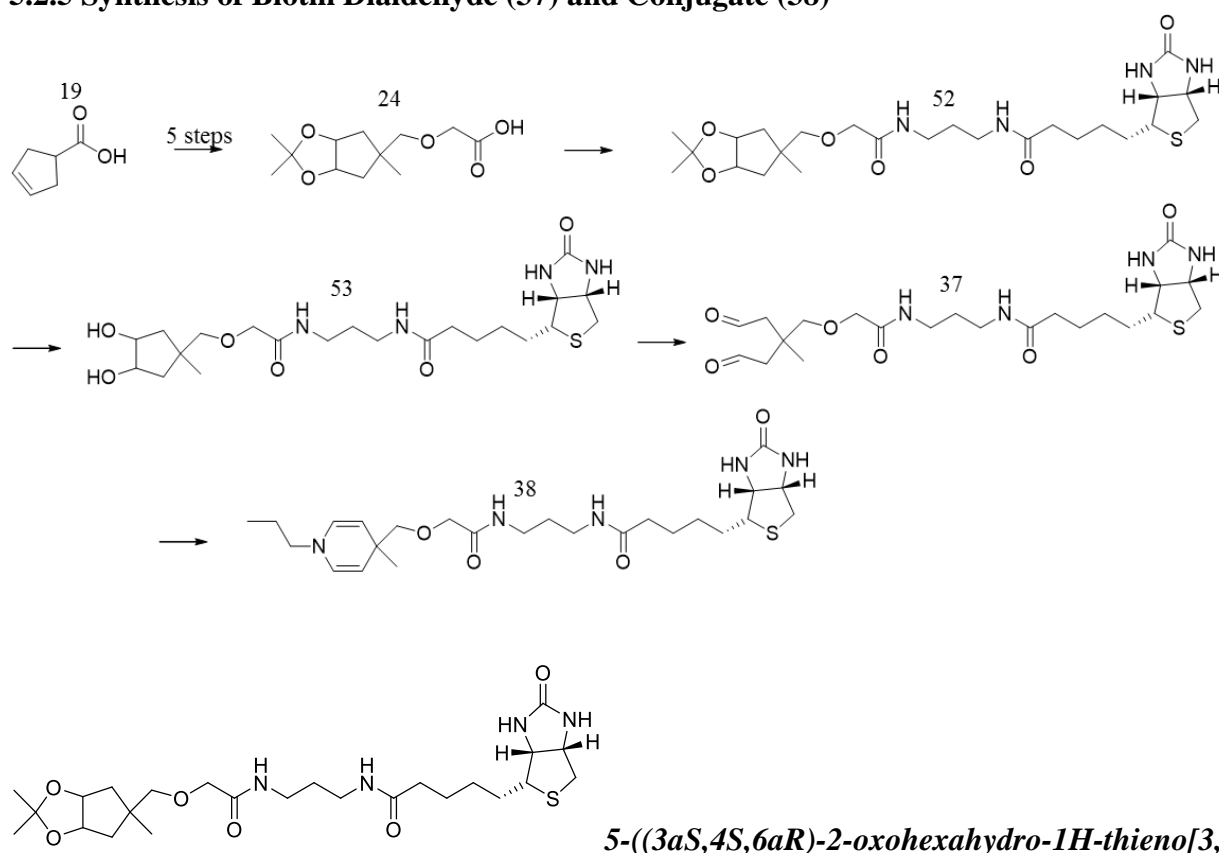
(33) To a solution of **(49)** (2.2647 g, 7.377 mmol) in H_2O :methanol (1:9) was added NaIO_4 and stirred for 1 hour until a flakey white, solid iodate salt appeared. Solvent was distilled off under vacuum and the product was taken into diethyl ether and dried over MgSO_4 and used for subsequent reactions.



2-((4-methyl-1-propyl-1,4-dihydropyridin-4-yl)methoxy)-N-

phenethylacetamide (51) To a solution of (33) (20 mg, 0.4000 mmol) in DCM was added excess propylamine and stirred for 30 minutes at 23°C. Solvent and excess propylamine were distilled off under vacuum and the final product was taken into diethyl ether and dried over MgSO₄ to afford clear oil.

5.2.5 Synthesis of Biotin Dialdehyde (37) and Conjugate (38)

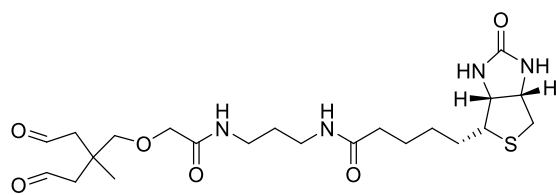


5-((3a*S*,4*S*,6a*R*)-2-oxohexahydro-1*H*-thienof[3,4-

***d*]imidazol-4-yl)-N-(3-(2-((2,2,5-trimethyltetrahydro-3a*H*-cyclopenta[*d*][1,3]dioxol-5-**

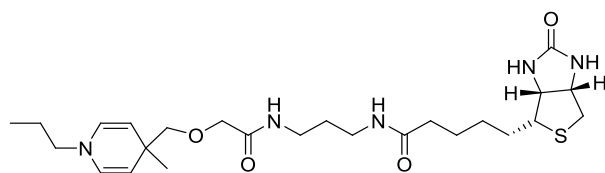
yl)methoxy)acetamido)propyl)pentanamide (52) To a solution of (24) mixed isomers (0.0589 g, 0.2415 mmol) in MeOH/ACN and excess of sodium bicarbonate was added HBTU (0.0917 g, 0.2656 mmol, 1.1 eq). The reaction was monitored with TLC for complete disappearance of starting material. Once the activated carboxylic acid was generated, confirmed by TLC, biotin

cadaverine trifluoroacetate (0.1000 g, 0.2415 mmol, 1 eq) was added to the reaction vessel. Mixture was stirred for 30 minutes, then concentrated and flushed through a pad of silica MeOH:EtOAc (1:4) to white crystal. ¹H-NMR (700 MHz; MeOD): δ 4.74-4.73 (m, 2H), 4.51 (dd, *J* = 7.8, 5.0 Hz, 1H), 4.32 (dd, *J* = 7.8, 4.5 Hz, 1H), 3.95 (s, 2H), 3.37 (s, 2H), 3.33 (q, 1H), 3.25 (s, 2H), 3.23 (d, *J* = 6.9 Hz, 2H), 2.95 (dd, *J* = 12.7, 5.0 Hz, 2H), 2.72 (d, *J* = 12.7 Hz, 2H), 2.24 (t, *J* = 7.3 Hz, 2H), 1.94 (dd, *J* = 14.2, 5.1 Hz, 2H), 1.71-1.66 (m, 4H), 1.49 (d, *J* = 4.9 Hz, 2H), 1.46 (d, *J* = 6.9 Hz, 2H), 1.46 (s, 3H), 1.30 (s, 3H), 1.24 (s, 3H).



2-(2-methyl-4-oxo-2-(2-oxoethyl)butoxy)-N-

phenethylacetamide (37) To a solution of **(52)** (87.74 mg, 0.1800 mmol) in H₂O:methanol (1:9) was added 3 drops of dilute acid and stirred for 30 minutes, then NaIO₄ was added and stirred for 1 hour until a flakey white, solid iodate salt appeared. Solvent was distilled off under vacuum and the product was taken into diethyl ether and dried over MgSO₄ and used for subsequent reactions.

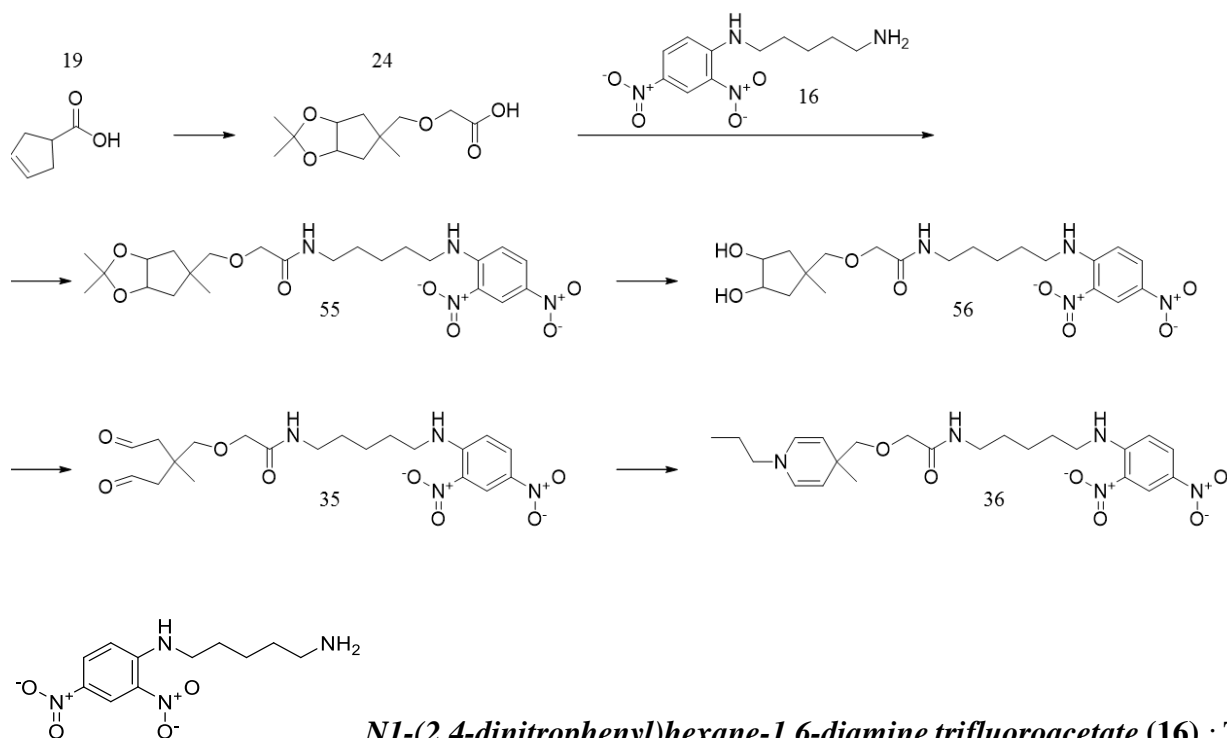


N-(3-(2-((4-methyl-1-propyl-1,4-dihydropyridin-

4-yl)methoxy)acetamido)propyl)-5-((3a*S*,4*S*,6a*R*)-2-oxohexahydro-1*H*-thieno[3,4-*d*]imidazol-

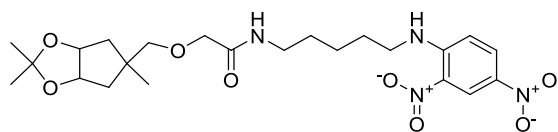
4-yl)pentanamide (38) To a solution of **(37)** (20 mg, 0.4000 mmol) in MeOH was added excess propylamine and stirred for 30 minutes at 23°C. Solvent and excess propylamine were distilled off under vacuum and the final product was taken into diethyl ether and dried over MgSO₄ to afford white solid.

5.2.6 Synthesis of DNP Dialdehyde (35) and Conjugate (36)

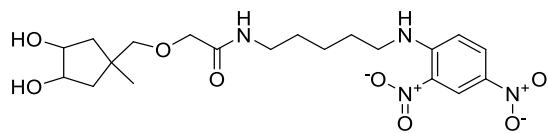


*N*1-(2,4-dinitrophenyl)hexane-1,6-diamine trifluoroacetate (16) : To

a solution of *N*-Boc-1,6-hexanediamine hydrochloride (0.2000 g, 0.793 mmol) in dimethyl formamide (DMF)/H₂O in (9:1) and excess of sodium bicarbonate was added **24** (0.1771 g, 0.9523 mmol, 1.2 eq) and stirred overnight. The solvents were stripped off under high vacuum and the content was dissolved in MeOH and treated with 80 % trifluoroacetic acid (TFA) and stirred for 1 hour at 23°C. After complete evaporation of solvent, fresh MeOH was added and filtered. Final product was isolated as yellow crystals of trifluoroacetate quaternary salt. ¹H-NMR (700 MHz; MeOD): δ 9.05 (dd, *J* = 5.5, 2.9 Hz, 1H), 8.30 (ddd, *J* = 9.5, 2.4, 1.9 Hz, 1H), 7.19-7.18 (m, 1H), 3.53 (d, *J* = 7.1 Hz, 2H), 2.97-2.94 (m, 2H), 1.80 (t, *J* = 7.3 Hz, 2H), 1.72-1.70 (m, 2H), 1.55-1.49 (m, 4H). ¹³C-NMR (700 MHz; MeOD): δ 161.74, 161.55, 148.3, 135.5, 130.1, 129.7, 123.38, 123.37, 119.3, 117.7, 116.0, 114.3, 42.7, 39.2, 28.1, 27.1, 26.0, 25.7

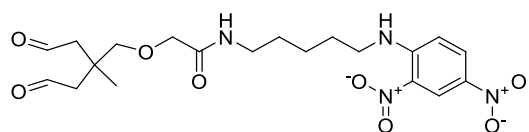


N-(6-(2,4-dinitrophenylamino)hexyl)-2-((2,2,5-trimethyltetrahydro-3aH-cyclopenta[d][1,3]dioxol-5-yl)methoxy)acetamide (55): To a solution of **(16)** mixed isomers (0.2000 g, 0.8196 mmol) in MeOH/ACN and excess of sodium bicarbonate was added HBTU (0.3426 g, 0.901 mmol, 1.1 eq) and stirred for 1 hour at 23°C. Reaction was monitored with TLC for complete disappearance of the starting material carboxylic acid. Once the activated carboxylic acid was generated, confirmed by TLC, **(59)** (0.4643 g, 0.901 mmol, 1.1 eq) was added to the reaction vessel. Mixture was stirred for 30 minutes, then concentrated and flushed through a pad of silica Hex:EtOAc (4:1) to afford yellow crystal (0.737 mmol, 90 %). ¹H-NMR (700 MHz; CDCl₃): δ 9.17 (d, *J* = 2.5 Hz, 1H), 8.57 (s, 1H), 8.31-8.30 (m, 1H), 6.94 (d, *J* = 9.5 Hz, 1H), 6.63 (d, *J* = 5.9 Hz, 1H), 4.72 (d, *J* = 4.7 Hz, 2H), 3.99 (s, 2H), 3.54 (s, 2H), 3.43 (q, *J* = 6.4 Hz, 3H), 3.33 (q, *J* = 6.7 Hz, 3H), 1.99 (d, *J* = 14.7 Hz, 2H), 1.82 (t, *J* = 7.3 Hz, 3H), 1.62-1.59 (m, 3H), 1.57 (s, 2H), 1.54 (td, *J* = 9.8, 4.0 Hz, 6H), 1.49-1.48 (m, 4H), 1.46 (q, *J* = 7.5 Hz, 3H), 1.30 (s, 3H), 1.09 (s, 3H). ¹³C-NMR (700 MHz; CDCl₃): δ 170.1, 148.3, 136.0, 130.4, 124.4, 113.8, 110.0, 81.3, 70.7, 44.5, 43.5, 41.8, 38.5, 29.5, 28.6, 26.56, 26.43, 26.2, 26.0, 23.4



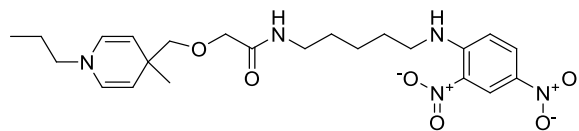
2-((3,4-dihydroxy-1-methylcyclopentyl)methoxy)-N-(6-(2,4-dinitrophenylamino)hexyl)acetamide (56) To a solution of **(55)** (0.3747 g, 0.737 mmol) in methanol:H₂O (1:1), 3 drops of 1N HCl was added. The reaction was monitored with TLC for complete disappearance of the starting material. Solvent was distilled off under vacuum and the product was taken into ethyl acetate and dried over MgSO₄, further purified with silica MeOH:EtOAc (0.5:9.5) to afford yellow crystals (0.700 mmol, 95 %). ¹H-NMR (700 MHz;

CDCl₃): δ 9.16 (d, J = 2.6 Hz, 1H), 8.57 (s, 1H), 8.30 (dd, J = 9.5, 2.5 Hz, 1H), 6.94-6.93 (m, 1H), 6.46 (s, 1H), 4.13 (q, J = 4.3 Hz, 2H), 4.03 (s,), 3.96 (s, 2H), 3.43 (q, J = 6.2 Hz, 3H), 3.34 (q, J = 6.8 Hz, 3H), 3.32 (d, J = 10.3 Hz, 1H), 3.20 (d, J = 6.7 Hz, 2H). ¹³C-NMR (700 MHz, CDCl₃): δ 169.6, 148.3, 136.0, 130.4, 124.4, 113.9, 80.8, 74.4, 70.9, 43.5, 41.9, 39.8, 38.6, 29.5, 28.6, 27.5, 26.56, 26.45



***N*-(6-(2,4-dinitrophenylamino)hexyl)-2-(2-methyl-4-**

oxo-2-(2-oxoethyl)butoxy)acetamide (35) To a solution of **(56)** (32.7 mg, 0.700 mmol) in H₂O:methanol (1:9) was added NaIO₄ and stirred for 1 hour until a flakey white, solid iodate salt appeared. Solvent was distilled off under vacuum and the product was taken into diethyl ether and dried over MgSO₄ and used for subsequent reactions.

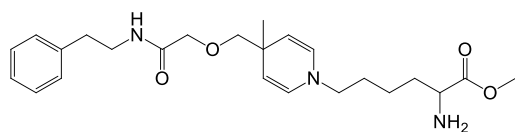


***N*-(3-(2-((4-methyl-1-propyl-1,4-dihydropyridin-4-**

yl)methoxy)acetamido)propyl)-5-((3a*S*,4*S*,6a*R*)-2-oxohexahydro-1*H*-thienof[3,4-*d*]imidazol-4-

yl)pentanamide (36) To a solution of **(35)** (20 mg, 0.4291 mmol) in MeOH/DCM was added excess propylamine and stirred for 30 minutes at 23°C. Solvent and excess propylamine were distilled off under vacuum and the final product was taken into diethyl ether and dried over MgSO₄ to afford yellow solid.

5.2.7 Synthesis of Lysine O-methyl Dialdehyde Conjugate (36)



Methyl-2-amino-6-(4-methyl-4-((2-oxo-2-(phenethylamino)ethoxy)methyl)pyridin-1(4H)-

yl)hexanoate (36) To a solution of L-Lysine methyl ester dihydrochloride (20 mg, 0.8583 mmol) in H₂O and excess bicarbonate was added (26 mg, 0.8583 mmol) (**49**) and stirred for 30 minutes at 23°C. Solvent was distilled off under vacuum and the final product was taken into MeOH and filtered through a layer of MgSO₄ to afford white solid.

5.2.8 Synthesis of Dialdehyde Glass Surfaces

Acetonide Surface: A (1 x 1 cm) glass SuperAmine substrate (Arrayit) was carefully cut and submerged in a solution of excess bicarbonate and water. The glass substrate was stirred at 23°C for 30 minutes to generate a free-base amine surface. In another vial, excess dicyclohexylcarbodiimide (DCC)/N-hydroxysuccinimide and bicarbonate was mixed in THF and stirred for 15 minutes to which, 0.001 moles of substrate **24** was added. Once the activated ester was generated, the glass substrate was submerged into the vial to allow for formation of the amide bond between substrate **24** and the amine surface over 3 hours at 23°C. The glass substrate was removed and rinsed 3X with MeOH/H₂O to remove all by-products and impurities. The generated protected diol surface is stable and could be stored at 4-8°C indefinitely.

Dialdehyde Surface (44): The acetonide glass surface is submerged in a mixture of MeOH/H₂O (1:9) to which 1 drop of dilute HCl acid is added and stirred for 4 hours to ensure the acetonide protecting group was completely removed. The substrate was then removed from the solution and rinsed with MeOH/H₂O five times. The resulting surface displays a 1,2 vicinal diol and was submerged into a vial containing excess NaIO₄ in MeOH/H₂O and stirred for 4 hours at 23°C. The

glass substrate presenting dialdehyde was then rinsed thoroughly with MeOH/H₂O and used for immobilization applications.

5.2.9 Immobilization of Fluorescent Beads onto Dialdehyde Glass Surfaces

Immobilization of fluorescent amine beads to dialdehyde surface. Synthesized surface displaying dialdehyde headgroup was submerged into a 12 mL vial charged with 10 µL of L1030 (Sigma Aldrich) amine presenting latex beads in an aqueous solution for 4 hours. The substrate was removed and rinsed with aqueous solution to remove any non-specific and non-covalent interaction from the surface. The resulting solid surface was rinsed and images were obtained using fluorescent microscopy.

Control Dialdehyde surface quenched with propylamine displays no fluorescent amine bead immobilization. Synthesized surface displaying dialdehyde headgroup was submerged into a 12 mL vial charged with MeOH and treated with excess propylamine for 4 hours. The substrate was then removed and washed with MeOH/H₂O thoroughly. The glass substrate was submerged into a 12 mL vial containing 10 µL of L1030 (Sigma Aldrich) amine presenting latex beads in an aqueous solution for 4 hours. The resulting surface was rinsed and images were obtained showing no fluorescent bead immobilized.

5.2.10 Cell Surface Engineering via Liposome Fusion using Dialdehyde Liposomes (15)

Dialdehyde Liposome (Pathway A)

General Dialdehyde Liposomes

The dialdehyde lipid molecule **9** (0.6451 mmol, 3.2 mg) in chloroform was aliquoted into a 5 mL autoclaved glass vial, followed by the addition of 295 µL of POPC (10 mg/mL) in chloroform (Avanti Polar) and 25.6 µL of DOTAP (10 mg/mL) in chloroform (Avanti Polar). The lipid

solution was then evaporated under a stream of air for 1 hour until dry. Then 1.92 mL of culture grade PBS (Sigma Aldrich) was added to the dry lipids and immediately tip sonicated (Fisher Scientific) for 10 minutes at 30 W in a 23°C water bath. The resulting lipid suspension was used within 24 hours or stored at 4°C until use.

General Blank Liposomes:

Into an autoclaved 5 mL glass vial, 295 µL of POPC (10 mg/mL) in chloroform and 25.6 µL of DOTAP (10 mg/mL) in chloroform were added, followed by evaporation using a stream of air for 1 hour. Then 1.92 mL of culture grade PBS was added to the dry lipids and immediately sonicated for 10 minutes at 30 W in a 23°C water bath. The resulting lipid suspension was used within 24 hours or stored at 4°C until use.

General Control Liposomes [Liposome with no dialdehyde lipid molecule (9)]:

Into an autoclaved 5 mL glass vial, reporter-amine (0.9677 mmol) was added followed by 295 µL of POPC (10 mg/mL) in chloroform and 25.6 µL of DOTAP (10 mg/mL) in chloroform were added, followed by evaporation using a stream of air for 1 hour. Then 1.92 mL of culture grade PBS was added to the dry lipids and immediately tip sonicated for 10 minutes at 30 W in a 23°C water bath. The resulting lipid suspension was used within 24 hours or stored at 4°C until use.

General Quenched Dialdehyde Liposomes:

The dialdehyde lipid molecule **9** (0.6451 mmol, 3.2 mg) in chloroform was treated with excess propylamine and stirred for 4 hours. The excess reagents and all other volatiles were evaporated. The content was aliquoted into a 5 mL autoclaved glass vial, followed by the addition of 295 µL of POPC (10 mg/mL) in chloroform and 25.6 µL of DOTAP (10 mg/mL) in chloroform. The lipid solution was then evaporated under a stream of air for 1 hour until dry. Then 1.92 mL of culture grade PBS was added to the dry lipids and immediately tip sonicated for 10 minutes at 30 W in a

23°C water bath. The resulting lipid suspension was used within 24 hours or stored at 4 °C until use.

5.2.11 Synthesis of Cell Surface Engineering Liposome Probes

DNPC-Dialdehyde Conjugation Liposome Preparation

Dialdehyde liposome **14** was transferred into a 5 mL autoclaved glass vial and treated with DNP-amine (0.9677 mmol, 4.8 mg). The mixture was incubated for 2 hours at 23°C with moderate agitation.

Biotin-Dialdehyde Conjugation Liposome Preparation

Dialdehyde liposome **14** was transferred into a 5 mL autoclaved glass vial and treated with biotin cadaverine **17** (0.9677 mmol, 4.6 mg). The mixture was incubated at 23°C for 2 hours with moderate agitation.

FLAG-Dialdehyde Conjugation Liposome Preparation

Dialdehyde liposome **14** was transferred into a 5 mL autoclaved glass vial and treated with FLAG peptide **18** (4.0 mg). The mixture was incubated at 23°C overnight with moderate agitation.

5.2.12 Cell Surface Engineering via Liposome Fusion using Dialdehyde Liposomes (15)

Dialdehyde Liposome (Pathway B)

DNPC-Dialdehyde Conjugation Liposome Preparation

The dialdehyde lipid molecule **9** (0.6451 mmol, 3.2 mg) was transferred into a 5 mL autoclaved glass vial and dissolved through the addition of 1.5 mL of a mixed solvent system (1:3) of THF and methanol respectively. To this solution, molecule **16** DNP cadaverine (0.9677 mmol, 4.8 mg) was added, along with a magnetic stir bar and reacted for 2 hours at 23°C. The product was

then obtained by evaporating the solvent under a stream of air. The conjugate product was then immediately used to form conjugate liposomes **15**.

To the 5 mL glass vial of synthesized DNP-dialdehyde conjugate, 295 μ L of POPC (10 mg/mL) in chloroform and 25.6 μ L of DOTAP (10 mg/mL) in chloroform were added, followed by evaporation using a stream of air for 1 hour. Then 1.92 mL of culture grade PBS was added to the dry lipids and immediately tip sonicated for 10 minutes at 30 W in a 23°C water bath. The resulting lipid suspension was used within 24 hours or stored at 4°C until use.

Biotin-Dialdehyde Conjugation Liposome Preparation

The dialdehyde lipid molecule **9** (0.6451 mmol, 3.2 mg) was transferred into a 5 mL autoclaved glass vial and dissolved through the addition of 1.5 mL of a mixed solvent system (1:3) of THF and methanol respectively. To this solution, molecule **17** biotin-amine (0.9677 mmol, 4.6 mg) was added, along with a magnetic stir bar and reacted for 2 hours at 23°C. The product was then obtained by evaporating the solvent under a stream of air. The product was then immediately used to form a single batch of liposomes.

To the 5 mL glass vial of synthesized biotin-Dialdehyde conjugate 295 μ L of POPC (10 mg/mL) in chloroform and 25.6 μ L of DOTAP (10 mg/mL) in chloroform were added, followed by evaporation using a stream of air for 1 hour. Then 1.92 mL of culture grade PBS was added to the dry lipids and immediately tip sonicated for 10 minutes at 30 W in a 23°C water bath. The resulting lipid suspension was used within 24 hours or stored at 4°C until use.

FLAG-Dialdehyde Conjugation Liposome Preparation

The dialdehyde lipid molecule **9** (0.6451 mmol, 3.2 mg) was transferred into a 5 mL autoclaved glass vial and dissolved through the addition of 1.5 mL of a mixed solvent system (1:1) of H₂O

and methanol, respectively. To this solution, molecule **18** FLAG peptide (4.0 mg) was added, along with a magnetic stir bar and reacted overnight (16 hours) at 23°C. The product was then obtained by evaporating the solvent under a stream of air. The product was then immediately used to form a single batch of liposomes.

To the 5 mL glass vial of synthesized FLAG-Dialdehyde conjugate 295 µL of POPC (10mg/mL) in chloroform and 25.6 µL of DOTAP (10 mg/mL) in chloroform were added, followed by evaporation using a stream of air for 1 hour. Then 1.92 mL of culture grade PBS was added to the dry lipids and immediately tip sonicated for 10 minutes at 30 W in a 23°C water bath. The resulting lipid suspension was used within 24 hours or stored at 4°C until use.

5.2.13 Mammalian Cell Surface Engineering via Dialdehyde Conjugate Liposome (15)

DNPC-dialdehyde (A) or Biotin-dialdehyde (B) Conjugate Liposome Delivery

C3H/10T1/2 cells (ATCC) were cultured using DMEM media supplemented with 10% FBS and 1% P/S under standard growth conditions. For experiments, the cells were treated with 3 mL trypsin for three minutes to place cells in suspension and then quenched using 6 mL of growth media. The suspension was then centrifuged at 800 RPM for 5 minutes, the media decanted and the cells re-suspended in 500 µL of PBS. To the prepared cell suspension, 500 µL of the liposomal solution of pathway **A** or **B** DNP-dialdehyde was added and incubated at 23°C for 10 minutes followed by the addition of 9 mL of PBS and centrifuged at 800 RPM for 5 minutes and decanting of the supernatant. The resulting pellet was then re-suspended in 500 µL of PBS and 40 µL of 2 mg/mL anti-dinitrophenyl-KLH, Alexa Fluor 488 conjugate (Life Technologies) and was incubated at 23°C for 1 hour. After incubation, the samples were diluted with 9 mL of PBS, centrifuged and the resulting pellet was washed again using 9 mL of PBS and centrifuged. The

pellet was then re-suspended in 500 μ L of PBS. Flow cytometry and fluorescence microscopy was used to characterize the resulting cell suspension.

Biotin-Dialdehyde Conjugate Liposome Delivery

C3H/10T1/2 cells were cultured using DMEM media supplemented with 10 % FBS and 1 % P/S under standard growth conditions. For experiments, the cells were treated with 3 mL trypsin for 3 minutes to place cells in suspension and then quenched using 6 mL of growth media. The suspension of cells was then centrifuged at 800 RPM for 5 minutes, the media decanted and the cells re-suspended in 500 μ L of PBS. To the prepared cell suspension, 500 μ L of the liposomal solution **A** or **B** biotin-dialdehyde was added and incubated at 23°C for 10 minutes followed by the addition of 9 mL of PBS and centrifuged at 800 RPM for 5 minutes, and decanting of the supernatant. The resulting pellet was then re-suspended in 500 μ L of PBS and 40 μ L of Streptavidin-(FITC) 1 mg/mL and was incubated at 23°C for 1 hour. After incubation, the samples were diluted with 9 mL of PBS, centrifuged and the resulting pellet was washed again using 9 mL of PBS and centrifuged. The pellet was then re-suspended in 500 μ L of PBS. Flow cytometry and fluorescence microscopy was used to characterize the resulting cell suspension.

FLAG-Dialdehyde Conjugate Liposome Delivery

C3H/10T1/2 cells were cultured in 10 cm plates for 2 days until 90% confluent using High Glucose DMEM supplemented with 10% FBS and 1% P/S at 37°C and 5% CO₂. The cells were removed using 3 mL trypsin for 4 minutes followed by addition of 6 mL media. The cells were collected and centrifuged at 800 RPM for 5 minutes followed by decanting of the media. The cells were re-suspended in 500 μ L PBS and treated with 500 μ L of the pathway **A** or **B** FLAG-dialdehyde prepared liposome suspension. The contents were incubated for 10 minutes followed by dilution with 9 mL of PBS and centrifuged followed by decantation. The pellet was re-suspended in 500

μL of PBS. The resulting pellet was then re-suspended in 500 μL of PBS, the C3H/10T1/2 cells were treated with 5 μL of 2 mg/mL anti-FLAG peptide (Life Technologies) and incubated at 23°C for 1 hour followed by dilution with 9 mL of PBS. Content was centrifuged and re-suspended in 500 μL of PBS and then further characterized by flow cytometry and fluorescence microscopy.

5.2.14 Bacteria Cell Surface Engineering via Dialdehyde Conjugate Liposome (15)

Biotin-Dialdehyde Conjugate Liposome Delivery

Bacteria *E. coli* BL21, were grown to $\text{OD}^{650} = 0.6$, corresponding to approximately 4×10^8 CFU/mL. The cells were harvested by centrifugation at 6000 RPM for 10 minutes, washed with 100 mM CaCl_2 and re-suspended in 6 mL of 100 mM CaCl_2 for 2 hours at 4°C. Aliquoted cells were suspended in 10 mL of 0.5 mM HEPES buffer pH 4.3. Cells were then treated with 6 μL EDTA (50 mM pH 8.4) and incubated at 37°C for 1 hour. 550 μL of liposomal solution obtained from pathway **A** or **B** was added to the cell culture and incubated at 23°C for 30 minutes. Cells were then spun down and the resulting pellet was re-suspended in 500 μL of PBS and 40 μL of STREPT-(FITC) 1 mg/mL. Content was incubated at 25°C for 1 hour or 15 minutes at 37°C. After incubation, cells were centrifuged and the resulting pellet was washed three times using 2 mL of fresh PBS. The pellet was then re-suspended in 500 μL of PBS. Flow cytometry and fluorescence microscopy was then used to characterize the resulting cell suspension.

5.2.15 Cell Surface Engineering via Liposome Fusion using Amine Liposomes (42)

Amine Liposome (Pathway A)

General Dodecylamine Liposomes

The dodecylamine molecule **39** (0.02702 mmol, 5.0 mg) in chloroform was aliquoted into a 5 mL autoclaved glass vial, followed by the addition of 295 μL of POPC (10 mg/mL) in chloroform and

25.6 μL of DOTAP (10 mg/mL) in chloroform. The lipid solution was then evaporated under a stream of air for 1 hour until dry. Then 1.92 mL of culture grade PBS was added to the dry lipids and immediately tip sonicated for 10 minutes at 30 W in a 37°C water bath. The resulting lipid suspension was used within 24 hours or stored at 4°C until use.

General Blank Liposomes:

Into an autoclaved 5 mL glass vial 295 μL of POPC (10 mg/mL) in chloroform and 25.6 μL of DOTAP (10 mg/mL) in chloroform were added, followed by evaporation using a stream of air for 1 hour. Then 1.92 mL of culture grade PBS was added to the dry lipids and immediately tip sonicated for 10 minutes at 30 Watts in a 37°C water bath. The resulting lipid suspension was used within 24 hours or stored at 4°C until use.

General Control Liposomes (No Dodecylamine):

Into an autoclaved 5 mL glass vial reporter-dialdehyde (0.4054 mmol) was added followed by 295 μL of POPC (10 mg/mL) in chloroform and 25.6 μL of DOTAP (10 mg/mL) in chloroform were added, followed by evaporation using a stream of air for 1 hour. Then 1.92 mL of culture grade PBS was added to the dry lipids and immediately tip sonicated for 10 minutes at 30 W in a 37°C water bath. The resulting lipid suspension was used within 24 hours or stored at 4°C until use.

General Quenched Dodecylamine Liposomes:

The dodecylamine molecule **39** (0.1081 mmol, 20.0 mg) in DCM was treated with excess HCl and stirred for 1 hour. The excess reagents and all other volatiles were evaporated. The content was aliquoted into a 5 mL autoclaved glass vial, followed by the addition of 295 μL of POPC (10 mg/mL) in chloroform and 25.6 μL of DOTAP (10 mg/mL) in chloroform. The lipid solution was then evaporated under a stream of air for 1 hour until dry. Then 1.92 mL of culture grade PBS was

added to the dry lipids and immediately tip sonicated for 10 minutes at 30 W in a 37°C water bath. The resulting lipid suspension was used within 24 hours or stored at 4°C until use.

DNPC-Dialdehyde-Dodecylamine Conjugation Liposome Preparation

Amine liposome **41** was transferred into a 5 mL autoclaved glass vial and treated with molecule **35** DNP-dialdehyde (0.04054 mmol, 2.0 mg). The batch was then incubated at 23°C for 2 hour with moderate agitation.

Biotin-Dialdehyde-Dodecylamine Conjugation Liposome Preparation

Amine liposome **41** was transferred into a 5 mL autoclaved glass vial and treated with molecules **37** biotin-dialdehyde (0.04054 mmol, 1.9 mg). The batch was then incubated at 25°C for 2 hours with moderate agitation.

5.2.16 Cell Surface Engineering via Liposome Fusion using Amine Liposomes (42)

Amine Liposome (Pathway B)

DNPC-Dialdehyde Conjugation Liposome Preparation

Dodecylamine molecule **39** (0.02688 mmol, 5.0 mg) was transferred into a 5 mL autoclaved glass vial and dissolved with the addition of 1.5 mL of a mixed solvent system (1:3) of THF and methanol, respectively. To this solution, molecule **35** DNP-dialdehyde (0.04032 mmol, 18 mg) was added, along with a magnetic stir bar and reacted for 2 hours at 23°C. The product was then obtained by evaporating the solvent under a stream of air. The product was then immediately used to form a single batch of liposomes.

To the 5 mL glass vial of synthesized DNP-dialdehyde-dodecylamine conjugate, 295 µL of POPC (10 mg/mL) in chloroform and 25.6 µL of DOTAP (10 mg/mL) in chloroform were added, followed by evaporation using a stream of air for 1 hour. Then 1.92 mL of culture grade PBS was

added to the dry lipids and immediately tip sonicated for 10 minutes at 30 W in a 23°C water bath. The resulting lipid suspension was used within 24 hours or stored at 4°C until use.

Biotin-Dialdehyde-Dodecylamine Conjugation Liposome Preparation

Dodecylamine molecule **39** (0.02688 mmol, 5.0 mg) was transferred into a 5 mL autoclaved glass vial and dissolved with the addition of 1.5 mL of a mixed solvent system (1:3) of THF and methanol respectively. To this solution, molecule **37** biotin-dialdehyde (0.04032 mmol, 20 mg) was added, along with a magnetic stir bar and reacted for 2 hours at 23°C. The product was then obtained by evaporating the solvent under a stream of air. The product was then immediately used to form a single batch of liposomes.

To the 5mL glass vial of synthesized biotin-dialdehyde-dodecylamine conjugate 295 µL of POPC (10 mg/mL) in chloroform and 25.6 µL of DOTAP (10 mg/mL) in chloroform were added, followed by evaporation using a stream of air for 1 hour. Then 1.92 mL of culture grade PBS was added to the dry lipids and immediately tip sonicated for 10 minutes at 30 W in a 23°C water bath. The resulting lipid suspension was used within 24 hours or stored at 4°C until use.

5.2.17 Mammalian Cell Surface Engineering via Amine Conjugate Liposome (42)

DNPC-Dialdehyde-Dodecylamine Conjugate Liposome Delivery

C3H/10T1/2 cells were cultured in 10 cm plates for 2 days until 90% confluent using High Glucose DMEM supplemented with 10% FBS and 1% P/S at 37°C and 5% CO₂. For experiments, the cells were treated with 3 mL trypsin for 3 minutes to place cells in suspension and then quenched using 6 mL of growth media. The suspension of cells was then centrifuged at 800 RPM for 5 minutes, the media was decanted and the cells re-suspended in 500 µL of PBS. To the prepared cell suspension, 500 µL of the liposomal solution of pathway **A** or **B** DNP-dialdehyde-dodecylamine

was added and incubated at 23°C for 10 minutes followed by the addition of 9 mL of PBS and centrifuged at 800 RPM for 5 minutes, followed by decanting of the supernatant. The resulting pellet was then re-suspended in 500 µL of PBS and 40 µL of 2 mg/mL anti-dinitrophenyl-KLH, Alexa Fluor 488 conjugate (Life Technologies) and was incubated at 23°C for 1 hour. After incubation, the samples were diluted with 9 mL of PBS, centrifuged and the resulting pellet was washed again using 9 mL of PBS and centrifuged. The pellet was then re-suspended in 500 µL of PBS. Flow cytometry and fluorescence microscopy was used to characterize the resulting cell suspension.

Biotin-Dialdehyde-Dodecylamine Conjugate Liposome Delivery

C3H/10T1/2 cells were cultured in 10 cm plates for 2 days until 90% confluent using High Glucose DMEM supplemented with 10% FBS and 1% P/S at 37°C and 5% CO₂. For experiments, the cells were treated with 3 mL trypsin for 3 minutes to place cells in suspension and then quenched using 6 mL of growth media. The suspension of cells was then centrifuged at 800 RPM for 5 minutes, the media was decanted and the cells re-suspended in 500 µL of PBS. To the prepared cell suspension, 500 µL of the liposomal solution **A** or **B** biotin-dialdehyde-dodecylamine was added and incubated at 23°C for 10 minutes followed by the addition of 9 mL of PBS, centrifuged at 800 RPM for 5 minutes, followed by decanting of the supernatant. The resulting pellet was then suspended in 500 µL of PBS and 40 µL of STREPT-FITC (1 mg/mL) and then incubated at 25°C for 1 hour. After incubation, the samples were diluted with 9 mL of PBS, centrifuged and the resulting pellet was washed again using 9 mL of PBS and centrifuged again. The pellet was then re-suspended in 500 µL of PBS. Flow cytometry and fluorescence microscopy was used to characterize the resulting cell suspension.

5.2.18 Bacteria Cell Surface Engineering via Amine Conjugate Liposome (42)

DNP-Dialdehyde-dodecylamine Conjugate Liposome Delivery

E. coli BL21, were grown to $OD^{650} = 0.6$, corresponding to approximately 4×10^8 CFU/mL. The cells were harvested by centrifugation at 6000 RPM for 10 minutes, washed with 100 mM $CaCl_2$ and re-suspended in 6 mL of 100 mM $CaCl_2$ for 2 hours at 4°C. Aliquoted cells were suspended in 10 mL of 0.5 mM HEPES buffer (pH 4.3). Cells were then treated with 6 μ L EDTA (50 mM pH 8.4) and incubated at 37°C for 1 hour. 550 μ L of liposomal solution obtained from pathway **A** or **B** was added to the cell culture and incubated at 23°C for 30 minutes. Cells were then spun down and the resulting pellet was re-suspended in 500 μ L of PBS and 40 μ L of 2 mg/mL anti-dinitrophenyl-KLH, Alexa Fluor 488 conjugate (Life Technologies) and then incubated at 23°C for 1 hour. Content was incubated at 25°C for 1 hour or 15 minutes at 37 °C. After incubation, cells were centrifuged and the resulting pellet was washed three times using 2 mL of fresh PBS. The pellet was then re-suspended in 500 μ L of PBS. Flow cytometry and fluorescence microscopy was used to characterize the resulting cell suspension.

Biotin-Dialdehyde-dodecylamine Conjugate Liposome Delivery

E. coli BL21, were grown to $OD^{650} = 0.6$, corresponding to approximately 4×10^8 CFU/mL. The cells were harvested by centrifugation at 6000 RPM for 10 minutes, washed with 100 mM $CaCl_2$ and re-suspended in 6 mL of 100 mM $CaCl_2$ for 2 hours at 4°C. Aliquot cells were suspended in 10 mL of 0.5 mM HEPES buffer (pH 4.3). Cells were then treated with 6 μ L EDTA (50 mM pH 8.4) and incubated at 37°C for 1 hour. 550 μ L of liposomal solution obtained from pathway **A** or **B** was added to the cell culture and incubated at 23°C for 30 minutes. Cells were then spun down and the resulting pellet was re-suspended in 500 μ L of PBS and 40 μ L of STREPT-FITC (1 mg/mL). Content was incubated at 25°C for 1 hour or 15 minutes at 37°C. After incubation, cells

were centrifuged and the resulting pellet was washed three times using 2 mL of fresh PBS. The pellet was then re-suspended in 500 μ L of PBS. Flow cytometry and fluorescence microscopy was used to characterize the resulting cell suspension.

5.2.19 Cross-linking of Protein LAR D1D2 and CS2 Domain

20 μ L of Protein LAR D1D1 18.5 μ M was mixed with 20 μ L of CS2 domain 20 μ M and incubated for 30 minutes for complete interactive binding, to which, 20 μ L of homobifunctional cross-linker dialdehyde (**70**) 20 mg/mL was added. The mixture was further diluted to a total of 50 μ L volume using PBS pH 8.4 buffer and incubated at 25°C and 37°C for 15 minutes.

Control protein (Cross-linker Deficient): A native control experiment was also conducted by mixing 20 μ L of Protein LAR D1D2 18.5 μ M and 20 μ L of CS2 20 μ M, incubated for 30 minutes for complete interactive binding for complex formation.

Control Cross-linker reagent (Quenched Head Groups): A native control experiment was also conducted using quenched linker with propylamine, presenting a terminated head group dialdehyde functional group. 20 μ L of homobifunctional cross-linker dialdehyde (**70**) 20 mg/mL was mixed with excess propylamine in a 1 mL vial and incubated at 23°C for 5 hours to ensure both head groups were terminated. The solvent and excess volatile reagents were evaporated using a stream of air overnight. The content was resolved in 20 μ L of fresh PBS (pH 8.4) and added to 20 μ L of protein complex which was further diluted to a total of 50 μ L volume using PBS pH 8.4 buffer and incubated at 25°C and 37°C for 15 minutes.

Positive Control Cross-linker Reagent (Glutaraldehyde): To investigate the extent of cross-linking, a positive control experiment was also performed with conventional 50% glutaraldehyde consistent with the total concentration of the protein-protein complex. 20 μ L of Protein LAR D1D2

was mixed with 20 μL of CS2 20 μM and incubated for 30 minutes for complete interactive binding, to which, 5 μL of homobifunctional cross-linker glutaraldehyde was added, further diluted to a total of 50 μL volume using PBS buffer (pH 8.4) and incubated at 25°C and 37°C for 15 minutes.

5.2.20 Cross-linking of Protein EA22

3 μL of Protein EA22 Lambdaphage 1 mg/ml was mixed with 15 μL of homobifunctional cross-linker dialdehyde (**72**) 20 mg/ml, further diluted to a total of 50 μL volume using PBS buffer (pH 8.4) and incubated at 25°C for 15 minutes.

Control Cross-linker Reagent (Quenched Head Groups): A native control experiment was also conducted using quenched linker with propylamine, presenting a terminated head group dialdehyde functional group. 3 μL of homobifunctional cross-linker dialdehyde (**70**) 20 mg/ml was mixed with excess propylamine in a 1 mL vial and incubated at 23°C for 5 hours to ensure both head groups were terminated. The solvent and excess volatile reagents were evaporated using a stream of air overnight. The content was resolved in 10 μL of PBS (pH 7.8) and added to 3 μL of protein EA22 further diluted to a total of 50 μL volume using PBS buffer (pH 8.4) and incubated at 25°C for 15 minutes.

5.2.21 Cross-linking of Protein PP16

3 μL of Protein PP16 Lambdaphage (1 mg/mL) was mixed with 15 μL of homobifunctional cross-linker dialdehyde (**70**) 20 mg/mL, further diluted to a total of 50 μL volume using PBS buffer (pH 8.4) and incubated at 25°C for 15 minutes.

Control Cross-linker reagent (Quenched Head Groups): A native control experiment was also conducted using quenched linker with propylamine, presenting a terminated head group

dialdehyde functional group. 15 μ L of homobifunctional cross-linker dialdehyde (**70**) 20 mg/ml was mixed with excess propylamine in a 1 ml vial and incubated at 23°C for 5 hours to ensure both head groups were terminated. The solvent and excess volatile reagents were evaporated using a stream of air overnight. The content was resolved in 10 μ L of PBS (pH 7.8) and added to 3 μ L of protein PP16 further diluted to a total of 50 μ L volume using PBS buffer (pH 8.4) and incubated at 25°C for 15 minutes.

SDS Gel Electrophoresis Analysis: A 20 μ L aliquot of each complex above was mixed with equal volume of 2X SDS dye and resolved on a 12% SDS-PAGE gel. The gel was stained with Coomassie Brilliant Blue staining solution and imaged.

5.2.22 Dialdehyde Cross-linking and Acid Release of Commercial Latex-Amine Beads in Aqueous Solution

In a 5 mL test tube, 10 μ L of L1030 (Sigma Aldrich) amine presenting latex beads in aqueous solution were aliquoted and diluted with 500 μ L of ddH₂O and then gently agitated. An aqueous solution of cross-linking tetraethylene glycol (TEG)-dialdehyde (**70**) in 250 μ L (0.011 mM) using ddH₂O or methanolic solution of cross-linker dialdehyde (**66**) in methanol was made. 250 μ L of either solutions of cross-linker dialdehyde was aliquoted into the latex-amine bead suspension, gently agitated and reacted overnight at 23°C. Examination of the overnight reaction yielded precipitated beads.

Blank Control Liposomes (dialdehyde deficient): In a 5 mL test tube, 10 μ L of L1030 amine presenting latex beads in aqueous solution were aliquoted and diluted with 500 μ L of ddH₂O and then gently agitated. Next, 100 μ L of ddH₂O was aliquoted into the latex-amine bead suspension and reacted overnight at 25°C. No change in opaque suspension of beads was observed.

N-propylamine Quenched Aldehyde Control: An aqueous solution of cross-linking TEG containing dialdehyde (**70**) in 250 μL (0.011 mM) was made using ddH₂O and solution of cross-linker (**66**) in 250 μL of methanol (0.011 mM). N-propylamine was added and reacted at 25°C for 1 hour to both solutions separately. Then 250 μL of the quenched cross-linking dialdehyde was added to a suspension of latex amine presenting beads formed through the dilution of 15 μL of L1030 beads diluted using 500 μL of ddH₂O. No change in opaque suspension of beads was observed.

Cross-linked Dialdehyde Acid Release: First a precipitated cross-linked bead sample was produced using a 5 mL test tube 10 μL of L1030 (Sigma Aldrich) amine presenting latex beads in aqueous solution were aliquoted, diluted with 500 μL of ddH₂O and then gently agitated. An aqueous solution of (**70**) in 250 μL (0.011 mM) was made using ddH₂O. Similar methanolic solution was made using (**66**). 250 μL of cross-linker solution was aliquoted into the latex-amine bead suspension, gently agitated and reacted overnight at 25°C. Examination upon overnight reaction yielded precipitated beads. The remaining liquid was decanted using a micropipette, leaving behind only the precipitated beads. To the beads 450 μL of ddH₂O treated with 1M HCl to pH 2.0 was added and agitated. The suspension was then allowed to react and then visualized to determine if the beads continued to precipitate or remained in suspension. Then, after a 12 hour reaction of the cross-linked beads with water (pH 2.0), the bead suspensions were centrifuged at 8000 RPM for 10 minutes, followed by decanting of the supernatant and the addition of fresh 500 μL of ddH₂O (pH 2.0) and re-suspended. The beads were allowed to react for a further 30 minutes and then centrifuged at 8000 RPM for 10 minutes, followed by decanting of the supernatant and the addition of fresh 500 μL of ddH₂O and re-suspended. The beads were allowed to sit for 16 hours and images were obtained of the final suspension along with controls using fluorescent microscopy.

Fluorescent Microscopy of Dialdehyde Cross-linking of Amine Beading in Solution: In a 5 mL test tube, 10 μ L of L1030 amine presenting latex beads in aqueous solution were transferred and diluted with 500 μ L of ddH₂O and gently agitated. An aqueous solution of cross-linker TEG containing dialdehyde (**70**) in 250 μ L (0.011 mM 1.5 mg) was made using ddH₂O and solution of cross-linker (**66**) in 250 μ L of methanol (0.011 mM, 1.5 mg). 250 μ L of the cross-linker solution was aliquoted into the latex-amine bead suspension, gently agitated and reacted overnight at 25°C. Examination of the overnight reaction yielded precipitated beads. The beads were transferred onto glass slides and imaged using phase contrast and fluorescent microscopy to visualize aggregation.

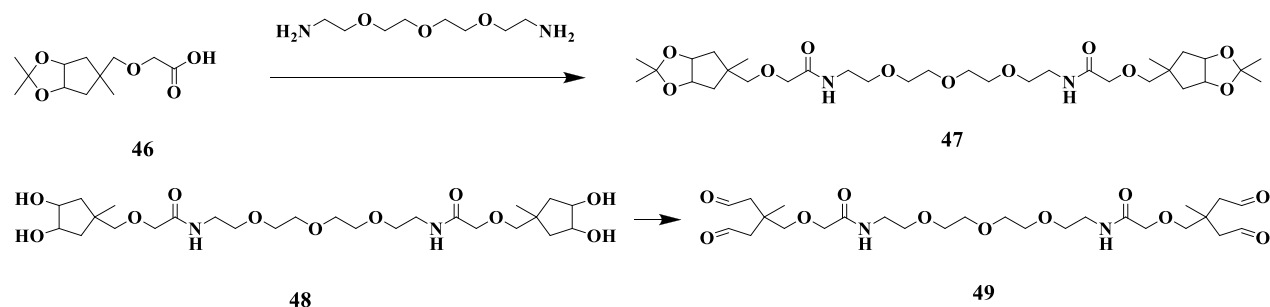
5.2.23 Cross-linker Dialdehyde Generation of Tissue Constructs

General Tissue Formation through Dialdehyde Cross-linking: C3H/10T1/2 cells were cultured in 10 cm tissue for 2 days until 90% confluent using optimal growth conditions. For experiments, cell cultures were suspended using 3 mL trypsin for 4 minutes followed by addition of 6 mL DMEM media. The cells were collected and centrifuged at 800 RPM for 5 minutes followed by decanting. The pellet was re-suspended in approximately 650 μ L of serum free media to obtain a concentration of 4×10^6 cells/mL using a hemocytometer. The suspension was then treated with 2 μ L of a 20 mg/mL dialdehyde cross-linker aqueous solution. Then 200 μ L of the treated suspension was carefully added on top of a sterile 1 cm² glass slide and incubated for 1 hour at 37°C and 5% CO₂. The glass slides were then washed once with PBS, fresh serum containing media and the plates were further incubated for 16 hours (overnight), then washed twice with PBS and fixed with 4% formalin solution. For confocal microscopy, the cells were stained with DAPI and TRITC for 3D visualization using the manufacturers protocol. The images were obtained by mounting onto thin glass slides with LIGHT DIAGNOSTICS Mounting Fluid (Millipore) for 3D confocal microscopy using a Zeiss LSM 700.

Tissues were also formed using RFP and GFP expressing cell lines by using the above protocol. The cells were combined in suspension with 1:1 ratio with an overall concentration of 4 million cells/mL. These tissues were visualized without staining by mounting onto thin glass slides with LIGHT DIAGNOSTICS Mounting Fluid (Millipore) for 3D confocal microscopy using a Zeiss LSM 700.

Cell Viability Assay of C3H/10T1/2 cells with Cross-linker Dialdehyde: The cell viability assay was performed using C3H/10T1/2 cells using the general tissue engineering protocol. After cells were treated with the cross-linker dialdehyde molecule (**70**), washed and replaced with fresh serum media, following 16 hours of incubation (overnight) the cells were re-suspended and the cell viability assay was performed using Trypan Blue (Sigma Aldrich) staining, following the manufacturer's protocol.

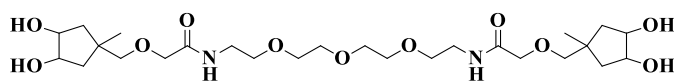
5.2.24 Synthesis of Dialdehyde Cross-linker (49)



N,N'-(2,2'-(2,2'-oxybis(ethane-2,1-diyl))bis(oxy))bis(ethane-2,1-diyl)bis(2-((2,2,5-trimethyltetrahydro-3aH-

cyclopenta[d][1,3]dioxol-5-yl)methoxy)acetamide) (**47**) To a solution of (**46**) mixed isomers (0.0635 g, 0.2604 mmol) in MeOH/ACN and excess of sodium bicarbonate was added HBTU (0.2078 g, 0.546 mmol, 2.1 eq). Reaction was monitored with TLC for complete disappearance of

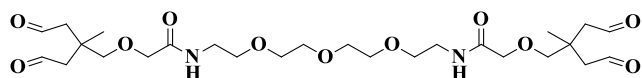
starting material. Once the activated carboxylic acid is generated, confirmed by TLC, 1,11-diamino-3,6,9-trioxaundecane (0.0250 g, 0.1302 mmol) was added to the reaction vessel. Mixture was stirred for 0.5 hours, then concentrated and flushed through a pad of silica MeOH:EtOAc (1:4) to afford clear oil (0.1236 mmol, 95%). The product was not purified as an isolated compound as it was used in subsequent steps.



N,N'-(2,2'-(2,2'-oxybis(ethane-2,1-

diyl))bis(oxy))bis(ethane-2,1-diyl))bis(2-

((3,4-dihydroxy-1-methylcyclopentyl)methoxy)acetamide) (**47**) To a solution of (**47**) (0.8000 g ,0.1236 mmol) in methanol:H₂O (1:1), 3 drops of 1N HCl was added. The reaction was monitored with TLC for complete disappearance of the starting material. Solvent was distilled off under vacuum and the product was taken into ethyl acetate and dried over MgSO₄, further purified with silica MeOH:EtOAc (1:4) to afford a clear oil (0.1236 mmol, 100%). ¹H-NMR (700 MHz, CDCl₃): 1.28-1.39 (4s, 12H), 1.518 (s, 3H), 1.540 (s, 3H), 1.92- 1.95 (d, 2H, J= 14.59Hz), 2.28-2.30 (d, 2H), 2.68-2.70 (d, 2H, J= 14.51Hz), 4.682-4.689 (d, 1H, J= 4.38Hz), 4.760-4.769 (d, 1H).



N,N'-(2,2'-(2,2'-oxybis(ethane-2,1-

diyl))bis(oxy))bis(ethane-2,1-diyl))bis(2-(2-

methyl-4-oxo-2-(2-oxoethyl)butoxy)acetamide)(**49**) To a solution of (**48**) (0.8000 g ,0.1236 mmol) in H₂O:methanol (1:9) was added NaIO₄ and stirred for 1 hour until a flakey white, solid iodate salt appeared. Solvent was distilled off under vacuum and the product was taken into diethyl ether and dried over MgSO₄ and used for subsequent reactions.

5.3 Results and Discussion

To show the utility of the modified glutaraldehyde moiety for primary amine conjugation we synthesized a number of dialdehyde containing molecules for a wide range of applications. Figure 5.3 depicts the synthetic scheme used to produce the lipidated dialdehyde molecule (9), which was used as a ‘liposome loading’ or ‘lipidation strategy’ for delivery of amine containing molecules to cells. These molecules can be useful for conjugating a variety of probes for biophysical, cell membrane and biology studies. The synthetic strategy for the lipid dialdehyde (9) only requires 5 synthetic steps, which also proceed with high yields as a straightforward and robust methodology.

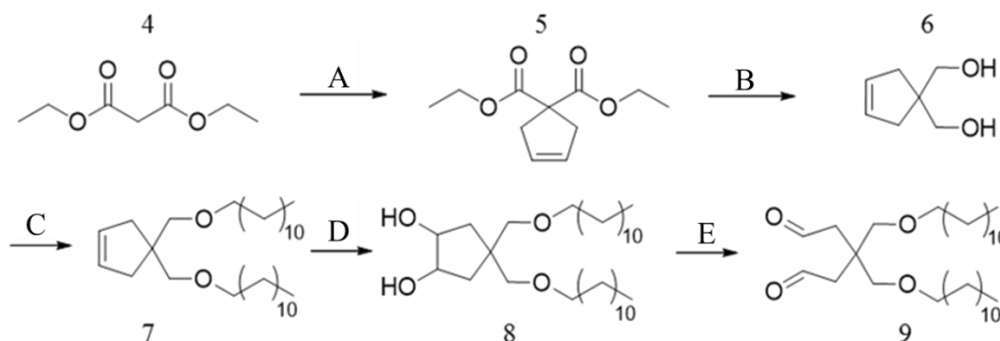


Figure 5.3: Lipidated dialdehyde reagent synthetic route. (A) cis-1,4-Dichloro-2-butene (1.0 equiv), Na (2.2 equiv), anhydrous t-butanol, 12 hours, 95%. (B) LiAlH₄ (3.0 equiv), -78°C, dry THF, 2 hours, CH₃COOH/H₂O 1 M, 3 hours, 95%. (C) NaH (excess), dry THF, Argon, 1-bromododecane (2.2 equiv) 24 hours, 80%. (D) OsO₄, N-methylmorpholine N-oxide (excess), CH₃CN/acetone/H₂O, 12 h, 90%. (E) NaIO₄, Acetone/H₂O, 2 hours, 75%.

Using ¹H-NMR, we studied the conjugation of dialdehyde (9) containing a quaternary carbon as our model by reacting (9) with propyl amine, (Figure 5.4). To probe the reactivity of the quaternary dialdehyde (9) we performed the reaction under aqueous conditions at 23°C to produce conjugate (10). We found dialdehyde (9) to be stable under aqueous 23°C conditions and neat conditions. Under aqueous conditions for proton NMR analysis, the unreacted dialdehyde molecule (9) did not polymerize or undergo intermolecular reactions but rather

existed as a cyclic hydrate pyran diol. After exposure of dialdehyde (9) to a primary amine such as propylamine shown in Figure 5.4, one aldehyde quickly reacts with the amine to form an imine, but due to the close proximity of the second aldehyde group a fast intramolecular reaction occurs trapping the amine to form a six-membered diol piperidine-type moiety, which then undergoes dehydration to form the 1,4-dihydropyridine conjugate (10). Proton NMR analysis of dialdehyde (9) and conjugate (10) shown in Figure 5.5 was used to follow the reaction by focusing on the appearance of the vinylic and alpha proton peaks of propylamine. The reaction kinetics were quantified using NMR by following the formation of vinylic peaks to obtain $t_{1/2}$ of less than 5 seconds ($k_{\text{obs}} = 0.14 \text{ s}^{-1} \pm 0.02$), with a subsequently slow hydration step to form the 1,4-dihydropyridine group. Without the proximity of the intramolecular second aldehyde group to trap the amine, the initial imine formation was not favorable under aqueous conditions and became quickly hydrolyzed due to the equilibrium heavily favoring the reactants (dialdehyde and amine).^{14 15} Yet, at low pH (< 3.0) conditions the conjugate (10) undergoes cleavage, which may permit the release of the dialdehyde and amine molecule. The release of these molecules may have utility for incorporation into fluorescence resonance energy transfer (FRET) probes or pH biosensors for aggregate nanoparticles, which would enable switchable conjugation using high pH reactions and low pH release of the parent reactants. The dialdehyde-amine conjugation reaction is a true click reaction which does not require an activating agent, while also releasing no other by-products other than water, proceeds rapidly, is traceless and reacts with high atom economy.

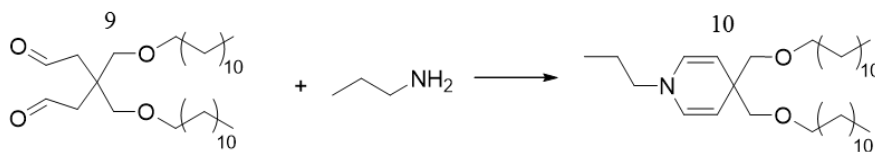


Figure 5.4: Reaction of lipidated dialdehyde (9) with propyl amine to produce the lipid conjugate (10). The reaction occurs in aqueous media at 23°C with propylamine to produce the desired conjugate (10) in high yield with no byproducts in under 30 minutes.

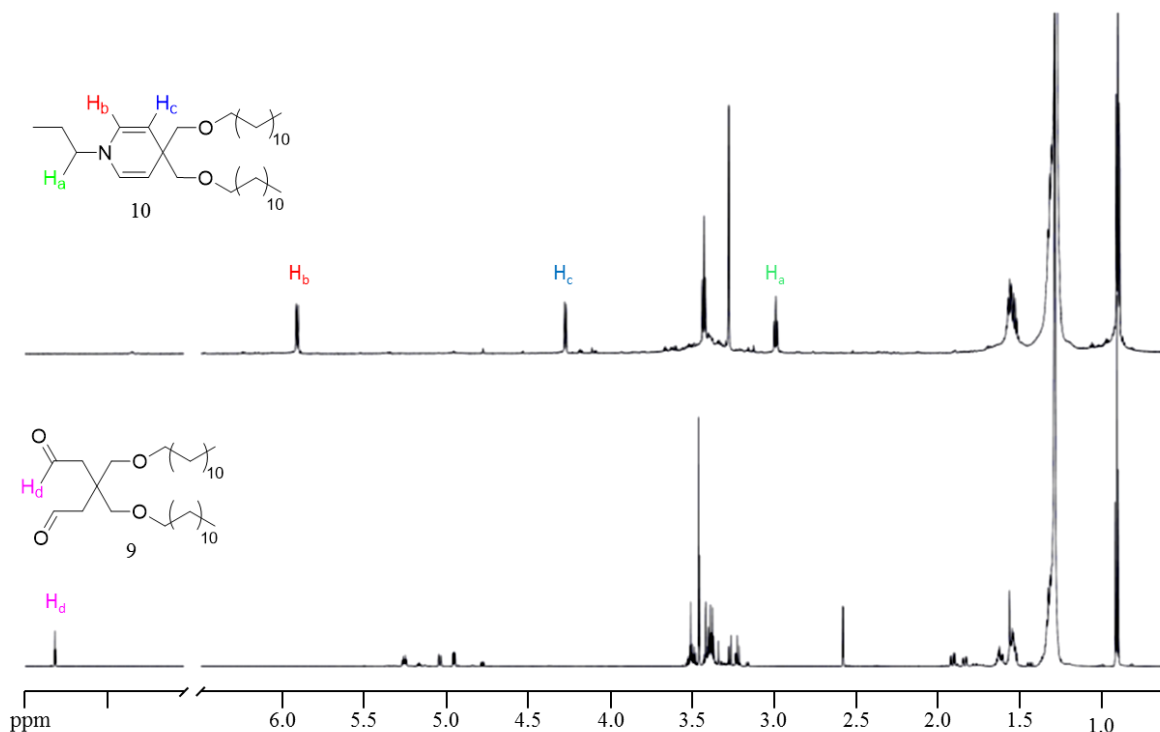


Figure 5.5: ^1H -NMR spectra comparison of the modified glutaraldehyde molecule (9) and the conjugated molecule (10). The reaction of the dialdehyde with primary propylamine rapidly generated the conjugate. Comparison of the final conjugate with the starting material dialdehyde NMR spectra show key proton peaks which were used for kinetic studies. The key proton peaks include the 9.6 ppm H_d aldehyde proton and peaks in the 4.7-5.3 ppm region (dialdehyde cyclic pyran hydrate). The key peaks for the conjugate (10) include H_c at 6.0 ppm and H_b at 4.3 ppm vinylic protons and H_d at 3.1 ppm α nitrogen protons.

The utility of our lipid dialdehyde conjugation strategy was demonstrated using a liposome nanoparticle delivery and CSE to perform various applications. Liposomes have been an effective component of biological research, understanding molecular signalling and the synthesis, adaptation and delivery of these lipid nanoparticles as a fundamental instrument for

biophysical research as probe and drug delivery mechanism and model membrane system.^{16 17 18}

19 20

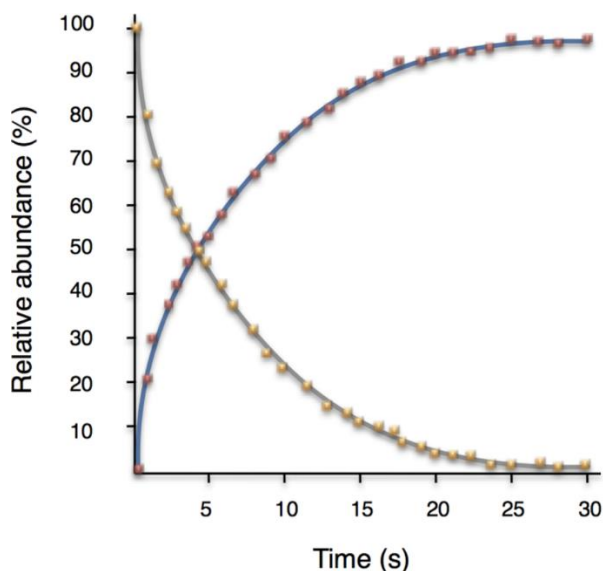


Figure 5.6: Reaction rate of primary amine (propylamine) and dialdehyde (9) to generate the dihydro pyridine conjugate (10). With a short half-life (25°C, pH 7.0) of $t_{1/2}$ of less than 5 seconds ($k_{\text{obs}} = 0.14 \text{ s}^{-1} \pm 0.02$) it also subsequently undergoes a slow dehydration step.

Current research performed by the Yousaf group focused on the use of liposomes as lipid delivery vehicles via liposome fusion with cell membranes to insert bio-orthogonal-like lipids into membranes for a range of applications.^{21 22 23 24 25} This method was used to engineer plasma membranes which present lipid molecules that impart new capabilities to the cell including redox, photoswitchable and fluorescent properties.^{24 25 26} This system was also used to

incorporate complementary bio-orthogonal moieties into multiple cell types to form scaffold free spheroids and functional 3D cardiac and liver tissues.^{23 27 26}

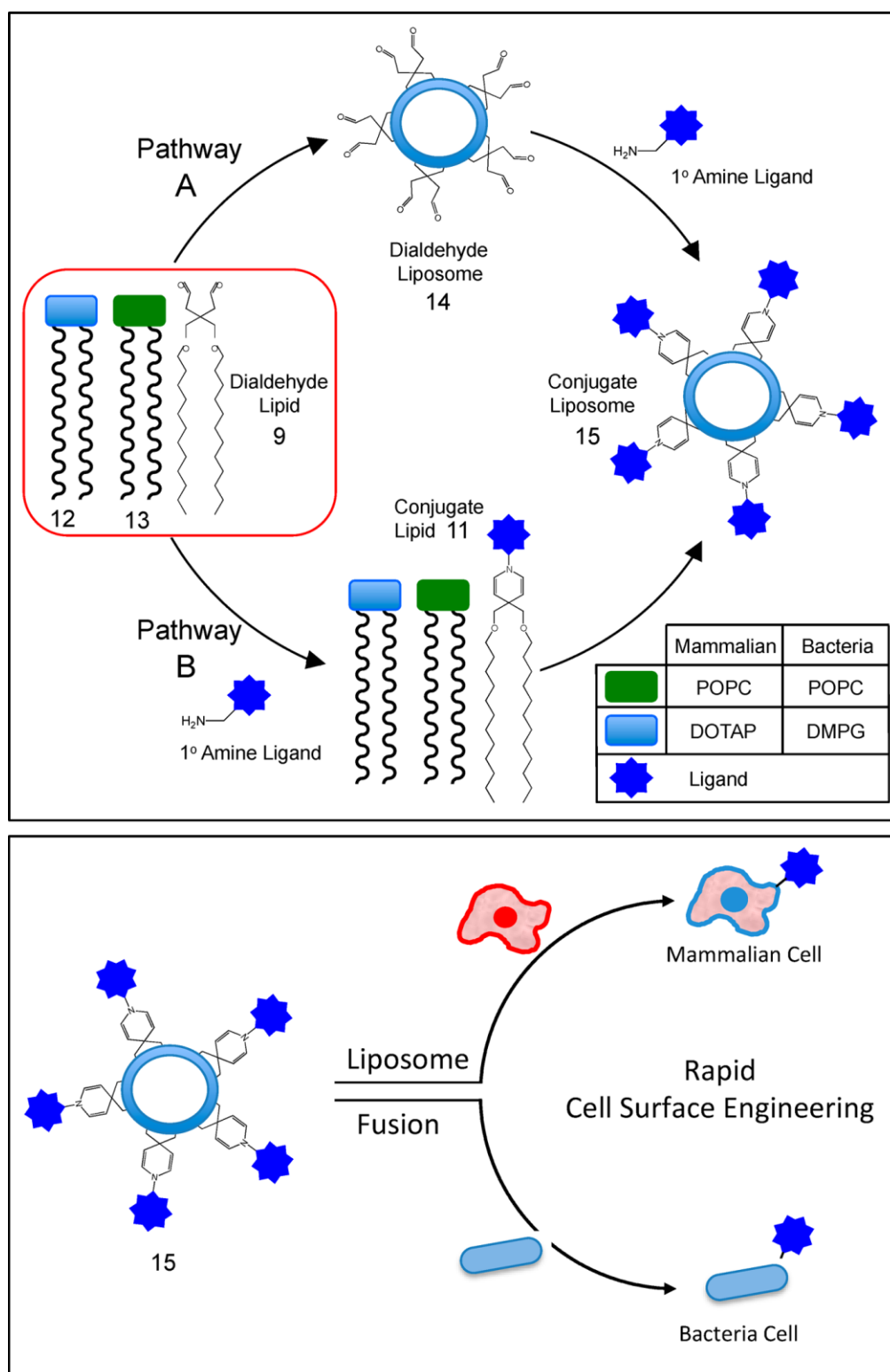


Figure 5.7: Scheme depicting the flexible liposome functionalization strategy using incorporated dialdehyde lipids. (A) Pathway A describes incorporating dialdehyde lipids (9) into a fully formed liposome suspension using background lipids (12 and 13), to produce dialdehyde liposomes (14). These dialdehyde liposomes can then be reacted with primary amine containing ligands, small molecules or probes to form useful conjugate liposomes (15). (B) Pathway B describes reacting the dialdehyde lipid (9) with probes, peptides or other amine small molecules first to form the conjugate lipid (11), followed by mixing with background lipids (12 and 13) to form the conjugate presenting liposome (15). (Bottom) The formed conjugate presenting liposome (15) can then be delivered to both bacterial or mammalian cell membranes via liposome fusion.

Figure 5.7 demonstrates two competing methods to generate conjugate liposomes (15) using our lipid dialdehyde (9) with a variety of primary amine containing molecules for delivery to the plasma membrane. Due to the flexibility of our dialdehyde bioconjugation strategy, two different pathways for the formation of conjugated liposomes (15) may be used to tailor membranes. Pathway A illustrates the synthesis of liposomes containing background lipids and dialdehyde molecule (ratio of lipids 12:13:9 at 86%/ 7%/ 7%). After self-assembly of the nanoparticle (14), a number of amine containing reporter molecules can then be reacted with the dialdehyde to form a stable conjugate with the liposome leaflet (15). It is possible to couple multiple different ligands to a single liposome using the primary amine and dialdehyde click reaction to form multiplexed liposomes.

Pathway B demonstrates an alternative method to synthesize conjugate liposomes. The active dialdehyde (9) is initially reacted with an amine ligand to form the conjugate molecule (11), which is then mixed with the background lipids (12 and 13) to then form the conjugate liposome (15). This strategy requires no activating groups or catalysts and generates no by-

products, while also being straightforward and enables the formation of complex multimodal liposomes without the need of subsequent dialysis or purification.

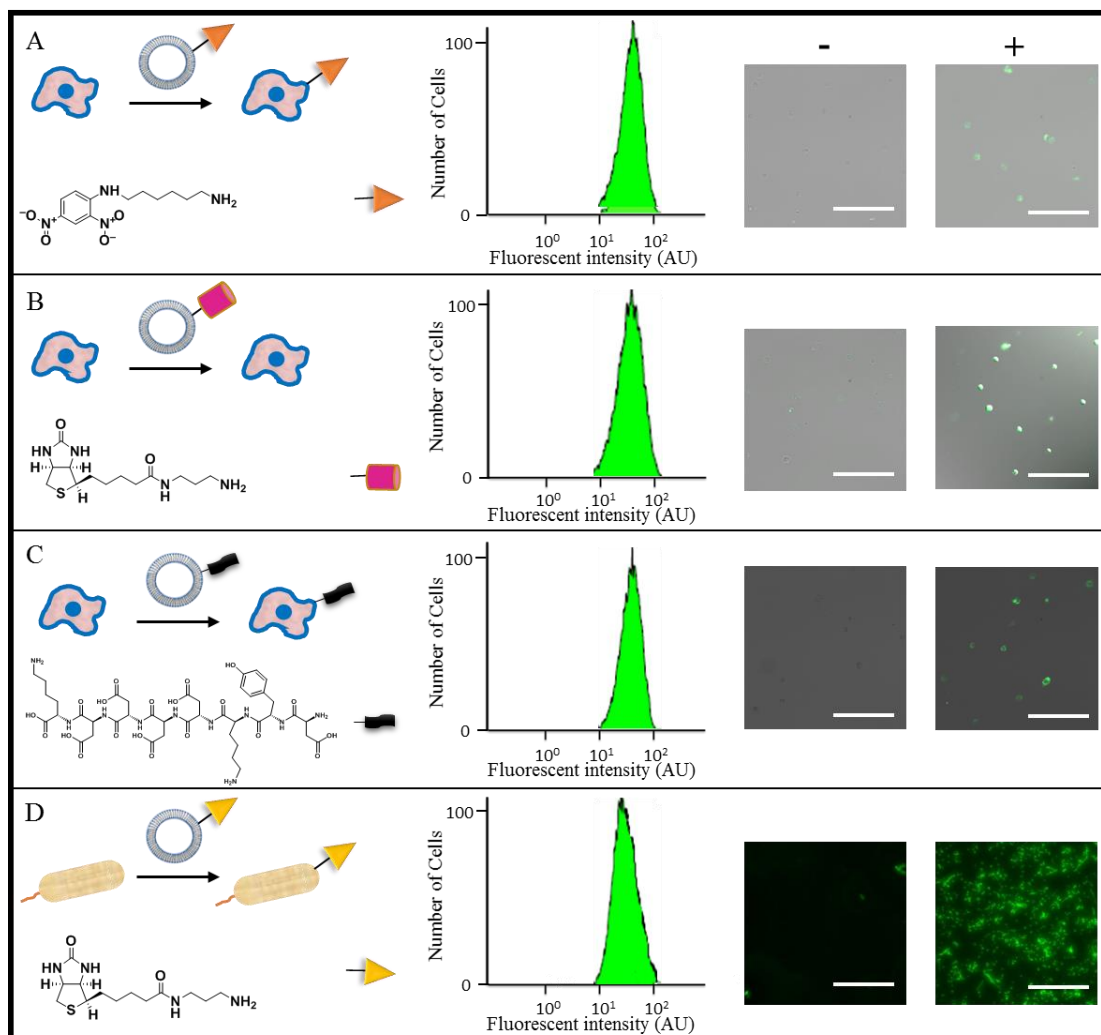


Figure 5.8: Flow cytometry scheme of cells rapidly treated with amine containing bio-molecular probes conjugated to lipid dialdehyde liposomes using CSE via liposome fusion. (A) Amine-DNP cadaverine conjugated liposomes treated to mammalian fibroblast cells via dialdehyde click chemistry and characterized using FITC antibody coupled with flow cytometry and fluorescent microscopy (+). Cells do not fluoresce when treated with liposomes devoid of the dialdehyde or when the dialdehyde was first reacted with propylamine (quenched) under identical conditions (-). (B,C) Fibroblasts cells were treated with biotin cadaverine and FLAG peptide conjugated to dialdehyde liposomes and exposed to STREPT-FITC and anti-FLAG respectively (+). (D) *E. coli* BL21 were engineered with biotin cadaverine via dialdehyde liposome fusion and characterized with STREPT-FITC in flow cytometry. Scale bar: 20 μ m.

Figure 5.8 illustrates an assortment of liposome conjugates expressing a variety of surface coupled ligands for delivery to the cell surface. The liposomes were functionalized using Pathway A, where the dialdehyde liposomes were treated with primary amine ligands and delivered to mammalian fibroblasts and bacteria (*E. coli*) cells, that underwent rapid liposome fusion to deliver the ligands onto the cell surface. For bacterial cells, liposome background lipids included POPC and 1,2-dimyristoyl-sn-glycero-3-phospho-(1'-rac-glycerol) (sodium salt) (DMPG) lipids, while POPC and DOTAP (12 and 13) were used due to physiological differences in cell membrane properties.^{19 21}

Characterization of liposome conjugate ligand delivery to the cell surface was performed using the ligand tailored cells through exposure to their specific fluorescent antibodies, followed by flow cytometry analysis and fluorescent microscopy. Figure 5.8 demonstrates that our ligand conjugated fusion liposomes were successful incorporating ligands on the cell surface.

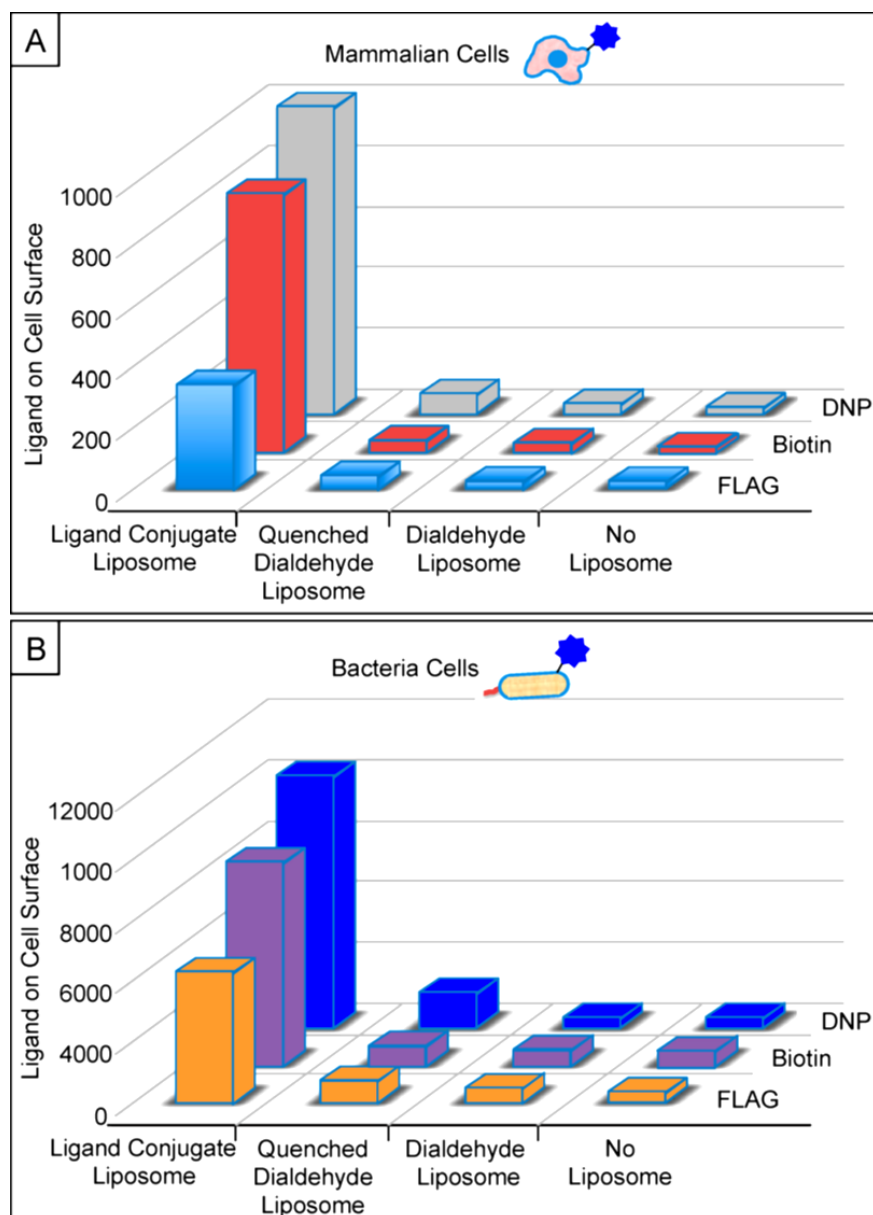


Figure 5.9: 3D plots of various ligands delivered to the cell membrane by dialdehyde amine click chemistry using liposome fusion describing the relationship concerning the amount of ligand characterized using flow cytometry. (A) Mammalian membrane fusion using dialdehyde liposome fusion quantifies lipid incorporation using liposome fusion and flow cytometry. (B) Prokaryotic membrane fusion using dialdehyde liposome fusion quantified lipid incorporation using liposome fusion and flow cytometry. Control cells do not display ligands nor do quenched dialdehyde show any fluorescence signal. Only positive liposomes bearing dialdehyde groups which were reacted with primary amine ligands showed cell surface ligand display through fluorescence.

To quantify the number of conjugated ligands to the cell surface via dialdehyde-amine click chemistry and liposomes, we utilized flow cytometry. Figure 5.9 is a 3D plot displaying the relationship between liposome composition and amount of ligand delivered onto mammalian and bacterial cell surfaces. The relationship between the identity of the ligand, concentration of the liposome conjugates and the duration of exposure influenced the delivered number of conjugate ligand molecules.^{20 21} These elucidated parameters are important to engineer cells with known ligand density for a variety of applications. Previous work has shown that application of CSE liposomes to cells does not result in changes to viability or cell behavior for a range of cell types and bacteria.^{23 24 25 26} For our control experiments, when blank liposomes and quenched dialdehyde liposomes were used, no ligands were found on the cell surface.

Figure 5.10 demonstrates the broad utility of our bioconjugation strategy by synthesizing a small set of dialdehyde coupling reagents and by developing a synthesis strategy for dialdehyde moieties. These dialdehyde reagents were made using minimal steps and high yields to generate a key intermediate (24) to allow the convergent synthesis of a variety of ligands, probes and monomers. Figure 5.11 describes our synthesized list of dialdehyde containing molecules and their conjugate forms. To illustrate the bioconjugation strategy, dialdehyde molecules were tethered to lysine (34) and other known recognition small molecules such as biotin (37) and DNP (35).^{28 29}

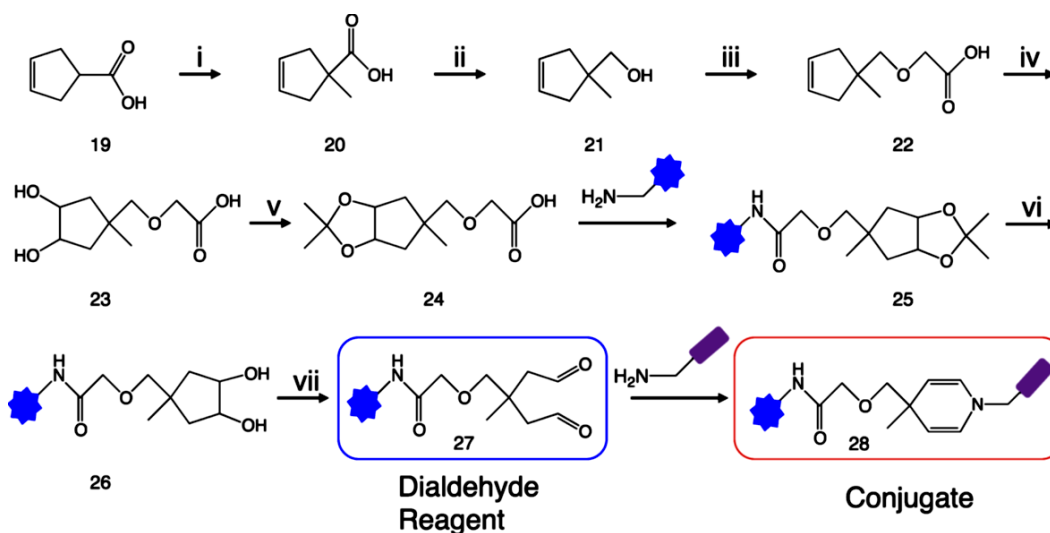


Figure 5.10: A general synthetic methodology to generate dialdehyde reagents. (i) t-Butyl lithium (3.0 equiv), -78°C , dry THF, 6 hours, MeI (excess), 12 hours, 100%. (ii) LiAlH_4 (3.0 equiv), -78°C , dry THF, 2 hours, $\text{CH}_3\text{COOH}/\text{H}_2\text{O}$ 1 M, 3 hours, 85%. (iii) NaH (excess), dry THF, Argon, chloroacetic acid (1.2 equiv) 24 hours, 95%. (iv) OsO_4 , N-methylmorpholine N-oxide (excess), $\text{CH}_3\text{CN}/\text{acetone}/\text{H}_2\text{O}$, 12 hours, 60%. (v), 1,2 Dimethoxypropane, dry THF, pTsOH (cat), 2 hours, 95%. (vi) Dry THF, sodium bicarbonate, DCC, N-hydroxysuccinimide, 1 hours, general amine, 30 minutes. (vii) $\text{MeOH}/\text{H}_2\text{O}$ (1:9) dilute HCl, 2 hours. (viii) $\text{H}_2\text{O}/\text{methanol}$ (1:9), NaIO_4 , 1 hour.

Figure 5.11 depicts our general strategy for engineering cell surfaces with ligands through the initial coupling of dialdehyde containing ligands with amine-terminated lipids or liposomes for delivery to the plasma membrane via fusion.

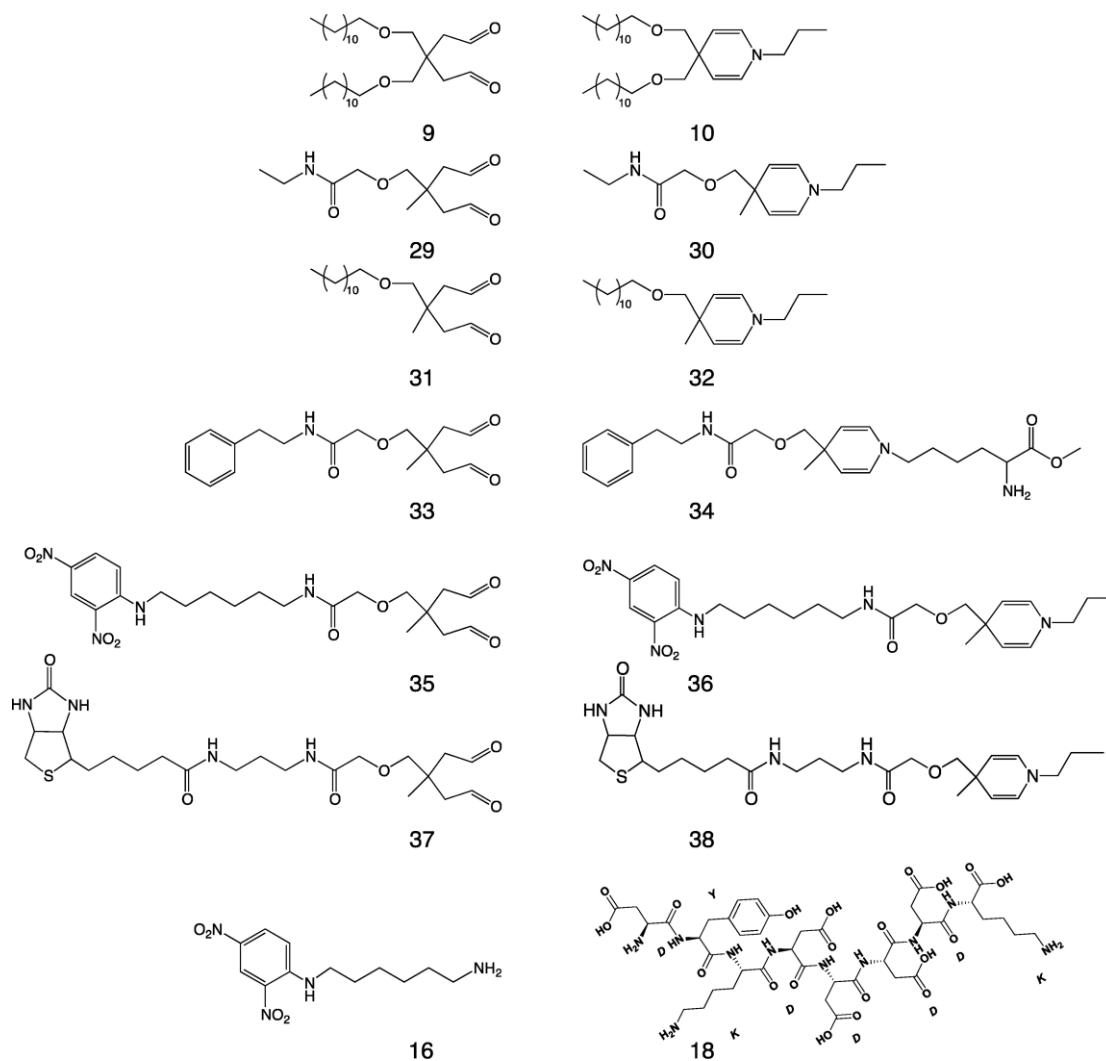


Figure 5.11: List of synthesized dialdehyde molecules and dialdehyde conjugates used in this study.

Pathway A in Figure 5.12 depicts the formation of an amine engineered liposome (41) through mixing terminal amine lipids (39) with background lipids (12 and 13). The amine liposome can then be loaded or reacted with dialdehyde presenting ligands (27), which undergo fast reaction to ligate with the liposome via dialdehyde and amine click chemistry (42). Pathway B describes the reaction of amine lipids (39) with dialdehyde ligands (27) first to form a lipid conjugate (40), followed by the mixing and assembly with background lipids to synthesize the

ligand engineered liposome (42). The generated ligand presenting liposomes are then added to mammalian or bacterial cells (*E. coli*), which undergo rapid fusion followed by ligand display.

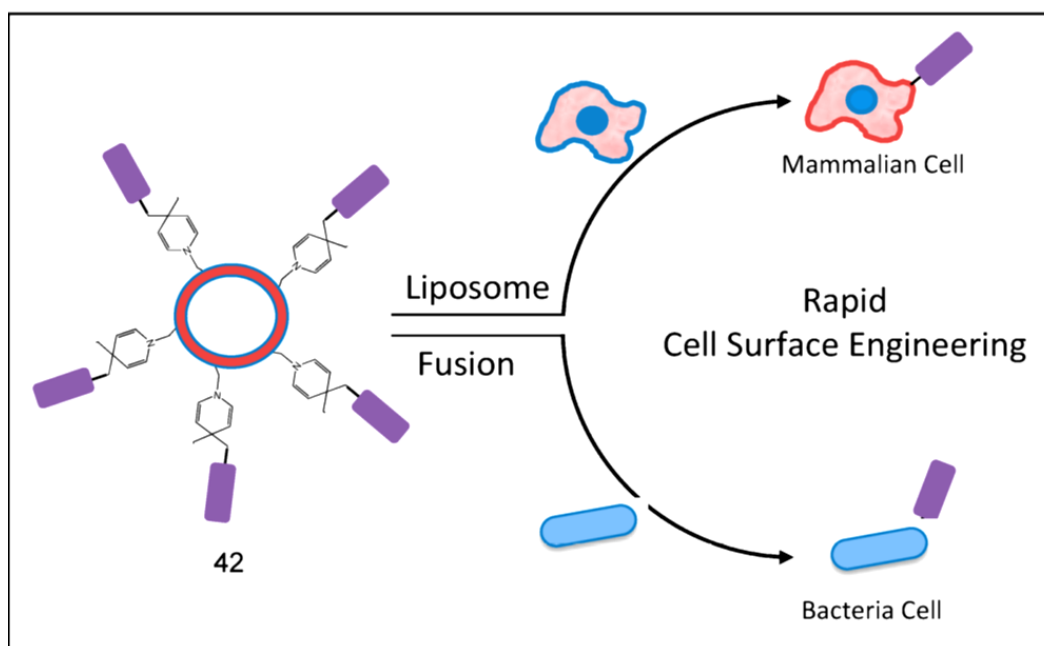
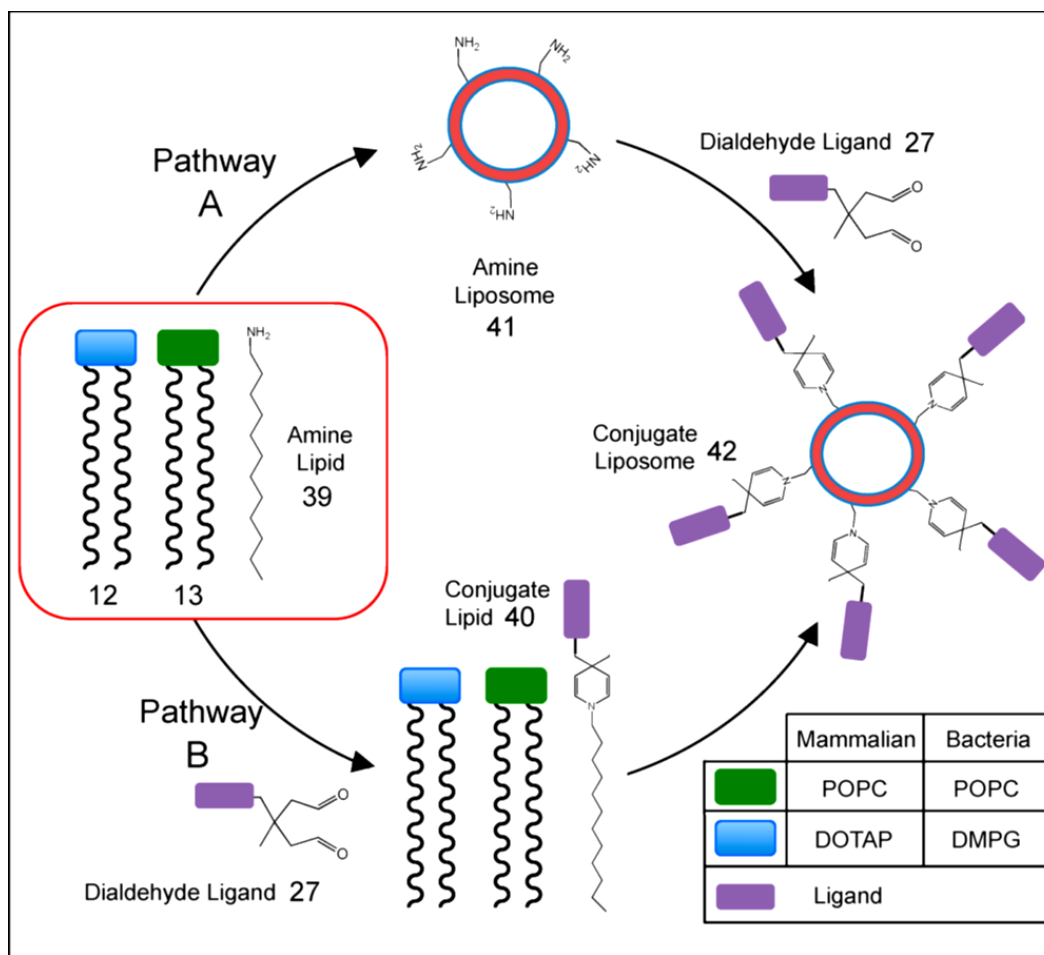


Figure 5.12: Scheme depicting the flexible liposome functionalization strategy using incorporated dialdehyde lipids. Pathway A describes incorporating amine lipids (**39**) into a full formed liposome suspension using background lipids (**12** and **13**), to produce amine presenting liposomes (**41**). These liposomes can then be reacted with dialdehyde containing ligands, small molecules or probes to form useful conjugate liposomes (**42**). Pathway B describes reacting the amine lipid (**39**) with probes, peptides or other dialdehyde containing small molecules first to form the conjugate lipid (**40**), followed by mixing with background lipids (**12** and **13**) to form the conjugate presenting liposome (**42**). The formed conjugate presenting liposome can then be delivered to both bacterial and mammalian cell membranes via liposome fusion.

Figure 5.13 presents flow cytometry and fluorescence data gathered from the conjugation of dialdehyde terminated DNP and biotin (**37** and **35**) to amine lipids (**39**), and amine liposomes (**41**) delivered using liposome fusion. The generation of ligand presenting liposomes (**42**), DNP-dialdehyde and biotin-dialdehyde are mixed with amine liposomes for 2 hours with a mole ratio (amine/dialdehyde) of 1.5:1. The final dialdehyde conjugate DNP or biotin liposome was then treated to cultured fibroblasts for 2 hours with a mole ratio (amine/dialdehyde) of 1.5:1. Fluorescent DNP or streptavidin antibodies for were added and followed by flow cytometry and fluorescent microscopy to characterize our CSE strategy. Results indicate a clear successful conjugation and delivery of our designed ligands to cells. Control experiments where performed through quenching the dialdehyde with propylamine or the amine liposomes were not exposed to the relevant ligand resulting in no cell fluorescence. Results for biotin and DNP dialdehyde conjugation and delivery for *E. coli* cells was similar. These experiments demonstrate the efficient conjugation of our dialdehyde modified ligands to liposomes for delivery via liposome fusion.

not fluoresce (-). (C,D) Delivery of biotin and DNP (**37** and **35**) via liposome fusion to bacterial cells (*E. coli*). The reagents were conjugated to amine bearing liposomes using dialdehyde ligands to form ligand presenting liposomes (**42**). The cells were then treated with fluorescent antibodies or adhesion proteins for flow cytometry and fluorescent microscopy for analysis (+). Control experiments were performed where either the dialdehyde, amine terminated liposome, or quenched dialdehyde ligand with propylamine were delivered to cells do not fluoresce (-). Scale bar: 20 μm .

This general click chemistry conjugation strategy can be applied to many different applications including the immobilization of ligands to inorganic substrate materials or a cross-linking strategy to combine proteins, peptides or small molecule containing amines.^{30 31 32}

Figure 5.14 depicts the general applicability of the dialdehyde-amine reaction method for tailoring material surface modification and reaction. To demonstrate the method, we converted an amine presenting glass slide (**43**) into a dialdehyde modified glass slide (**44**) using precursor molecule (**24**) followed by oxidation. To the modified dialdehyde surface, we added fluorescent polystyrene beads with amine presenting groups. The amine beads became efficiently bound to the dialdehyde surface via click chemistry. However, in the control no beads attached to dialdehyde surfaces when deactivated using propylamine or when the amine beads were first reacted with a dialdehyde capping reagent.

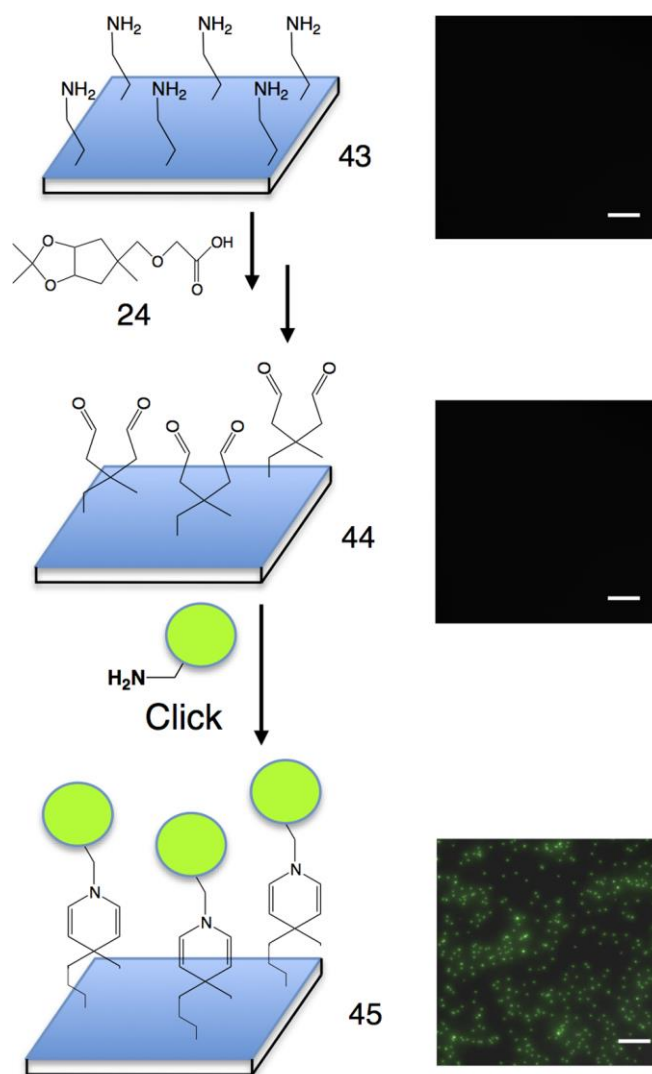


Figure 5.14: Diagram and images depicting the production of a dialdehyde modified glass substrate for primary amine terminated immobilization. An amine presenting substrate (43) was converted to a dialdehyde terminated surface (44) through the reaction of intermediate (24) with the surface amines followed by oxidation. To show conjugation, fluorescent latex beads (45) which have surface presenting amine groups are treated to the dialdehyde engineered substrate. When dialdehyde groups are present upon the solid substrate, the fluorescent beads become immobilized to the surface via click chemistry. While control experiments comprised of the dialdehyde surface deactivated using propylamine did not result in bead adhesion to the substrate. Scale bar: 5 mm.

These results demonstrate that our dialdehyde presents an adaptable conjugation method and can be used on different materials including nanoparticles, inorganic and organic materials, and as a method for synthesizing smart materials and coatings.^{33 34 35 36 37} An additional potential

feature of our conjugation strategy involves the reaction of two moles of oxyamine or hydrazine containing ligands with one mole of dialdehyde reagent to form oxime or hydrazone through classical aldehyde chemistry. Using our organic and inorganic work as a foundation for expanding the scope of the dialdehyde methodology, we furthered our work to include biological manipulation, cellular manipulation for protein cross-linking, stapling of enzymes, biomacromolecules and tissue generation.

The study of associated protein complexes is vital in the discovery of transitory signalling complexes. These complexes form transitory structures with short half-lives that are difficult to study due to their short lifespans and weak binding interactions, which readily dissociate in laboratory conditions. Protein stapling or cross-linking provides a methodology to permanently associate and stabilize these complexes in their native form for study.

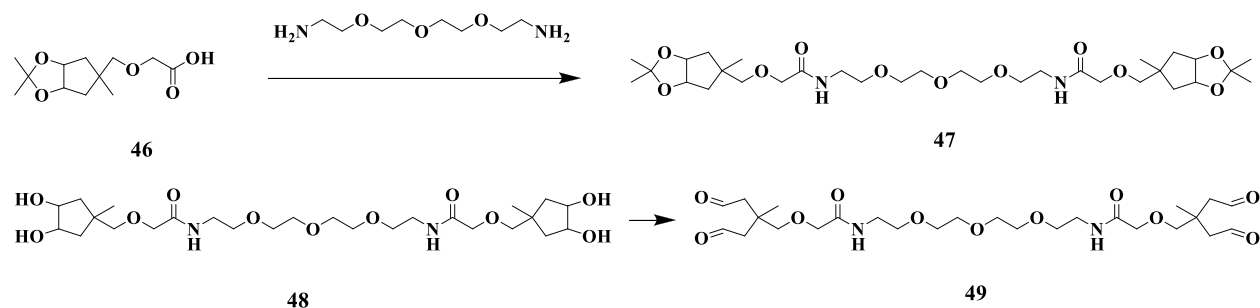


Figure 5.15: Scheme depicting the synthesis of cross-linking dialdehyde molecule (49). Starting from the general dialdehyde building block (46), the cross-linker (49) was achieved in 3 steps using a similar methodology to other dialdehyde molecules.

Figure 5.15 outlines the synthetic methodology for synthesizing a water soluble molecule containing two dialdehyde moieties that has significant chain length to act as a cross-linking molecule (49) to covalently bridge two intramolecular or intermolecular primary amines. Our cross-linking strategy using our dialdehyde cross-linker reacts with N-terminus amines and the primary amine side chains of lysine, which are readily abundant in most proteins. By cross

reacting primary amines, both through inter- and intramolecular stapling, the proteins can be characterized and studied in their native form.

Figure 5.16 shows the ability of (49) to cross-link lysine containing macromolecules. We treated a solution containing LAR D1D21 and Caskin SAM2 (48), proteins that form a complex during embryonic motor axon development in *Drosophila* as a method to irreversibly bind the protein complex (50). Under electrophoretic separation (SDS-PAGE) proteins are denatured and separated based on their size and charge, while addition of the dialdehyde cross-linker (49) results in the covalent binding of the two proteins into a single protein band of 250 kDa (Lane 2) (Figure 5.16). The control (Lane 1) shows the untreated complex (48) readily dissociates under electrophoretic conditions.

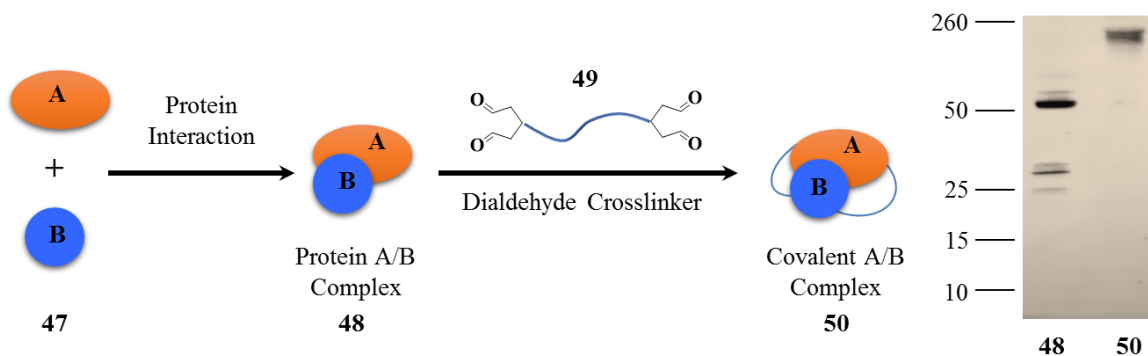


Figure 5.16: Depiction and data of protein stapling of LAR D1D21 (A) and Caskin 2 SAM2 (B) (47) using the dialdehyde cross-linker (49). LAR D1D21 and Caskin 2 SAM2 undergo natural association (A/B) when incubated in solution (48). Once treated with the dialdehyde cross-linker (49) the lysine amino acids become cross-linked into a covalently bound (A/B) complex, which does not dissociate following gel electrophoresis (50). The control (Lane 1) shows the electrophoretic separation of the native bound (A/B) complex (48), while Lane 2 demonstrates the covalently crosslinked (A/B) complex, which remains as a single complex under separation conditions.

Although the study of associated complexes such as those comprised of enzymes, are important there are also numerous applications for single protein aggregation studies such as amyloid plaques and tangles associated with Alzheimer's disease. In Figure 5.17, we

demonstrate the dialdehyde cross-linker capability to form dimers and stapled complexes from single protein solutions of PP16 and EA22, RNA binding and DNA translation proteins, respectively. The addition of our cross-linker (49) to individual protein solutions resulted in the formation of dimerized proteins and stapled proteins under SDS gel conditions (Figure 5.17). The crosslinked PP16 (53) and EA22 (56) SDS gel demonstrates the irreversible doubling of the mass (kDa) of the respective protein solutions. Control experiments, where the propylamine quenched cross-linker (51) was treated to PP16 (54) and EA22 (57) did not produce a dimerized product. Therefore, this methodology has applications for producing aggregates of amine presenting macromolecules for studies *in vitro*. The assembly of advanced macroscopic materials is also of considerable interest, for colorimetric probes, sensors and drug delivery vehicles.

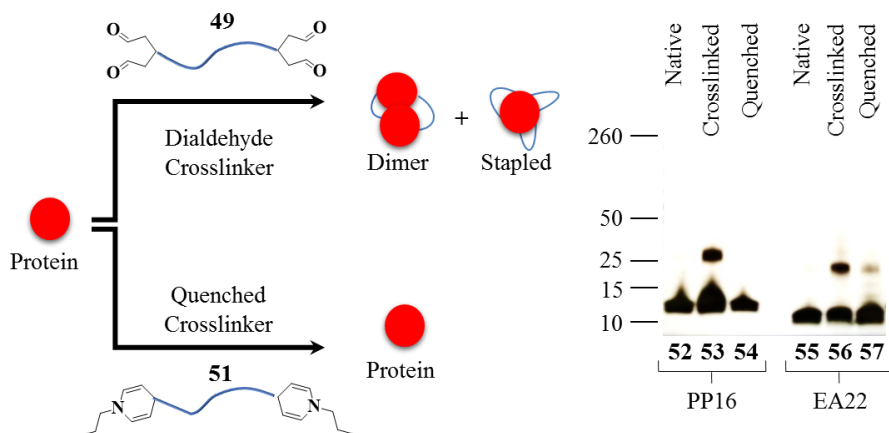


Figure 5.17: Depiction of proteins PP16 and EA22, RNA binding and DNA translation proteins respectively, treated with dialdehyde cross-linker (49) conditions to form dimers and stapled protein complexes. Treatment of individual proteins with (49) cross-linker resulted in the formation of dimers and stapled protein aggregates (53 and 56) with doubled masses (kDa). Two identical proteins treated with (49) results in intramolecular crosslinks to produce covalently bound dimers and stapled proteins which have intermolecular binding of the dialdehyde molecule to amine groups within the same protein. Control experiments used the cross-linker quenched with propylamine (51) and did not result in dimerized proteins (54 and 57), respectively.

The aggregation of solid nanoparticles is a broad field of study that encompasses colorimetric assays, pH tests and biophysical analyses for both academic and commercial

applications. The utility of surface chemical groups of materials are essential, since they confer stability and functionality, while imbuing the material with covalent and non-covalent properties with further characteristics based upon the type of chemistry used. Adsorption or covalent interactions between the solid particle and ligand or cross-linker of interest produce a measurable response upon reaction and incorporate switchable mechanisms for purification, drug release, assembly and spectroscopic output. Figure 5.18 outlines our demonstration of the dialdehyde cross-linker (49) as a method to aggregate fluorescent beads into spheroid like structures, and release as individual beads upon addition of acid ($\text{pH} < 3.0$). Initially, the amine presenting beads were treated with molecule (49) to allow cross-linking of the solid particles in aqueous solution, which resulted in the aggregate cross-linked spheroids under fluorescent microscopy. While the addition of HCl (aq) to reduce the pH of the solution resulted in the quick release of the beads into their native form (Figure 5.18). Controls using quenched dialdehyde cross-linker (51) did not result in bead aggregation. Further incorporation of additional subunits into the cross-linker ethoxy chain could possibly produce further functionality for a variety of solid materials applications such as smart plastics, bioimplants and tissue engineering.

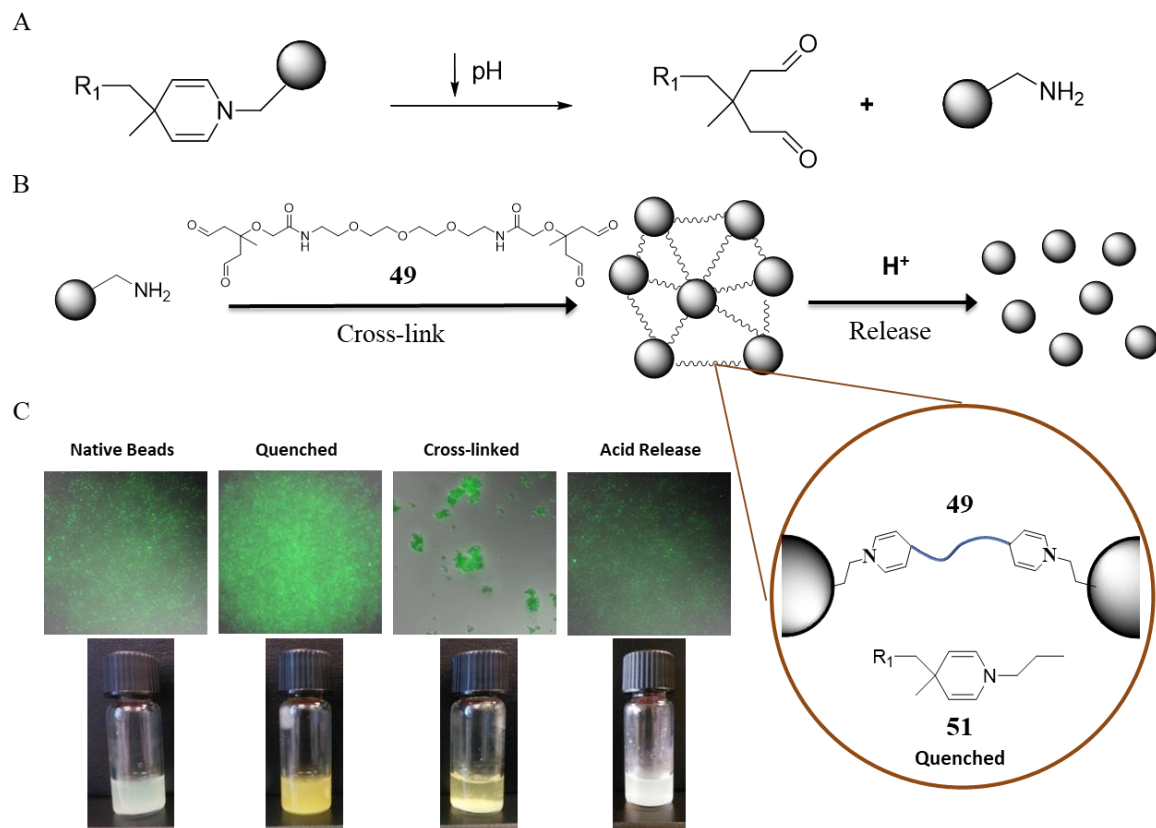


Figure 5.18: Scheme depicting the assembly and release of primary amine presenting fluorescent beads using dialdehyde cross-linker (49). (A) Chemical scheme depicting the lowering of pH ($\text{pH} < 3.0$) results in the release of the primary amines from the dihydropyridine ring. (B) Amine presenting beads treated with cross-linker (49) in aqueous solution assemble clusters, where upon lowering of pH with HCl (aq) to approximately pH 3.0 results in the release of the beads from the clusters to individual beads. (C) Fluorescent microscopy and macroscopic images of the resulting bead solutions shows efficient assembly of the beads using the cross-linker dialdehyde molecule, while lower pH solutions result in bead release. Control experiments with quenched dialdehyde (51) demonstrates no assembly occurs if (49) is first reacted with propylamine.

Spheroids and tissue products are important substrates for regenerative medicine, drug testing and engineered bioproducts, such as biologics. In vitro formation of tissues is important for the discovery and elucidation of molecular signaling pathways, which is hindered by *in vitro* cellular contact inhibition, preventing the growth of 3D tissues in the Z plane. To demonstrate the use of dialdehyde cross-linker (49) as a method to grow 3D co-cultures, suspended cells were mixed with aqueous soluble molecule (49) (Figure 5.19). The reaction between the amine

containing cell membrane surface proteins and cross-linker (49) resulted in adhesion and formation of tissues through the deposition of cells upon glass substrates. We studied the formation of our co-culture tissues in Figure 5.19B using confocal microscopy to show that the dialdehyde cross-linker generated tissues were similar to previous tissue work using bio-orthogonal insertion of complimentary groups delivered via liposome fusion. Our control experiments did not produce multilayers, but rather single layers of contact inhibited cells. Although the cross-linker molecule has a similar moiety as glutaraldehyde (fixing agent), Trypan Blue staining assays (Figure 5.19C) demonstrate that the cells retained high viability following 24 hours of treatment, possibly due to the inability of the molecule to cross the plasma membrane.

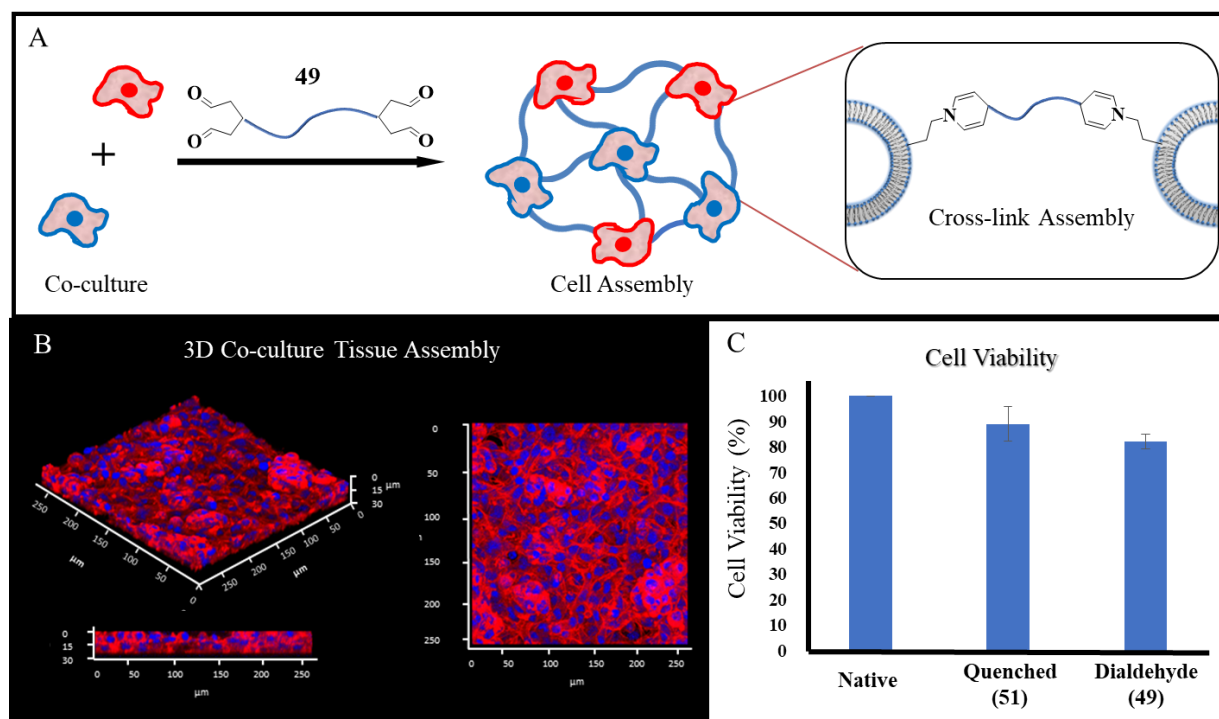


Figure 5.19: Cell assembly of large scale cell aggregates into 3D co-culture tissues using dialdehyde cross-linker (49). (A) Co-culture suspensions of one or more cell types treated with aqueous soluble cross-linker (**49**) assembles cells through intercellular amine surface reactions. (B) Confocal microscopy of C3H/10T1/2 and NIH3T3 cells treated with cross-linker in suspension and deposited on glass slides in high concentration to form viable tissues of 3-4 cell layers thick using contact inhibited cell types. (C) Trypan Blue cell viability assay performed using the propylamine treated (**51**) quenched and active dialdehyde cross-linker (**49**) to determine cell viability after cell assembly conditions.

5.4 Conclusion

In conclusion, we have developed a novel general click chemistry strategy which can conjugate dialdehyde substituents and primary amine containing molecules. The resulting dihydropyridine moiety is stable and the reaction does not require activation or a catalyst. Moreover, the reaction displays fast kinetics and high yield under aqueous conditions and 25°C conditions. The dialdehyde and amine reaction proceeds with high atom efficiency, with only water as a byproduct. Therefore, purification is not necessary to remove toxic byproducts. This is an advantageous system, where amines are an abundant moiety in biological and chemical

systems, is a major group in bioconjugation chemistry and a key chemical handle for material and nanoparticle tailoring. We designed and synthesized a range of dialdehyde containing molecules, while demonstrating their applicability in a diverse range of applications in CSE, materials and tissue engineering. This novel general amine conjugation system has great potential in future applications in green chemistry, molecular tagging, antibody drug conjugates, nanoparticle modification, biosensors and polymers.

5.5 References

- (1) Pearson, R. G. *J. Am. Chem. Soc.* **1963**, 85 (22), 3533–3539.
- (2) Jencks, W. P. *Chem. Rev.* **1972**, 72 (6), 705–718.
- (3) Ritchie, C. D. *Acc. Chem. Res.* **1972**, 5 (10), 348–354.
- (4) Hoffman, A. S.; Stayton, P. S. *Macromol. Symp.* **2004**, 207 (1), 139–152.
- (5) Raindlová, V.; Pohl, R.; Hocek, M. *Chem. – A Eur. J.* **2012**, 18 (13), 4080–4087.
- (6) McKay, C. S.; Finn, M. G. *Chem. Biol.* **2014**, 21 (9), 1075–1101.
- (7) Gildersleeve, J. C.; Oyelaran, O.; Simpson, J. T.; Allred, B. *Bioconjug. Chem.* **2008**, 19 (7), 1485–1490.
- (8) Montalbetti, C. A. G. N.; Falque, V. *Tetrahedron* **2005**, 61 (46), 10827–10852.
- (9) Ozaki, S. *Chem. Rev.* **1972**, 72 (5), 457–496.
- (10) Wangler, C.; Schirmacher, R.; Wangler, P. B. and B. *Current Medicinal Chemistry*. 2010, pp 1092–1116.
- (11) Roy, R.; Katzenellenbogen, E.; Jennings, H. J. *Can. J. Biochem. cell Biol. - Rev. Can. Biochim. Biol. Cell.* **1984**, 62 (5), 270–275.
- (12) Migneault, I.; Dartiguenave, C.; Bertrand, M. J.; Waldron, K. C. *Biotechniques* **2004**, 37 (5), 790–802.
- (13) Elahipanah, S.; O'Brien, P. J.; Rogozhnikov, D.; Yousaf, M. N. *Bioconjug. Chem.* **2017**, 28 (5), 1422–1433.
- (14) Cordes, E. H.; Jencks, W. P. *J. Am. Chem. Soc.* **1963**, 85 (18), 2843–2848.
- (15) Cordes, E. H.; Jencks, W. P. *J. Am. Chem. Soc.* **1962**, 84 (5), 832–837.
- (16) Nicolson, G. L. *Biochim. Biophys. Acta - Biomembr.* **2014**, 1838 (6), 1451–1466.
- (17) Faneca, H.; Düzgüneş, N.; de Lima, M. C. P. Weissig, V., Ed.; Humana Press: Totowa, NJ, 2010; pp 425–437.
- (18) Kumar, K.; Isa, L.; Egner, A.; Schmidt, R.; Textor, M.; Reimhult, E. *Langmuir* **2011**, 27 (17), 10920–10928.
- (19) Dutta, D.; Pulsipher, A.; Luo, W.; Yousaf, M. N. *J. Am. Chem. Soc.* **2011**, 133 (22), 8704–8713.
- (20) Dutta, D.; Pulsipher, A.; Luo, W.; Mak, H.; Yousaf, M. N. *Bioconjug. Chem.* **2011**, 22 (12), 2423–2433.
- (21) Elahipanah, S.; Radmanesh, P.; Luo, W.; O'Brien, P. J.; Rogozhnikov, D.; Yousaf, M. N. *Bioconjug. Chem.* **2016**, 27 (4), 1082–1089.
- (22) O'Brien, P. J.; Luo, W.; Rogozhnikov, D.; Chen, J.; Yousaf, M. N. *Bioconjug. Chem.* **2015**, 26 (9), 1939–1949.
- (23) Luo, W.; Westcott, N.; Dutta, D.; Pulsipher, A.; Rogozhnikov, D.; Chen, J.; Yousaf, M. N. *ACS Chem. Biol.* **2015**, 10 (10), 2219–2226.

- (24) Pulsipher, A.; Dutta, D.; Luo, W.; Yousaf, M. N. *Angew. Chemie Int. Ed.* **2014**, 53 (36), 9487–9492.
- (25) Luo, W.; Pulsipher, A.; Dutta, D.; Lamb, B. M.; Yousaf, M. N. *Sci. Rep.* **2014**, 4, 6313.
- (26) Rogozhnikov, D.; O'Brien, P. J.; Elahipanah, S.; Yousaf, M. N. *Sci. Rep.* **2016**, 6, 39806.
- (27) Rogozhnikov, D.; Luo, W.; Elahipanah, S.; O'Brien, P. J.; Yousaf, M. N. *Bioconjug. Chem.* **2016**, 27 (9), 1991–1998.
- (28) Wang, X.; Liu, L.; Luo, Y.; Zhao, H. *Langmuir* **2009**, 25 (2), 744–750.
- (29) Vretblad, P. *FEBS Lett.* **1974**, 47 (1), 86–89.
- (30) Sigrist, H.; Gao, H.; Wegmuller, B. *Nat Biotech* **1992**, 10 (9), 1026–1028.
- (31) Hodneland, C. D.; Lee, Y.-S.; Min, D.-H.; Mrksich, M. *Proc. Natl. Acad. Sci.* **2002**, 99 (8), 5048–5052.
- (32) Love, J. C.; Estroff, L. A.; Kriebel, J. K.; Nuzzo, R. G.; Whitesides, G. M. *Chem. Rev.* **2005**, 105 (4), 1103–1170.
- (33) Park, S.; Westcott, N. P.; Luo, W.; Dutta, D.; Yousaf, M. N. *Bioconjug. Chem.* **2014**, 25 (3), 543–551.
- (34) Luo, W.; Yousaf, M. N. *J. Am. Chem. Soc.* **2011**, 133 (28), 10780–10783.
- (35) Lamb, B. M.; Yousaf, M. N. *J. Am. Chem. Soc.* **2011**, 133 (23), 8870–8873.
- (36) Lee, E.; Luo, W.; Chan, E. W. L.; Yousaf, M. N. *PLoS One* **2015**, 10 (6), e0118126.
- (37) Medintz, I. L.; Uyeda, H. T.; Goldman, E. R.; Mattoussi, H. *Nat Mater* **2005**, 4 (6), 435–446.

Chapter 6

Conclusions and Future Directions

6.1 Conclusions

In this work, several cell surface engineering techniques and technologies were developed for the control and study of cellular behavior for in vitro research applications. In Chapters 2 and 3 NMR spectroscopy, oxime reaction kinetics and oxime cell surface engineered cell adhesion was correlated and probed under microfluidic conditions, while the robustness of adhesion and flexibility of cluster and tissue formation was established using live cell techniques microfluidics. The rapidity and general applicability of bioorthogonal CSE was also probed under a variety of conditions, while tissues formed using this technology were studied for biological activity.^{1 2 3} Using this as a base strategy, we developed a general method for the microfluidic manipulation and cell surface engineering of cells for dual labelling and flexible delivery of nucleic acids and small molecule ligands (unpublished work).

In Chapter 4 the bioorthogonal liposomal strategy originally utilized for cell adhesion and cell membrane ligand integration was modified and extended to transfect mammalian cell lines with nucleic acids limiting the use of cationic charge as a mild and general method to tag and target cells in monocultures and cocultures.⁴ This methodology using complimentary oxime chemistry on the cell membrane and the lipoplex allowed for the reduction of cationic charge for cell-lipoplex interaction and internalization to occur, while the method was characterized using microscopy, protein production quantification and targeting in complex cocultures for selective internalization.

Finally, in Chapter 5 a new chemical moiety termed a dialdehyde was designed and synthesized for the easy and mild conjugation of primary amine containing molecules.⁵ This conjugation strategy was used to deliver small molecule ligands and macromolecules to bacterial and mammalian cell membranes using a generalized liposomal formation method. The

dialdehyde moiety was characterized and modified to contain two dialdehyde moieties with a PEG linker for crosslinking proteins, inorganic surface functionalization, organic bead aggregation and cell aggregation for tissue formation.⁶

6.2 Future Directions

Regarding the studies conducted in Chapter 2, future directions include the precision delivery of two or more bioorthogonal ligands to achieve simultaneous multiplexed delivery of biomolecular ligands for cellular studies of complex cell membrane biophysics, clinical tissue engineering, membrane biophysics, and immobilization. Surface labelling of cells for complex applications can benefit from the extension of this methodology by giving access to wider arrays of molecular probes for live cell staining and lipid trafficking studies. Ongoing work includes assembly and transfection of co-culture tissues containing stem cells for stem cell niche studies and cancer metastasis, tumor penetration studies.

Future research for work conducted in Chapter 3 include the generation of complex 3D tissues containing 3 or more cell types for paracrine or autocrine signaling, stem cell differentiation, stem cell growth and maintenance or development of blood-brain barrier models for drug screening studies. This methodology can also be extended to the study of macroscopic in vivo cell migration of implanted cellular patches through a pulse-chase model of bioorthogonal delivery, implantation and selective labelling of cells. This could enable the monitoring of spatio-temporal events including teratoma formation, tumor metastasis and developmental biology milestones.

With the introduction of cell surface engineering driven transfection in Chapter 4, the development of the future technology requires the further optimization of the liposomes and CSE for higher transfection rates, efficiencies and cell viability. This methodology can also be

extended to polymer based transfection methods using the installation of complimentary methodology into transfection polymers to drive transfection. Other future work should include transfection of primary cells, stem cells and other difficult to transfect cell lines to determine the overall applicability and general cellular mechanisms of the endocytic process of internalizing a neutral lipoplex using chemical reactions at the membrane interface.

Lastly, Chapter 5 was developed as an extension or add-on to the original liposome methodology, where a dialdehyde moiety could be used to conjugate amine containing biomolecules and small molecule to liposomes or other molecules for delivery to the plasma membrane of T-cells, stem cells or other cell types for biological study or therapeutic applications. Future studies based could include the development of magnetic or polymeric solid particles with surface presenting dialdehydes for solid based enzymatic reactions and purifications for biological applications and research. The conjugation and release of dialdehydes and primary amines through the lowering of pH should be pursued as a methodology for lysosomal antibody-drug conjugate release, surface modification using macromolecules for functional studies and cell delivery applications. The crosslinking dialdehyde has applications for functional studies of short-lived protein complexes, protein aggregate studies, colorimetric sensors and further studies into tissue formation using soluble cross-linkers for drug testing assays.

6.3 References

- (1) O'Brien, P. J.; Luo, W.; Rogozhnikov, D.; Chen, J.; Yousaf, M. N. *Bioconjug. Chem.* **2015**, 26 (9), 1939–1949.
- (2) Rogozhnikov, D.; Luo, W.; Elahipanah, S.; O'Brien, P. J.; Yousaf, M. N. *Bioconjug. Chem.* **2016**, 27 (9), 1991–1998.
- (3) Rogozhnikov, D.; O'Brien, P. J.; Elahipanah, S.; Yousaf, M. N. *Sci. Rep.* **2016**, 6, 39806.
- (4) O'Brien, P. J.; Elahipanah, S.; Rogozhnikov, D.; Yousaf, M. N. *ACS Cent. Sci.* **2017**, 3 (5), 489–500.
- (5) Elahipanah, S.; Radmanesh, P.; Luo, W.; O'Brien, P. J.; Rogozhnikov, D.; Yousaf, M. N. *Bioconjug. Chem.* **2016**, 27 (4), 1082–1089.
- (6) Elahipanah, S.; O'Brien, P. J.; Rogozhnikov, D.; Yousaf, M. N. *Bioconjug. Chem.* **2017**, 28 (5), 1422–1433.

7.0 Appendix

Theoretical Microsphere Calculations of Diffusion Time

Sample calculation of diffusion coefficient for spheres (rounded cells)

We estimated the (R_h) Hydrodynamic radii or Stokes radius as 10 micrometers, where larger proteins are ~6-8 Angstroms. The Stokes radius estimates a hard sphere that diffuses at the same rate as a molecule of roughly the same size.

(hydrodynamic radii) $R_h = 1E-5m$

(temperature) $T = 37^\circ C$ (310.15K)

(Boltzmanns constant) $k_b = (1.3806E-23kg\ m^2\ s^{-2}\ K^{-1})$

(kinematic viscosity of water) $\eta = 0.000426kg\ m^{-1}s^{-1}$

$$D = \frac{k_b T}{6\pi\eta R_h}$$
$$D = \frac{(1.3806E-23kgm^2s^{-2}K^{-1})(310.15K)}{6\pi(0.001004kgm^{-1}s^{-1})(1E-5m)}$$
$$D = 2.26E-14m^2s^{-1}$$

Therefore the estimated diffusion coefficient for rounded 10 μm is 5.34E-14m²s⁻¹. While at 75nm sphere has a $D = 3.02E-12$

Calculation of diffusion time of spheres through water across a 200 μm channel width

(smallest channel dimension) $w = 0.0002m$

(diffusion coefficient) $D = 5.34E-14m^2\ s^{-1}$

$$T_{diff} = \frac{\left(\frac{2}{3}w\right)^2}{D}$$
$$T_{diff} = \frac{\left(\frac{4}{9}\right)(2E-4m)^2}{2.26E-14m^2s^{-1}}$$
$$T_{diff} = 13110min$$

A 75nm has a $T_{diff} = 98min$

Renoldys number calculation for the microfluidic flow in the PMMA device

(channel area) $A = hb/2 = (1.70E-4\ m)(2E-4\ m)/2 = 1.70E-8\ m^2$

(channel length) $L = 0.015m$

(total flow rate) $Q = 1.2\mu L/min = 2.00E-11m^3/s$

(kinetic viscosity of water) $\eta = 0.001004\ m^2s^{-1}$

$$Re = \frac{QL}{\nu A}$$

$$Re = \frac{(2.00E-11 m^3 s^{-1})(0.015m)}{(1.70E-8 m^2)(1.004E-3 kg m^2 s^{-1})}$$

$$Re = 1.76E-2$$

Supplemental Linear Plots depicting the Effective Relationship of Cell Density, Flow Rate and Channel Distance upon number of cells per cluster (Spheroids) using our general microfluidic Y-channel device Using data for Figure 3.6.

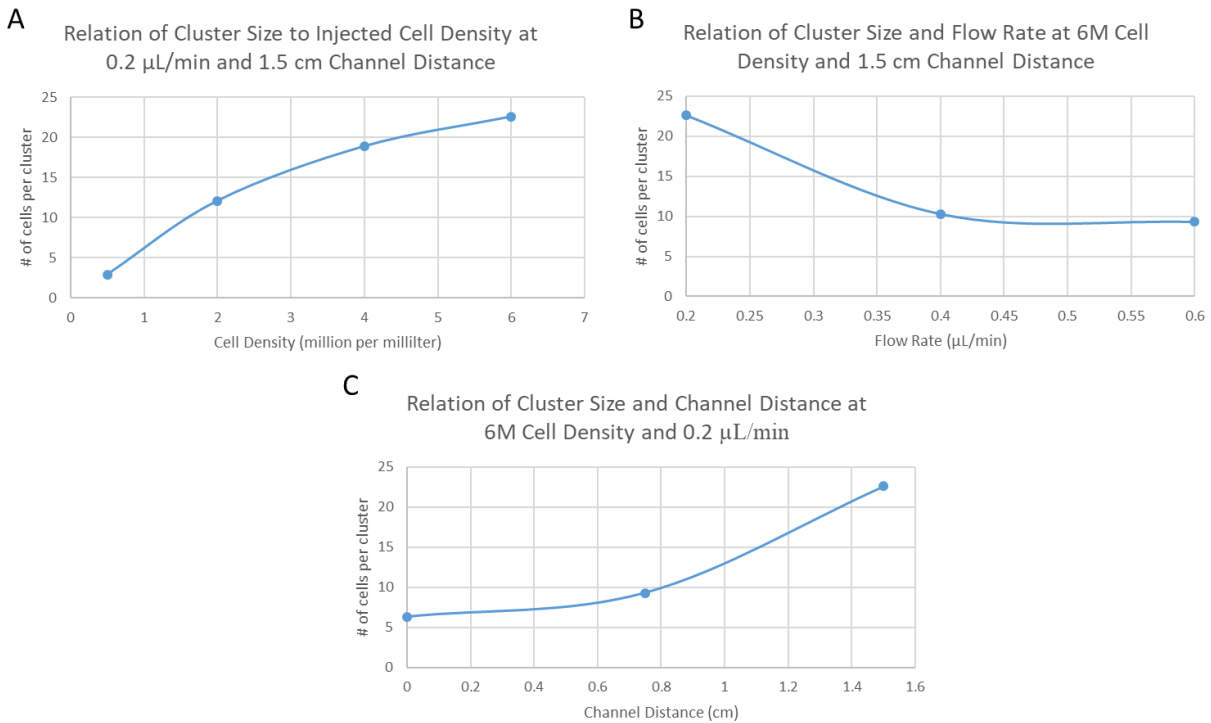


Table 1: Experimental results depicting changing conditions of liposome delivery to cells in flow to achieve cell surface engineering to form tissues. Thick tissue formation was observed (YES) when varying liposome concentration and changing the % composition of background lipids (DOTAP and POPC) in relation to concentration in our dual Y-joint microfluidic device (Fig 3) as a result of sufficient CSE. When liposomal CSE was not in sufficient concentrations or the biorthogonal chemistry was in low mol% there was only monolayers of cells observed (NO).

				Total Lipid Conc. [M] _b			Total Lipid Conc. [M] _b			Total Lipid Conc. [M] _b		
				6.2×10 ⁻⁴ M			1.6×10 ⁻³ M			3.1×10 ⁻³ M		
				2-dodecanone (%) _a			2-dodecanone (%) _a			2-dodecanone (%) _a		
				0	1.1	8.2	0	1.1	8.2	0	1.1	8.2
Total Lipid Conc. [M] _b	6.2×10 ⁻⁴ M	Dodecyloxyamine (mol%) _c	0	No	No	No	No	No	No	No	No	No
			1.1	No	No	No	No	No	No	No	No	No
			8.2	No	No	No	No	No	Yes	No	Yes	Yes
Total Lipid Conc. [M] _b	1.6×10 ⁻³ M	Dodecyloxyamine mol(%) _c	0	No	No	No	No	No	No	No	No	No
			1.1	No	No	No	No	Yes	Yes	No	Yes	Yes
			8.2	No	No	Yes	No	Yes	Yes	No	Yes	Yes
Total Lipid Conc. [M] _b	3.1×10 ⁻⁴ M	Dodecyloxyamine (mol%) _c	0	No	No	No	No	No	No	No	No	No
			1.1	No	No	Yes	No	Yes	Yes	No	Yes	Yes
			8.2	No	No	Yes	No	Yes	Yes	No	Yes	Yes